



Flávio Luis Portas Pinheiro Células solares e sensores de filme fino de silício depositados sCharacterization of Self-organization Processes in Complex Networks sobre substratos flexíveis

UMinho | 2015



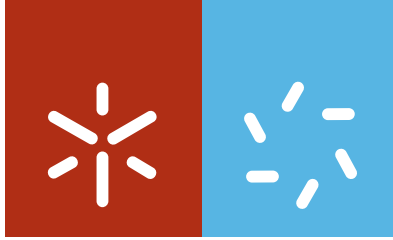
Universidade do Minho
Escola de Ciências

Flávio Luis Portas Pinheiro

Characterization of Self-organization Processes in Complex Networks

outubro de 2015





Universidade do Minho

Escola de Ciências

Flávio Luis Portas Pinheiro

Characterization of Self-organization Processes in Complex Networks

Programa Doutoral em Física (MAP-fis)

Trabalho realizado com a orientação do

Professor Doutor Jorge M. Pacheco

do

Professor Doutor Nuno M. Peres

e do

Professor Doutor Francisco C. Santos

DECLARAÇÃO

Nome **Flávio Luís Portas Pinheiro**

Endereço electrónico: **flavio.lpp@gmail.com** Telefone: **+351 916750763**

Número do Bilhete de Identidade: **13228061**

Título tese: **(PT)** *Caracterização de Processos de Auto-Organização em Redes Complexas* ou **(EN)**
Characterization of Self-Organization Processes in Complex Networks

Orientador(es): **prof Doutor Jorge M. Pacheco, prof Doutor Nuno M. Peres e prof Doutor Francisco C. Santos** Ano de conclusão: 2015

Designação do Doutoramento: **Programa Doutoral em Física**
(MAP-FIS)

É AUTORIZADA A REPRODUÇÃO INTEGRAL DESTA TESE/TRABALHO APENAS PARA EFEITOS DE INVESTIGAÇÃO, MEDIANTE DECLARAÇÃO ESCRITA DO INTERESSADO, QUE A TAL SE COMPROMETE;

Universidade do Minho, ___/___/_____

Assinatura: _____

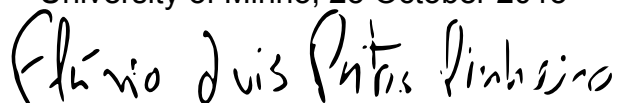
25 10 2015
Flávio Luís Portas Pinheiro

STATEMENT OF INTEGRITY

I hereby declare having conducted my thesis with integrity. I confirm that I have not used plagiarism or any form of falsification of results in the process of the thesis elaboration.

I further declare that I have fully acknowledge the Code of Ethical Conduct of the University of Minho

University of Minho, 25 October 2015

A handwritten signature in black ink, reading "Flávio Luís Portas Pinheiro". The signature is written in a cursive style with some capital letters.

Flávio Luís Portas Pinheiro

– *That’s why I like to listen to Schubert while I’m driving. As I said, it’s because all the performances are imperfect. A dense, artistic imperfection stimulates your consciousness, keeps you alert. If I listen to some utterly perfect performance of an utterly perfect piece while I’m driving, I might want to close my eyes and die right then and there. But listening to the D major, I can feel the limits of what humans are capable of – that a certain type of perfection can only be realised through a limitless accumulation of the imperfect. And personally, I find that encouraging. Do you see what I’m getting at?*

– *Sort of . . .*

Haruki Murakami, *Kafka on the Shore*

ACKNOWLEDGEMENTS

I acknowledge the financial support of FCT-Portugal through fellowship SFRH/BD/77389/2011.

I would like to express my gratitude to Jorge M. Pacheco, Nuno M. Peres and Francisco C. Santos for their support and tutoring over the last years. This extends back to 2009 when I first joined the ATP-Group and later when they actively supported my application to the FCT Phd fellowship.

My thanks to all the people I have had the pleasure to meet and collaborate during my time at the ATP-Group, these include Marta D. Santos, Carlos L. Reis, Jeromos Vukov, Marcos Gaudiano, João Moreira, João Braz, Vitor V. Vasconcelos and Fernando Santos.

My thanks to all the Macro Connections group, and in particular to César Hidalgo, who welcomed me in their group during the first half of 2015.

Finally, a special thanks to my family and to my girlfriend, for they have shared with me the ups and downs in the life of a doctoral student.

Thank you!

RESUMO

A estrutura de interações sociais numa população é muitas vezes modelada através de uma rede complexa que representa os indivíduos e respetivas relações sociais. Estas estruturas são conhecidas por afetarem de forma fundamental os processos dinâmicos que suportam. A caracterização desse efeito é, no entanto, uma tarefa complicada pois o tratamento matemático destes sistemas requer o estudo de um espaço de estados de grande dimensão, limitando a aplicabilidade de abordagens analíticas e numéricas. Esta tese teve como objetivo desenvolver métodos, inspirados na Física Estatística dos Sistemas Fora do Equilíbrio, com o fim de caracterizar processos dinâmicos em redes complexas.

Nesta tese demonstramos que a estrutura de uma população naturalmente induz a emergência de padrões de correlações entre indivíduos que partilham traços semelhantes, um fenómeno também identificado em estudos empíricos. Estes padrões de correlações são independentes do tipo de processo dinâmico considerado, do tipo de informação que se propaga sendo observados numa classe alargada de redes complexas. Mostramos também que propriedades como o clustering e a densidade de ligações da rede têm um papel fundamental nos padrões de correlações emergentes.

Outra questão fundamental diz respeito à relação entre as dinâmicas local e a global em redes sociais. De facto, as redes sociais afetam de forma tão fundamental os processos dinâmicos que suportam que em muitas situações o comportamento coletivo observado não tem qualquer relação aparente com a dinâmica local na sua génese. Este é um problema comum a muitos sistemas complexos e tipicamente associado a fenómenos emergentes e de auto-organização. Neste trabalho esta questão é explorada no contexto do problema da Cooperação e no âmbito da *Teoria de Jogos Evolutiva*. Para esse fim introduzimos uma quantidade que é estimada numericamente e a que damos o nome de *Average Gradient of Selection (AGOS)*. Esta quantidade, relaciona de forma efetiva as dinâmicas local e global, possibilitando a descrição do processo de auto-organização em populações estruturadas.

Através do **AGOS** mostramos que quando as interações entre indivíduos são descritas através do *Dilema do Prisioneiro*, uma metáfora popular no estudo da cooperação, a dinâmica coletiva emergente é sensível à forma da rede de interações entre os indivíduos. Em particular, demonstramos que quando a rede é homogénea (heterogénea) no que respeita à distribuição de grau o *Dilema do Prisioneiro* é transformado numa dinâmica coletiva de coexistência (coordenação). Mostramos ainda que esta transformação depende da pressão de seleção (associada ao grau de determinismo no processo de decisão dos indivíduos) e de taxa de mutações (a adoção espontânea de um novo comportamento por parte de um indivíduo) consideradas. A relação entre estas duas variáveis pode também resultar em alterações de regimes dinâmicos cujo o resultado pode, em casos particulares, resultar no desfecho drástico para a evolução da cooperação.

Finalmente, fazemos uso do **AGOS** para caracterizar a dinâmica evolutiva da cooperação no caso em que a estrutura co-evolve. Demonstramos que na presença de uma estrutura social a dinâmica global é semelhante à de um jogo de coordenação entre N -pessoas, cujas características dependem de forma

sensível das escalas de tempo relativas entre a evolução de comportamentos e a evolução da estrutura. Uma vez mais, a dinâmica global emergente contrasta com o *Dilema do Prisioneiro* que caracteriza as interações locais entre os indivíduos.

Acreditamos que o **AGOS**, que pode ser facilmente aplicado no estudo de outros processos dinâmicos, proporciona uma contribuição significativa para o melhor entendimento de Sistemas Complexos, em particular aqueles em que as interações entre os elementos constituintes são bem definidos através uma rede complexa.

ABSTRACT

The structure of social interactions in a population is often modeled by means of a complex network representing individuals and their social ties. These structures are known to fundamentally impact the processes they support. However, the characterization of how structure impacts a dynamical process is by no means an easy task. Indeed, the large configuration space spanned tends to limit the systematic applicability of numerical methods, while analytical treatments have failed to provide a good description of the system dynamics. The aim of this thesis was to develop methods inspired in the Statistical Physics of Systems far from equilibrium to characterize dynamical processes on complex networks.

In this thesis we show how the structure of a population naturally induces the emergence of correlations between individuals that share similar traits, which is in accordance empirical evidence. These, so called, '*peer-influence*' correlation patterns are independent of the type of dynamical process under consideration, the type of information being spread while being ubiquitous among a wide variety of network topologies. We have also find evidence that central to the '*peer-influence*' patterns are topological features such as the clustering and the sparsity of the underlying network of interactions.

Another fundamental problem concerns the relationship between local and global dynamics in social networks. Indeed, social networks affect in such a fundamental way the dynamics of the population they support that the collective, population-wide behavior that one observes often bears no relation to the individual processes it stems from. This is in fact a common problem among many Complex Systems typically associated with self-organization and emerging phenomena. Here we study this issue in the context of the problem of Cooperation and in the realm of *Evolutionary Game Theory*. To that end we introduce a numerically estimated mean-field quantity that we call the *Average Gradient of Selection* (**AGOS**). This quantity is able to effectively connect the local and global dynamics, providing a way to track the self-organization of cooperators and defectors in networked populations.

With the **AGOS** we show that when individuals engage in a *Prisoner's Dilemma*, a popular cooperation metaphor, the emerging collective dynamics depends on the shape of the underlying network of interactions. In particular, we show that degree homogeneous (heterogeneous) networks the *Prisoner's Dilemma* is transformed into a collective coexistence (coordination) dynamics, contrasting with the defector dominance of the local dynamics. We further show that the extent to which these emergent phenomena are observed in structured populations is conditional on the selection pressure (the uncertainty associated with the decision making) and the rate of mutations (the spontaneously adoption of new behaviors by individuals) under consideration. Interestingly, the interplay between selection pressure and mutation rates can lead to drastic regime shifts in the evolution of cooperation.

Finally, we make use of the **AGOS** to characterize the evolutionary dynamics of cooperation in the case of a co-evolving social structure. We demonstrate that in an adaptive social structure the population-wide dynamics resembles that of a N -person coordination game, whose characteristics depend sensitively on the relative time-scales between behavioral and network co-evolution. Once more,

the resulting collective dynamics contrasts with the two-person *Prisoner's Dilemma* that characterizes how individuals interact locally.

We argue that the **AGOS**, which can be readily applied to other dynamical contexts and processes, provides a significant contribution to a better understanding of Complex Systems involving populations in which who interacts with whom is well-defined by a complex network.

CONTENTS

1	INTRODUCTION	1
1.1	Overview	3
1.2	The Science of Networks	5
1.2.1	Degree	6
1.2.2	Clustering Coefficient	8
1.2.3	Average Path Length	9
1.2.4	Models of Networks	11
1.3	Evolutionary Game Theory	14
1.3.1	Finite Populations	16
1.3.2	Two Person Games	21
1.3.3	Social Dilemmas of Cooperation	23
1.3.4	Evolving Cooperation	26
1.4	Evolutionary Games in Structured Populations	31
1.4.1	Homogeneous Networks	32
1.4.2	Heterogeneous Networks	34
1.4.3	Gradient of Selection in networks	36
1.4.4	Co-Evolutionary Dynamics	39
1.5	Bibliography	42
2	ORIGINS OF PEER INFLUENCE IN SOCIAL NETWORKS	57
2.1	Manuscript	57
2.2	Supplemental Material	62
2.2.1	Social Structure	62
2.2.2	Peer Influence	65
2.2.3	SIR Dynamics	66
2.2.4	Voter Model	68
2.2.5	Prisoner's Dilemma	69
2.3	Bibliography	71
3	FROM LOCAL TO GLOBAL DILEMMAS IN SOCIAL NETWORKS	77
3.1	Manuscript	77
3.1.1	Introduction	77
3.1.2	Dynamical Model	78
3.1.3	Results	80
3.1.4	Discussion	83
3.1.5	Methods	84
3.2	Supporting Information	86

Contents

3.2.1	Evolutionary steady states in homogeneous networks	86
3.3	Bibliography	87
4	HOW SELECTION PRESSURE CHANGES THE NATURE OF SOCIAL DILEMMAS IN STRUCTURED POPULATIONS	93
4.1	Manuscript	93
4.1.1	Introduction	93
4.1.2	Model	95
4.1.3	Results and Discussion	97
4.2	Additional Results	103
4.3	Bibliography	105
5	EVOLUTION OF COOPERATION UNDER VARIABLE MUTATION RATES	109
5.1	Manuscript	109
5.1.1	Model	110
5.1.2	Materials and Methods	113
5.1.3	Results and Discussion	114
5.2	Bibliography	116
6	LINKING INDIVIDUAL AND COLLECTIVE BEHAVIOR IN ADAPTIVE SOCIAL NETWORKS	119
6.1	Manuscript	119
6.2	Supplemental Material	126
6.2.1	Computer Simulations	126
6.2.2	Time-Dependent Gradient of Selection	127
6.2.3	Time-Independent Gradient of Selection	128
6.2.4	Selection Pressure	129
6.3	Bibliography	130
7	EVOLUTION OF ALL-OR-NONE STRATEGIES IN REPEATED PUBLIC GOODS DILEMMAS	133
7.1	Manuscript	133
7.1.1	Introduction	133
7.1.2	Model	134
7.1.3	Results and Discussion	136
7.2	Supporting Information	139
7.2.1	The Small Mutation Limit	139
7.2.2	Evolution without errors	141
7.2.3	Validity of the Small-Mutation Limit	142
7.2.4	All-or-None versus ALLD	142
7.3	Bibliography	143
8	CONCLUSION	147
8.1	Bibliography	150

LIST OF FIGURES

Figure 1	Adjacency Matrix	6
Figure 2	Graphs	7
Figure 3	Clustering Coefficient	8
Figure 4	Paths and Distance	10
Figure 5	<i>Watts-Strogatz</i> Model	10
Figure 6	<i>Barabási-Albert</i> Model	12
Figure 7	Complex Networks	13
Figure 8	Pairwise Comparison Rule	15
Figure 9	Markov Chain	18
Figure 10	Fixation Probability	20
Figure 11	Payoff Matrix	22
Figure 12	Two Person Games	25
Figure 13	Fixation Probability in the $T \times S$ domain	26
Figure 14	Cooperation Level in the $T \times S$ domain	27
Figure 15	Five Mechanisms to Evolve Cooperation	29
Figure 16	Pairwise Comparison Rule on Networks	32
Figure 17	Level of Cooperation in Homogeneous Networks	33
Figure 18	Spatial Patterns in Lattices	34
Figure 19	Level of Cooperation in Heterogeneous Networks	35
Figure 20	Double-Star Dynamics	36
Figure 21	Gradient of Selection in Networks	38
Figure 22	Dynamical Feedback in Co-Evolutionary Systems	40
Figure 23	Peer Influence Patterns in Homogeneous Networks	58
Figure 24	Peer Influence Patterns in Social Networks	60
Figure 25	Summary of Network Properties	62
Figure 26	Networks Diameter	63
Figure 27	Critical distances for the SIR	64
Figure 28	Peer Influence patterns generated by SIR model on Small World Networks	65
Figure 29	Peer Influence patterns generated by SIR model on Heterogeneous Networks	66
Figure 30	Critical distances for the Voter Model	67
Figure 31	Peer Influence patterns generated by the Voter Model on Small World Networks	68
Figure 32	Peer Influence patterns generated by the Voter Model on Heterogeneous Networks	69
Figure 33	Critical distances for the Prisoner's Dilemma	70

List of Figures

Figure 34	Peer Influence patterns generated by the Prisoner's Dilemma on Small World Networks	71
Figure 35	Peer Influence patterns generated by the Prisoner's Dilemma on Heterogeneous Networks	72
Figure 36	Time-independent AGoS	79
Figure 37	Time-dependent AGoS	81
Figure 38	AGoS on BA-networks	84
Figure 39	Evolutionary dynamics cooperation in homogeneous networks	86
Figure 40	Effective games in structured populations	94
Figure 41	Average Gradient of Selection on Homogeneous Random graphs	97
Figure 42	Average Gradient of Selection on strongly Heterogeneous graphs	98
Figure 43	Level of Cooperation in Structured Populations	99
Figure 44	Meta-Network description	100
Figure 45	Meta-network imitation probabilities	102
Figure 46	Level of Cooperation in Heterogeneous Populations	103
Figure 47	Evolutionary Dynamics on Random Networked Populations	104
Figure 48	Evolutionary Dynamics on Exponential Networked Populations.	105
Figure 49	The impact of Variable Mutations	110
Figure 50	Average Gradient of Selection with Variable Mutations	111
Figure 51	Level of Cooperation with Variable Mutations	113
Figure 52	Time Evolution with Decaying Mutations	115
Figure 53	Level of Cooperation in Adaptive Networks	121
Figure 54	Average Gradient of Selection in Adaptive Networks	122
Figure 55	Level of Cooperation in Adaptive Networks	125
Figure 56	Time-Dependent Gradient of Selection	126
Figure 57	Time-Independent Gradient of Selection	127
Figure 58	Time-Independent Gradient of Selection Fit	128
Figure 59	Selection Pressure in Adaptive Networks	129
Figure 60	Stationary bit Distribution	135
Figure 61	Stationary bit Distribution	136
Figure 62	Level of Cooperation	138
Figure 63	Markov Chain	140
Figure 64	Stationary-bit-Strategy	141
Figure 65	Validity of Small Mutation Limit	142
Figure 66	Gradient of Selection	143

LIST OF PUBLICATIONS INCLUDED

This thesis is written as a compilation of articles published, submitted or ready for submission during the period of the doctoral program. Bellow is a list of the articles included in this thesis and the respective chapter.

CHAPTER 2 - *Origin of Peer Influence in Social Networks,*

Physical Review Letters, 112, 098702 (2014),

Flávio L. Pinheiro, Marta D. Santos, Francisco C. Santos and Jorge M. Pacheco.

CHAPTER 3 *From Local to Global Dilemmas in Social Networks,*

PLoS ONE 7(2): e32114 (2012),

Flávio L. Pinheiro, Jorge M. Pacheco and Francisco C. Santos.

CHAPTER 4 *How selection pressure changes the nature of social dilemmas in structured populations,*

New Journal of Physics 14 073035 (2012),

Flávio L. Pinheiro, Francisco C. Santos and Jorge M. Pacheco.

CHAPTER 5 *Evolution of Cooperation under variable Mutation Rates,*

To be Submitted (2015),

Flávio L. Pinheiro, Francisco C. Santos and Jorge M. Pacheco.

CHAPTER 6 *Linking Individual and Collective Behaviour in Adaptive Social Networks,*

Submitted (2015),

Flávio L. Pinheiro, Francisco C. Santos and Jorge M. Pacheco.

CHAPTER 7 *Evolution of All-or-None strategies in repeated public goods dilemmas,*

PLoS Computational Biology 10(11): e1003945 (2014),

Flávio L. Pinheiro, Vitor V. Vasconcelos, Francisco C. Santos and Jorge M. Pacheco.

INTRODUCTION

“Things became duplicated in Tlön; they also tend to become effaced and lose their details when they are forgotten. A classic example is the doorway which survived so long as it was visited by a beggar and disappeared at his death. At times some birds, a horse, have saved the ruins of an amphitheater.”

Jorge Luis Borges, *Ficciones*

Social structure is often associated with the web of social relationships interconnecting individuals in a group, community or population [1, 2]. In that context, networks or graphs provide an intuitive and powerful conceptual tool to model and study the properties of such structures. In a ‘Social Network’ nodes correspond to individuals and links, connecting two nodes, highlight the existence of a social tie between a pair of individuals. Different types of social interactions may lead to different types of social networks, such as networks of scientific collaborations [3], sexual partnerships [4], communication [5], friendship [6], among others. Real world social networks are complex, in the sense that they often exhibit topological features that strongly deviate from the regular and homogeneous topologies commonly found in Physics textbooks [7] and from the random structures at the genesis of graph theory [8, 9].

The ubiquity of complex networks far extends social systems. Examples range from Technological systems (*e.g.* power grid [10], airline [11], roads [12, 13], telecommunications [14], the Internet [15]) to Information (*e.g.* world wide web [16], citations [17], blogs [18]) but are also common in Biological (*e.g.* metabolic [19, 20], food web [3], gene regulation [21], protein-protein interactions [22, 23]), Language (*e.g.* semantic [24]) and other natural systems. Their abundance has justified the big effort that has been made to understand how they emerge and the role they play in the functioning of the different systems at their genesis. In that context, Physics has played an important part, since as a science it is known for the development of tools that successfully predict the behavior of large scale systems from the properties of its constituents [25]. Example of that are several review articles [26, 25, 27, 28, 29] and books [30, 31, 32, 33] that summarize the fundamental contributions of Physics to the Science of Networks, constituting the backbone of any modern course in Complex Networks. Section 1.2 provides an introduction to the fundamental concepts of Network Science necessary for a full comprehension of the topics discussed along the following Chapters.

While the shape of Social Networks stems from individuals’ choices [34], individuals’ dynamical state and traits are, in the same way, largely influenced by the shape of the social network they are part of [35]. For instance, the susceptibility of an individual to acquire and infectious disease, such

Chapter 1. INTRODUCTION

as flu, is largely influenced by the individuals he chooses to interact with, whose susceptibility, in turn, depends on whom they interact with, and so forth. Following the same logic, being friends with a highly popular and, as consequently, highly susceptible individual, certainly increases our chances of getting infected. In that context *Santorras et al* [36] have shown that Social Structures decrease the resilience of populations to epidemic outbreaks, by increasing the susceptibility of individuals to become infected [37, 38, 39].

Contagious diseases are not the only dynamical element that propagates along the nodes of Social Networks. Ideas, innovations and behaviors are also transmitted from individual to individual throughout social interactions. In the same way our opinions and behaviors influence our peers, we are also influenced by theirs. Furthermore, the '*peer-influence*' patterns found in empirical social networks show that they extend individuals' range of interactions, beyond those they are directly connected to. For instance, *Fowler and Christakis* [40, 41, 42] have compiled empirical evidence that supports the idea that individuals' habits (*e.g.* smoking) and behaviors are not only influenced by the people we choose to interact directly with but also by their friends and by their friends' friends as well. This phenomenon, coined as the three-degrees of influence, highlights how Social Networks generate non-intuitive patterns and calls for a closer attention on how these impact the dynamical processes they support. In Chapter 2 we explore the universality of these network patterns by testing how different dynamical processes generate similar *peer-influence* patterns in a wide range of network topologies [43].

Social structure also plays a central role in the evolution of Cooperative behavior [44]. Mostly studied employing Evolutionary Game Theory [45, 46, 47], it has been shown theoretically that an underlying network of interactions between individuals facilitates the emergence of cooperation [48, 49]. This becomes particularly effective when such structure closely resembles the shape of real world social networks [50, 51, 52, 53]. Empirical evidence is, however, less conclusive. Some studies support the idea that structure indeed promotes cooperative behavior in human populations [54, 55, 56, 57, 58, 59], while recent studies have raised some questions on that evidence [60, 61, 62, 63, 64]. In Chapter 3 we proposed a novel approach to characterize dynamical processes on structured populations, thus effectively unveiling the role that different types of social structures have in the emerging collective dynamics. In Chapters 4 and 5 we extend this approach to more dynamically complex scenarios.

In the same way we adopt new traits and our health condition changes, we also constantly revise with whom we interact. Indeed, the assumption that social structures are static, is but a simplification [65]. The real world social networks are evolving structures driven by decision making of individuals. Studying dynamical processes in complex networks thus requires to take into consideration also this aspect of social structures. In Chapter 6 we explore the evolutionary consequences of adaptive social networks in the context of the evolution of cooperation by adapting the approach introduced in Chapter 3.

Dynamical processes are not restricted to situations that involve interactions between pairs of individuals. Indeed, many situations are better understood when interactions between groups are considered [66]. In that scope, networks, whose structure stems from pairwise relationships, are not necessarily

the most convenient way to map individuals' participation in groups [67]. In fact, decision making in groups have been recently used to study the implication of individuals' decision making in international agreements [68, 69]. Whenever a social network plays a smaller role, we extend the study of an evolving population in which individuals only interact in pairs to the more complex scenario of groups of interacting individuals. In Chapter 7 we explicitly explore the evolutionary dynamics of a population whose individuals participate in repeated group interactions [70]. We consider the entire strategy space spanned when considering strategies in which individuals react to the actions of the group in the previous round.

Overall, in this thesis we explore questions that consider finite populations of individuals. We model both the rules and the scheme (*i.e* network) of interactions between individuals, our goal being to characterize the process of self-organizing, emerging collective phenomena. This is a problem well framed within the Physics of Complex Systems, whose state of the art approaches often stem directly from tools developed in the scope of Statistical Physics and Dynamical Systems Theory. This is not surprising, since the study of systems composed by many interacting units is a secular topic in Physics [71]. Here, in order to characterize the self-organization processes in complex networks we introduce a novel approach that makes use of Computational Physics methods to run large scale numerical (Monte-Carlo) simulations to estimate a quantity that proves to be sensitive to the network context in which it is computed. Furthermore, the work developed in this thesis tackles problems and questions that are inherently multidisciplinary. For instance, the problem of Cooperation, which is the focus of Chapters 3 to 7, is considered of major importance in Biological [72] and Social [73, 66] sciences, where it is believed to be an essential building block to the evolution of complex biological organisms and of human civilization.

In the next section we provide a brief overview of this thesis, highlighting the main contributions of each chapter.

1.1 OVERVIEW

This thesis is organized as a collection of independent articles developed during the time period of the doctoral program. The modular structure invites the reader to jump to the chapter that he/she feels more interested in. In the following I provide an overview of the remaining thesis, summarizing the major contributions per chapter.

The remaining of Chapter 1 is composed by three sections. The first two introduce fundamental concepts of Network Science (1.2) and Evolutionary Game Theory (1.3) while the third (1.4) reviews the main results available in existing literature of Evolutionary Games on Structured Populations [53].

Chapters 2, 3, 4, 5, 6 and 7 correspond to articles developed during the doctoral program. Each starts with an introductory note that contextualizes the reader to the importance of the work included. While some of these chapters correspond to articles published in peer-reviewed journals (Chapters 2, 3, 4 and 7) others are either submitted or (Chapter 6) close to submission (Chapter 5).

In Chapter 2, entitled *Origins of Peer Influence in Social Networks*, we study how the empirically identified 'peer-influence' patterns of correlations between individuals emerge in networked populations [43]. We employ a range of models of information spreading, well-known in the Physics of

Chapter 1. INTRODUCTION

Complex Systems, to argue that empirically observed patterns of correlation among peers emerge naturally from a wide range of dynamics, being essentially independent of the type of information, on how it spreads, and even on the class of underlying network that interconnects individuals. Moreover, we show that the sparser and clustered the network, the more far reaching the influence of each individual will be.

In Chapter 3, *From Local to Global Dynamics in Social Networks*, we study the evolution of cooperation in networked populations when individuals interact according to the two-person Prisoner's Dilemma, the most famous social metaphor of cooperation developed to date [74]. We show how degree homogeneous networks transform a *Prisoner's Dilemma* into a population-wide evolutionary dynamics that promotes the coexistence between cooperators and defectors, while degree heterogeneous networks promote their coordination. Central to this analysis is the development of a novel methodology to analyze the macroscopic, population-wide dynamics on structured populations. This is done through the computation of a numerically mean-field quantity that we refer to the *Average Gradient of Selection*, which returns dynamical information similar to the classical replicator equation from Evolutionary Game Theory but with information that is context dependent, namely, that reflects the nature of the underlying network supporting the evolutionary dynamics.

In Chapter 4, *How Selection Pressure Changes the Nature of Social Dilemmas in Structured Populations*, we use the *Average Gradient of Selection* to investigate how selection pressure (here associated with the stochasticity of the individuals decision making) contributes to change the fate of the population in a broader range of network topologies [75]. We recover the analytical results from degree homogeneous networks (valid only in the limit of weak selection, that is, weak coupling amenable to a first order perturbation theory analysis), whereas strongly heterogeneous networks are more resilient to natural selection, dictating an overall robust evolutionary dynamics of coordination. Between these extremes, a whole plethora of behaviors are predicted, showing how selection pressure can change the nature of dilemmas populations effectively face. We further demonstrate how the present results for homogeneous networks bridge the existing gap between analytic predictions obtained in the framework of the pair-approximation from very weak selection and simulation results obtained from strong selection.

In Chapter 5, *Evolution of Cooperation Under Variable Mutation Rates*, we use the *Average Gradient of Selection* to investigate how the introduction of mutation rates in structured population influences the evolutionary dynamics of cooperation. We show that when individuals engage in a *Prisoner's Dilemma* game on degree heterogeneous networks, mutation rates induce regime shifts, from the defection dominance that characterises the standard *Prisoner's Dilemma* into a regime of coexistence among Cooperators and Defectors, as well as into a regime of coordination, often revealing more than one basin of attraction. Moreover, we predict that under strong selection regimes, cooperation is undermined by variations in the mutation rate, whereas under weak selection one witnesses a subtle balance between selection and mutation, which is favourable to defectors. Interestingly, there exists a range of selection pressures in which structured populations are most resilient to variations in mutation rates.

In Chapter 6, *Linking Individual and Collective behavior in Adaptive Social Networks*, we use the *Average Gradient of Selection* to explore the evolutionary dynamics on adaptive social networks, establishing a link between the global and the local dynamics in co-evolutionary systems. We demonstrate that adaptive social structures change the two-person social dilemmas locally faced by individuals into an evolutionary dynamics that resembles that of a N-person coordination game, whose characteristics depend sensitively on the relative time-scales between behavioral and network co-evolution. Indeed, we show that the faster the relative rate of adaptation of the network, the smaller the critical fraction of Cooperators required for cooperation to prevail, thus establishing a direct link between network adaptation and the evolution of cooperation.

Chapter 7, *Evolution of All-or-None strategies in repeated public goods dilemmas*, is devoted to investigate the evolutionary dynamics of direct group reciprocity, considering the complete sub-space of reactive strategies, where individuals behave conditionally on what they observed in the previous round [70]. This sub-space, although not complete, is by far the largest strategy subspace employed to date in the study of reciprocity within groups. We study both analytically and by computer simulations the evolutionary dynamics encompassing this extensive strategy space, witnessing the emergence of a surprisingly simple strategy that we call All-Or-None. This strategy consists in cooperating only after a round of unanimous group behavior (cooperation or defection), and proves robust in the presence of errors, thus fostering cooperation in a wide range of group sizes. The principles encapsulated in this strategy share a level of complexity reminiscent of that found already in two-person games under direct reciprocity, reducing, in fact, to the well-known *Win-Stay-Lose-Shift* strategy in the limit of the repeated 2-person *Prisoner's Dilemma*.

Finally, Chapter 8 concludes with a recap of the main results obtained during this thesis, a critique to the work developed during the doctoral program, which also includes work developed and published during the same period but not included in the thesis, and notes of future research directions.

1.2 THE SCIENCE OF NETWORKS

A network is any system that admits an abstract mathematical representation as a graph whose nodes or vertices identify the elements of the system and in which the set of connecting links or edges represent the existence of a relation or interaction among those elements [35]. In that sense a network can be represented by a graph \mathcal{G} composed by a set \mathcal{Z} of Z vertices $\{n_1, n_2, \dots, n_{Z-1}, n_Z\}$ and another set \mathcal{L} of L edges $\{e_{ij}, \dots, e_{nm}\} \forall (i, j, n, m) \in [1, Z]$. Edges connect pairs of vertices and can have additional properties, for instance a weight (w_{ij}) or a direction (*i.e.* $e_{ij} \neq e_{ji}$). A graph is also said to be sparse if $L \ll Z^2$ and dense if $L = \mathcal{O}(Z^2)$.

A network is completely described by means of the so-called adjacency matrix, \mathcal{A} . This is a $Z \times Z$ square matrix whose entries a_{ij} are 1 when exists a link connecting nodes n_i and n_j , being 0 otherwise. In weighted networks, the entries of \mathcal{A} are replaced by the respective weights of the edges (*i.e.* $a_{ij} = w_{ij}$), while in undirected networks \mathcal{A} is becomes symmetric since $a_{ij} = a_{ji}$. Finally, the diagonal elements of \mathcal{A} concern self-connections or loops, that is, links that start and end at the same node (e_{ij} for $i = j$).

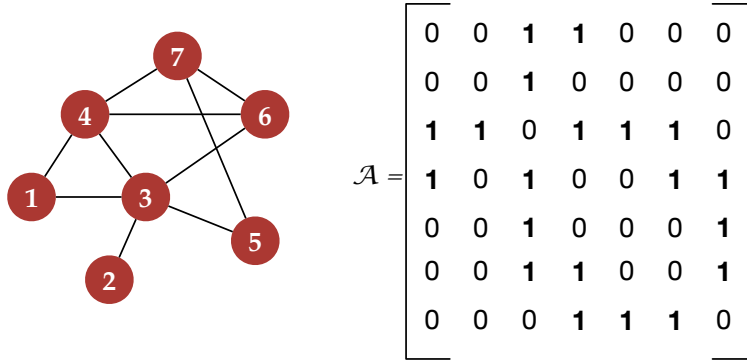


Figure 1: Graphical representation of an undirected network and the respective Adjacency matrix \mathcal{A} . Each entry of the adjacency matrix a_{ij} is 1 if i is connected to j and 0 otherwise. In the case of undirected network $a_{ij} = a_{ji}$, and moreover when links are weighted, the entries of the matrix are replaced by the weight.

The maximum number of edges in an undirected graph is $Z(Z - 1)/2$ while in directed graphs there are at most $Z(Z - 1)$ edges. A complete graph corresponds to a network whose entries are all 1, *i.e.* $a_{ij} = 1 \forall i, j \in \{1, \dots, Z\} \wedge i \neq j$. Likewise, cliques refer to fully connected components of graphs.

Although weighted and directed networks provide a more realistic representation of real world systems, for the purpose of this thesis we shall focus our attention in the simpler case of undirected and unweighted networks that do not have loops.

1.2.1 Degree

The degree of a node corresponds to the total number of connections a node i is part of, which in terms of \mathcal{A} reads

$$k_i = \sum_{j=1}^Z a_{ij} \tag{1}$$

Networks are characterized by the degree distribution, $D(k)$, that corresponds to the fraction of nodes with degree k . The first moment of $D(k)$ corresponds to the mean degree

$$\langle k \rangle = \sum_{k=1}^{max(k)} kD(k) \tag{2}$$

while the second moment $\langle k^2 \rangle$ measures fluctuations in $D(k)$. We shall also consider the variance of $D(k)$, that is given by

$$var(k) = \langle k^2 \rangle - \langle k \rangle^2 \tag{3}$$

The Degree distribution ($D(k)$) is the simplest, yet the most common property used to classify networks. Indeed, real world networks often exhibit different degree distributions. In particular, when $D(k)$ falls in the category of heavy-tailed distributions, we face several technical challenges that undermine a good estimation of the distribution parameters. These are distributions characterized by a tail that decays slower than an exponential or geometric distribution. As a result empirical samples

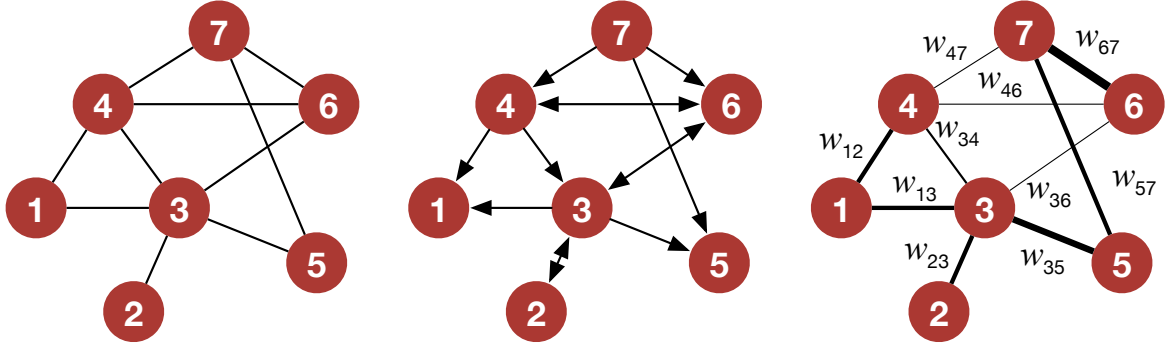


Figure 2: Graphical representation of an undirected (left), directed (middle) and weighted network (right). The weighted and undirected graphs are composed by $Z = 7$ vertices (nodes) and $L = 10$ edges (links). In the directed graph arrows point to the direction of the link and the total number of links is $L = 13$. In the weighted graph w_{ij} indicates the weight of each link. Graphically, the weight is represented with different thicknesses.

tend to be very noisy for values $k \gg 1$. One approach is to compute the complementary cumulative distribution (CDF) of $D(k)$, that is defined as

$$\bar{D}(k) = 1 - \sum_{j=1}^{k-1} D(j) \quad (4)$$

and provides a smoother distribution for analysis. Currently the most accepted approach to estimate the parameters of heavy tail distribution relies on the maximum likelihood fit in conjunction with a goodness-of-fit test. In reference [76] *Clauset et al* detail the applicability of this approach to arbitrary distributions.

Although the degree distribution describes the statistical properties of an uncorrelated network, it fails to capture *degree-degree* correlations, which are present in many real world networks [77, 78, 79]. A more general and accurate definition would be provided by the conditional probability that a node with degree k is connected to a node with degree k' , *i.e.* $D(k|k')$. Although such the formal definition, it is often unfeasible to estimate the conditional distribution from finite size empirical networks. A more feasible approach to identify and classify *degree-degree* correlations explores the so-called *average nearest neighbors degree* of a node i , which reads as

$$k_{nn}^i = \frac{1}{k_i} \sum_{j=1}^Z a_{ij} k_j \quad (5)$$

that allows the computation of the average degree of nearest neighbors of nodes with degree k , denoted as $k_{nn}(k)$, that is

$$k_{nn}(k) = D(k) \sum_{i=1}^Z \delta(k - k_i) k_{nn}^i \quad (6)$$

In the absence of degree correlations $k_{nn}(k)$ should be independent of k , while a dependence on this parameter highlights the existence of correlations.

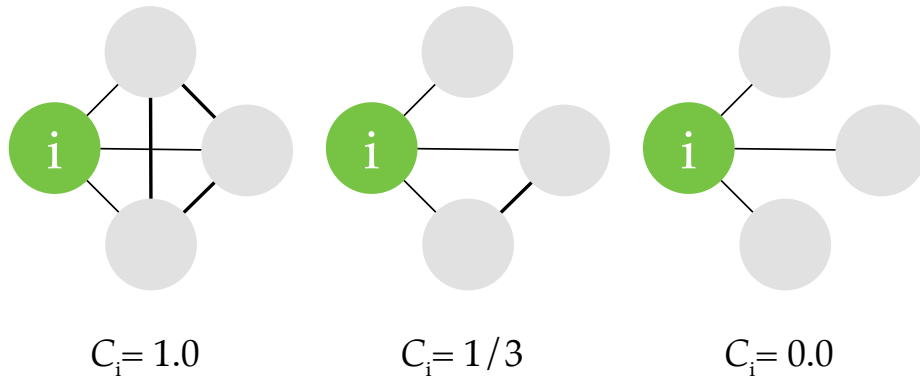


Figure 3: Graphic representation of the computation of the Clustering Coefficient of node i in different iterations of a graph with $Z = 4$.

Networks showing *degree-degree* correlations are classified either as assortative if $k_{nn}(k)$ increases with k and disassortative if it decreases with k [80], thus indicating how probable is for nodes of similar degree to cluster together. Another way to measure degree assortativity is by means of the Pearson correlation coefficient, r , which is computed as

$$r = \frac{1}{\sigma_q^2} \sum_{jk} jk(a_{jk} - q_j q_k) \quad (7)$$

where q_k is obtained from the degree distribution and reads

$$q_k = \frac{D(k+1)}{\sum_{j \geq 1} D(j)} \quad (8)$$

and σ_q the variance of q_k . This quantity measures the correlation between the degrees of nodes that share an edge. A positive (negative) r indicates a correlation between nodes of similar (dissimilar) degree. In the context of social sciences, assortativity (disassortativity) is associated with homophilic (heterophilic) behavior in individuals choice of social interactions. Assortativity in social networks is most likely the result of our natural homophilic behavior [80, 81].

1.2.2 Clustering Coefficient

It is often the case that a network can also be characterized by the abundance of particular arrangements of nodes. These topological building blocks [82], also called motifs, constitute patterns of interconnections occurring in complex networks at an abundance higher than expected from a random network. That is, motifs are statistically significant sub-graphs or patterns.

The simplest motif involves three nodes (n_i , n_j and n_k) with at least two (e.g. e_{ij} and e_{jk}) and at most three (e.g. e_{ij} , e_{jk} and e_{ki}) links, the first case corresponds to an 'open' and the second to a 'closed' triangle. The study of the abundance of 'closed' triangles on networks takes a particular interest mainly because of its intuitive meaning in real world social networks. For instance in social

networks, whose nodes correspond to individuals and links to a social tie connecting them, triangles identify a pair of friends (nodes) of a focal individual (node) that are also friends (connected) between themselves.

The abundance of triangles is also associated with clustering, that is the tendency for nodes in a graph to cluster together, in the sense that 'closed' triangles correspond to a fully connected motif. Hence, let us consider λ_i as the number of 'closed' triangles a node i belongs over the total number of 'open' triangles $((k_i(k_i - 1))/2)$. The clustering coefficient of individual i is

$$C_i = 2 \frac{\lambda_i}{k_i(k_i - 1)} \quad (9)$$

and the *average clustering coefficient* of a network \mathcal{G} , as introduced by *Duncan J. Watts* and *Steven Strogatz* [83], becomes

$$C_{\mathcal{G}} = \frac{1}{Z} \sum_{i=1}^Z C_i \quad (10)$$

Alternatively, one can also compute the distribution of clustering coefficients $(C(K))$, which corresponds to the average clustering of nodes with degree k

$$C(k) = D(k) \sum_{i=1}^Z \delta(k, k_i) C_i \quad (11)$$

where $\delta(k, k_i)$ is one when $k = k_i$, and zero otherwise.

The shape of $C(k)$ has been connected with the hierarchical structure of networks [84]. In particular, when $C(k) \sim k^{-\beta}$ networks exhibit properties associated with modular hierarchical structure. That is, one can easily identify nodes that are highly interconnected with each other, but have only a few, or none connections with nodes outside of the group to which they belong to. This is at the genesis of the high clustering coefficients that characterize real world structures.

Higher order clustering coefficients, involving an arbitrary number of nodes, have also been proposed [85] although its applicability is always dependent on the problem at hand.

1.2.3 Average Path Length

Networks provide an intuitive and natural metric to measure the distance between the different elements of a system. The distance between the two nodes $d_s(n_i, n_j)$ corresponds to the minimum number of links a walker starting from one node would need to transverse to reach the other end, that is

$$d_s(n_i, n_j) = \min(d(n_i, n_j)) \quad (12)$$

where $d(n_i, n_j)$ represents a list of the distances corresponding to all paths that connect nodes n_i and n_j . The *average (shortest) path length* ($\langle l_{\mathcal{G}} \rangle$) of a network is defined as

$$\langle l_{\mathcal{G}} \rangle = \frac{1}{Z(Z-1)} \sum_{i \neq j} d(n_i, n_j) \quad (13)$$

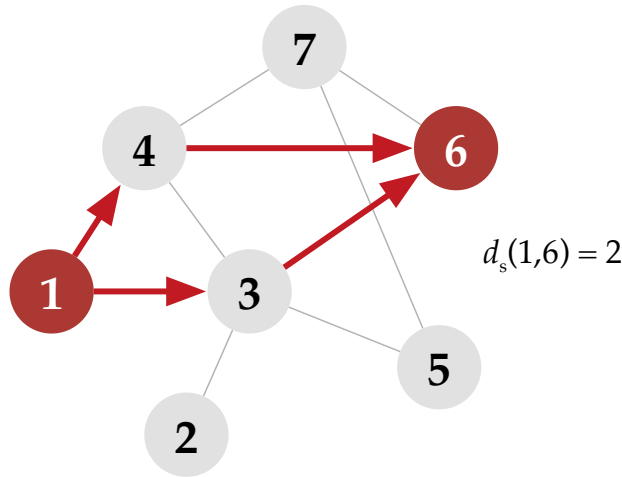


Figure 4: Graphic representation of the distance between a pair of nodes in a unweighted and undirected Graph. Highlighted are all equidistant paths connecting nodes 1 and 6.

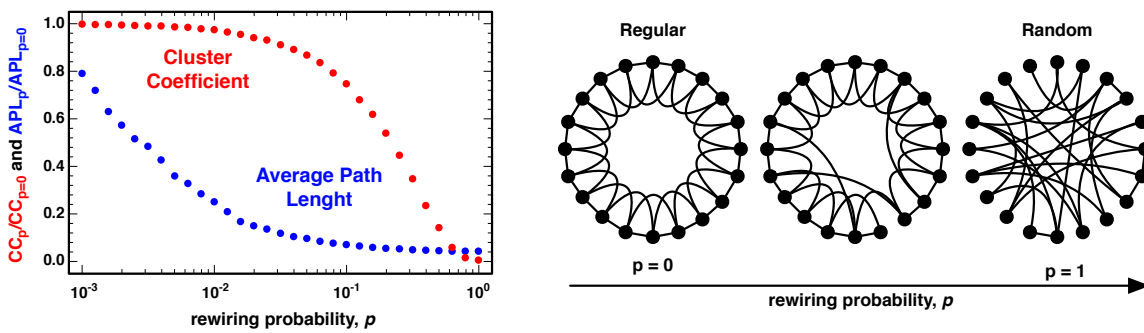


Figure 5: Schematisation of Watts-Strogatz Model used to explore the Small-World phenomena in complex networks. (Left) Relationship between clustering coefficient and Average Path Length as a function of the probability p of rewiring links. (Right) layout of the *Watts-Strogatz* model to generate networks that exhibit the small-world phenomena.

and gives an estimate of the average distance between any two random nodes sampled from the network.

Similarly, the diameter of a network ($diam(\mathcal{G})$) corresponds to the maximum distance between any pair of nodes,

$$diam(\mathcal{G}) = \max(d(n_i, n_j)), \quad \forall i, j \tag{14}$$

Both measures require the network to be composed by a single connected component, that is, there is at least path connecting every pair of nodes in the network.

One can also expand the notion of degree under the concept of network distance. Hence, the degree k_i of a node n_i corresponds to the number of nodes at distance of 1 one link. Likewise we can define k_i^n as the degree of node n_i at distance n , that is, how many nodes are at distance of n links from n_i .

1.2.4 *Models of Networks*

Real world networks exhibit a wide range of properties. Several models have been proposed to explain how these networks can be generated. These help us explain the identified underlying properties and patterns of such networks along with the dynamical processes they stem from. The success with which network science has explained several real world features was one of the major contributors for its growing popularity in past twenty five years.

Random and Regular Structures

To understand and quantify the properties and patterns of empirical networks we require the understanding of the shape and structure of a network that is free of correlations and strong generative assumptions. Such networks can be devised by means of a purely random process. The study of these structures comprised the bulk of graph theory research for much of the XX century [9]. One of the most popular methods to generate random networks was proposed by *Paul Erdős* and *Alfréd Rényi*. The algorithm that become known as *Erdős–Rényi* model [8] considers a set of initially disconnected nodes, after which each pair of nodes is independently connected with probability p . For large networks ($Z \gg 1$) the distribution of degrees is well approximated by a Poisson distribution

$$D(k) \sim \frac{\langle k \rangle^k}{k!} e^{-\langle k \rangle} \quad (15)$$

For this reason, *Erdős–Rényi* networks are also known as Poisson or Random networks and are by definition uncorrelated networks, since links are created regardless of the nodes' degree.

Networks can also be generated following a more constrained set of conditions. Take for instance a network whose nodes are spatially arranged in a symmetric configuration (*e.g.* a grid) and where each node is connected to his closest k neighbors (in an Euclidean metric). The resulting networks exhibit a regular structure and are commonly known as a Lattices with the degree distribution being characterized by a single peak over k , *i.e.* $D(k) = \delta(k)$ where $\delta(k)$ is the Kronecker delta. What Lattices and *Erdős–Rényi* networks offer in mathematical simplicity (*i.e.* high symmetries and regularities in one case and the absence of correlations in the other) they lack in being good representatives of real world networks. Indeed, random networks typically exhibit low clustering coefficient levels and a single scale¹ degree distribution [10]. While the highly constrained topology of Lattices only finds a real world counter part in the molecular structure of crystals [86]. Despite the lack of similarities with real networks, the interpolation between these two types of networks (*Erdős–Rényi* and Lattices) was central to explain a phenomena that is ubiquitous among real-world social networks: the small world effect.

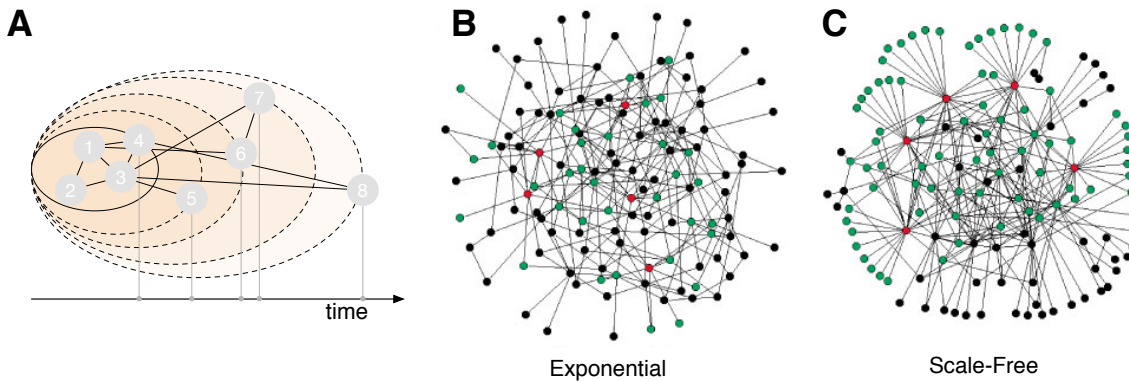


Figure 6: **A** Schematic representation of the Barabási-Albert Model of growth to generate networks. At each time step a new node is added to the network and connects to m pre-existing nodes. The resulting structure is an Exponential structure (**B**) if attachment occurs linearly and Scale-Free network (**C**) when nodes attached preferentially to the most connected nodes of the pre-existing nodes. Panels **B** and **C** were extracted from [87].

Small World

If one work has to be regarded as the starting point of modern Network Science, the prize would be awarded to the 1998 seminal work of *Duncan J. Watts* and *Steven Strogatz* [83]. The authors successfully joined the mathematical framework of graph theory with the real world features that have been associated with large structured populations.

Let us consider the *Watts-Strogatz* model [83], which is used to generate the networks represented in the right panel of Fig. 5. Starting from a regular ring network (nodes are arranged along a circle and connected to their k nearest neighbors) each node rewires his rightmost $k/2$ connections with probability p towards another node of the network. For $p = 0$ the network retains the initial structure (high clustering coefficient and large Average Path Length) while for $p = 1$ the network is qualitatively equivalent to an *Erdős-Rényi* network except that $k_{min} = k/2$, thus holding no similarities with the initial network. However, as *Duncan J. Watts* and *Steven Strogatz* have shown, it is only necessary to rewire a few connections (small $p \approx Z - 1$) of a ring network drastically decrease the *Average Path Length* of the network while retaining the local properties (*i.e.* the clustering coefficient), a phenomena commonly referred as *Small World* [83] and which was formulated in mathematical terms, for the first time, in 1998. Not only did their work explain several properties found in real world networks but it also draw an amazing parallel with the concept of six degrees of separation popularized by *Stanley Milgram* forty years before in the social sciences [88].

In fact, the ideas behind small-world phenomena are older, tracing back to the work of social scientist *de Sola Pool* and mathematician *Manfred Kochen* [89] in the early 1960, which despite having only published their work after *Milgram's* [88] had made available a pre print version of the work since the early 1960.

¹ Implying that the network has a distribution with a well-defined scale, this is the case of the Lattices or any Degree distribution whose degree distribution decays exponentially.

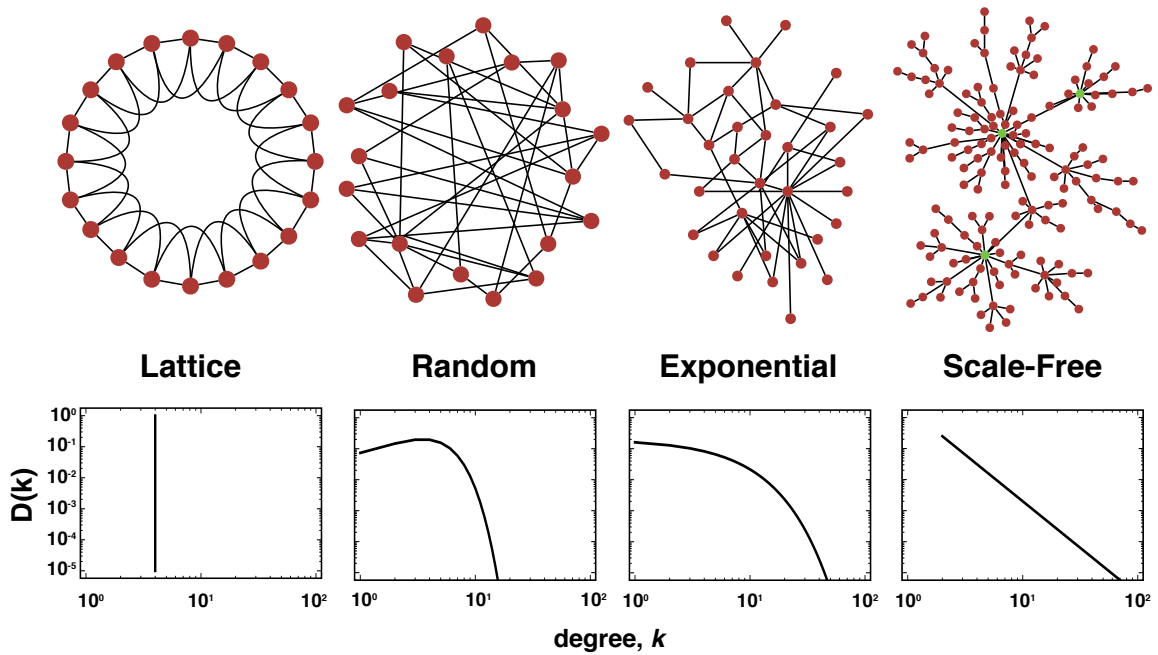


Figure 7: Schematic representation of different network topologies (top) and respective degree distributions (bottom). Degree distributions ($D(k)$) are plotted in a *log-log* plot.

The World is Scale-Free

The most recognisable fingerprint of many empirical networks, however, is their distinctive power-law degree distribution, that is

$$D(k) \sim k^{-\gamma} \quad (16)$$

This profile, intimately related to scale-invariant behavior in non-linear physical systems, led these networks to be coined as scale-free. They are characterized for having a few nodes that accumulate a large number of connections (the hubs) while the majority of the nodes only have a few connections (the leaves), leading to fat-tail degree distributions. As pointed by *Lazlo Barabási* and *Reka Albert* [90], two important ingredients are necessary to generate scale-free networks: a) the network needs to be the result of a growth process where nodes are iteratively added over time and b) new nodes should preferentially connect to pre-existing ones proportional to their degree.

The algorithm proposed by *Barabási* and *Albert* to generate scale-free networks starts from a clique with $m + 1$ nodes (*i.e.* a set fully connected nodes) and adds the remaining $Z - m - 1$ nodes sequentially (growth); each node added connects to other m pre-existing nodes sampled proportional to their degree (preferential attachment, see illustration in Figure 6). In the limit of large network size Z , this algorithm generates scale-free networks with a power of $\gamma = 3.0$ and average degree of $\langle k \rangle = 2m$

Later adaptations of this model allowed for the generation of scale-free networks with larger clustering coefficients [91], hierarchical structure [84] or with a particular power [92] of the degree distribution. When the preferential attachment is replaced by a linear attachment (*i.e.* nodes connect to pre-existing

Chapter 1. INTRODUCTION

ones at random) the resulting network shows a degree distribution whose tail follows an exponential distribution

$$D(k) \sim e^{-\lambda k} \quad (17)$$

and that, as we see, is also common in real world networks.

Figure 7 shows a representation of the four network topologies discussed in this section together with their respective degree distributions. Networks are ordered according to their degree variance (increasing from left to right).

1.3 EVOLUTIONARY GAME THEORY

The central description in Evolutionary Game Theory is the replicator equation [93, 94, 46, 95]. It corresponds to a set of $S - 1$ non-linear differential equations describing how the frequencies of S different types of individuals evolve in a population. It has the form

$$\dot{x}_i = x_i(f_i - \sum_{j=1}^S x_j f_j) \quad (18)$$

where x_i is the fraction of individuals of type i with fitness f_i , and where $\sum_{j=1}^S x_j f_j$ is the average fitness of the population. Here a type is also associated with a strategy. Fitness accounts for the ability of individuals to replicate themselves. The replicator equation describes the frequency dependent evolution of an infinite population, in this context fitter individuals replicate more often.

In an evolutionary sense, the replicator equation only accounts for the effects of selection due to competition. A more general approach would include the role of mutations [96], which can be added with the introduction of an additional term to Equation 18

$$\dot{x}_i = x_i(f_i - \sum_{j=1}^S x_j f_j) + \mu(1 - Sx_i) \quad (19)$$

where μ corresponds to the relative intensity of mutations and S to the number of strategies.

A key insight of Evolutionary Game Theory is that behaviors involve the interaction of multiple organisms in a population, the success of any organism depends on how its behaviors interacts with that of others. So, the fitness of an individual organism cannot be measured in isolation; rather it has to be evaluated in the context of the whole population in which it lives. This opens the door to a natural game-theoretic analogy: an organism's genetically-determined characteristics and behaviors are like strategies in a game, its fitness is like its payoff, and this payoff depends on the strategies of the organisms with which it interacts.

One of the central assumption in Evolutionary Game Theory is that the evolution of a population depends on the outcome of the interactions that occur between individuals that make it up. So the fitness of an individual is not an isolated quantity predefined by an individual full set of traits, but rather a context-dependent quantity. In the sense of Evolutionary Game Theory, interactions between individuals can be modeled in light of Game Theory, in the sense that an individual genetically-determined

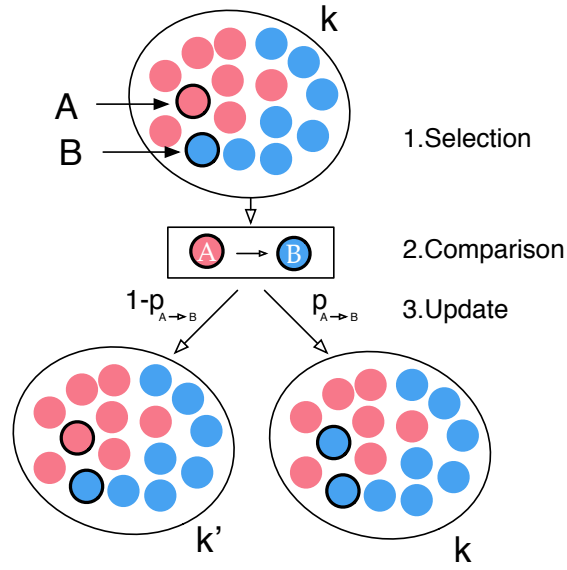


Figure 8: Depiction of the Pairwise Comparison Rule to model Birth-Death processes in finite populations. In the first step two individuals are randomly selected from the population. Secondly one of these individuals compares his fitness with the other. Finally, at a third step with a probability defined by the Fermi Distribution the first individual imitates the strategy of the second. Disks represent individuals in a population, with different colors representing different types.

characteristics and behaviors are like strategies in a game, its fitness is a function of the payoff, which depends on the the strategies adopted/played by the other individuals with whom he interacts [97]. In simple terms, the fitness is a frequency dependent quantity

$$f_i = f_i(\mathbf{x}) = f_i(x_1, x_2, \dots, x_{S-1}) \quad (20)$$

that is, it is a function of the composition of strategies in the population. Another important, but implicit, assumption in Evolutionary Game Theory is that individuals are effectively rationality-bounded, in the sense that individuals are not aware of the payoff structure of the game nor do any consideration on the rationality of their peers. Individuals behave unconditionally according to their strategy, as if it was a phenotype in a biological sense. Hence, in a biological sense, evolution is driven by selection, reproduction and replacement of strategies. In a social scope evolution happens by social learning (*e.g.* imitation), or the desire of individuals to adopt the most fitted behaviors, regardless of the strategy that they stem from.

When mutations are absent ($\mu = 0$) and the population is only composed by individuals of two strategies (*e.g.* A and B), Equation 18 simplifies to

$$\dot{x} = x(1 - x)(f_A(x) - f_B(x)) \quad (21)$$

Chapter 1. INTRODUCTION

where x is the fraction of A individuals. This is the most popularized form of the replicator equation, and also corresponds to the most studied regime (no mutations and two-strategies). This expression holds two trivial solutions $x = 0$ and $x = 1$, while additional fixed points in $]0, 1[$ exist for all values of x that are solution of $f_a(x) = f_b(x)$. In this context we are left with the definition and computation of the fitness function for each strategy.

It has been shown that the replicator equation is equivalent to other models in Population Dynamics [98]. For instance, it can be derived from the *Lotka-Volterra* system of equations, which is the classical description for the evolution of species abundances under a predator-prey dynamics [99, 93]. The derivation requires a rescaling of time and does not result in a *one-to-one* equivalence, in the sense that S strategies in the Evolutionary Game Theory description map into $N - 1$ species in the *Lotka-Volterra*.

Furthermore, it has also been shown [100, 101, 102, 103] the replicator equation can be derived from the exponential growth model

$$\dot{y}_i = y_i(t)g_i \quad (22)$$

where y_i is the abundance of strategy i and $g_i = f_i(y_1, y_2, \dots, y_S)$ its fitness. The equivalence is done by means of a change of variables

$$x_i = \frac{y_i}{\sum_i^S y_i} \quad (23)$$

where it is also fundamental to ensure that fitness is a function of the frequencies of each strategy only and not of the population size.

1.3.1 Finite Populations

The replicator equation provides a mean-field deterministic description of a population evolutionary dynamics. This implies studying a population in the limit of an infinite and well-mixed population driven by a continuous time dynamical process. Such utopian assumptions might hold in the limit of a very large population, but this is rarely the case of Natural systems where stochastic effects matter.

Let us consider a population of Z individuals of which n_A play strategy $S_1 = A$ and n_B strategy $S_2 = B$. The population size remains constant ($\dot{Z} = 0$) throughout evolution and corresponds to $Z = n_A + n_B$. Besides a strategy, each individual is also characterised by a fitness (f_i) that translates his ability to replicate himself.

For $S = 2$ the population can only be in one of $Z + 1$ available states. Each state corresponds to one of the available strategy configurations, *i.e.* combinations of n_A and n_B . Each state k is enumerated according to the number of A individuals in the population ($n_A = k$), since $n_B = Z - n_A$ this suffices to have a *one-to-one* mapping between strategy configurations and system states.

Evolution can be modelled by means of the so-called *fermi update* or *pairwise comparison* rule [104, 105], which considers that at each time step (Δt) a randomly sampled individual (i) compares

1.3. Evolutionary Game Theory

his fitness with another randomly sampled individual (j). The former (i) adopts the strategy of the latter (j) with probability given by the Fermi distribution from statistical physics, that is

$$p_{i \rightarrow j} = \frac{1}{1 + e^{-\beta(f_j - f_i)}} \quad (24)$$

where β plays the role of the inverse of the temperature regulating the stochasticity of the decision making of i . When $\beta = 0$ individuals decide at random regardless of the fitness difference while for $\beta \gg 1$ individuals take a deterministic stance revising their strategies as long as $|f_j - f_i| > 0$.

The evolutionary dynamics of such population corresponds to a Stochastic Markov, Birth-Death process whose dynamics becomes fully described upon the computation of all transition probabilities between available configurations. The state space in this scenario corresponds to a chain, with transitions occurring only between adjacent states (see Figure 9). Transitions that correspond to jumps from state k to $k + 1$ ($T^+(k)$) are associated with a B individual adopting strategy A ($T(k)^{B \rightarrow A}$), conversely jumps from k to $k - 1$ ($T^-(k)$) correspond to transitions where an individual A changes to strategy B ($T(k)^{A \rightarrow B}$), see Equation 25.

$$\begin{aligned} T(k)^{A \rightarrow B} \equiv T^+(k) &= \frac{k}{Z} \frac{Z - k}{Z - 1} p_{A \rightarrow B} \\ T(k)^{B \rightarrow A} \equiv T^-(k) &= \frac{Z - k}{Z} \frac{k}{Z - 1} p_{B \rightarrow A} \end{aligned} \quad (25)$$

The transition probabilities allow us to write down the master equation associated with this stochastic process [106, 107]

$$\begin{aligned} p(k, \tau + 1) - p(k, \tau) &= p(k - 1, \tau) T^+(k - 1) + \\ & p(k + 1, \tau) T^-(k + 1) - \\ & p(k, \tau) T^+(k) - p(k, \tau) T^-(k) \end{aligned} \quad (26)$$

where $p(k, \tau)$ is the probability that the system occupies configuration k at time τ . Solving Equation 26 for $p(k, \tau + 1) - p(k, \tau) = 0$ and $\tau \rightarrow \infty$ we are left with an eigenvector problem, the solution of which, after the appropriate normalisation, indicates the likelihood of finding the population in each state at the equilibrium or, in other words, the fraction of time the population occupies each state. In this particular example the solution is achieved upon solving the recurrence relationship

$$p(k)(T^+(k) + T^-(k)) = p(k - 1)T^+(k - 1) + p(k + 1)T^-(k + 1) \quad (27)$$

in order to $p(k)$, which leads [46] to

$$p(k) = \frac{\prod_{i=0}^{k-1} \frac{T^+(i)}{T^-(i+1)}}{\sum_{l=0}^Z \prod_{i=0}^{l-1} \frac{T^+(i)}{T^-(i+1)}} \quad (28)$$

a result that we can obtain from a recurrence relationship in relation to $p(k)$.

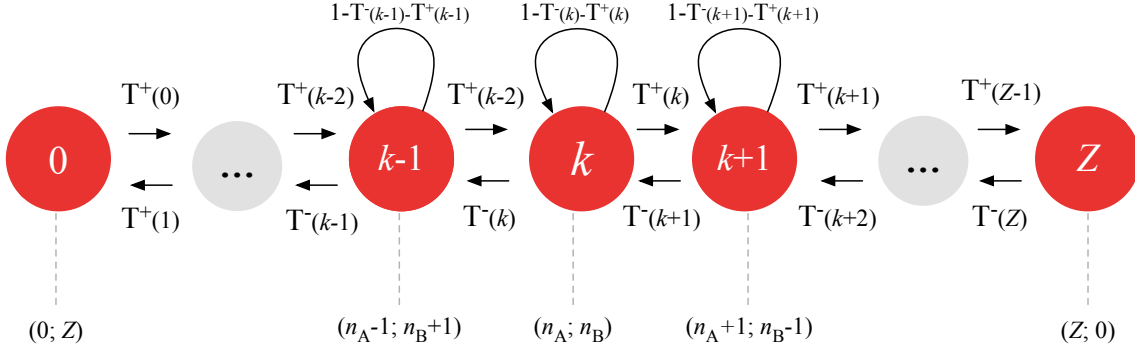


Figure 9: Schematic representation the state space of a finite population of Z individuals and two strategies $S_1 = A$ and $S_2 = B$. Each state corresponds to a strategy configuration, that is a combination n_A (number of A individuals) and n_B (number of B individuals). Each state is enumerated according to the number of A individuals in the population (n_A) since $Z = n_A + n_B$. Transitions associated with jumps between states are denoted by $T(k)^{X \rightarrow Y}$, where $X \rightarrow Y$ indicates that an individual with strategy X adopted strategy Y .

However, if we perform a system size expansion [108, 106] of Equation 26 through a change of variables $k = x/Z$ and $t = \tau/Z$, while considering $\rho(x, t) = Zp(k, \tau)$, we obtain

$$\begin{aligned} \rho(x, t + Z^{-1}) - \rho(x, t) = & \rho(x - Z^{-1}, t)T^+(x - Z^{-1}) + \\ & \rho(x + Z^{-1}, t)T^-(x + Z^{-1}) - \\ & \rho(x, t)T^+(x) - \rho(x, t)T^-(x) \end{aligned} \quad (29)$$

and Taylor expanding both sides in order to x and t , rearranging terms in powers of Z^{-1} , while neglecting terms of order above Z^{-2} , yields

$$\frac{d}{dt}\rho(x, t) = -\frac{d}{dx}\rho(x, t)(T^+(x) - T^-(x)) - \frac{1}{2Z}\frac{d^2}{dx^2}(T^+(x) + T^-(x)) + \mathcal{O}(Z^{-2}), \quad (30)$$

which holds the form of a Fokker-Planck equation for large but finite population size $Z \gg 1$. In this expression the term $T^+(x) - T^-(x)$ corresponds to the drift and $T^+(x) + T^-(x)/Z$ to the diffusion. Moreover, being the noise uncorrelated, this expression is equivalent to the Langevin description

$$\dot{x} = (T^+(x) - T^-(x)) + \sqrt{\frac{T^+(x) + T^-(x)}{Z}}\eta \quad (31)$$

where η corresponds to white noise. The drift term is of particular interest as it represents the so-called gradient of selection ($g(x)$) [104, 109, 110], which for the Fermi update rule takes the form²

$$g(x) = T^+(x) - T^-(x) = \frac{k}{Z}\frac{Z-k}{Z-1}\tanh\left(\frac{\beta}{2}(f_A - f_B)\right) \quad (32)$$

² We make use of the definition $\tanh(x) = (e^x - e^{-x})/(e^x + e^{-x})$ and of equation 24

1.3. Evolutionary Game Theory

where f_A and f_B are respectively the average fitness of strategy A and B . This quantity provides the most likely direction of evolution at state x , in the sense that a positive (negative) $g(x)$ indicates that the number of A tends to increase (decrease).

In the limit $Z \rightarrow \infty$ and $\beta \rightarrow 0$, the term $g(x)$ is the only one that does not vanish from Equation 31, thus holding the same form of the replicator equation. Moreover if we also consider the limit of $\beta \rightarrow 0$, a Taylor expansion $\tanh(\frac{\beta}{2}(f_A - f_B)) \propto (f_A - f_B)$ leads to an expression that holds the same form of the replicator equation. The replicator description is thus a deterministic limit of the Birth-Death stochastic processes.

In order to simplify the discussion in the following sections, let us introduce a more general and less ambiguous notation for the gradient of selection as

$$g_{s_A, s_B}(n_A, n_B) = \frac{n_A}{Z} \frac{n_B}{Z-1} \tanh\left(\frac{\beta}{2}(f_{s_A} - f_{s_B})\right) \quad (33)$$

which refers to the gradient of selection between pair of strategies s_A and s_B in a configuration with n_A many s_A individuals and n_B many s_B individuals.

In this thesis, we shall focus on the Fermi update rule, as the stochastic process of update to model evolution. This is so because it offers a broader applicability, in the sense that it can be conceptually used to model evolution in a biological or social context. In the first, evolution would imply the birth and death (replication) of individuals of a species, while in the social scope it can be understood as an imitation dynamics or any other mechanism of social learning. Nevertheless, there are other stochastic processes of which it is noteworthy to mention the Moran Process for its wide application in the biological context [111]. Both stochastic processes, Fermi and Moran, have been shown to correspond to a limit of the replicator equation.

Fixation Probability

One question of particular interest, when dealing with finite populations, concerns the probability of a population reaching a state dominated by a single species [46]. Let us define by ϕ_k as the probability of a population reaching state Z when starting from state k . In the the absence of mutations, and in a scenario with only two species there are only two absorbing states: 0 and Z , which imply

$$\begin{aligned} \phi_0 &= 0 \\ \phi_Z &= 1 \end{aligned} \quad (34)$$

since from $k = 0$ the system will never reach Z . For the remaining starting configurations we have

$$\phi_k = \phi_{k-1}T^-(k) + \phi_k(1 - T^+(k) - T^-(k)) + \phi_{k+1}T^+(k) \quad (35)$$

where $T^+(k)$ is the probability to jump from state $k - 1$ to k and $T^-(k)$ the probability to jump from state $k + 1$ to k . Equation 35 expresses the probability of reaching Z from k and corresponds to the sum of three terms: the probability of jumping to state $k - 1$ and reach Z from there; the probability of staying in k and reach Z ; probability of jumping to state $k + 1$ and reaching Z from there. This

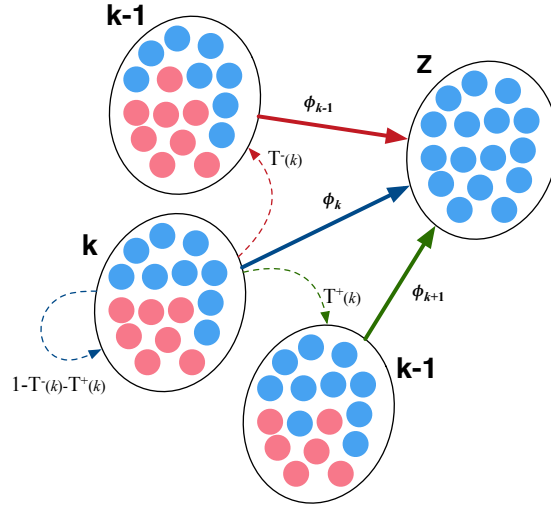


Figure 10: Schematic representation of the terms involved in the computation of the fixation probability (ϕ_k) when starting from state k . Each event is depicted by an arrow, the fixation probabilities are the sum of the three terms, each term is the multiplication of all arrows with the same colour. Dashed lines identify transition probabilities between states, while full lines indicates fixation probabilities. Disks represent individuals in a population, with different colors representing different types.

is also graphically represented in Figure 10. From this recursive relationship involving ϕ_k , and after some algebra, we arrive at a closed form expression for the fixation probability [46]

$$\phi_k = \frac{1 + \sum_{j=1}^{k-1} \prod_{i=1}^j \gamma(i)}{1 + \sum_{j=1}^{Z-1} \prod_{i=1}^j \gamma(i)} \quad (36)$$

where $\gamma(i) = T^-(i)/T^+(i)$. Finally, the probability of fixation of a single mutant in a resident population (*i.e.* $k = 1$) simplifies to [46]

$$\phi_1 = \frac{1}{1 + \sum_{j=1}^{Z-1} \prod_{i=1}^j \gamma(i)} \quad (37)$$

and for the particular case of the fermi update rule the fixation probability becomes [112]

$$\phi_1^{fermi} = \frac{1}{1 + \sum_{j=1}^{Z-1} \prod_{i=1}^j e^{\beta(f_{s_A}(i) - f_{s_B}(i))}} \quad (38)$$

Small Mutation Limit

When mutations are taken into consideration but at a sufficiently small rates, such that the fixation time of any mutant in a population is much smaller than the waiting time between any two mutations, the population is said to be evolving under the *small mutation limit* [113] and therefore at any moment in time it hosts a maximum of two different strategies (s_i and s_j).

1.3. Evolutionary Game Theory

Under these assumptions a system with S strategies can be conveniently described by means of a *reduced Markov chain*, where each state is associated with a strategy s_i and where transitions between states ($T_{s_i s_j}$) are defined by the renormalised fixation probability

$$T_{s_i s_j} = \frac{\phi_{s_i s_j}}{S-1}, (i \neq j) \quad (39)$$

where $\phi_{s_i s_j}$ is the fixation probability of single s_i mutant in a population composed by $Z - 1$ s_j individuals.

Upon computing all $T_{s_i s_j}$ (*i.e.* $\phi_{s_i s_j}$) we can build a Transition Matrix (*i.e.* a stochastic matrix) whose eigenvector (τ) associated with the largest eigenvalue, returns the stationary distribution of the population [108]. Each entry of τ conveniently describes the average time the population spends in each of the S possible monomorphic configurations that correspond to states in which all individuals of the population adopt the same strategy. The small mutation limit provides an approach to inspect the evolutionary dynamics of systems with a large number of strategies ($S > 4$) and in which other conventional approaches become too complicated [114, 115, 116].

Neutral Drift

In the limit in which evolution does not select any of the strategies preferentially, evolution proceeds randomly without a dominant selection direction. A population evolving under such conditions is said to be evolving under neutral drift.

This limiting scenario can be recovered in the fermi update rule (see Equation 24) when one considers $\beta = 0$, which results in

$$p_{i \rightarrow j} = \frac{1}{2} \quad (40)$$

consequently, gradient of selection is $g(x) = 0$ over the entire domain of $x \in [0, 1]$ and the fixation probability becomes $\phi_k = k/Z$.

The study of evolution close to neutral drift has been important in Biology [117]. Moreover, pure neutral drift provides us with the necessary point of reference to classify and quantify the strength of different mechanisms in the evolutionary dynamics of populations.

1.3.2 *Two Person Games*

Let us consider two individuals, A and B , engaging in a single shot interaction. Each is required to independently and simultaneously choose/play a strategy from a predefined pool with S many strategies, *i.e.* $\{s_1, s_2, \dots, s_S\}$. Both individuals have full knowledge of the game but don't have memory of past interactions with the opponent. Out of interaction results a payoff to each individual that depends only on the combination of strategies adopted, that is, A obtains payoff $\pi_{\sigma_A \sigma_B}^A$ and B collects $\pi_{\sigma_A \sigma_B}^B$ where σ_A and σ_B are the strategies played respectively by A and B .

All possible outcomes can be represented by means of a $S \times S$ payoff matrix, see Figure 11, which in Game Theory is known as the normal form representation of a game.

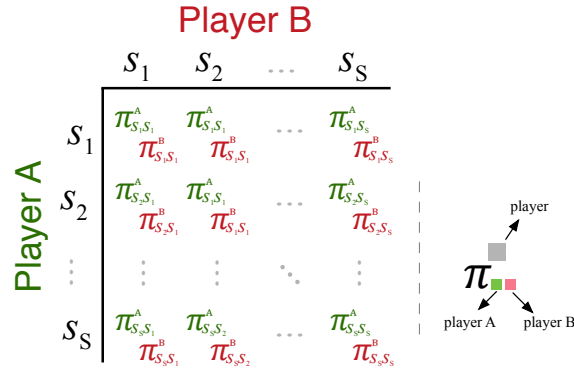


Figure 11: The Payoff Matrix is the normal form representation of two-person and S -strategy games. Each entry represents the payoffs of each player for a given combination of strategies.

When $\pi_{\sigma_A \sigma_B}^A + \pi_{\sigma_A \sigma_B}^B = 0$, for all $\sigma_A, \sigma_B \in \{s_1, s_2, \dots, s_S\}$, the game is said to be zero-sum, since the gains of a player represent the loss of the other. Moreover a game is said to be symmetric when payoffs are player independent. That is, the payoff of player A when playing strategy $\sigma_A = X$ and facing player B with strategy $\sigma_B = Y$ is the same as the payoff attained by B when playing strategy $\sigma_B = X$ against a player A playing strategy $\sigma_A = Y$. The payoff structure of Symmetric games can be simplified to

	s_1	s_2	\dots	s_S
s_1	$\pi_{s_1 s_1}$	$\pi_{s_1 s_2}$	\dots	$\pi_{s_1 s_S}$
s_2	$\pi_{s_2 s_1}$	$\pi_{s_2 s_2}$	\dots	$\pi_{s_2 s_S}$
\vdots	\vdots	\vdots	\ddots	\vdots
s_S	$\pi_{s_S s_1}$	$\pi_{s_S s_2}$	\dots	$\pi_{s_S s_S}$

where each entry ($\pi_{\sigma_A \sigma_B}$) indicates the payoff obtained by a player playing the Row strategy while facing an opponent adopting the Column strategy. All asymmetric games can be transformed into symmetric games by assuming that the game is played sequentially and the order of decision of the players is random [95]. This creates a new game in which the payoffs are linear combinations of the original game.

Evolutionary Stable Strategies

The concept of Evolutionary Stable Strategy was first introduced in 1973 by *John Maynard Smith* [118]. It tries to assess the evolutionary viability of a strategy by analysing the payoff structure of the game. A strategy s_i is said to be Evolutionary Stable (*ESS*) if a population composed only by s_i individuals is resilient to the invasion from a mutant of any other strategy.

In a context with S different strategies ($\{s_1, s_2, \dots, s_S\}$), a strategy s_i is *ESS* if for all $s_i \neq s_j$ we have that

$$\pi_{s_i s_i} > \pi_{s_i s_j} \tag{41}$$

or

$$\begin{aligned}\pi_{s_i s_i} &= \pi_{s_i s_j} \\ \pi_{s_i s_j} &> \pi_{s_j s_j}\end{aligned}\tag{42}$$

which means that to be an *ESS*, selection needs to opposes mutant strategies, since the payoff attained by an individual with strategy s_i against another individual play s_i is greater than the payoff of playing against the mutant individual s_j . A weaker definition of *ESS* assumes that $\pi_{s_i s_j} \geq \pi_{s_j s_j}$ instead of $\pi_{s_i s_j} > \pi_{s_j s_j}$.

Evolutionary Stable Strategies in Finite Populations

The original definition of *ESS* is based on a pure analysis of the payoff matrix. It provides intuition to the deterministic invasion dynamics of a population, it fails however to take into consideration stochastic effects in finite populations, since in that situation the probability of a mutant to invade a resident population as non-zero. An alternative definition, can be formalised by means of the likelihood with which a mutant can invade a resident population (*i.e.* fixation probability).

Let us consider a population of size Z , and a strategy space with S strategies. Then according to *Nowak et al* [113] a strategy s_i is ESS_Z if for all strategies $s_j \neq s_i$

$$\phi_{s_j s_i} < \frac{1}{Z}\tag{43}$$

and

$$g_{s_i s_j}(Z - 1, 1) > 0\tag{44}$$

where $g_{s_i s_j}(Z - 1, 1)$ denotes the gradient of selection of a single mutant s_j in a populations of s_i , which for being positive means that selection favours s_i . Strategies that only hold the condition expressed in equation 43 are said to be Evolutionary Robust (*ERS*)[119, 120, 121].

The concepts of *ESS*, ESS_Z and *ERS* fail to capture other types of stability that do not correspond to monomorphic configurations of strategies. It is essentially a biological concept which clashes with the definition of stability in dynamical systems, where stability can also correspond to limit cycles or strange attractors [108].

1.3.3 *Social Dilemmas of Cooperation*

Let us a consider a situation in which an individual A has the chance to incur in a cost (c) to offer a benefit (b) to an individual B . We say that in this situation A plays the role of the donor and B that of the recipient. The act of paying the cost is associated with Cooperative or Altruistic behaviour while refusing to do so corresponds to a Defective or selfish action [122]. When both individuals have the opportunity to act/play simultaneously and independently, the possible outcomes can be summarised by the payoff matrix

whenever $b > c$ the best action for any rational individual looking to optimise his own gains is to not contribute, thus avoiding being cheated while trying to exploit any incautious Cooperator. Ironically,

	C	D
D	$b - c$	$-c$
C	b	0

the expected outcome from two rational individuals, mutual defection, leads to an aggregated payoff that is smaller when compared with the result from mutual cooperation ($0 < 2(b - c)$). This game corresponds to the so-called Prisoner’s Dilemma [123, 95] and is often considered as the best metaphor for Cooperative social dilemmas, since it highlights the conflict between self and collective interests.

We can further generalise the payoff matrix for two-person, two-strategy games by rewriting the above matrix into a more general form

	C	D
D	R	S
C	T	P

where mutual cooperation is associated with the *Reward* (**R**) payoff while mutual defection generates a *Punishment* (**P**) payoff for both players. When a Defector successfully exploits a Cooperator, the former obtains the *Temptation* (**T**) payoff while the latter obtains the *Sucker’s* payoff (**S**). Besides the Prisoner’s Dilemma ($T > R > P > S$) we can derive three new situations depending on the relative order of the payoffs, namely the Stag Hunt when $R > T > P > S$ [124], the Snowdrift Game when $T > R > S > P$ [125, 126] and the Harmony Game for $R > T > S > P$.

It is common practice to simplify the analysis by normalising the difference $R - P = 1$ with $R = 1$ and $P = 0$ and thus reducing our analysis to the domain bounded by $0 \leq T \leq 2$ and $-1 \leq S \leq 1$ [127].

Each game presents different metaphors of real-life social dilemmas, thus putting into evidence the nature of social dilemmas since the solution attained by the players’ rational course of action leads to an aggregated outcome that is not the best collective outcome.

Evolving Cooperation

Let us consider a population of individuals whose interactions fall in one of the scenarios described above. Individuals play one of the available strategies, unconditionally, as if the strategy was a behaviour or a phenotype. Every now and then, individuals revise their strategies by means of some type of social learning and in such a way that more successful individuals replicate more often, assuming that the social success is measured by the expected payoff over many interactions, and is analogous to biological fitness. Then, the evolution of a well-mixed population can then be described by the replicator dynamics, and thus we are left with the estimation of the fitnesses.

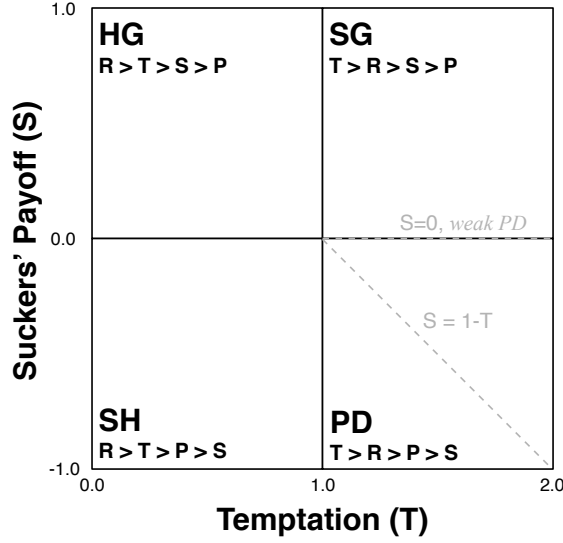


Figure 12: Parameter space of the *two-person* and *two-strategy* game. The horizontal axis represented the Temptation (T) payoff, while in the vertical axis is the Sucker's Payoff (P) [127]. Each color represents a different game, in particular the Prisoner's Dilemma (Right Bottom); the Stag Hunt game (Left Bottom); the Snowdrift Game (Right Top) and the Harmony Game (Left Top). Grey dashed lines highlight parameterisations of the Prisoner's Dilemma commonly found in Literature.

In a well-mixed population of size Z , composed by k cooperators (C) and $Z - k$ defectors (D). The average fitness of each strategy is

$$\begin{aligned} f_C &= \frac{k-1}{Z}R + \frac{Z-k}{Z}S \\ f_D &= \frac{k}{Z}T + \frac{Z-k-1}{Z}P \end{aligned} \quad (45)$$

where we take into account that individuals do not play with themselves.

In the limit of $Z \rightarrow \infty$ we define $k/Z \equiv x$ and the evolutionary dynamics can be well approximated by the replicator equation (see Equation 21), which, solving for $\dot{x} = 0$, renders, in addition to the two trivial solutions $x^* = 0$ and $x^* = 1$, an additional internal fixed located at

$$x^* = \frac{S - P}{R + P - T - S} = \frac{S}{1 - T - S} \quad (46)$$

when $f_C - f_D = 0$.

Because only solutions that lie in the interval $[0, 1]$ are valid, additional fixed points only exist in the domains defined by $S > 0 \wedge T > 1$ (*Snowdrift Game*) or $S < 0 \wedge T < 1$ (*Stag Hunt*). The stability of the fixed points is readily computed by inspecting the signal of \dot{x} in the vicinity of x^* .

Hence the Stag Hunt is characterised by an unstable fixed point that renders the evolution a Coordination like dynamics, since the population will converge to either $x = 1$ or $x = 0$ depending on whether the initial fraction of cooperators x_i is, respectively, above ($x_i > x^*$) or below ($x_i < x^*$) the internal fixed point x^* . In contrast, the Snowdrift is characterised by a stable fixed point that dictates

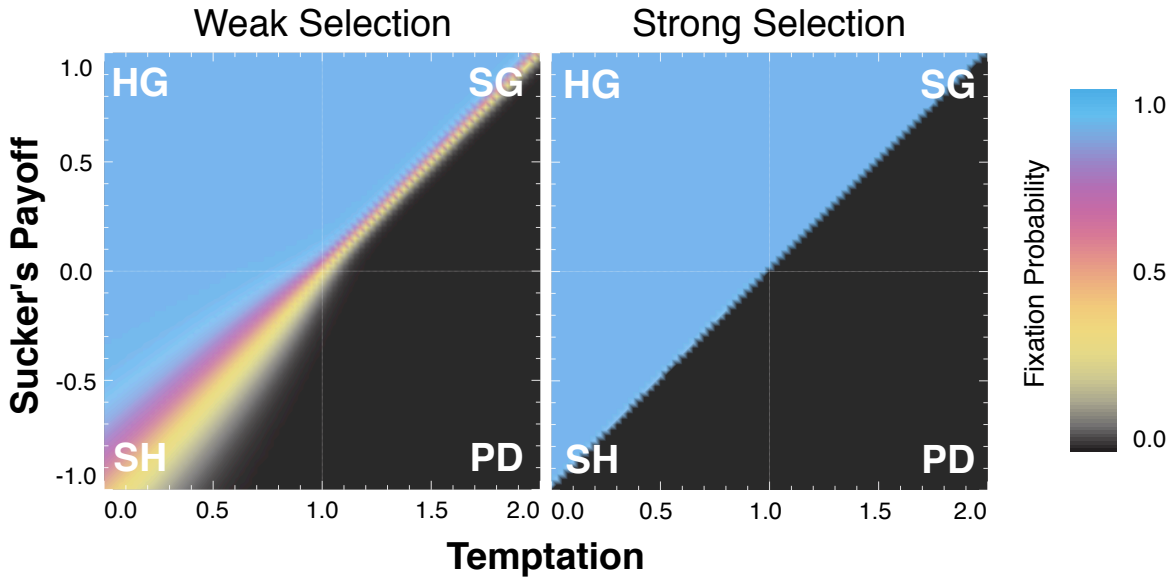


Figure 13: Probability of Fixation, ϕ_k , on well-mixed populations with $Z = 100$ individuals under weak selection left ($\beta = 0.01$) and strong selection right ($\beta = 10.0$) regimes starting with 50 cooperators ($\phi_{k=50}$) for the entire parameter space bounded by $R = 1$, $P = 0$, $0 \leq T \leq 2$ and $-1 \leq S \leq 1$. Regions are identified according to the associated social dilemma, namely Harmony Game (**HG**), Snowdrift Game (**SG**), Stag Hunt (**SH**) and Prisoner's Dilemma (**PD**)

a stable coexistence of strategies, with the population converging for a state with x^* cooperators and $1 - x^*$. Because of these two distinct characters the Stag Hunt is often associated with Coordination Game and the Snowdrift to a Co-existence game.

In the absence of internal fixed points, the dynamics is characterised by the Dominance of one of the strategies, that is, the population evolves deterministically to a configuration dominated by a single strategy regardless of its initial composition. In particular, Cooperators dominate in the Harmony Game ($T < 1 \wedge S > 0$), as indicated by the positive \dot{x} in the entire domain, conversely the fully negative \dot{x} hints at the Defector dominance that characterises the Prisoner's Dilemma ($T > 1 \wedge S < 0$).

Figure 14 shows how these dynamics influence the evolutionary outcome of a finite population with $Z = 10^3$ individuals evolving from an initial configuration with equal composition of strategies. The outcome for each pair of parameters (T, S) was estimated through Monte-Carlo simulations and corresponds to the average over the final fraction of cooperation after 10^6 time steps. A similar result can be obtained through the estimated value of k from the stationary distribution associated with each pair (T, S) .

1.3.4 Evolving Cooperation

Evolutionary Game Theory provides a powerful mathematical framework to study the evolutionary dynamics of populations. However, as shown in the previous sections, whenever individuals engage in

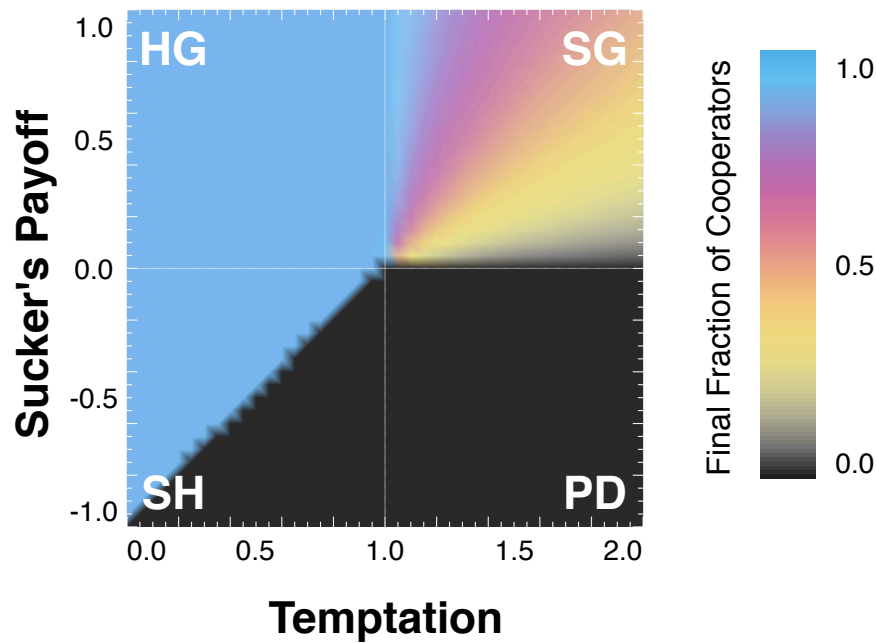


Figure 14: Level of cooperation on well-mixed population with $Z = 10^3$ individuals for the entire parameter space. Evolution proceeds under a strong selection ($\beta = 10.0$) starting from a configuration with equal composition of strategies. Regions are identified according to the associated social dilemma, namely Harmony Game (**HG**), Snowdrift Game (**SG**), Stag Hunt (**SH**) and Prisoner's Dilemma (**PD**)

the Prisoner's Dilemma it leads to the same paradoxical outcome that the theory of Natural Selection seemingly suggests: The demise of altruistic individuals in favour of those acting selfishly.

The failure to understand how evolution might select Cooperative behaviour in the Prisoner's Dilemma has been regarded as one of the major scientific questions of our times [128]. For the past sixty years, several solutions have been proposed. To date, five canonical mechanisms are accepted to facilitate the evolution of cooperation. Even though other mechanisms have been proposed, these five constitute the main line of research.

Direct Reciprocity

Direct reciprocity was originally proposed in 1971 by *Robert Trivers* [129] as a mechanism to explain the evolution of Cooperation. It is based on the idea that repeated interactions between individuals facilitate the coordination towards an outcome that is best for both, which in the context of Cooperation Social Dilemmas, is mutual cooperation.

The central situation studied in direct reciprocity considers a pair of individuals, *A* and *B*, playing iterated rounds of the Prisoner's Dilemma. At each round, individuals need to decide simultaneously whether to Cooperate (donate) or Defect (do not donate). Contrarily to the one-shot scenario, considered so far, in repeated games individuals have memory of the previous interactions, thus strategies

Chapter 1. INTRODUCTION

are necessarily conditional on the opponent previous actions. A new round is played with probability w . A central result is that cooperation becomes favourable if

$$w > \frac{c}{b} \quad (47)$$

which means that the probability of a new round should be greater than the cost-benefit ratio of an altruistic action.

Direct Reciprocity became widely popular with a series of computer tournaments organised by *Robert Axelrod* [73] in the late 70s, which pitted different strategies – submitted by independent researchers – in an evolutionary contest. Surprisingly, the winner in both occasions was a simple strategy of Tit-for-Tat (TFT) that consists on Cooperating in the initial round and then do exactly the same as the opponent did in the previous round. Tit-for-Tat was able to outperform other strategies while, at the same time, attaining high levels of Cooperation, which supported the argument that Direct Reciprocity could effectively support the evolutionary emergence of cooperative strategic profiles.

However, Tit-for-That suffers from several drawbacks, the major being its lack of resilient to behavioural errors [130, 131]. In its place, it was suggested a strategy of Win-Stay Lose-Shift [132, 133, 134] (WSLS), which in the Prisoner's Dilemma implies that individuals should Cooperate after a round of mutual behaviour and defect otherwise. This strategy also exhibits a strong Cooperative character while performing better in noisy environments.

Repeated games can be extended to Public Goods Game [135]. In that scope, recent works have shown that a strategy of Contributing to the Public Good only after a round of group unanimity outperforms all other strategies in an evolutionary sense [70]. This strategy of All-or-None is resilient to mild behavioural errors rates and follows a similar philosophy to the Win-Stay-Lose-Shift. This work is discussed in Chapter 7

Another variant of the Repeated Prisoner's Dilemma considers probabilistic strategies. For instance, assuming that players only have 1-step memory, strategies correspond to a vector with four components: $\{p_{cc}, p_{cd}, p_{dc}, p_{dd}\}$. Each entry p_{XY} represents the probability of Cooperating after a round where the focal player adopted strategy X and the opponent strategy Y . Making use of this notation Tit-for-Tat corresponds to $\{1, 0, 1, 0\}$ and Win-Stay Lose-Shit to $\{1, 0, 0, 1\}$. In this context, behavioural errors can be accounted by a adding/subtracting a real-valued error probability $\epsilon \in]0, .5]$ to each component p_{XY} .

A recent work by *Press* and *Dyson* [136] has shown that if individuals are able to adjust the probabilities from round to round, then exists a class of strategies – so called Zero-Determinant – that are able to manipulate the game in such a way that long term payoffs of players can be controlled, despite the opponent intentions. Initial research focused in a subclass of Zero-Determinant strategies that guarantees, to the player adopting it, a better payoff than the opponent, or in the worst case scenario, the payoff for mutual defection. Such extortionist strategy showed to be quite successful, but its aggressiveness and unfriendly stance contrasts with the nice character Tit-for-Tat and Win-Stay-Lose-Shift. This finding largely revived the study in directed reciprocity [137, 138, 121, 139, 140]. One noteworthy result shows that despite its success in the Game Theoretical sense, the Zero-Determinant Extortion strategies have a perform poorly in an evolutionary context [120, 141, 142].

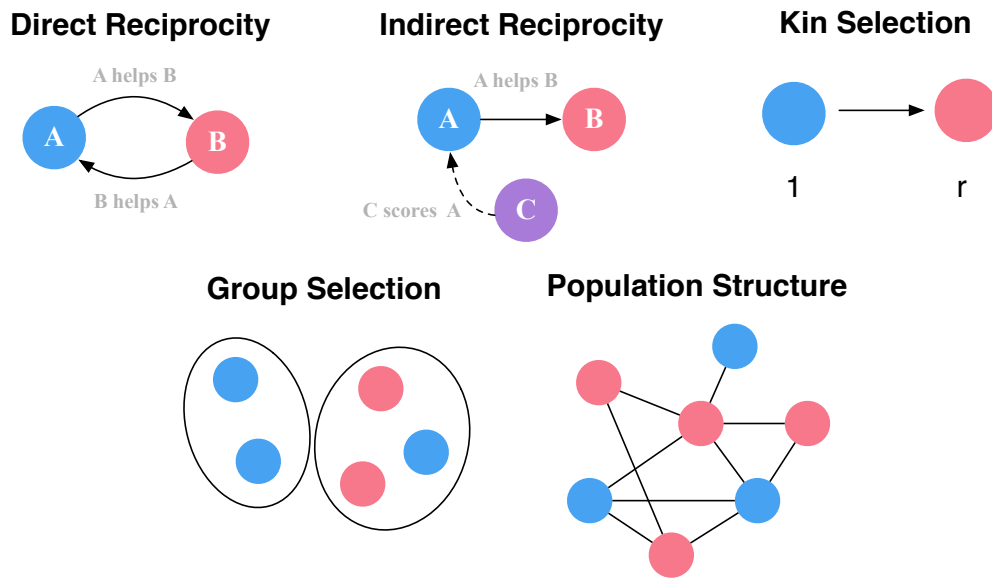


Figure 15: Schematic representation of the five fundamental mechanisms for the evolution of cooperation, inspired by [143]. Direct reciprocity implies the repeated interaction between individuals. Indirect reciprocity is sustained by a reputation dynamics. Kin selection operates between individuals that are relatives. Group or multi-level selection implies that selection might not act on the individuals but on higher order scales, for instance selecting the most sustainable groups. Population structure allows for cooperators to outcompete defectors in local clusters.

Indirect Reciprocity

The emergence of cooperation is not limited to the repeated and direct interaction between individuals. Indeed, in one-shot interactions it suffices to provide the donor with indirect information on whether the recipient is worth or not cooperating with. Such information can be provided by a Reputation based system [144] that continuously monitors and scores individuals' according to their actions. This is the main concept behind the so called Indirect Reciprocity [145, 146]: a population of individuals co-evolving strategies and Reputations.

The evolution of Reputation is largely driven by a Social Norm³, that is, a set of rules that classify the donor whether as Good or Bad depending on his action and the context they are embedded in [147, 148, 149]. One can devise Norms with different levels of complexity: first order Norms only take into account the action of the donor; second order Norms that take into account the donor action and the recipient reputation; third order Norms involve additionally the reputation of the donor besides the actions of the latter. On the other hand, strategies⁴ employed by individuals are conditional to the recipient and donor reputations.

³ In some literature Social Norms are also called Rules of Assessment, since they assess the individual Reputation after a given action

⁴ In the context of Indirect Reciprocity strategies are also known as action rules, since they are a set of rules that dictate how individuals act, given the reputations of the opponents (or even self reputations).

Chapter 1. INTRODUCTION

Ohtsuki & Iwasa [150, 151] have shown that only 8 of the 4096 combinations of the 256 third order norms with the 16 available strategies are evolutionary stable and effectively promote cooperation. These correspond to eight norms supported by a single strategy of Cooperating against good guys and Defecting bad guys. Later *Pacheco et al* [152] used a model with multi-level selection to show that a Norm of *Stern Judging* is the most evolutionary successful among all third order norms. This norm classifies as good donors that cooperate with a good or refuse to help to a bad recipient, whereas refusing help to a good recipient or helping a bad one leads to a bad reputation.

Empirical evidence supporting Indirect Reciprocity has come mostly from Economical experiments [153, 154, 155] but also from field experiences [156, 157].

Kin Selection

Kin Selection builds on the idea that cooperating towards a closely related individual can favour the evolution of Cooperation. This concept builds on the notion of Inclusive Fitness, which assumes that one's fitness is not only a measure of his direct reproduction but also accounts for indirect reproduction of individuals that share similar traits. The reasoning is that close relatives will, somehow, contribute to the evolutionary success of one's traits. The theory of Inclusive Fitness was initially developed by *W.D. Hamilton* [158] and was latter mathematically formalised by *George R. Price* [159]. One of its the major results is the so called *Hamilton's rule*, which states that the emergence of cooperative behaviour requires the relatedness, r , between individuals to exceed the cost-to-benefit ratio of an altruistic act:

$$r > \frac{c}{b} \quad (48)$$

where r is a measure of the genetic distance between individuals.

Kin selection has been used to explain the emergence of Eusociality [160] in biological communities. Following previous works [161, 162, 163], *Nowak et al* [164] have recently argued that the assumptions underlying inclusive fitness theory are unnecessary since its predictions can be explained through other, more well founded and simpler, mechanisms such as multilevel selection. These ideas have however been received with strong criticism [165, 166], particularly from the Biological community.

Group Selection

Selection can also act on groups, by selecting groups that are more fitted in detriment of others [167, 168, 169]. This concept is contrary to the traditional biological view that selection acts solely on individuals or on genes. It is straightforward to understand why Group selection would be advantageous for Cooperation, since groups composed mostly by Cooperators benefit from the fact that a Cooperator in a group increases the overall fitness of the group while Defectors decrease it.

Several theoretical works have supported the idea of group selection [170, 171]. Nowadays it is usual to refer to Group Selection as Multi-level Selection, as it is a more accurate definition for the different selection forces that drive evolution.

Population Structure

So far we have dealt with models and situations that consider well-mixed populations. However, as shown in Section 1.2, the real world is hardly close to the a well-mixed scenario. Indeed, individuals tend to interact with a limit number of peers either for cognitive or spatial constrains. One way to capture this structure in evolutionary models is by assuming that individuals of a population correspond to nodes of a complex network, with interactions constrained to nodes directly connected through links.

It was shown that structured populations prompt a more beneficial scenario for the emergence of Cooperation. This is in part because small groups of Cooperators are able to cluster and "solve" the collective dilemma, opening the chance for them to invade, fixate and "dominate" the whole population.

Section 1.4 summarises the most important results that involve static and dynamical Population Structures in the scope of the Cooperation problem.

Additional Mechanisms

Besides the five canonical mechanisms described above, others have been suggested to promote the emergence of cooperation. For instance peer and pool punishment of free riders has been shown to be an effective mechanism both theoretically [172, 173, 174, 175, 176, 177, 178, 179, 180] and experimentally [181, 182]. On the other hand, Cooperation can be facilitated by the presence of additional strategies [183, 184, 185, 186, 187], which can include Punishers or a strategy of Voluntary participation.

The addition of cooperation thresholds [110, 188] and risk perception of collective failure [189, 190, 191] have also been shown to facilitate the emergence of cooperation in Public Goods Games, a class of games that involves interactions between groups of individuals.

Diversity in both social networks or among individual's traits is also pointed as one of the main drivers of cooperation [192, 52, 193, 53].

Moreover, *Matjaz Perc* has reviewed the impact of different co-evolutionary dynamics [194] that show a positive impact in the evolution of cooperation. In this context, co-evolution implies that, alongside strategy abundance, an additional trait co-evolves. Examples range from the co-evolution of social structure [195, 196, 197, 65, 198, 59, 199], population size [200, 201], learning rate [202, 192, 203], mobility [204, 205], individuals ageing [206, 207], etc.

While many of these mechanisms are additive [208], in the sense that two mechanisms together facilitate even more cooperation than each alone, some are not. For instance, *Vukov et al* [209] has shown that depending on the choice of parameters on the Prisoner's Dilemma in a structured population, evolution might result in a worse outcome when peer-punishment is considered.

1.4 EVOLUTIONARY GAMES IN STRUCTURED POPULATIONS

Since the 1992 seminal work by *Nowak and May* [211] that others have explored the role of population structure in the evolutionary dynamics of Cooperation [49].

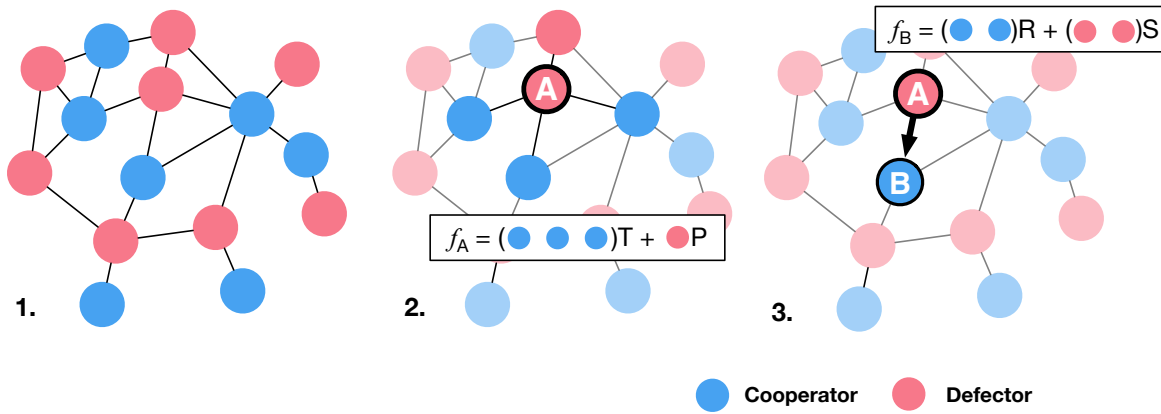


Figure 16: One individual is selected at random from the population (A) and a second (B) is selected at random from the neighbourhood of A . The fitness of each individual is now context dependent and is a function of the accumulated payoff over all interactions with their neighbours [210].

While theoretical works support the idea that population structure does indeed facilitate the emergence and sustainability of Cooperative behaviour, empirical evidence is not so clear: some authors argue that indeed static [54, 55, 56] and adaptive [57, 58, 59] structures promote cooperation, others say the opposite [60, 61, 62, 63, 64]. The latter have been criticised for not exploring the right conditions and to reach conclusions based in insufficient data to be statistically sound. The former for performing experiments under unrealistic conditions.

Update Rule on Structured Populations

In order to account for the effects of structure we need to revise our stochastic update rule. Hence, instead of sampling two individuals (say i and j) at random from the population, the second is sampled from the sub-set of individuals that are directly connected with the first. In other words, the focal individual can only revise his strategy by looking at his nearest neighbours.

Moreover, the fitness now corresponds to the accumulated payoffs over all interactions individuals that engage with the nearest neighbours. For instance, if we consider a two-person, two-strategy game, the fitness $f_i^{s_i}$ of an individual i adopting strategy s_i is

$$\begin{aligned} f_i^C &= k_i^C R + k_i^D S \\ f_i^D &= k_i^C T + k_i^D P \end{aligned} \tag{49}$$

where k_i^C and k_i^D are respectively the number of Cooperators and Defectors in the neighbourhood of i , with $k_i^C + k_i^D = k_i$.

1.4.1 Homogeneous Networks

Figure 18 shows the *average final fraction of cooperators* obtained along the $T \times S$ domain for three distinct network topologies: Square Lattice (left), Regular Ring (middle) and Homogeneous Random

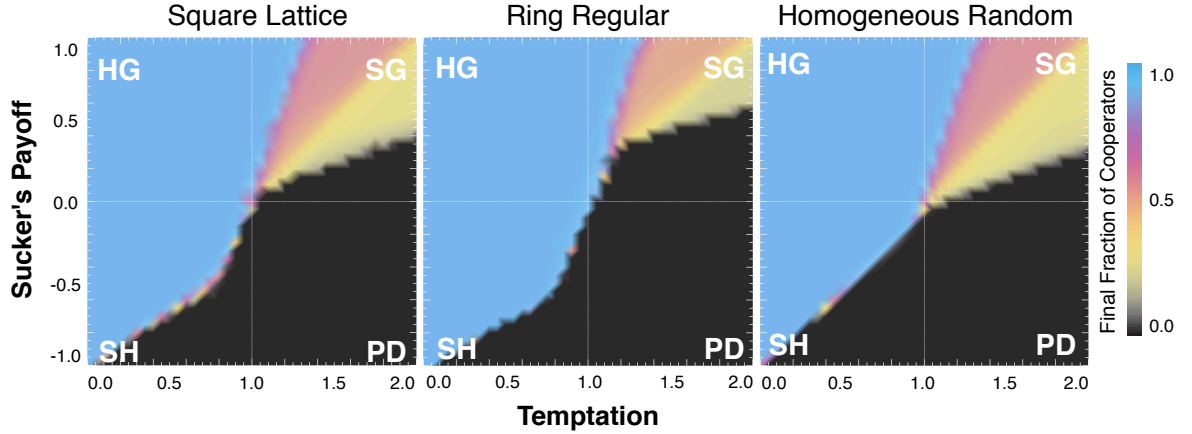


Figure 17: Level of Cooperation measured through the expected Final Fraction of Cooperators [127, 53] for three types of degree Homogeneous networked populations in the entire space of parameters and under a strong selection regime ($\beta = 10.0$). Regions are identified according to the associated social dilemma, namely Harmony Game (**HG**), Snowdrift Game (**SG**), Stag Hunt (**SH**) and Prisoner's Dilemma (**PD**)

Graph (right). The latter being obtained by the complete randomisation of the links ends from any of the two first topologies [212]. All three networks are characterised for having all nodes engaging in the same number of interactions, thus leading to a degree distribution that corresponds to a peak over $\langle k \rangle$.

Homogenous networks allow Cooperators to form clusters [48, 213, 214]. In this context, clustering implies that cooperators are more likely to interact with other cooperators, and therefore to achieve higher fitnesses. However, these are only stable for a narrow range of the parameters in the Prisoner's Dilemma (that is, in comparison with the well-mixed scenario, see Figure 14) and highly dependent on the selection pressure [215, 216, 217, 75].

The consistency of such clusters depends on the payoff structure of the game. For instance, *Hauert* and *Doebeli* [218, 219] showed that, in homogeneous structures, cooperation can be inhibited in the Snowdrift domain. They concluded that the clusters that form in this scenario tend to be smaller and more disperse, when compared with what is observed in the Prisoner's Dilemma [220], since players benefit from playing with individuals of the opposite strategy.

Ohtsuki et al [221] suggested that selection favours cooperation whenever

$$\frac{b}{c} > \langle k \rangle \quad (50)$$

where b is the benefit and c the cost of an altruistic act, with $\langle k \rangle$ being the average degree of the network. This result, derived analytically and derived resorting to the pair-approximation [222], is based on the idea that the fixation probability (ϕ_k) of a single Cooperator is greater than the outcome of neutral drift ($1/Z$) when this condition holds. The results show a good agreement with numerical simulations on regular networks with low degree, low selection pressure (β), however it fails for networks with that exhibit degree heterogeneity.

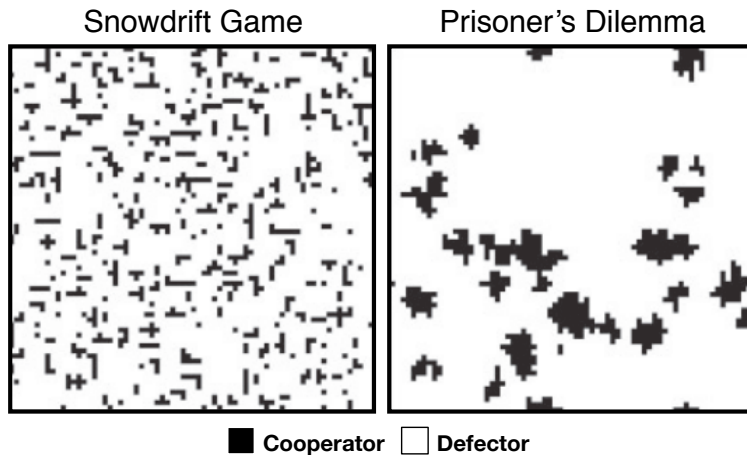


Figure 18: Snapshot of the typical spatial patterns found in the Snowdrift Game (left) and Prisoner's Dilemma (right) games played on a squared lattice. Both situations correspond to parameters close to the D-Dominance parameter region. Both panels are found in [219]

1.4.2 Heterogeneous Networks

Figure 19 shows the *average final fraction of cooperators* obtained along the $T \times S$ domain for three heterogeneous network topologies: Erdős–Rényi Random (left), Exponential (middle) and *Barabási-Albert* Scale Free (right). From left to right in Figure 19, the diversity⁵ in the interaction patterns of the population increases. Empirical distributions collected from real-world social networks fall somewhere between the limits bounded by these structures [223, 25, 10]. Hence it is without surprise that they are the best at promoting the emergence and sustainability of cooperation for a broader domain of the Prisoner's Dilemma.

In heterogeneous structures, different individuals typically participate in a different number of interactions, as dictated by the position occupied by each individual in the social network and pattern of connectivity. Given that the fitness of each individual is directly related with his success, social diversity will certainly impact social evolution. Moreover, because the position that each individual occupies largely defines who he is able to imitate and who imitates him, heterogeneous networks prompts a diversity in the influence of individuals: highly connected individuals (hubs) are imitated more often than individuals with few connections.

Underlying the ability of heterogeneous networks to promote cooperation is the interplay between these two types of social diversity: diversity in fitness and diversity of influence. The positive impact of heterogeneous networks in the evolution of cooperation was first shown in 2005 by *Pacheco* and *Santos* [50, 212, 127, 53] in the context of two-person games and later extended to Public Goods Games [52] by the same authors. Many other works have studied the role of heterogeneous networks in the evolution of cooperation, exploring, for instance, the impact of different topological features [224, 225, 226, 227, 228, 229, 127, 212, 230, 231, 232, 109].

⁵ Here diversity is measured in terms of the variance of the degree distribution $D(k)$, that is $var(k) = \langle k \rangle^2 - \langle k^2 \rangle$

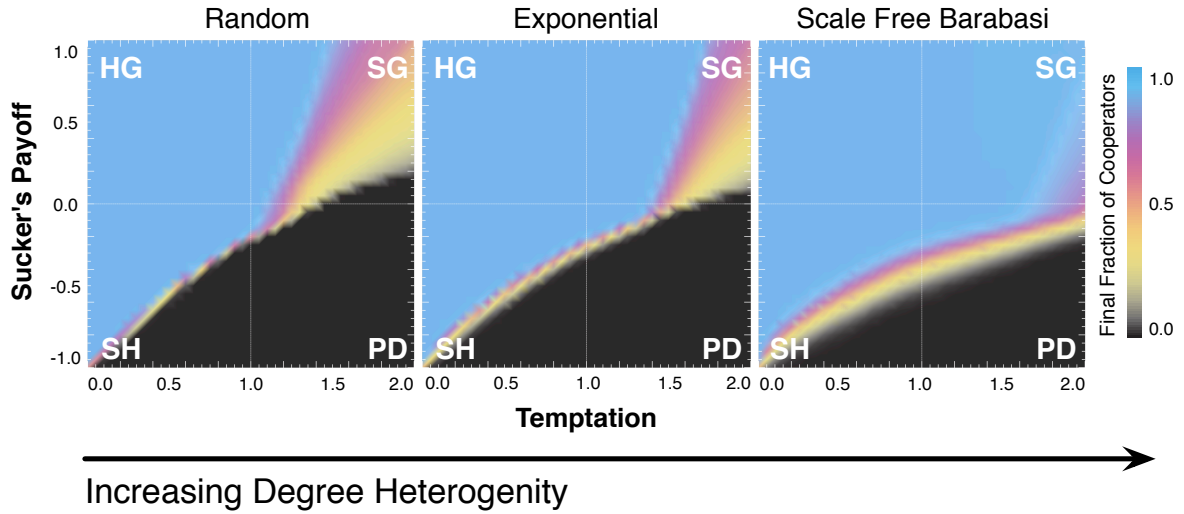


Figure 19: Level of Cooperation obtained on three types of degree Heterogeneous networked populations [127, 53] along the $T \times S$ parameter space and under a strong selection regime ($\beta = 10.0$). Degree Heterogeneity is here associated with the variance of the degree distribution $D(k)$ and it increases from the left to the right. Regions are identified according to the associated social dilemma, namely Harmony Game (**HG**), Snowdrift Game (**SG**), Stag Hunt (**SH**) and Prisoner's Dilemma (**PD**)

While the spatial nature of regular structures, like the Lattice, allows for an intuitive visual inspection of the patterns generated by the evolutionary process, in more complex structures this approach is often unfeasible. Alternatively, one can resort to the study of prototype, and simpler network structures (*i.e.* motifs) that play capture the functioning of the structure under analysis. In the particular case of scale-free networks a motif of particular interest considers two connected stars [52, 233], see Figure 20 sheds some light on the hub centric dynamics that drives the evolution on strongly heterogeneous populations. In Figure 20, two stars i and j are completely surrounded by Cooperators. However i is a Defector and j a Cooperator. The centre of the stars correspond to high fitness positions. As a consequence, i will be imitated by the individuals around him, same for j , who is resilient to invasion as he holds a relatively high fitness. Ironically, j becomes a victim of his early success and ends at the centre of a star surrounded by Defectors, deeming him with a relatively low fitness. At this stage j becomes a role model for i , and the latter is likely to change his strategy to Cooperator. Finally, because i occupies a position in which he is imitated more often than he imitates, his influence ends up turning all the Defectors surrounding him to Cooperation.

Scale-free networks provide the ideal conditions for the *hub-hub* dynamics describe above. Indeed, they are often characterized for having interconnected *hubs* with a broad range of connectivities, creating star-like structures of different sizes, in which Cooperators may play a central role with a high resilience to the invasion of Defectors, as a result of the large number of mutual Cooperative interactions they participate. Moreover, the role of these highly influential individuals have also been analyzed through the study of the fixation probability. It was shown that the fixation of a single mutant

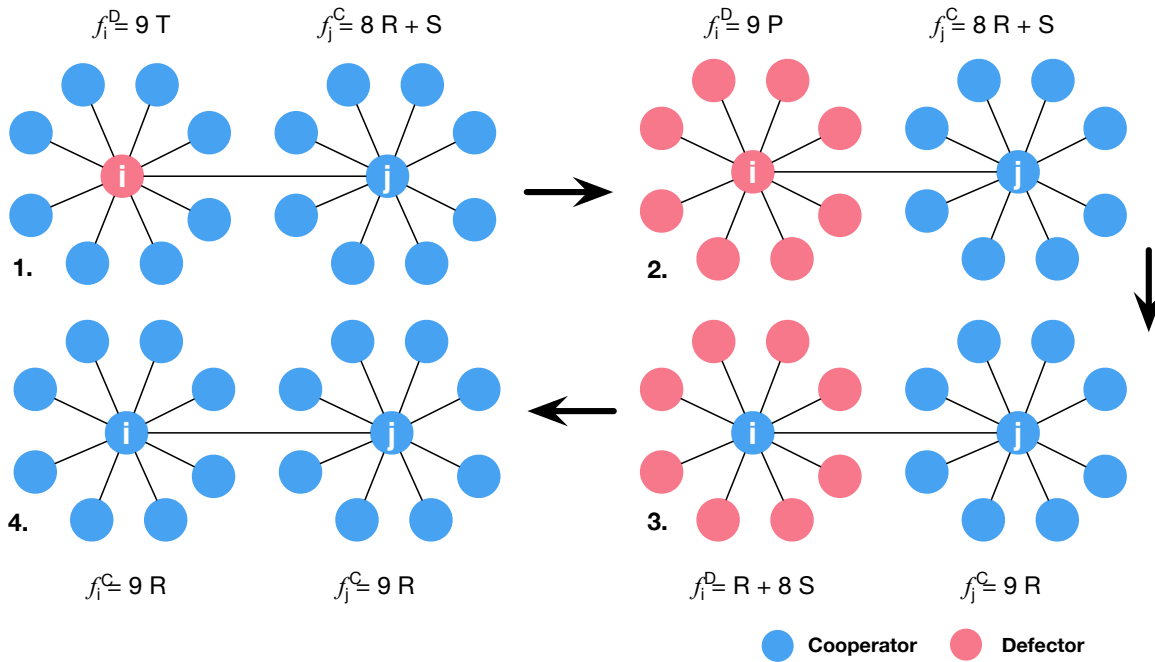


Figure 20: Dynamics of a double star. In the context of the Prisoner's Dilemma ($T > R > P > S$), when a Defector i invades the centre of a star he positions himself in a high-fitness location. The natural process is for the leaves around his position to change to Defector, which in turn decrease the fitness of i leaving him vulnerable to be invaded by j . Ironically i is a victim of his own success. For more details see [52]

Cooperator is strongly correlated with the degree, thus the influence, of the initial location: a mutant invading a hub has more chances of invading the network [234, 235].

1.4.3 Gradient of Selection in networks

Several works have explored the impact of population structured in the evolutionary dynamics through analytical inspection. The accuracy and validity of the used techniques often require assuming the limiting scenario of weak-selection ($\beta \ll 1$) [221, 236, 237, 238, 239] and/or fairly unrealistic population structures [49]. The quantities obtained, are in most cases of little interest to the understanding of how population structure shapes the evolutionary dynamics as they tend to focus in the fixation probabilities, a question of more relevance to biology.

A more adequate approach to quantify the role of population structure in the evolutionary dynamics of populations is to estimate the gradient of selection, see Section 1.3.1. This quantity indicates the expected direction of selection. In network populations it is difficult to derive a closed form expression for the gradient of selection, it can, however, be estimated numerically. And since it is qualitatively similar to the replicator equation and to its analogous in finite well-mixed populations, it allows us to assess the role of population structure in the evolutionary dynamics.

1.4. Evolutionary Games in Structured Populations

In that scope, let us define as $\zeta^\pm(k)$ the probability to increase/decrease the number of cooperators by one in a structured population composed by k Cooperators and $Z - k$ Defectors. The equivalent to the gradient of selection becomes

$$\Gamma(k) = \zeta^+(k) - \zeta^-(k) \quad (51)$$

thus being positive/negative if the number of cooperators is more likely to increase/decrease. We are left with the estimation of $\zeta^\pm(k)$, which requires computing

$$\zeta^\pm(k) = \frac{1}{Z} \sum_{i=0}^Z \frac{1}{k_i} \sum_{j \in \zeta_i} \frac{s_j(1 - s_i)}{1 + e^{\pm\beta(f_j - f_i)}} \quad (52)$$

where ζ_i is the set of neighbours of j and s_i is 1 if i is a Cooperator and 0 if a Defector. To estimate $\zeta^\pm(k)$ we sum all available transitions available, which requires iterating over all pairs of connected individuals with different strategies.

By estimating $\Gamma(k)$ numerically we obtain a context dependent (in the sense that it effectively differentiates different topologies) mean-field description for structured populations which contrasts with other techniques, *e.g.* pair-approximation that only works for regular and random structures[240, 241, 242, 243, 221, 49].

Strategy Assortment

To compute $\Gamma(k)$ we need to somehow place k cooperators along the nodes of the network. Different assortments k will likely return different values of $\Gamma(k)$. Choosing the right one from the total (maximum) of $Z! / (k!(Z - k)!)$ can be a daunting task.

We want to know why evolution promotes cooperation when the population structure of interactions follows a specific pattern. Unfortunately evolution does not occupy each configuration with equal probability. This is because there are transitions between strategy assortments that are more probable than others. For instance, it is more likely that evolution leads to assortments where strategies become clustered, more on this bellow.

Furthermore, since we are dealing with extremely large space state, the computation of the transition probabilities between states is humanly and computationally impossible. This is, after all, the main challenge of studying dynamical processes on networks: the size of the strategy assortments space state and the asymmetry of their likelihood does not allow us to properly average $\Gamma(k)$.

Nevertheless, we can make some good educated guesses about some extreme conditions. For instance, and by definition, at the beginning of evolution, strategies are randomly placed along the nodes of the network. This allows to estimate $\Gamma(k)$ for all $k \in [0, Z]$ by performing a sample average over many randomly picked strategy assortments. The result is shown in panels A and B of Figure 21 for Homogeneous Random and Heterogeneous networks respectively. Despite quantitatively different, $\Gamma(k) < 0$ for all $k \in [0, Z]$ suggests that at the beginning of the evolution is more probable for the number of cooperators to decrease. This is the same paradoxical result that is obtained for well-mixed populations.

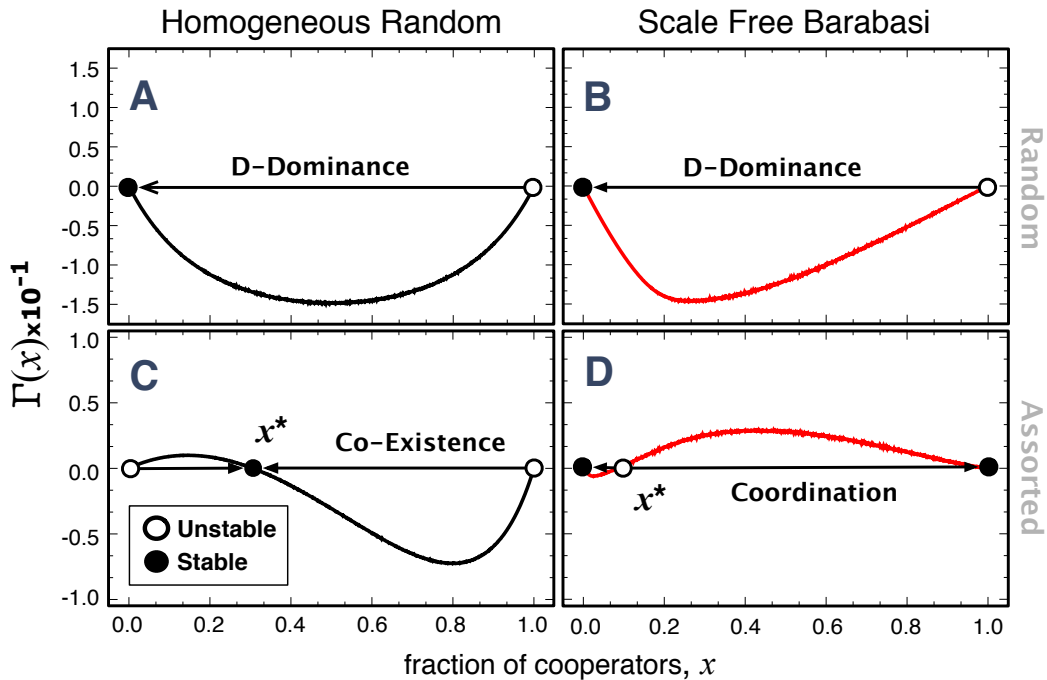


Figure 21: Gradient of Selection in Structured populations [109]. Top panels consider a situation where both Cooperators and Defectors are placed at random along the nodes of the network. Bottom panels consider a scenario where Cooperators are placed preferentially around other Cooperators, thus generating a positive assortment among Cooperators.

However as evolution proceeds, we observe the building-up of correlations between individuals of the same strategy. The nature of these correlations are complex, which clearly bounds our ability to predict them. They stem from the balance of two processes. On one hand the stochastic birth-death process is associated with dynamics of *Cooperators breeding Cooperators* and that *Defectors breeding Defectors* [109]. While in the other, the nature of the interaction structure gives rise to different patterns depending of the particular features of the network topology under study.

Hence, at the other extreme of evolution, it is more likely to find Cooperators closer to other Cooperators and Defectors close to other Defectors. However, because as we seen with the dual star example discussed previously, only Cooperative clusters remain sustainable and thus we could argue that a possible strategy assortment would percolate k cooperators. Panels C and D of Figure 21 show the impact of such assortment strategy in the shape of $\Gamma(k)$ for the network topologies. In particular homogeneous networks change the nature of the Prisoner's Dilemma from a Defector-Dominance to a Co-existence game. On the other hand, heterogeneous networks change the Prisoner's Dilemma from a Defector-Dominance to a Coordination game.

This connection implies that studying a Prisoner's Dilemma in a complex network is similar to study a different game in a well-mixed scenario. The new game is conditional to the underlying structure of interactions between individuals. More importantly, although individual pairwise interactions follow the Prisoner's Dilemma, the collective dynamics of populations becomes very different.

1.4. Evolutionary Games in Structured Populations

The proposed approaches to distribute strategies along the nodes of the network are: at random and with a positive assortment of Cooperators [109]. These two extreme scenarios fail to capture the true strategy assortments that emerge with evolution. In chapter 3 we introduce a way to estimate such assortments that allow us to estimate expected $\Gamma(k)$ (gradient of selection) for a predefined time-window of the evolutionary process. More interestingly, we can capture the evolution of the effective dilemma along the evolutionary dynamics.

1.4.4 Co-Evolutionary Dynamics

Population structure is not static, for instance, we often change our e-mail contacts, our social interactions and the internet is constantly changing shape as we add new devices to replace old ones [244, 245, 246]. Hence, studying evolutionary processes on static networks, is but an approximation that allows us to characterise the scheme of interactions of a system along a particular time interval of observation. Through the repeated observation of a system along successive time intervals one often unveils a structure evolving under its own set of rules. The characterization of these rules largely defines the study of dynamical networks [247, 65]. Although these rules are in most cases local, *i.e.* take place at the level of the node, they can lead to dramatic changes in the global topology of the network, identified by phase transitions along paths established by different order parameters. For instance, the *Watts-Strogatz* model may be (qualitatively) associated with a dynamical process⁶ that leads to the emergence of an entirely different network topology with respect to the topology of the initial structure [83].

Adaptive Networks

Apart from the evolutionary process of strategy adaptation, it is also reasonable to expect that individuals try to exert some local control over their gains by choosing with whom they interact [248, 249]. In particular, when interactions conform with the Prisoner's Dilemma [250, 251], one should expect that rational individuals look to avoid interactions with defectors, which would spare them from obtaining the *Sucker's* or the *Punishment* payoffs. In a dynamical network, one can model this behavior by either assuming that individuals break their connections with defectors or that they opt to rewire from non-beneficial interactions towards another individual of the population.

To account for the evolution of both processes it is appropriate to consider that each evolves independently of the other and thus allow for separate timescales: one for strategy evolution (τ_S) and another for network adaptation (τ_N). Let us define the ratio of both timescales as

$$W = \frac{\tau_S}{\tau_N} \quad (53)$$

and assume that $\tau_S = 1$. Then, at each time step, a strategy update event shall occur with probability $p_{strategy} = (1 + W)^{-1}$ and a network update with $p_{network} = 1 - p_{strategy}$. Here W provides a measure of population inertia to react to their rational choices: Large W reflects populations in which

⁶ Although a strongly constrained dynamics which bears no comparison with any real world process

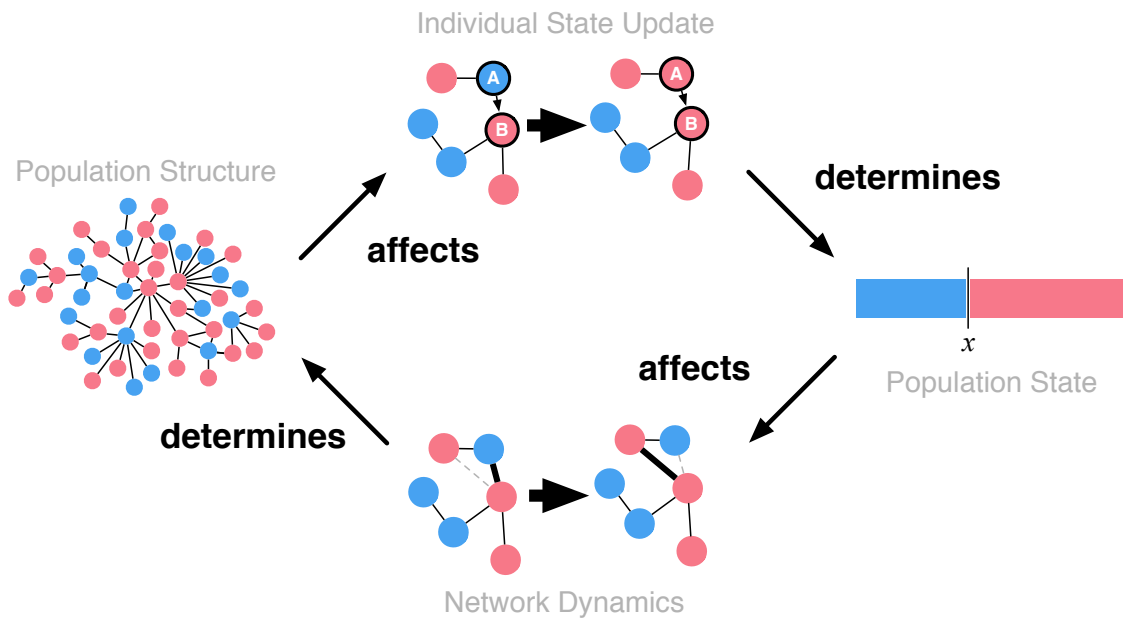


Figure 22: Scheme that summarizes the feedback between Strategy and Structure Evolution. The assortment of strategies in a network dictates the effective dilemma as identified by the Gradient of Selection thus affecting strategy update, which determines how the frequency of strategies in the population changes in time. In turn the amount of individuals of each type affects the underlying decision making driving network dynamics, thus determining the interaction structure of the population.

individuals react promptly to adverse ties, whereas small W reflects the overall inertia for topological change (compared with strategy change) [252].

In the previous section, by using the gradient of selection, we explored the idea that population structure fundamentally changes the effective dynamics of strategy evolution and more importantly how different types of structures lead to distinct dynamical portraits. Now, on the other hand, we realize that the evolution of structure seemingly depends on both the composition of strategies in the population as well as their particular assortment along the network. Thus, although formally independent, both processes remain coupled through the seemingly feedback that is schematized in Figure 22 [65, 253, 254].

Active Linking

Two limits bring us back to charted territory. In the limit of $W \rightarrow 0$ the static network scenario is recovered and the evolutionary dynamics of structured populations can be extracted through the computational computation of $\Gamma(k)$. When $W \rightarrow \infty$ the network evolution is much faster than strategy evolution and reaches a stationary topology in between any pair of strategy update events. In this limit, and under additional constraints, it is also possible to understand and quantify the impact of the network dynamics on the strategy evolution of the population.

1.4. Evolutionary Games in Structured Populations

Concerning the latter case ($W \rightarrow \infty$), a very successful approach known as *Active Linking* [254, 255, 256, 199, 196, 195] considers the state space spanned by the different types of links⁷ plus their rates of creation ($\alpha_{s_i s_j}$ for all $i, j \in \{C, D\}$) and destruction ($\beta_{s_i s_j}$ for all $s_i, s_j \in \{C, D\}$). Each state in this space, that we call Active Linking configuration space, is defined by a different combination of the total number of links of each type in the population. In this framework the creation and destruction of links does not depend on the composition of strategies of the population, thus the fraction of active links is governed by a set of ordinary (linear) differential equations of the form

$$\dot{\psi}_{s_i s_j} = \alpha_{s_i s_j}(\bar{\psi}_{s_i s_j} - \psi_{s_i s_j}) - \beta_{s_i s_j} \psi_{s_i s_j} \quad (54)$$

where $\psi_{s_i s_j}$ is the fraction of links that connect individuals of strategy s_i to individuals of strategy s_j , and $(\bar{\psi}_{s_i s_j})$ is the maximum possible number of links of each type. The computation of the equilibrium fraction of active links in the steady state ($\psi_{s_i s_j}^*$) leads to an expression that depends only on the quantities $\alpha_{s_i s_j}$ and $\beta_{s_i s_j}$,

$$\psi_{s_i s_j}^* = \bar{\psi}_{s_i s_j} \eta_{s_i s_j} = \bar{\psi}_{s_i s_j} \frac{\alpha_{s_i s_j}}{\alpha_{s_i s_j} + \beta_{s_i s_j}} \quad (55)$$

The computation of the equilibrium fraction of each type of link introduces a correction to the replicator equation. Hence in the case of a two-person and two strategy the resulting effective evolutionary dynamics corresponds to a rescaling of the payoff matrix of the form,

	C	D
C	$\eta_{CC}R$	$\eta_{DC}S$
D	$\eta_{DC}T$	$\eta_{DD}P$

which, as pointed out by *Pacheco et al* [196, 195, 257, 254], under the right conditions can prompt a milder dilemma, distinct from Prisoner's Dilemma initially faced by individuals. Surprisingly, the results computed with the Active Linking tend to hold for a wide range of timescales ($W \gg 1$) [254]. A similar description with qualitatively the same results, but that takes into account the stochastic effects that arise from the finite number of links, was developed by *Bin Wu et al* [256].

In sum, both Active Linking (for adaptive networks) and the $\Gamma(k)$ (on static networks) suggest that the introduction of structure shifts the population-wide dynamics towards a milder dynamical scenario (compared to the Prisoner's Dilemma) that allows for the emergence and evolution of cooperation. This can be interpreted as if the population-wide dynamics in structured populations is akin to study a well-mixed population evolving under a different dilemma [74, 195].

Co-evolutionary Dynamics

Ecosystems hardly evolve under such limiting conditions, *i.e.* in an overly fast adaptation or in a static scenario. In fact, it is more reasonable to expect that real world systems support both processes to co-evolve with timescales of a similar order of magnitude ($W \approx 1$), a scenario for which we are left

⁷ In a population where individuals are either Cooperators or Defectors there are three types of links: those connecting two cooperators, those connecting two defectors and links that connect cooperators and defectors.

Chapter 1. INTRODUCTION

without an appropriate approach to extract/compute the evolutionary dynamics of strategy and structure co-evolution at a macro-level. So far, several works have inspected this regime resorting mostly to Monte-Carlo simulations [258, 259, 260], concluding that the co-evolution of network structure and strategy composition promote cooperation as long as W is above a certain critical threshold W_{crit} [197].

In contrast with the Active Linking, where the network dynamics is introduced by means of the rates of creation/destruction of links, the slower timescale of network update in the regime W_{crit} requires a more microscopic modeling of the network update process. The simplest process would consider that at each network update event a random individual breaks a link with a Defector and creates a new one towards another individual in the population, thus keeping the number of links constant. Several variations of this model consider that the target individual is selected proportional to his age, degree or fitness potentially leading to different evolutionary outcomes. Contrary to the Active Linking framework, it is common in this regime (W_{crit}) to quantify the resulting structure [197], although this is not in the scope of this thesis.

In Chapter 6 we propose a methodology to adapt the computation of $\Gamma(k)$ to this co-evolutionary scenario. As we show this methodology provides a dynamical analysis that is independent of the relative times scales.

1.5 BIBLIOGRAPHY

- [1] Albert-László Barabási. *Linked: How everything is connected to everything else and what it means*. Plume Editors, 2002.
- [2] Nicholas A Christakis and James H Fowler. *Connected: The surprising power of our social networks and how they shape our lives*. Little, Brown, 2009.
- [3] Michelle Girvan and Mark EJ Newman. Community structure in social and biological networks. *Proceedings of the National Academy of Sciences*, 99(12):7821–7826, 2002.
- [4] Fredrik Liljeros, Christofer R Edling, Luis A Nunes Amaral, H Eugene Stanley, and Yvonne Åberg. The web of human sexual contacts. *Nature*, 411(6840):907–908, 2001.
- [5] Gueorgi Kossinets, Jon Kleinberg, and Duncan Watts. The structure of information pathways in a social communication network. In *Proceedings of the 14th ACM SIGKDD international conference on Knowledge discovery and data mining*, pages 435–443. ACM, 2008.
- [6] Nathan Eagle, Alex Sandy Pentland, and David Lazer. Inferring friendship network structure by using mobile phone data. *Proceedings of the National Academy of Sciences*, 106(36):15274–15278, 2009.
- [7] Michael O’Keeffe and Bruce G Hyde. *Crystal Structures, No. 1: Patterns & Symmetry*, volume 3. Mineralogical Society of Amer, 1996.
- [8] Paul Erdős and Alfréd Rényi. On the evolution of random graphs. *Publications of the Mathematical Institute of the Hungarian Academy of Sciences*, 5:17–61, 1960.
- [9] Béla Bollobás. *Random graphs*. Springer, 1998.
- [10] Luis A Nunes Amaral, Antonio Scala, Marc Barthelemy, and H Eugene Stanley. Classes of small-world networks. *Proceedings of the National Academy of Sciences*, 97(21):11149–11152,

- 2000.
- [11] Trivik Verma, Nuno AM Araújo, and Hans J Herrmann. Revealing the structure of the world airline network. *Scientific reports*, 4, 2014.
 - [12] F Benjamin Zhan and Charles E Noon. Shortest path algorithms: an evaluation using real road networks. *Transportation Science*, 32(1):65–73, 1998.
 - [13] Feng Xie and David Levinson. Measuring the structure of road networks. *Geographical analysis*, 39(3):336–356, 2007.
 - [14] Vincent D Blondel, Jean-Loup Guillaume, Renaud Lambiotte, and Etienne Lefebvre. Fast unfolding of communities in large networks. *Journal of Statistical Mechanics: Theory and Experiment*, 2008(10):P10008, 2008.
 - [15] Reuven Cohen, Keren Erez, Daniel Ben-Avraham, and Shlomo Havlin. Resilience of the internet to random breakdowns. *Physical Review Letters*, 85(21):4626, 2000.
 - [16] Réka Albert, Hawoong Jeong, and Albert-László Barabási. Internet: Diameter of the worldwide web. *Nature*, 401(6749):130–131, 1999.
 - [17] Norman P Hummon and Patrick Dereian. Connectivity in a citation network: The development of dna theory. *Social Networks*, 11(1):39–63, 1989.
 - [18] Lada A Adamic and Natalie Glance. The political blogosphere and the 2004 us election: divided they blog. In *Proceedings of the 3rd international workshop on Link discovery*, pages 36–43. ACM, 2005.
 - [19] Roger Guimera and Luis A Nunes Amaral. Functional cartography of complex metabolic networks. *Nature*, 433(7028):895–900, 2005.
 - [20] Hawoong Jeong, Bálint Tombor, Réka Albert, Zoltan N Oltvai, and A-L Barabási. The large-scale organization of metabolic networks. *Nature*, 407(6804):651–654, 2000.
 - [21] Eric Davidson and Michael Levin. Gene regulatory networks. *Proceedings of the National Academy of Sciences*, 102(14):4935–4935, 2005.
 - [22] Benno Schwikowski, Peter Uetz, and Stanley Fields. A network of protein–protein interactions in yeast. *Nature Biotechnology*, 18(12):1257–1261, 2000.
 - [23] Hawoong Jeong, Sean P Mason, A-L Barabási, and Zoltan N Oltvai. Lethality and centrality in protein networks. *Nature*, 411(6833):41–42, 2001.
 - [24] Javier Borge-Holthoefer and Alex Arenas. Semantic networks: structure and dynamics. *Entropy*, 12(5):1264–1302, 2010.
 - [25] Réka Albert and Albert-László Barabási. Statistical mechanics of complex networks. *Reviews of Modern Physics*, 74(1):47, 2002.
 - [26] Steven H Strogatz. Exploring complex networks. *Nature*, 410(6825):268–276, 2001.
 - [27] Sergey N Dorogovtsev and Jose F F Mendes. Evolution of networks. *Advances in Physics*, 51(4):1079–1187, 2002.
 - [28] Stefano Boccaletti, Vito Latora, Yamir Moreno, Martin Chavez, and D-U Hwang. Complex networks: Structure and dynamics. *Physics Reports*, 424(4):175–308, 2006.
 - [29] Mark EJ Newman. The structure and function of complex networks. *SIAM Review*, 45(2):167–256, 2003.

Chapter 1. INTRODUCTION

- [30] Duncan J Watts. *Small worlds: the dynamics of networks between order and randomness*. Princeton university press, 1999.
- [31] Romualdo Pastor-Satorras and Alessandro Vespignani. *Evolution and structure of the Internet: A statistical physics approach*. Cambridge University Press, 2007.
- [32] Mark EJ Newman. *Networks: an introduction*. Oxford University Press, 2010.
- [33] Sergei N Dorogovtsev and José F F Mendes. *Evolution of networks: From biological nets to the Internet and WWW*. Oxford University Press, 2013.
- [34] Miller McPherson, Lynn Smith-Lovin, and James M Cook. Birds of a feather: Homophily in social networks. *Annual review of sociology*, pages 415–444, 2001.
- [35] Alain Barrat, Marc Barthelemy, and Alessandro Vespignani. *Dynamical processes on complex networks*, volume 1. Cambridge University Press Cambridge, 2008.
- [36] Romualdo Pastor-Satorras and Alessandro Vespignani. Epidemic spreading in scale-free networks. *Physical Review Letters*, 86(14):3200, 2001.
- [37] Lisa F Berkman and Thomas Glass. Social integration, social networks, social support, and health. *Social epidemiology*, 1:137–173, 2000.
- [38] James Holland Jones and Mark S Handcock. Social networks (communication arising): Sexual contacts and epidemic thresholds. *Nature*, 423(6940):605–606, 2003.
- [39] Mark EJ Newman. Spread of epidemic disease on networks. *Physical Review E*, 66(1):016128, 2002.
- [40] Nicholas A Christakis and James H Fowler. The spread of obesity in a large social network over 32 years. *New England Journal of Medicine*, 357(4):370–379, 2007.
- [41] James H Fowler and Nicholas A Christakis. Dynamic spread of happiness in a large social network: longitudinal analysis over 20 years in the framingham heart study. *BMJ: British Medical Journal*, 337, 2008.
- [42] Nicholas A Christakis and James H Fowler. The collective dynamics of smoking in a large social network. *New England Journal of Medicine*, 358(21):2249–2258, 2008.
- [43] Flavio L Pinheiro, Marta D Santos, Francisco C Santos, and Jorge M Pacheco. Origin of peer influence in social networks. *Physical Review Letters*, 112(9):098702, 2014.
- [44] Martin A Nowak. Evolving cooperation. *Journal of Theoretical Biology*, 299:1–8, 2012.
- [45] Herbert Gintis. *Game theory evolving: A problem-centered introduction to modeling strategic behavior*. Princeton University Press, 2000.
- [46] Martin A Nowak. *Evolutionary dynamics: exploring the equations of life*. Harvard University Press, 2006.
- [47] Ross Cressman. *The stability concept of evolutionary game theory: a dynamic approach*, volume 94. Springer Science & Business Media, 2013.
- [48] György Szabó and Csaba Tóke. Evolutionary prisoner’s dilemma game on a square lattice. *Physical Review E*, 58(1):69, 1998.
- [49] György Szabó and Gábor Fáth. Evolutionary games on graphs. *Physics Reports*, 446(4):97–216, 2007.

1.5. Bibliography

- [50] Francisco C Santos and Jorge M Pacheco. Scale-free networks provide a unifying framework for the emergence of cooperation. *Physical Review Letters*, 95(9):098104, 2005.
- [51] Julia Poncela, Jesús Gómez-Gardeñes, LM Floría, and Yamir Moreno. Robustness of cooperation in the evolutionary prisoner’s dilemma on complex networks. *New Journal of Physics*, 9(6):184, 2007.
- [52] Francisco C Santos, Marta D Santos, and Jorge M Pacheco. Social diversity promotes the emergence of cooperation in public goods games. *Nature*, 454(7201):213–216, 2008.
- [53] Francisco C Santos, Flavio L Pinheiro, Tom Lenaerts, and Jorge M Pacheco. The role of diversity in the evolution of cooperation. *Journal of Theoretical Biology*, 299:88–96, 2012.
- [54] David G Rand, Martin A Nowak, James H Fowler, and Nicholas A Christakis. Static network structure can stabilize human cooperation. *Proceedings of the National Academy of Sciences*, 111(48):17093–17098, 2014.
- [55] James H Fowler and Nicholas A Christakis. Cooperative behavior cascades in human social networks. *Proceedings of the National Academy of Sciences*, 107(12):5334–5338, 2010.
- [56] Coren L Apicella, Frank W Marlowe, James H Fowler, and Nicholas A Christakis. Social networks and cooperation in hunter-gatherers. *Nature*, 481(7382):497–501, 2012.
- [57] David G Rand, Samuel Arbesman, and Nicholas A Christakis. Dynamic social networks promote cooperation in experiments with humans. *Proceedings of the National Academy of Sciences*, 108(48):19193–19198, 2011.
- [58] Jing Wang, Siddharth Suri, and Duncan J Watts. Cooperation and assortativity with dynamic partner updating. *Proceedings of the National Academy of Sciences*, 109(36):14363–14368, 2012.
- [59] Katrin Fehl, Daniel J van der Post, and Dirk Semmann. Co-evolution of behaviour and social network structure promotes human cooperation. *Ecology Letters*, 14(6):546–551, 2011.
- [60] Arne Traulsen, Dirk Semmann, Ralf D Sommerfeld, Hans-Jürgen Krambeck, and Manfred Milinski. Human strategy updating in evolutionary games. *Proceedings of the National Academy of Sciences*, 107(7):2962–2966, 2010.
- [61] Jelena Grujić, Constanza Fosco, Lourdes Araujo, José A Cuesta, Angel Sánchez, et al. Social experiments in the mesoscale: Humans playing a spatial prisoner’s dilemma. *PLoS One*, 5(11): e13749–e13749, 2010.
- [62] Carlos Gracia-Lázaro, Alfredo Ferrer, Gonzalo Ruiz, Alfonso Tarancón, José A Cuesta, Angel Sánchez, and Yamir Moreno. Heterogeneous networks do not promote cooperation when humans play a prisoner’s dilemma. *Proceedings of the National Academy of Sciences*, 109(32): 12922–12926, 2012.
- [63] Siddharth Suri and Duncan J Watts. Cooperation and contagion in web-based, networked public goods experiments. *ACM SIGecom Exchanges*, 10(2):3–8, 2011.
- [64] Jelena Grujić, Torsten Röhl, Dirk Semmann, Manfred Milinski, and Arne Traulsen. Consistent strategy updating in spatial and non-spatial behavioral experiments does not promote cooperation in social networks. *PLoS One*, 7(11):e47718, 2012.
- [65] Thilo Gross and Hiroki Sayama. *Adaptive networks*. Springer, 2009.

Chapter 1. INTRODUCTION

- [66] P. Kollock. Social dilemmas: The anatomy of cooperation. *Annual Review of Sociology*, 24: 183–214, 1998.
- [67] Jorge Peña and Yannick Rochat. Bipartite graphs as models of population structures in evolutionary multiplayer games. *PLoS One*, 7(9):e44514, 2012.
- [68] Vítor V Vasconcelos, Francisco C Santos, and Jorge M Pacheco. A bottom-up institutional approach to cooperative governance of risky commons. *Nature Climate Change*, 3(9):797–801, 2013.
- [69] Vítor V Vasconcelos, Francisco C Santos, Jorge M Pacheco, and Simon A Levin. Climate policies under wealth inequality. *Proceedings of the National Academy of Sciences*, 111(6): 2212–2216, 2014.
- [70] Flávio L Pinheiro, Vítor V Vasconcelos, Francisco C Santos, and Jorge M Pacheco. Evolution of all-or-none strategies in repeated public goods dilemmas. *PLoS Computational Biology*, 10 (11):e1003945, 2014.
- [71] Lev Davidovich Landau and EM Lifshitz. Statistical physics, part i. *Course of theoretical physics*, 5:468, 1980.
- [72] Martin Nowak and Roger Highfield. *SuperCooperators: Altruism, evolution, and why we need each other to succeed*. Simon and Schuster, 2011.
- [73] Robert Axelrod and William Donald Hamilton. The evolution of cooperation. *Science*, 211 (4489):1390–1396, 1981.
- [74] Flávio L Pinheiro, Jorge M Pacheco, and Francisco C Santos. From local to global dilemmas in social networks. *PLoS One*, 7(2):e32114, 2012.
- [75] Flávio L Pinheiro, Francisco C Santos, and Jorge M Pacheco. How selection pressure changes the nature of social dilemmas in structured populations. *New Journal of Physics*, 14(7):073035, 2012.
- [76] Aaron Clauset, Cosma Rohilla Shalizi, and Mark EJ Newman. Power-law distributions in empirical data. *SIAM Review*, 51(4):661–703, 2009.
- [77] Mark EJ Newman. Mixing patterns in networks. *Physical Review E*, 67(2):026126, 2003.
- [78] Mark EJ Newman and Juyong Park. Why social networks are different from other types of networks. *Physical Review E*, 68(3):036122, 2003.
- [79] Rogier Noldus and Piet Van Mieghem. Assortativity in complex networks. *Journal of Complex Networks*, page cnv005, 2015.
- [80] Mark EJ Newman. Assortative mixing in networks. *Physical Review Letters*, 89(20):208701, 2002.
- [81] Sinan Aral, Lev Muchnik, and Arun Sundararajan. Distinguishing influence-based contagion from homophily-driven diffusion in dynamic networks. *Proceedings of the National Academy of Sciences*, 106(51):21544–21549, 2009.
- [82] Ron Milo, Shai Shen-Orr, Shalev Itzkovitz, Nadav Kashtan, Dmitri Chklovskii, and Uri Alon. Network motifs: simple building blocks of complex networks. *Science*, 298(5594):824–827, 2002.

- [83] Duncan J Watts and Steven H Strogatz. Collective dynamics of ‘small-world’ networks. *Nature*, 393(6684):440–442, 1998.
- [84] Erzsébet Ravasz and Albert-László Barabási. Hierarchical organization in complex networks. *Physical Review E*, 67(2):026112, 2003.
- [85] Agata Fronczak, Janusz A Hołyst, Maciej Jedynek, and Julian Sienkiewicz. Higher order clustering coefficients in barabási–albert networks. *Physica A: Statistical Mechanics and its Applications*, 316(1):688–694, 2002.
- [86] Harald Ibach and Hans Lüth. Solid-state physics: an introduction to principles of material science. *Advanced Texts in Physics, Springer-Verlag berlin Heidelberg New York*, 2003.
- [87] Réka Albert, Hawoong Jeong, and Albert-László Barabási. Error and attack tolerance of complex networks. *Nature*, 406(6794):378–382, 2000.
- [88] Stanley Milgram. The small world problem. *Psychology today*, 2(1):60–67, 1967.
- [89] Ithiel de Sola Pool and Manfred Kochen. Contacts and influence. *Social Networks*, 1(1):5–51, 1979.
- [90] Albert-László Barabási and Réka Albert. Emergence of scaling in random networks. *Science*, 286(5439):509–512, 1999.
- [91] Sergey N Dorogovtsev, José Fernando F Mendes, and Alexander N Samukhin. Structure of growing networks with preferential linking. *Physical Review Letters*, 85(21):4633, 2000.
- [92] K-I Goh, B Kahng, and D Kim. Universal behavior of load distribution in scale-free networks. *Physical Review Letters*, 87(27):278701, 2001.
- [93] Josef Hofbauer and Karl Sigmund. *Evolutionary games and population dynamics*. Cambridge University Press, 1998.
- [94] Ross Cressman. *Evolutionary dynamics and extensive form games*, volume 5. MIT Press, 2003.
- [95] Karl Sigmund. *The calculus of selfishness*. Princeton University Press, 2010.
- [96] Mauro Mobilia. Oscillatory dynamics in rock–paper–scissors games with mutations. *Journal of Theoretical Biology*, 264(1):1–10, 2010.
- [97] David Easley and Jon Kleinberg. *Networks, crowds, and markets: Reasoning about a highly connected world*. Cambridge University Press, 2010.
- [98] Karen M Page and Martin A Nowak. Unifying evolutionary dynamics. *Journal of Theoretical Biology*, 219(1):93–98, 2002.
- [99] Immanuel M Bomze. Lotka-volterra equation and replicator dynamics: a two-dimensional classification. *Biological Cybernetics*, 48(3):201–211, 1983.
- [100] Peter D Taylor and Leo B Jonker. Evolutionary stable strategies and game dynamics. *Mathematical Biosciences*, 40(1):145–156, 1978.
- [101] Josef Hofbauer, Peter Schuster, and Karl Sigmund. A note on evolutionary stable strategies and game dynamics. *Journal of Theoretical Biology*, 81(3):609–612, 1979.
- [102] Erik Christopher Zeeman. Dynamics of the evolution of animal conflicts. *Journal of Theoretical Biology*, 89(2):249–270, 1981.
- [103] Jörgen W Weibull. *Evolutionary game theory*. MIT press, 1997.

Chapter 1. INTRODUCTION

- [104] Arne Traulsen, Martin A Nowak, and Jorge M Pacheco. Stochastic dynamics of invasion and fixation. *Physical Review E*, 74(1):011909, 2006.
- [105] Arne Traulsen, Jorge M Pacheco, and Martin A Nowak. Pairwise comparison and selection temperature in evolutionary game dynamics. *Journal of Theoretical Biology*, 246(3):522–529, 2007.
- [106] Arne Traulsen, Jens Christian Claussen, and Christoph Hauert. Coevolutionary dynamics: from finite to infinite populations. *Physical Review Letters*, 95(23):238701, 2005.
- [107] Jorge M Pacheco, Vítor V Vasconcelos, and Francisco C Santos. Climate change governance, cooperation and self-organization. *Physics of Life Review*, 11(4):573–586, 2014.
- [108] Nicolaas Godfried Van Kampen. *Stochastic processes in physics and chemistry*, volume 1. Elsevier, 1992.
- [109] Jorge M Pacheco, Flávio L Pinheiro, and Francisco C Santos. Population structure induces a symmetry breaking favoring the emergence of cooperation. *PLoS Computational Biology*, 5(12):e1000596, 2009.
- [110] Jorge M Pacheco, Francisco C Santos, Max O Souza, and Brian Skyrms. Evolutionary dynamics of collective action in n-person stag hunt dilemmas. *Proceedings of the Royal Society B: Biological Sciences*, 276(1655):315–321, 2009.
- [111] Patrick Alfred Pierce Moran. Random processes in genetics. In *Mathematical Proceedings of the Cambridge Philosophical Society*, volume 54, pages 60–71. Cambridge Univ Press, 1958.
- [112] Philipp M Altrock and Arne Traulsen. Fixation times in evolutionary games under weak selection. *New Journal of Physics*, 11(1):013012, 2009.
- [113] Martin A Nowak, Akira Sasaki, Christine Taylor, and Drew Fudenberg. Emergence of cooperation and evolutionary stability in finite populations. *Nature*, 428(6983):646–650, 2004.
- [114] Sven Van Segbroeck, Jorge M Pacheco, Tom Lenaerts, and Francisco C Santos. Emergence of fairness in repeated group interactions. *Physical Review Letters*, 108(15):158104, 2012.
- [115] The Anh Han, Luís Moniz Pereira, Francisco C Santos, Tom Lenaerts, et al. Good agreements make good friends. *Scientific Reports*, 3, 2013.
- [116] Luis A Martinez-Vaquero, The Anh Han, Luís Moniz Pereira, Tom Lenaerts, et al. Apology and forgiveness evolve to resolve failures in cooperative agreements. *Scientific Reports*, 5, 2015.
- [117] Motoo Kimura. *The neutral theory of molecular evolution*. Cambridge University Press, 1984.
- [118] J Maynard Smith and GR Price. The logic of animal conflict. *Nature*, 246:15, 1973.
- [119] Gary B Fogel, Peter C Andrews, and David B Fogel. On the instability of evolutionary stable strategies in small populations. *Ecological Modelling*, 109(3):283–294, 1998.
- [120] Alexander J Stewart and Joshua B Plotkin. Extortion and cooperation in the prisoner’s dilemma. *Proceedings of the National Academy of Sciences*, 109(26):10134–10135, 2012.
- [121] Alexander J Stewart and Joshua B Plotkin. Collapse of cooperation in evolving games. *Proceedings of the National Academy of Sciences*, 111(49):17558–17563, 2014.
- [122] William Donald Hamilton. *Evolution of social behaviour*. WH Freeman/Spektrum, 1996.
- [123] Anatol Rapoport and Albert M Chammah. *Prisoner’s dilemma: A study in conflict and cooperation*, volume 165. University of Michigan press, 1965.

- [124] Brian Skyrms. *The stag hunt and the evolution of social structure*. Cambridge University Press, 2004.
- [125] Morton Deutsch. *The resolution of conflict: Constructive and destructive processes*. Yale University Press, 1977.
- [126] R Cressman. Evolutionary stability for two-stage hawk-dove games. *Journal of Mathematics*, 25(1), 1995.
- [127] Francisco C Santos, Jorge M Pacheco, and Tom Lenaerts. Evolutionary dynamics of social dilemmas in structured heterogeneous populations. *Proceedings of the National Academy of Sciences*, 103(9):3490–3494, 2006.
- [128] Elizabeth Pennisi. How did cooperative behavior evolve? *Science*, 309(5731):93–93, 2005.
- [129] Robert L Trivers. The evolution of reciprocal altruism. *Quarterly review of biology*, pages 35–57, 1971.
- [130] Robert Boyd. Mistakes allow evolutionary stability in the repeated prisoner’s dilemma game. *Journal of Theoretical Biology*, 136(1):47–56, 1989.
- [131] Martin A Nowak, Karl Sigmund, and Esam El-Sedy. Automata, repeated games and noise. *Journal of Mathematical Biology*, 33(7):703–722, 1995.
- [132] Martin A Nowak, Karl Sigmund, et al. A strategy of win-stay, lose-shift that outperforms tit-for-tat in the prisoner’s dilemma game. *Nature*, 364(6432):56–58, 1993.
- [133] Martin Posch et al. Win stay—lose shift: An elementary learning rule for normal form games. Technical report, Santa Fe Institute, 1997.
- [134] Loren A Imhof, Drew Fudenberg, and Martin A Nowak. Tit-for-tat or win-stay, lose-shift? *Journal of Theoretical Biology*, 247(3):574–580, 2007.
- [135] Shun Kurokawa and Yasuo Ihara. Emergence of cooperation in public goods games. *Proceedings of the Royal Society of London B: Biological Sciences*, 276(1660):1379–1384, 2009.
- [136] William H Press and Freeman J Dyson. Iterated prisoner’s dilemma contains strategies that dominate any evolutionary opponent. *Proceedings of the National Academy of Sciences*, 109(26):10409–10413, 2012.
- [137] Christian Hilbe, Martin A Nowak, and Karl Sigmund. Evolution of extortion in iterated prisoner’s dilemma games. *Proceedings of the National Academy of Sciences*, 110(17):6913–6918, 2013.
- [138] Christian Hilbe, Martin A Nowak, and Arne Traulsen. Adaptive dynamics of extortion and compliance. *PLoS One*, 8(11):e77886, 2013.
- [139] Christian Hilbe, Torsten Röhl, and Manfred Milinski. Extortion subdues human players but is finally punished in the prisoner’s dilemma. *Nature Communications*, 5, 2014.
- [140] Christian Hilbe, Bin Wu, Arne Traulsen, and Martin A Nowak. Cooperation and control in multiplayer social dilemmas. *Proceedings of the National Academy of Sciences*, 111(46):16425–16430, 2014.
- [141] Alexander J Stewart and Joshua B Plotkin. From extortion to generosity, evolution in the iterated prisoner’s dilemma. *Proceedings of the National Academy of Sciences*, 110(38):15348–15353, 2013.

Chapter 1. INTRODUCTION

- [142] Christian Hilbe, Bin Wu, Arne Traulsen, and Martin A Nowak. Evolutionary performance of zero-determinant strategies in multiplayer games. *Journal of Theoretical Biology*, 374:115–124, 2015.
- [143] Martin A Nowak. Five rules for the evolution of cooperation. *Science*, 314(5805):1560–1563, 2006.
- [144] Martin A Nowak and Karl Sigmund. Evolution of indirect reciprocity by image scoring. *Nature*, 393(6685):573–577, 1998.
- [145] Martin A Nowak and Karl Sigmund. Evolution of indirect reciprocity. *Nature*, 437(7063):1291–1298, 2005.
- [146] Karthik Panchanathan and Robert Boyd. Indirect reciprocity can stabilize cooperation without the second-order free rider problem. *Nature*, 432(7016):499–502, 2004.
- [147] Robert Sugden. *The economics of rights, co-operation and welfare*. Blackwell Oxford, 1986.
- [148] Michihiro Kandori. Social norms and community enforcement. *The Review of Economic Studies*, 59(1):63–80, 1992.
- [149] Hannelore Brandt and Karl Sigmund. The logic of reprobation: assessment and action rules for indirect reciprocation. *Journal of Theoretical Biology*, 231(4):475–486, 2004.
- [150] Hisashi Ohtsuki and Yoh Iwasa. How should we define goodness?—reputation dynamics in indirect reciprocity. *Journal of Theoretical Biology*, 231(1):107–120, 2004.
- [151] Hisashi Ohtsuki and Yoh Iwasa. The leading eight: social norms that can maintain cooperation by indirect reciprocity. *Journal of Theoretical Biology*, 239(4):435–444, 2006.
- [152] Jorge M Pacheco, Francisco C Santos, and FACC Chalub. Stern-judging: A simple, successful norm which promotes cooperation under indirect reciprocity. *PLoS Computational Biology*, 2(12):e178, 2006.
- [153] Claus Wedekind and Manfred Milinski. Cooperation through image scoring in humans. *Science*, 288(5467):850–852, 2000.
- [154] Manfred Milinski, Dirk Semmann, Theo CM Bakker, and Hans-Jürgen Krambeck. Cooperation through indirect reciprocity: image scoring or standing strategy? *Proceedings of the Royal Society of London B: Biological Sciences*, 268(1484):2495–2501, 2001.
- [155] Manfred Milinski, Dirk Semmann, and Hans-Jürgen Krambeck. Reputation helps solve the ‘tragedy of the commons’. *Nature*, 415(6870):424–426, 2002.
- [156] Erez Yoeli, Moshe Hoffman, David G Rand, and Martin A Nowak. Powering up with indirect reciprocity in a large-scale field experiment. *Proceedings of the National Academy of Sciences*, 110(Supplement 2):10424–10429, 2013.
- [157] Melissa Bateson, Daniel Nettle, and Gilbert Roberts. Cues of being watched enhance cooperation in a real-world setting. *Biology Letters*, 2(3):412–414, 2006.
- [158] WD Hamilton. The genetical evolution of social behaviour. i. 1964.
- [159] George R Price et al. Selection and covariance. *Nature*, 227:520–21, 1970.
- [160] Malte Andersson. The evolution of eusociality. *Annual Review of Ecology and Systematics*, pages 165–189, 1984.

1.5. Bibliography

- [161] WJ Alonso. The role of kin selection theory on the explanation of biological altruism: a critical review. *Journal of Computational Biology*, 3:1–14, 1998.
- [162] Wladimir J Alonso and Cynthia Schuck-Paim. Sex-ratio conflicts, kin selection, and the evolution of altruism. *Proceedings of the National Academy of Sciences*, 99(10):6843–6847, 2002.
- [163] Edward O Wilson. One giant leap: how insects achieved altruism and colonial life. *BioScience*, 58(1):17–25, 2008.
- [164] Martin A Nowak, Corina E Tarnita, and Edward O Wilson. The evolution of eusociality. *Nature*, 466(7310):1057–1062, 2010.
- [165] Andy Gardner, Stuart A West, and Geoff Wild. The genetical theory of kin selection. *Journal of Evolutionary Biology*, 24(5):1020–1043, 2011.
- [166] Patrick Abbot, Jun Abe, John Alcock, Samuel Alizon, Joao AC Alpedrinha, Malte Andersson, Jean-Baptiste Andre, Minus van Baalen, Francois Balloux, Sigal Balshine, et al. Inclusive fitness theory and eusociality. *Nature*, 471(7339):E1–E4, 2011.
- [167] David Sloan Wilson. A theory of group selection. *Proceedings of the National Academy of Sciences*, 72(1):143–146, 1975.
- [168] M Slatkin and MJ Wade. Group selection on a quantitative character. *Proceedings of the National Academy of Sciences*, 75(7):3531–3534, 1978.
- [169] Edward O Wilson and Bert Hölldobler. Eusociality: origin and consequences. *Proceedings of the National Academy of Sciences*, 102(38):13367–13371, 2005.
- [170] Arne Traulsen and Martin A Nowak. Evolution of cooperation by multilevel selection. *Proceedings of the National Academy of Sciences*, 103(29):10952–10955, 2006.
- [171] Laurent Lehmann, Laurent Keller, Stuart West, and Denis Roze. Group selection and kin selection: two concepts but one process. *Proceedings of the National Academy of Sciences*, 104(16):6736–6739, 2007.
- [172] Christoph Hauert, Arne Traulsen, Hannelore Brandt, Martin A Nowak, and Karl Sigmund. Via freedom to coercion: the emergence of costly punishment. *Science*, 316(5833):1905–1907, 2007.
- [173] Karl Sigmund, Christoph Hauert, and Martin A Nowak. Reward and punishment. *Proceedings of the National Academy of Sciences*, 98(19):10757–10762, 2001.
- [174] Hannelore Brandt, Christoph Hauert, and Karl Sigmund. Punishment and reputation in spatial public goods games. *Proceedings of the Royal Society of London B: Biological Sciences*, 270(1519):1099–1104, 2003.
- [175] Karl Sigmund. Punish or perish? retaliation and collaboration among humans. *Trends in Ecology & Evolution*, 22(11):593–600, 2007.
- [176] Robert Boyd and Peter J Richerson. Punishment allows the evolution of cooperation (or anything else) in sizable groups. *Ethology and sociobiology*, 13(3):171–195, 1992.
- [177] James H Fowler. Altruistic punishment and the origin of cooperation. *Proceedings of the National Academy of Sciences*, 102(19):7047–7049, 2005.
- [178] Martijn Egas and Arno Riedl. The economics of altruistic punishment and the maintenance of cooperation. *Proceedings of the Royal Society of London B: Biological Sciences*, 275(1637):

Chapter 1. INTRODUCTION

- 871–878, 2008.
- [179] Mayuko Nakamaru and Yoh Iwasa. The coevolution of altruism and punishment: role of the selfish punisher. *Journal of Theoretical Biology*, 240(3):475–488, 2006.
- [180] Robert Boyd, Herbert Gintis, Samuel Bowles, and Peter J Richerson. The evolution of altruistic punishment. *Proceedings of the National Academy of Sciences*, 100(6):3531–3535, 2003.
- [181] Ernst Fehr and Simon Gächter. Cooperation and punishment in public goods experiments. *Institute for Empirical Research in Economics working paper*, (10), 1999.
- [182] Ernst Fehr and Simon Gächter. Altruistic punishment in humans. *Nature*, 415(6868):137–140, 2002.
- [183] Christoph Hauert, Silvia De Monte, Josef Hofbauer, and Karl Sigmund. Volunteering as red queen mechanism for cooperation in public goods games. *Science*, 296(5570):1129–1132, 2002.
- [184] Christoph Hauert, Silvia De Monte, Josef Hofbauer, and Karl Sigmund. Replicator dynamics for optional public good games. *Journal of Theoretical Biology*, 218(2):187–194, 2002.
- [185] György Szabó and Christoph Hauert. Evolutionary prisoner’s dilemma games with voluntary participation. *Physical Review E*, 66(6):062903, 2002.
- [186] Mauro Mobilia. Stochastic dynamics of the prisoner’s dilemma with cooperation facilitators. *Physical Review E*, 86(1):011134, 2012.
- [187] Mauro Mobilia. Evolutionary games with facilitators: When does selection favor cooperation? *Chaos, Solitons & Fractals*, 56:113–123, 2013.
- [188] Max O Souza, Jorge M Pacheco, and Francisco C Santos. Evolution of cooperation under n-person snowdrift games. *Journal of Theoretical Biology*, 260(4):581–588, 2009.
- [189] Jing Wang, Feng Fu, Te Wu, and Long Wang. Emergence of social cooperation in threshold public goods games with collective risk. *Physical Review E*, 80(1):016101, 2009.
- [190] Francisco C Santos, Vitor V Vasconcelos, Marta D Santos, PNB Neves, and Jorge M Pacheco. Evolutionary dynamics of climate change under collective-risk dilemmas. *Mathematical Models and Methods in Applied Sciences*, 22(supp01):1140004, 2012.
- [191] Francisco C Santos and Jorge M Pacheco. Risk of collective failure provides an escape from the tragedy of the commons. *Proceedings of the National Academy of Sciences*, 108(26):10421–10425, 2011.
- [192] Matjaž Perc and Attila Szolnoki. Social diversity and promotion of cooperation in the spatial prisoner’s dilemma game. *Physical Review E*, 77(1):011904, 2008.
- [193] Attila Szolnoki, Matjaž Perc, and György Szabó. Diversity of reproduction rate supports cooperation in the prisoner’s dilemma game on complex networks. *The European Physical Journal B*, 61(4):505–509, 2008.
- [194] Matjaž Perc and Attila Szolnoki. Coevolutionary games—a mini review. *BioSystems*, 99(2):109–125, 2010.
- [195] Jorge M Pacheco, Arne Traulsen, and Martin A Nowak. Coevolution of strategy and structure in complex networks with dynamical linking. *Physical Review Letters*, 97(25):258103, 2006.

- [196] Jorge M Pacheco, Arne Traulsen, and Martin A Nowak. Active linking in evolutionary games. *Journal of Theoretical Biology*, 243(3):437–443, 2006.
- [197] Francisco C Santos, Jorge M Pacheco, and Tom Lenaerts. Cooperation prevails when individuals adjust their social ties. *PLoS Computational Biology*, 2(10):e140, 2006.
- [198] Sven Van Segbroeck, Francisco C Santos, Tom Lenaerts, and Jorge M Pacheco. Reacting differently to adverse ties promotes cooperation in social networks. *Physical Review Letters*, 102(5):058105, 2009.
- [199] Joao A Moreira, Jorge M Pacheco, and Francisco C Santos. Evolution of collective action in adaptive social structures. *Scientific Reports*, 3, 2013.
- [200] Julia Poncela, Jesús Gómez-Gardeñes, Arne Traulsen, and Yamir Moreno. Evolutionary game dynamics in a growing structured population. *New Journal of Physics*, 11(8):083031, 2009.
- [201] Jie Ren, Xiang Wu, Wen-Xu Wang, Guanrong Chen, and Bing-Hong Wang. Interplay between evolutionary game and network structure: the coevolution of social net, cooperation and wealth. *arXiv preprint physics/0605250*, 2006.
- [202] Naoki Masuda. Oscillatory dynamics in evolutionary games are suppressed by heterogeneous adaptation rates of players. *Journal of Theoretical Biology*, 251(1):181–189, 2008.
- [203] Attila Szolnoki and György Szabó. Cooperation enhanced by inhomogeneous activity of teaching for evolutionary prisoner’s dilemma games. *EPL (Europhysics Letters)*, 77(3):30004, 2007.
- [204] Stephen J Majeski, Greg Linden, Corina Linden, and Aaron Spitzer. Agent mobility and the evolution of cooperative communities. *Complexity*, 5(1):16–24, 1999.
- [205] Te Wu, Feng Fu, Yanling Zhang, and Long Wang. Expectation-driven migration promotes cooperation by group interactions. *Physical Review E*, 85(6):066104, 2012.
- [206] John M McNamara, Zoltan Barta, Lutz Fromhage, and Alasdair I Houston. The coevolution of choosiness and cooperation. *Nature*, 451(7175):189–192, 2008.
- [207] Attila Szolnoki, Matjaž Perc, György Szabó, and Hans-Ulrich Stark. Impact of aging on the evolution of cooperation in the spatial prisoner’s dilemma game. *Physical Review E*, 80(2):021901, 2009.
- [208] Hisashi Ohtsuki and Martin A Nowak. Direct reciprocity on graphs. *Journal of Theoretical Biology*, 247(3):462–470, 2007.
- [209] Jeromos Vukov, Flavio L Pinheiro, Francisco C Santos, and Jorge M Pacheco. Reward from punishment does not emerge at all costs. *PLoS Computational Biology*, 9(1), 2013.
- [210] Francisco C Santos and Jorge M Pacheco. A new route to the evolution of cooperation. *Journal of Evolutionary Biology*, 19:726–733, 2006.
- [211] Martin A Nowak and Robert M May. Evolutionary games and spatial chaos. *Nature*, 359(6398):826–829, 1992.
- [212] F C Santos, J F Rodrigues, and J M Pacheco. Graph topology plays a determinant role in the evolution of cooperation. *Proceedings of the Royal Society B: Biological Sciences*, 273(1582):51–55, 2006.
- [213] György Szabó, Jeromos Vukov, and Attila Szolnoki. Phase diagrams for an evolutionary prisoner’s dilemma game on two-dimensional lattices. *Physical Review E*, 72(4):047107, 2005.

Chapter 1. INTRODUCTION

- [214] Jeromos Vukov and György Szabó. Evolutionary prisoner's dilemma game on hierarchical lattices. *Physical Review E*, 71(3):036133, 2005.
- [215] Jeromos Vukov, György Szabó, and Attila Szolnoki. Cooperation in the noisy case: Prisoner's dilemma game on two types of regular random graphs. *Physical Review E*, 73(6):067103, 2006.
- [216] Matjaž Perc. Double resonance in cooperation induced by noise and network variation for an evolutionary prisoner's dilemma. *New Journal of Physics*, 8(9):183, 2006.
- [217] Attila Szolnoki, Jeromos Vukov, and György Szabó. Selection of noise level in strategy adoption for spatial social dilemmas. *Physical Review E*, 80(5):056112, 2009.
- [218] Christoph Hauert and Michael Doebeli. Spatial structure often inhibits the evolution of cooperation in the snowdrift game. *Nature*, 428(6983):643–646, 2004.
- [219] Michael Doebeli and Christoph Hauert. Models of cooperation based on the prisoner's dilemma and the snowdrift game. *Ecology Letters*, 8(7):748–766, 2005.
- [220] Feng Fu, Martin A Nowak, and Christoph Hauert. Invasion and expansion of cooperators in lattice populations: Prisoner's dilemma vs. snowdrift games. *Journal of Theoretical Biology*, 266(3):358–366, 2010.
- [221] Hisashi Ohtsuki, Christoph Hauert, Erez Lieberman, and Martin A Nowak. A simple rule for the evolution of cooperation on graphs and social networks. *Nature*, 441(7092):502–505, 2006.
- [222] Hisashi Ohtsuki and Martin A Nowak. The replicator equation on graphs. *Journal of Theoretical Biology*, 243(1):86–97, 2006.
- [223] Sergei N Dorogovtsev. *Lectures on complex networks*, volume 24. Oxford University Press Oxford, 2010.
- [224] Guillermo Abramson and Marcelo Kuperman. Social games in a social network. *Physical Review E*, 63(3):030901, 2001.
- [225] Salvatore Assenza, Jesús Gómez-Gardeñes, and Vito Latora. Enhancement of cooperation in highly clustered scale-free networks. *Physical Review E*, 78(1):017101, 2008.
- [226] Jesús Gómez-Gardeñes, Julia Poncela, Luis Mario Floría, and Yamir Moreno. Natural selection of cooperation and degree hierarchy in heterogeneous populations. *Journal of Theoretical Biology*, 253(2):296–301, 2008.
- [227] C-L Tang, W-X Wang, X Wu, and B-H Wang. Effects of average degree on cooperation in networked evolutionary game. *The European Physical Journal B-Condensed Matter and Complex Systems*, 53(3):411–415, 2006.
- [228] Stephen Devlin and Thomas Treloar. Cooperation in an evolutionary prisoner's dilemma on networks with degree-degree correlations. *Physical Review E*, 80(2):026105, 2009.
- [229] Han-Xin Yang, Wen-Xu Wang, Zhi-Xi Wu, Ying-Cheng Lai, and Bing-Hong Wang. Diversity-optimized cooperation on complex networks. *Physical Review E*, 79(5):056107, 2009.
- [230] Julia Poncela, Jesús Gómez-Gardeñes, Luis M Floría, Yamir Moreno, and Angel Sánchez. Cooperative scale-free networks despite the presence of defector hubs. *EPL (Europhysics Letters)*, 88(3):38003, 2009.
- [231] J Gómez-Gardeñes, M Campillo, LM Floría, and Y Moreno. Dynamical organization of cooperation in complex topologies. *Physical Review Letters*, 98(10):108103, 2007.

- [232] Matjaž Perc. Evolution of cooperation on scale-free networks subject to error and attack. *New Journal of Physics*, 11(3):033027, 2009.
- [233] LM Floría, C Gracia-Lázaro, J Gómez-Gardeñes, and Y Moreno. Social network reciprocity as a phase transition in evolutionary cooperation. *Physical Review E*, 79(2):026106, 2009.
- [234] Cong Li, Boyu Zhang, Ross Cressman, and Yi Tao. Evolution of cooperation in a heterogeneous graph: Fixation probabilities under weak selection. *PLoS One*, 8(6):e66560, 2013.
- [235] Wes Maciejewski, Feng Fu, and Christoph Hauert. Evolutionary game dynamics in populations with heterogenous structures. *PLoS Computational Biology*, 10(4):e1003567, 2014.
- [236] M Broom, C Hadjichrysanthou, and J Rychtář. Evolutionary games on graphs and the speed of the evolutionary process. In *Proceedings of the Royal Society of London A: Mathematical, Physical and Engineering Sciences*, page rspa20090487. The Royal Society, 2009.
- [237] Martin A Nowak, Corina E Tarnita, and Tibor Antal. Evolutionary dynamics in structured populations. *Philosophical Transactions of the Royal Society B: Biological Sciences*, 365(1537):19–30, 2010.
- [238] Erez Lieberman, Christoph Hauert, and Martin A Nowak. Evolutionary dynamics on graphs. *Nature*, 433(7023):312–316, 2005.
- [239] Benjamin Allen, Arne Traulsen, Corina E Tarnita, and Martin A Nowak. How mutation affects evolutionary games on graphs. *Journal of Theoretical Biology*, 299:97–105, 2012.
- [240] Mayuko Nakamaru, H Matsuda, and Y Iwasa. The evolution of cooperation in a lattice-structured population. *Journal of Theoretical Biology*, 184(1):65–81, 1997.
- [241] Ulf Dieckmann, Richard Law, and Johan AJ Metz. *The geometry of ecological interactions: simplifying spatial complexity*. Cambridge University Press, 2000.
- [242] Kei-ichi Tainaka. Vortices and strings in a model ecosystem. *Physical Review E*, 50(5):3401, 1994.
- [243] Kazunori Sato, Norio Konno, and Tadashi Yamaguchi. Paper-scissors-stone game on trees. *Muroran Institute of Technology*, pages 109–114, 1997.
- [244] Ingmar Glauche, Wolfram Krause, Rudolf Sollacher, and Martin Greiner. Distributive routing and congestion control in wireless multihop ad hoc communication networks. *Physica A: Statistical Mechanics and its Applications*, 341:677–701, 2004.
- [245] May Lim, Dan Braha, Sanith Wijesinghe, Stephenson Tucker, and Yaneer Bar-Yam. Preferential detachment in broadcast signaling networks: connectivity and cost trade-off. *EPL (Europhysics Letters)*, 79(5):58005, 2007.
- [246] Wolfram Krause, Jan Scholz, and Martin Greiner. Optimized network structure and routing metric in wireless multihop ad hoc communication. *Physica A: Statistical Mechanics and its Applications*, 361(2):707–723, 2006.
- [247] Petter Holme and Jari Saramäki. Temporal networks. *Physics Reports*, 519(3):97–125, 2012.
- [248] Holger Ebel and Stefan Bornholdt. Coevolutionary games on networks. *Physical Review E*, 66(5):056118, 2002.
- [249] Brian Skyrms and Robin Pemantle. A dynamic model of social network formation. In *Adaptive Networks*, pages 231–251. Springer, 2009.

Chapter 1. INTRODUCTION

- [250] Martín G Zimmermann, Víctor M Eguíluz, and Maxi San Miguel. Coevolution of dynamical states and interactions in dynamic networks. *Physical Review E*, 69(6):065102, 2004.
- [251] Martín G Zimmermann and Víctor M Eguíluz. Cooperation, social networks, and the emergence of leadership in a prisoner’s dilemma with adaptive local interactions. *Physical Review E*, 72(5):056118, 2005.
- [252] Marta D Santos, Flavio L Pinheiro, Francisco C Santos, and Jorge M Pacheco. Dynamics of n-person snowdrift games in structured populations. *Journal of Theoretical Biology*, 315:81–86, 2012.
- [253] Sven Van Segbroeck, Francisco C Santos, Ann Nowé, Jorge M Pacheco, and Tom Lenaerts. The evolution of prompt reaction to adverse ties. *BMC Evolutionary Biology*, 8(1):287, 2008.
- [254] Sven Van Segbroeck, Francisco C Santos, and Jorge M Pacheco. Adaptive contact networks change effective disease infectiousness and dynamics. *PLoS Computational Biology*, 6(8):e1000895, 2010.
- [255] Bin Wu, Da Zhou, and Long Wang. Evolutionary dynamics on stochastic evolving networks for multiple-strategy games. *Physical Review E*, 84(4):046111, 2011.
- [256] Bin Wu, Da Zhou, Feng Fu, Qingjun Luo, Long Wang, and Arne Traulsen. Evolution of cooperation on stochastic dynamical networks. *PLoS One*, 5(6):e11187, 2010.
- [257] Jorge M Pacheco, Arne Traulsen, Hisashi Ohtsuki, and Martin A Nowak. Repeated games and direct reciprocity under active linking. *Journal of Theoretical Biology*, 250(4):723–731, 2008.
- [258] Jun Tanimoto. Dilemma solving by the coevolution of networks and strategy in a 2×2 game. *Physical Review E*, 76(2):021126, 2007.
- [259] Attila Szolnoki and Matjaž Perc. Resolving social dilemmas on evolving random networks. *EPL (Europhysics Letters)*, 86(3):30007, 2009.
- [260] Feng Fu, Te Wu, and Long Wang. Partner switching stabilizes cooperation in coevolutionary prisoner’s dilemma. *Physical Review E*, 79(3):036101, 2009.

ORIGINS OF PEER INFLUENCE IN SOCIAL NETWORKS

Physical Review Letters, 112, 098702 (2014)

Flávio L. Pinheiro, Marta D. Santos, Francisco C. Santos and Jorge M. Pacheco

Social networks pervade our everyday lives: we interact, influence, and are influenced by our friends and acquaintances. With the advent of the World Wide Web, large amounts of data on social networks have become available, allowing the quantitative analysis of the distribution of information on them, including behavioural traits and fads. Recent studies of correlations among members of a social network, who exhibit the same trait, have shown that individuals influence not only their direct contacts but also friends' friends, up to a network distance extending beyond their closest peers. Here, we show how such patterns of correlations between peers emerge in networked populations. We use standard models (yet reflecting intrinsically different mechanisms) of information spreading to argue that empirically observed patterns of correlation among peers emerge naturally from a wide range of dynamics, being essentially independent of the type of information, on how it spreads, and even on the class of underlying network that interconnects individuals. Finally, we show that the sparser and clustered the network, the more far reaching the influence of each individual will be.

2.1 MANUSCRIPT

Human societies are embedded in complex social networks on which information flow — associated with traits such as emotions, behaviors, ideas or fads — is ubiquitous [1, 2, 3, 4, 5, 6, 7, 8, 9, 10, 11, 12]. What determines the patterns observed has become extremely valuable, with applications extending to all areas of human activity. Several studies have focused on the role played by social networks on the spread of information between individuals, by making use of email and blog databases, and online social networks such as Twitter [4, 6] and Facebook [7, 8]. Such empirical studies have shown how social networks affect the propagation of health issues [13, 14], ideas [15], criminal behavior [16, 17], economic decisions [18, 19], school achievement [20] and cooperation [21, 22], among other human traits.

In what concerns the correlation patterns observed, Fowler and Christakis [23, 22, 24, 25] recently proposed a *3 degrees of influence* rule based on the statistical analysis of the Framingham Heart study database, from which a social network was inferred. Correlations among individuals were analyzed for traits as diverse as smoking habits, alcohol consumption, loneliness, obesity, cooperation or happiness. These correlations reflected the relative increase in probability — when compared with a random

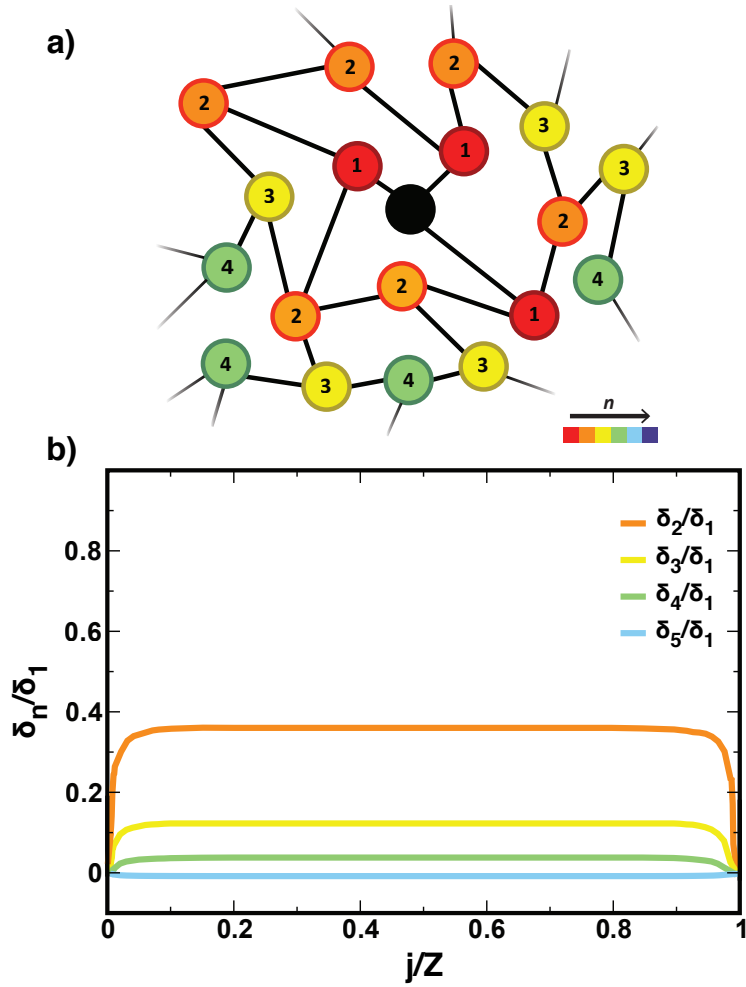


Figure 23: Peer Influence Patterns in Homogeneous Networks. (a) Network distance of a given node to the focal individual (black circle) defined as the smallest number of network links that separate the two (given by the number inside each circle). (b) Examples of correlation patterns as a function of j/Z (where j is the number of cooperators present in a population of size Z), emerging from the evolutionary **PD** game in homogeneous small world networks of size $Z = 10^3$ and degree $\langle k \rangle = 4$; the ratio $\delta_n(j/Z)/\delta_1(j/Z)$ provides an adequate normalisation which renders the correlation patterns approximately constant for most values of j/Z . Similar patterns are obtained both for **VM** and **SIR** dynamics.

arrangement — that two individuals share the same trait as a function of the network distance, defined as the smallest number of *links* connecting those individuals in the network (see Fig. 23a). They found that similar and non-trivial correlations emerge from distinct traits and persist in the period studied, suggesting the validity of a *3 degrees of influence* on social networks. In other words, not only our *friends*, but also our *friends' friends* together with their *friends* exhibit a positive correlation of traits. More recently, analysis of cooperation on social networks of hunter-gatherers revealed a degree of influence of 2 [26].

Here we investigate the degree of peer influence that emerges from different dynamical processes representative of a large plethora of phenomena occurring in networked populations — the spread of cooperative strategies, opinions and diseases. Individuals are assigned to nodes of a complex network, whereas links between them represent interactions. We show that, for each network class considered, *different* processes often lead to *the same* degrees of influence, suggesting that peer influence is insensitive to the process at stake. On the other hand, we find that simple topological properties of the underlying networks, such as the average connectivity ($\langle k \rangle$) and the clustering coefficient, ultimately determine the number of degrees of influence observed, which systematically falls between 3 and 2, in agreement with the results stemming from empirical analyses of correlations in present [23, 22, 24, 25] and past [26] social networks.

We start by studying the evolutionary dynamics of cooperation [27, 11], modeled as peer-to-peer interactions by means of the famous *Prisoner's Dilemma* (**PD**) metaphor [27]. The word dilemma in the **PD** stems from the decision conflict that occurs when 2 individuals must simultaneously decide whether to Cooperate (*C*) or to Defect (*D*) towards the other. The game returns $R = 1$ for mutual cooperation, $P = 0$ for mutual defection, $S = -\lambda$ when playing *C* against a *D*, and $T = 1 + \lambda$ when playing *D* against a *C* ($\lambda > 0$ measures both the temptation to defect and the fear of being cheated [28]). The ranking $T > R > P > S$ implies that maximizing one's own payoff leads each individual to choose *D*, irrespective of the decision of the other, such that the outcome will be mutual defection (pure Nash equilibrium for $\lambda > 0$). This outcome, however, is not the best for the pair, as mutual cooperation would lead to a better outcome for both of them. In the evolutionary version, the accumulated return from the interactions with all neighbors is interpreted as a measure of success (or *fitness*), such that some strategies – (*C*) or (*D*) – may become more attractive than others. We assume that individuals revise their behavior based on the perceived success of others: an individual *A* imitates a randomly chosen neighbor *B* with probability

$$p = \frac{1}{1 + e^{-\beta(f_B - f_A)}} \quad (56)$$

where f_A (f_B) stands for the fitness of *A* (*B*) and β denotes the intensity of selection [29]. In the mean-field limit, in which everyone is equally likely to interact with anyone else (also known as well-mixed population approximation, this dilemma inexorably condemns cooperation to extinction [27], a fate which may change when individuals are embedded in a social network represented by means of a graph, in which structural diversity is ubiquitous [1, 2, 10, 11, 8, 3, 12, 9, 22, 23, 24, 25, 26, 28, 30, 31, 32, 33, 34, 35].

Moreover, information transmission has been sometimes regarded as contagious [15, 36], similar to the propagation of infectious diseases [9]. Hence, we also study a widely used model of disease spreading — the *Susceptible-Infected-Recovered* model (**SIR**) [37], in which individuals can be either in a Susceptible (*S*), Infected (*I*) or Recovered (*R*) epidemiological state [9, 37]. An infected individual can either infect a susceptible neighbor at an infection rate α , or recover and become immune at a recovery rate γ .

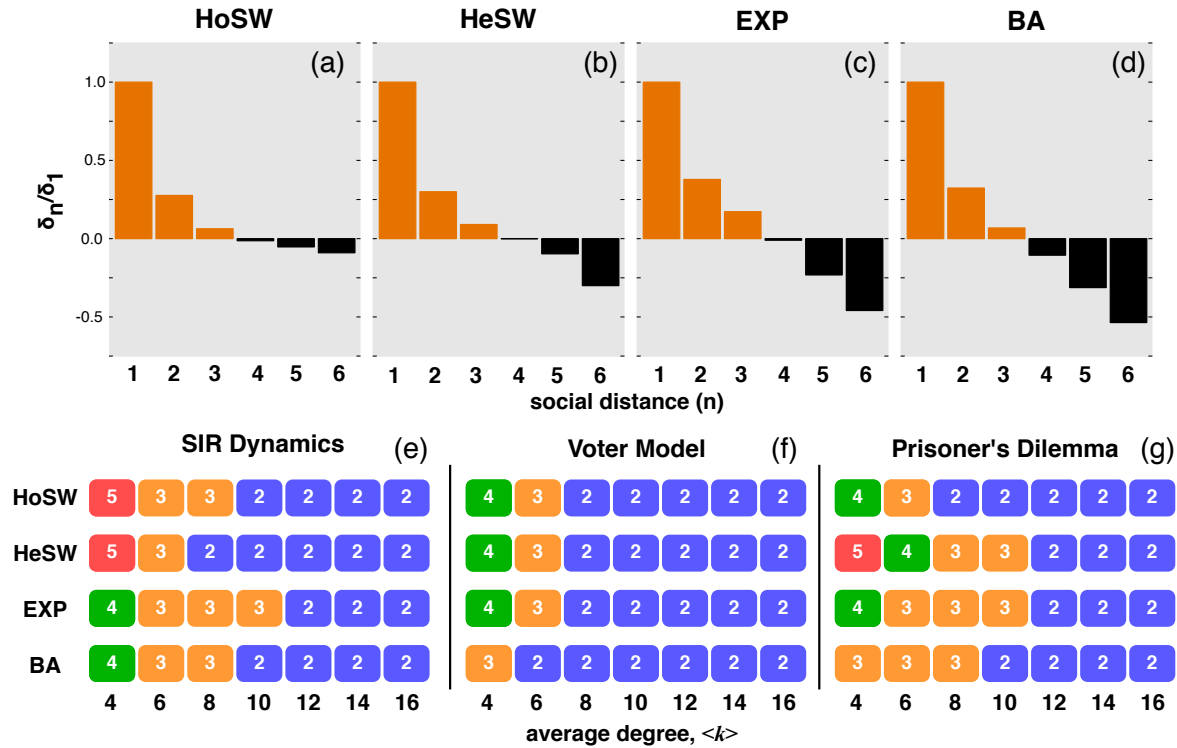


Figure 24: Peer influence in social networks. **Upper panels.** δ_n/δ_1 for Recovered and Infected individuals in the **SIR** Epidemic Model taking place in (a) Homogeneous small world networks; (b) Heterogeneous small world networks; (c) Exponential networks and (d) Scale-free networks. **Lower panels.** Critical degree of peer-influence n_c (defined as the largest network distance n for which $\delta_n > 0$) for different values of average degree $\langle k \rangle$ and network classes shown in the top panels, for the following traits and processes (see main text for details): (e) Recovered and Infected individuals in the **SIR** Epidemic Model (as above), (f) Individuals with the same opinion in the **VM**, and (g) Cooperators in the evolutionary **PD** game. All panels correspond to networks of size $Z = 10^3$ and results in the upper panels were obtained for networks with an average degree $\langle k \rangle = 6$. For larger network (and population) sizes, the negative values of the peer-influence correlation amplitudes that one obtains above n_c (see upper panels) will slowly approach 0 — highlighting the importance of finite-size effects in evaluating peer-to-peer processes. The reason for the negative correlation values for $n > n_c$ in finite (and small) networks is clear: at a network distance n_c , most of the individuals with the same trait have been already sampled (see Fig. 2 in Section 2.2); thus, for larger network distances, negative correlations will inevitably build up. At any rate, it is possible to clearly identify two regions of influence separated by n_c (see Section 2.2 for additional details).

Given the structural diversity of social networks [10, 33, 2, 34] in which some individuals interact and/or are taken as role models more and more often than others, we investigate the role played by the distribution of the number of first neighbors of each individual (the degree distribution, [2]) and clustering [2, 35] (a measure of the number of individuals' neighbors who are also neighbors of each other) in the emerging patterns of correlations. To this end, we employ four network classes [33] 2.2 with increasing variance of the degree distribution and similar low levels of clustering: homogeneous

and heterogeneous small-world networks, and exponential and scale-free networks [10, 33, 2]. Homogeneous small-world (**HoSW**) networks were obtained by repeatedly swapping the ends of pairs of randomly chosen links of a regular ring. Scale-free networks (**BA**) were obtained combining growth and preferential attachment, following the model proposed by Barabási and Albert [2]. Exponential networks (**EXP**) were obtained by adopting the same algorithm, with preferential attachment replaced by random attachment [2]. Heterogeneous small-world (**HeSW**) networks were built adopting the limit $p = 1$ of the Watts-Strogatz model [35], in which all links are rewired. Results reported in the main text refer to networks with $Z = 10^3$ (see Fig. 24) nodes, of the same order of magnitude of those investigated in [23, 22, 24, 25] and for which finite-size effects are non-negligible. In ??, we investigate in detail the behavior of correlations as a function of the network size.

To obtain $\epsilon_n(j/Z)$ we compute, for each network configuration, the average fraction of nodes that exhibit the same trait at a distance n . Hence, for each dynamical process, $\epsilon_n(j/Z)$ results from averaging over 10^6 independent network configurations. For the **PD** and **VM** processes, simulations were carried out starting from random configurations of traits; configurations included in the average were extracted after a transient of 10^3 generations (1 generation = Z iterations). For the **SIR** process, each simulation was started with a single I in a population of S ; α and γ were defined such that the population would often reach a state with no I s left, see Section 2.2.

The upper panels of Fig. 24 illustrate the normalized correlation values — δ_n/δ_1 , which, as shown in Fig. 23b, are approximately independent from j/Z — obtained for the **SIR** dynamics in **HoSW**, **HeSW**, **EXP** and **BA** networks. We observe that, regardless of the network topology, $n_c = 3$ as in Refs. [23, 22, 24, 25, 26]. Similar trends are also obtained for the two other dynamical processes introduced above, see Section 2.2. This is shown in the lower panels of Fig. 24, which also show how the critical network distance (n_c) stabilizes at $n_c = 2$ with increasing network connectivity (e.g., $\langle k \rangle$), independently of the network structure, cluster coefficient and dynamical process (see also Section 2.2). On the contrary, deviations from this universal behavior of n_c are obtained only whenever networks become very sparse, associated with the smallest values of the average connectivity. Counter-intuitively, the sparser the underlying network, the more far-reaching the influence of each individual will be, extending beyond the most pervasive value of 2. Needless to say, the absolute values of the correlations, depicted in the upper panels, will depend on the specific model parameters, but not the final value of n_c .

Besides being heterogeneous, social networks often exhibit sizable levels of clustering [2], contrary to the negligible values that characterize the ones utilized in Fig. 24. To evaluate the impact of this property, we generate, in 2.2, networks with arbitrary clustering for each network class [34]. We show how n_c remains limited between 2 and 4 for each of the three heterogeneous networks under study, irrespectively of their clustering coefficient and average degree. Nonetheless, we observe that increasing levels of clustering act to enlarge n_c , mostly whenever networks are very sparse, thus increasing sizeably their average path length, see Section 2.2.

Overall, our results suggest that the extent of peer influence emerges as a natural outcome of dynamical processes on structured populations, being pervasive in a wide-range of phenomena occurring in social networks. Despite the importance of social networks in defining the paths and ends of the

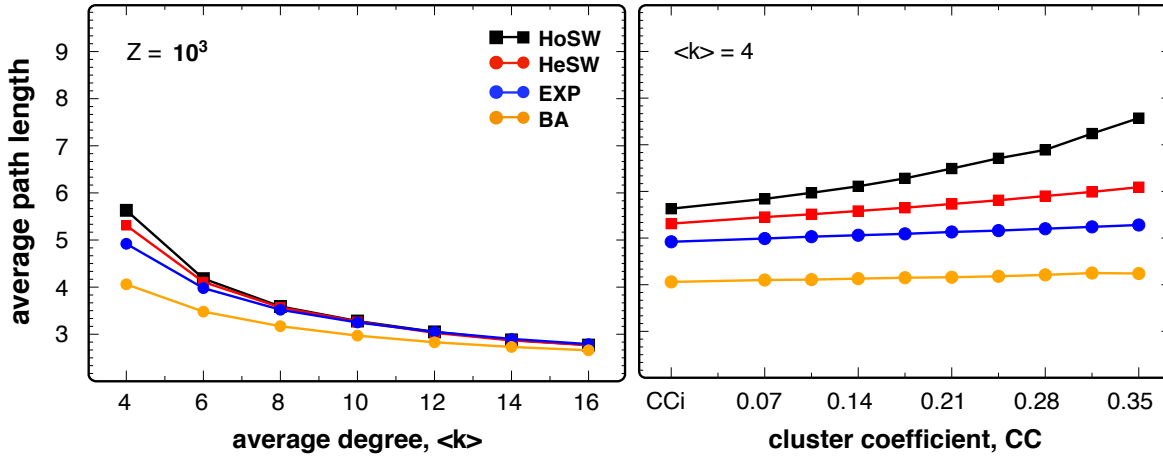


Figure 25: Network Properties. Average Path Length as a function of the average degree (left panel) and cluster coefficient (right panel). Different colors are used for each of the topologies studied (as indicated). Each network has $Z = 10^3$ individuals; each data point corresponds to an average over 100 different networks.

dynamical processes they support, showing how important it is to address and understand population dynamics from a complex networks perspective [9, 11, 31, 32, 38], the patterns of peer-influence they exhibit are surprisingly independent of their structure. On the other hand, when networks are very sparse, different network properties may contribute to enlarge the sphere of influence of each individual. Our results also show how networks naturally entangle individuals into interactions of many-body nature: Indeed, social networks effectively extend, in non-trivial ways, the dyadic interactions we started from. The fact that the network distance between any two individuals in social networks is small [2, 10] and comparable to n_c further enhances the significance of the present results, as they stress how our individual actions may have wide scopes and counter-intuitive repercussions.

2.2 SUPPLEMENTAL MATERIAL

This section provides supplementary information on the models and methodologies employed for the computation and analysis of the Peer Influence patterns discussed in section ?? of this chapter.

2.2.1 Social Structure

Let us consider a population of Z individuals embedded in a complex network of social interactions, where each node represents an individual and an undirected link a social interaction between two individuals. All links have the same weight equal to 1. The total number of interactions an individual i engages defines his degree k_i , while the fraction of individuals with degree k is given by the degree distribution $D(k)$. We shall refer to a network as homogeneous if all individuals have the same degree and heterogeneous otherwise. Moreover, we quantify the level of degree heterogeneity of a network by the variance of the degree distribution ($\sigma^2(k)$) [39].

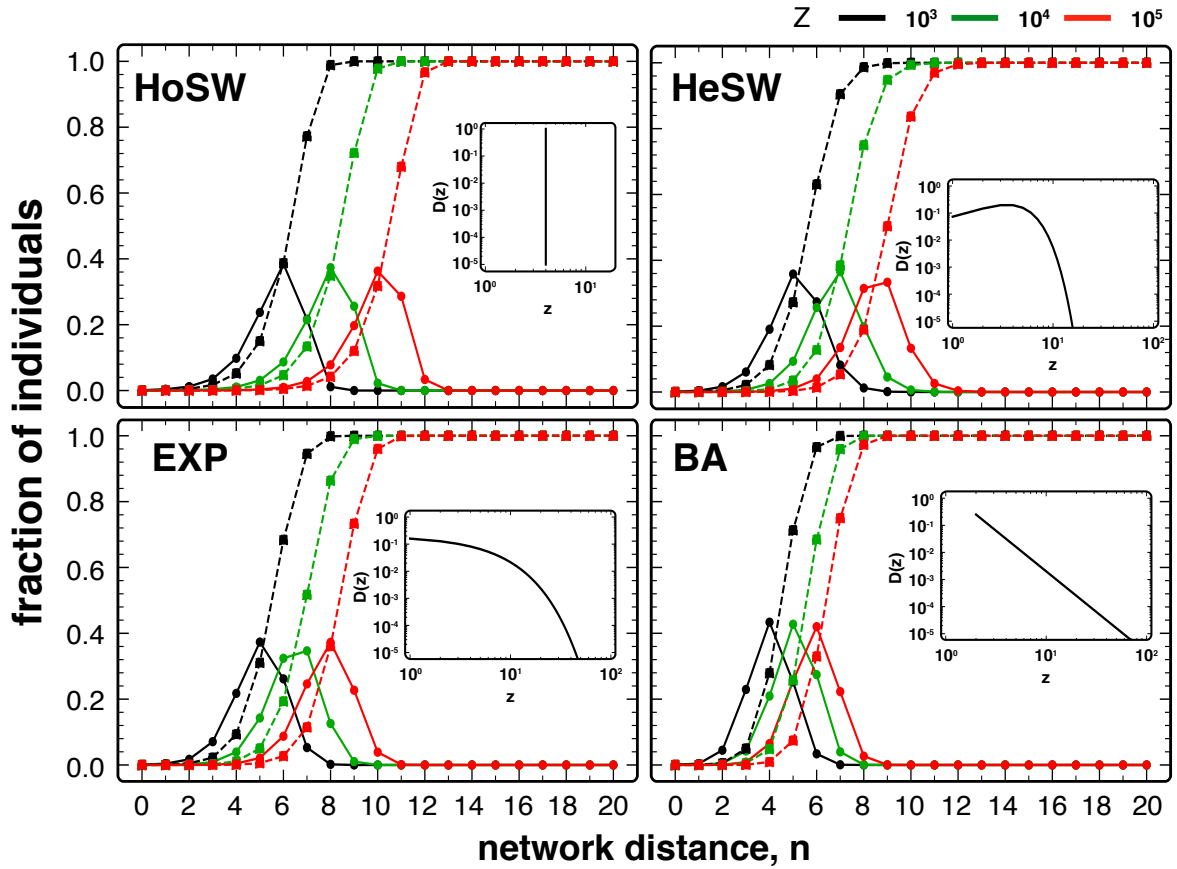


Figure 26: Average fraction of nodes at distance n , $\eta(n)$ from a random node of the population. Each panel shows the results for a different type of network: Homogeneous Small World networks (upper left panel); Heterogeneous Small World networks (upper right panel); exponential networks (bottom left panel) and scale-free networks (bottom right panel). Dashed lines denote the accumulated distribution, that is the fraction of nodes at a network distance lower or equal to n . Different colors refer to networks with different size: $Z = 10^3$ (black); 10^4 (green) and 10^5 (red).

Four different network topologies with different degree distributions are investigated in this work: Homogeneous Small World (HoSW) networks; Heterogeneous Small World (HeSW) networks; Exponential (EXP) and scale-free (BA) networks. Among these popular network types, BA and EXP networks are often regarded as good models of real world networks [33].

HoSW networks were generated by repeatedly swapping the ends of links from an initially regular network [40]. As a result all node-node correlations are eliminated while retaining their homogeneous character. HeSW networks were generated by rewiring half of the links of each node of a regular ring graph to a new random node in the population [35], forbidding link duplication and requiring overall network connectivity. The resulting degree distribution follows a Poisson distribution with k above $\langle k \rangle / 2$ [35], where $\langle k \rangle$ is the average connectivity of the network.

EXP networks are characterized by a degree distribution that follows an geometric distribution (exponential in the limit of very large populations) and were obtained by means of a growth mechanism with linear (random) attachment [10]. Similarly, BA networks were constructed by means of a growth

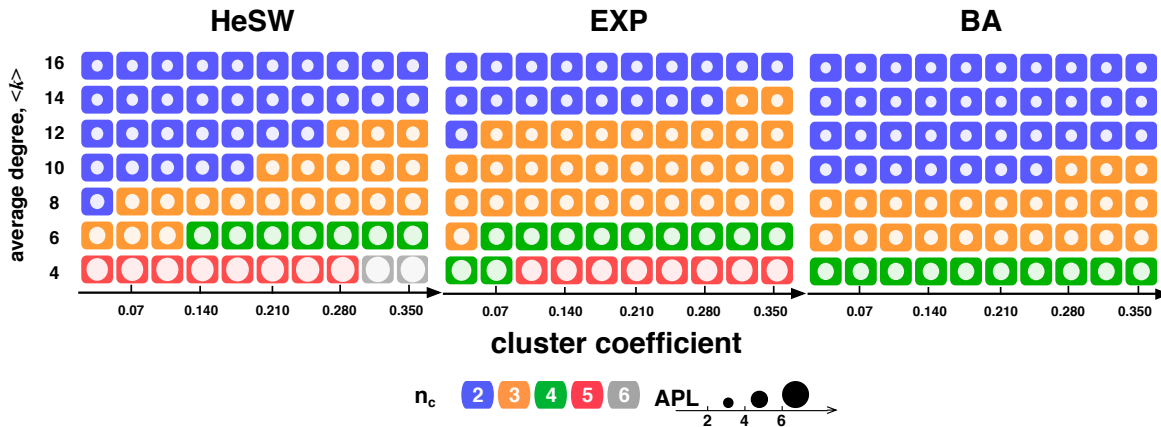


Figure 27: Critical network distance on heterogeneous social networks with different average degrees and cluster coefficient. Populations have $Z = 10^3$ individuals, each colored cell denotes a different network and circles correspond to their relative average path length (APL), which decreases with increasing average degree ($\langle k \rangle$) and decreasing cluster coefficient (CC).

mechanism combined with preferential attachment, which generates power law degree distribution [10, 2] characterized by the existence of a small group of nodes with a large number interactions, while the majority of the population engages in few.

Apart from the degree distribution, two other quantities of interest are used to characterize network topology: The clustering coefficient (CC) and the average path length (APL). The first concerns the fraction of neighboring individuals that share a common neighbor [41] and the second the average network distance (measured in terms of links traversed) between any two random individuals of the network [41].

By default, each network has a low CC (< 0.035); thus in order to inspect the impact of increasing CC on each topology we employ an algorithm proposed in [42] that increases the CC without changing the degree distribution, and that works as follows: at each iteration the ends of two randomly selected links are swapped; if the resulting network has a higher CC we validate this rewiring; otherwise we return to the initial network. These steps are repeated until the desired CC is attained.

Figure 25, shows how the APL changes with the $\langle k \rangle$ (left panel) and CC (right panel) for each of the topologies under study ($Z = 10^3$). Naturally, for a fixed CC, increasing $\langle k \rangle$ leads to a decrease of the APL; on the other hand, increasing CC for fixed $\langle k \rangle$ leads to an increase in the APL. Figure 26, in turn, shows the impact of network size on the average fraction of nodes at a distance of n links from any random node, a distribution that we denote as $\eta(n)$.

This network property provides a valuable indicator within this context, as it provides a measure of the sampling size available for each network distance and network topology (see Section 2). Interestingly, $\eta(n)$ peaks at different values of n for different population sizes (Z), shifting to larger n with larger Z , allowing for better statistics to be obtained for larger values of n . In the following sections we provide results of extensive numerical simulations in which we investigate the impact of different

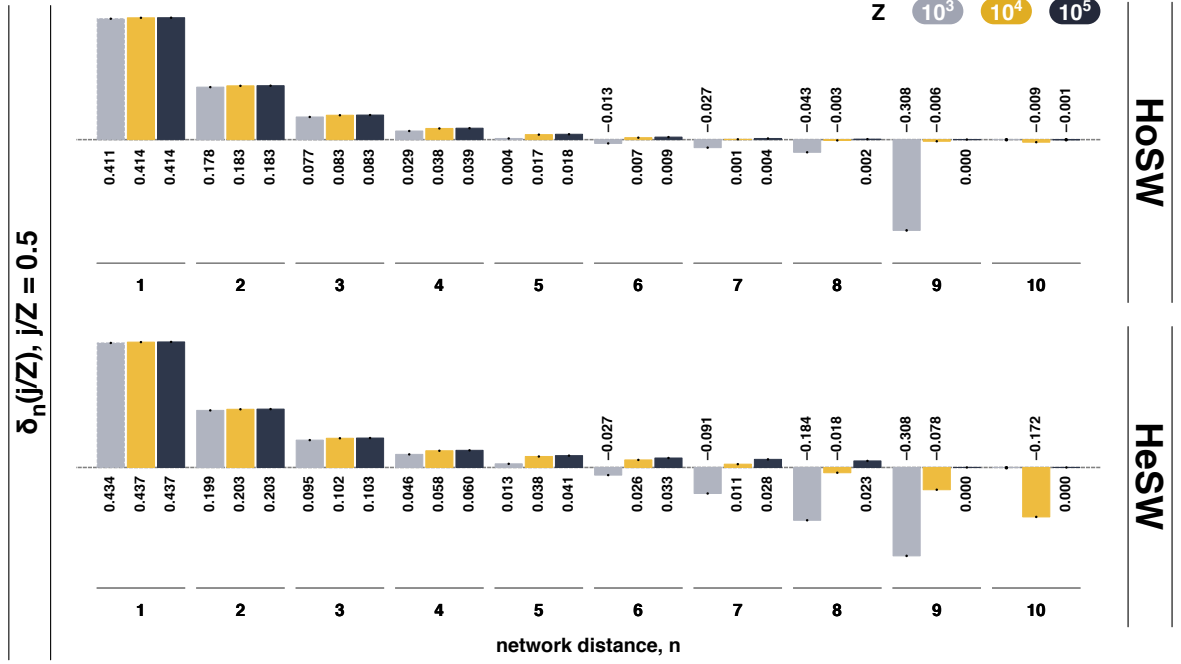


Figure 28: Peer Influence patterns on Homogeneous (upper panel) and Heterogeneous (bottom panel) Small World populations with different sizes. We assume populations composed by $Z = 10^3$ (gray), 10^4 (yellow) and 10^5 (black) individuals and average degree $\langle k \rangle = 4$ and show how the correlation values vary with the network distance.

dynamical processes on the peer influence patterns of structured populations with $Z = 10^3$, 10^4 and 10^5 . This is done for different levels of clustering coefficient CC and average degree $\langle k \rangle$.

2.2.2 Peer Influence

Let us consider a population of Z individuals in which j share a common trait. We designate by trait configuration any of the $Z + 1$ available states of the population characterized by j , that is $0 \leq j/Z \leq 1$.

Let us define $\epsilon_n(j/Z)$ as the probability that for a given j/Z two individuals at the distance of n links share the same trait. Therefore, if traits are distributed at random along the nodes of the population we expect $\epsilon_n(j/Z)$ to be, on average, equal to j/Z . The existence of positive/negative correlations of traits between individuals at a distance of n links can be conveniently measured by computing $\epsilon_n(j/Z) - j/Z$, where positive (negative) correlations of traits stand for individuals being assorted preferentially close to (away from) individuals with a similar trait.

For convenience, we also define $\delta_n(j/Z)$ as the average correlation of traits (normalized) between two nodes at the distance of n links, that is

$$\delta_n(j/Z) = \frac{\epsilon_n(j/Z) - j/Z}{j/Z} \quad (57)$$

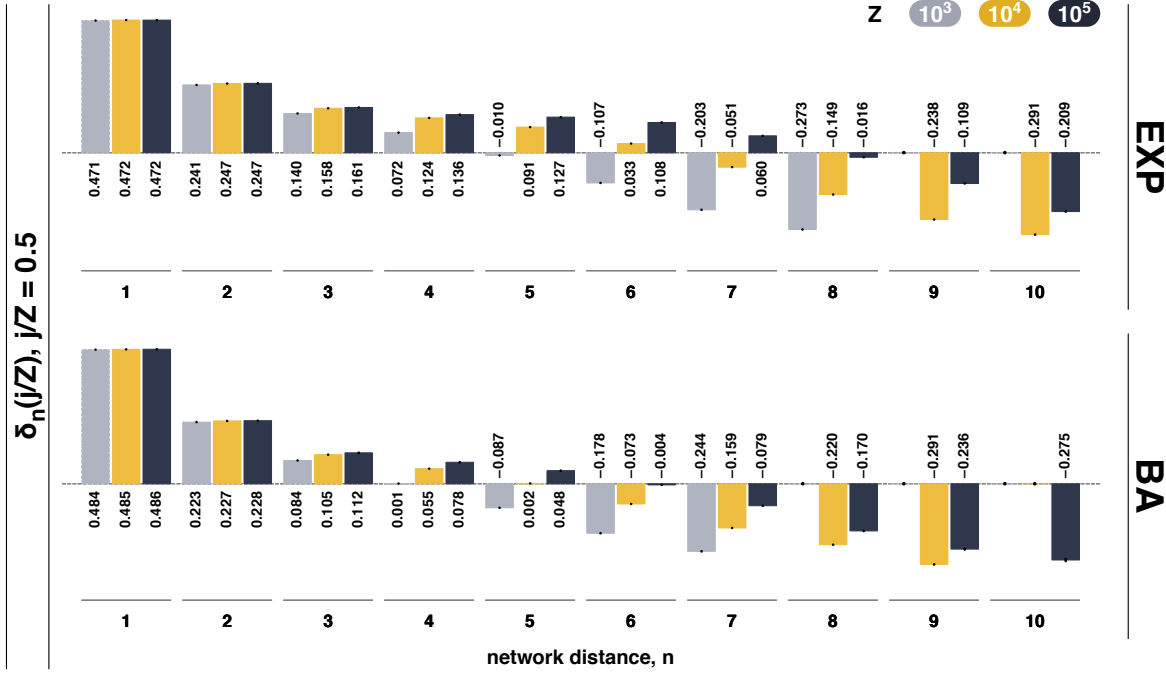


Figure 29: Peer Influence patterns on Exponential (upper panel) and scale free (bottom panel) populations of different sizes. We assume populations composed by $Z = 10^3$ (gray), 10^4 (yellow) and 10^5 (black) individuals and average degree $\langle k \rangle = 4$ and show how the correlation values vary with the network distance.

where the division by j/Z provides the convenient normalization that allows an easy interpretation and comparison with other works in the literature [23, 22, 24, 25].

The computation of $\delta_n(j/Z)$ requires the analysis of the network patterns of traits (that we refer to as network configurations) generated by each dynamical process under analysis. This task is divided in two steps: (1) a set of m network configurations produced by a dynamical process are extracted and (2) for each network configuration we compute $\delta_n(i; j/Z)$ (correlation at distance n for network configuration $1 \leq i \leq m$). The first step depends on the dynamical process at hand and hence the extraction of the network configurations is detailed at the beginning of the following three subsections. As for the second step, $\delta_n(j/Z)$ is computed as the average of $\delta_n(i; j/Z)$ over all m samples while the error bars shown in Figures below correspond to the expected deviations from the average, that is, $\sigma_n(j/Z)/\sqrt{m}$.

The quantity of interest in our analysis is the critical network distance above which $\delta_n(j/Z)$ becomes statistically negative, n_c , that is, when $\delta_n(j/Z) - \sigma_n/\sqrt{m} < 0$.

2.2.3 SIR Dynamics

SIR models and extensions have been extremely successful in investigating the propagation of contagious diseases from which individuals are able to acquire immunity. Chickenpox, measles and seasonal flu are a few real life examples of diseases that fall in this category. Here we follow closely the model studied in reference [43].

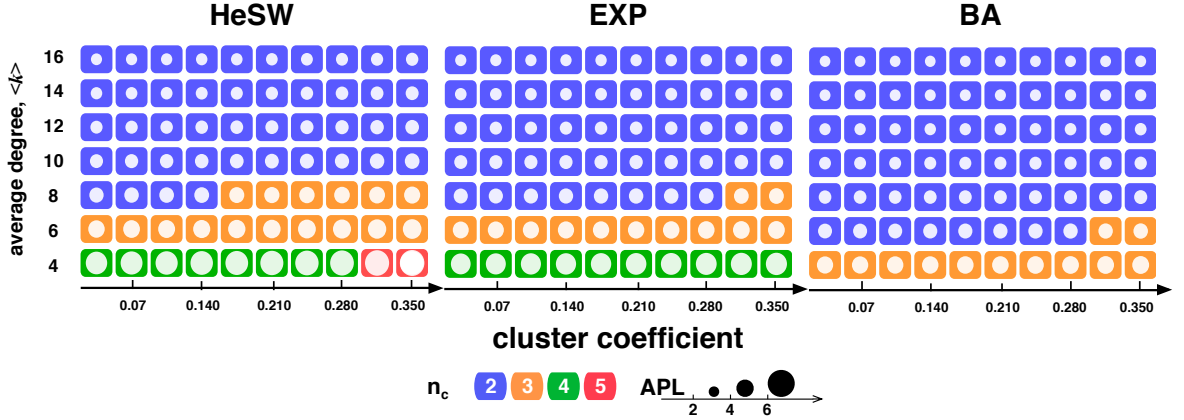


Figure 30: Critical network distance on heterogeneous social networks with different average degree and cluster coefficient. Populations have $Z = 10^3$ individuals. Each colored cell denotes a different network and circles correspond to their average path length (APL), which decreases with increasing average degree ($\langle k \rangle$) and decreasing cluster coefficient (CC).

Consider a population composed by individuals that can be, at any time, in one of three states: S (Susceptible); I (Infected) and R (Recovered), evolving under an asynchronous dynamics where at each time-step a recovery event occurs with probability p otherwise, with probability $1 - p$, an infection event occurs. Additionally, at each time step an individual A is selected at random from the population; if A is in state I and a recovery event was selected then I becomes R with probability α ; however if A was in state S and an infection event was selected then A becomes I with probability β if a randomly chosen neighbor of A is also in state I. For the purpose of computing correlations between traits, we consider correlations between S and both R and I, in the sense that the network pattern stems from the same dynamical event: S's becoming I's.

Each network configuration was extracted from a simulation that starts with a single source of infection. The outbreak evolved until the population reached the desired trait configuration. This procedure was repeated as many times as needed.

An appropriate β/α was chosen to ensure that most of the population becomes infected from a single infected individual regardless of the population structure, that is, above the most demanding epidemic threshold [44]. The peer influence patterns detected are, however, consistent for a wide range of β/α under this regime, thus providing a convenient set up in which to analyze the peer influence patterns that emerge for the entire domain of trait configurations.

Besides the results already shown in 24, Figure 27 shows how n_c changes with the CC (between 0 and 0.35, the range in which values obtained for real world networks fall) on heterogeneous populations.

Figure 27 evidences how n_c increases with increasing APL. This feature is explained by the fact that the network diameter (the maximum distance between any two nodes) follows the same trend of the APL, thus increasing with increasing CC and decreasing $\langle k \rangle$.

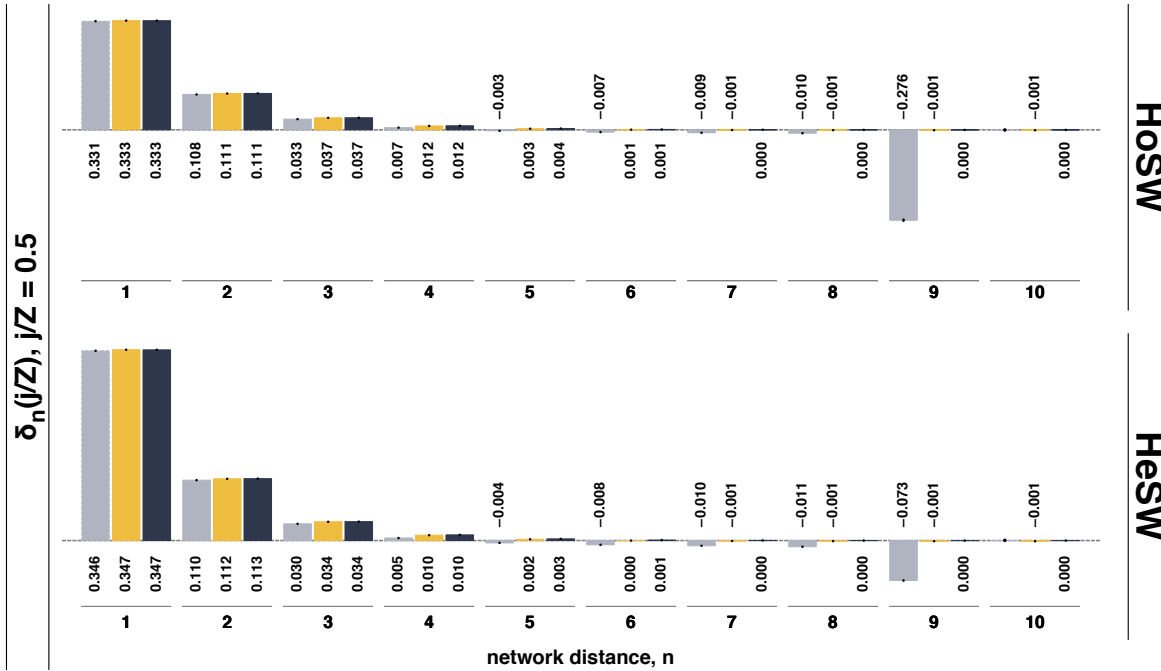


Figure 31: Peer Influence patterns on Homogeneous (upper panel) and Heterogeneous (bottom panel) Small World populations with different sizes. We assume populations composed by $Z = 10^3$ (gray), 10^4 (yellow) and 10^5 (black) individuals and average degree $\langle k \rangle = 4$ and show how the correlation values vary with the network distance.

Figures 28 and 29 show how the impact of population size (10^3 , 10^4 and 10^5) on the peer influence patterns generated from the SIR dynamics, putting in evidence the role of finite size effects. Values in the figures below (above) the bars identify a positive (negative) $\delta_n(j/Z)$. The absence of values above/below a certain value of n implies that there are no nodes at a distance of n links for that particular network size. Finally, bars of different colors represent populations of different sizes (gray correspond to 10^3 , yellow to 10^4 and black to 10^5).

For populations with 10^3 individuals, $\delta_n(j/Z)$ monotonically decreases with increasing n on all topologies. Thus there is a well defined critical network distance n_c above which $\delta_n(j/Z)$ become (increasingly) negative. For larger populations, however, this pattern is only kept on strongly heterogeneous populations (EXP and BA), while on Small World networks (HoSW and HeSW) $\delta_n(j/Z)$ tends to zero with increasing n , thus becoming difficult to identify n_c .

2.2.4 Voter Model

The Voter Model presents a simple yet highly successful framework in which to study opinion formation [9, 38, 45, 46]. Here we assume a structured population of individuals. Each individual can have one of two possible traits $S_i = 0$ or 1 . At each time-step (iteration) a randomly selected individual from the population imitates the trait of a randomly selected neighbor with probability p , which, without loss of generality, we consider equal to one.

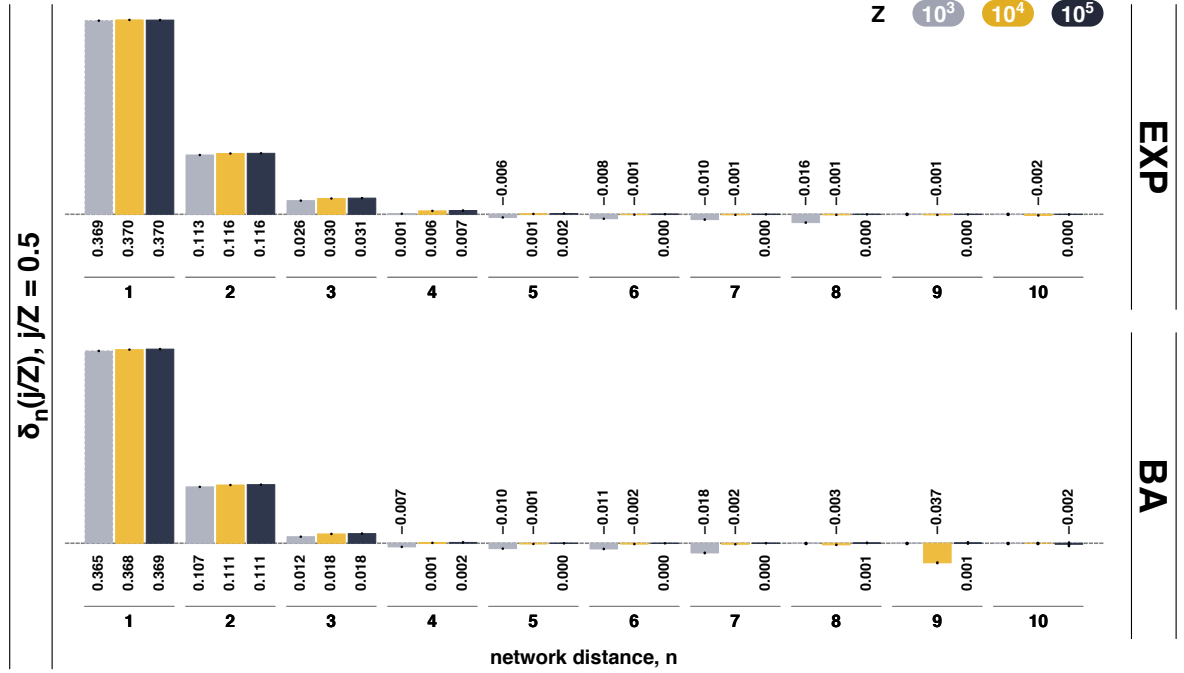


Figure 32: Peer Influence patterns on Exponential (upper panel) and scale free (bottom panel) populations of different sizes. We assume populations composed by $Z = 10^3$ (gray), 10^4 (yellow) and 10^5 (black) individuals and average degree $\langle k \rangle = 4$ and show how the correlation values vary with the network distance.

Each network configuration was extracted from populations that evolve from an initially random configuration of traits for a period of $\tau_t = 1.5 \times 10^3$.

A transient of $\tau_t = 10^3$ generations was considered. After the transient regime, network configurations associated with the desired trait configuration (j^*/Z) were stored with probability 10^{-3} , thus avoiding the same network configuration to be stored in consecutive time-steps. Once again we found that the critical network distance, n_c , tends to increase with increasing **APL** (white disks), see Figure 30. This happens for decreasing $\langle k \rangle$ or increasing **CC**. Figures 31 and 32 show the impact of population size (10^3 , 10^4 and 10^5) on the peer influence patterns generated from Voter Model dynamics.

Similar to the results obtained with the SIR dynamics, for populations with 10^3 , $\delta_n(j/Z)$ decreases monotonically with increasing network distance on all topologies. These results, however, contrast with the pattern of $\delta_n(j/Z)$ on larger populations that, overall (BA topologies constitute an exception) tend to zero with increasing network distance on all topologies.

2.2.5 Prisoner's Dilemma

Making use of Evolutionary Game Theory (EGT) [27, 47, 11, 48, 49] we now study the patterns of peer influence generated by a fitness driven evolutionary dynamics. Here we consider the most popular social dilemma of cooperation: The Prisoner's Dilemma (**PD** [27]).

Let us consider that each individual adopts unconditionally one of two strategies (to Cooperate or to Defect). Each interaction entails a payoff to both participating individuals that depends only on

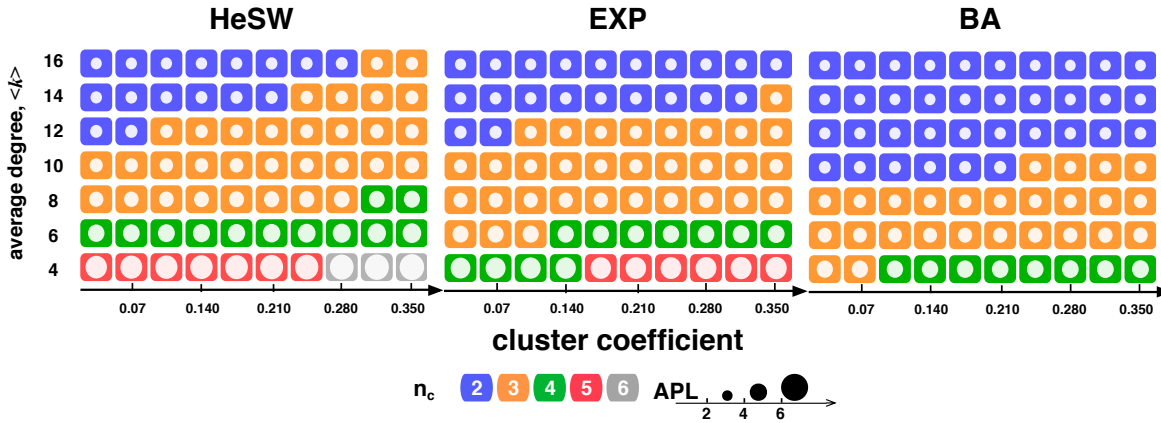


Figure 33: Critical network distance on heterogeneous social networks with different average degrees and cluster coefficient. Populations have $Z = 10^3$ individuals, each colored cell denotes a different network and circles correspond to their average path length (APL), which decreases with increasing average degree ($\langle k \rangle$) and decreasing cluster coefficient (CC)

the pair strategy. If both individuals cooperate each earns the reward (R) for mutual cooperation; if both defect each gets the punishment (P) for mutual defection; finally a cooperator facing a defector obtains the sucker's payoff (S) for being cheated upon, whereas the defector obtains the so called temptation (T) payoff. Here we shall adopt a standard parameterization of these four payoffs, making $R = 1.0$, $P = 0.0$, $T = 1 + \lambda$ and $S = -\lambda$; under these assumptions, $\lambda > 0$ ensures that individuals engage in a **PD**.

At each time-step a randomly selected individual A updates his/her strategy by imitating the strategy of a randomly selected neighbor B with probability [47, 11]

$$p_{fermi} = \frac{1}{1 - \exp(-\beta(f_B - f_A))} \tag{58}$$

where β is the intensity of selection (which regulates the randomness of the decision making process) and f_i is the fitness of individual i , which here is simply the accumulated payoff from all his interactions. Consequently, individuals imitate preferentially those peers that have a higher fitness, which may also be interpreted as a measure of social success.

Each network configuration was extracted from a time range of 2000 generations after an initial transient of 5 generations. Each evolution started from a random configuration of traits. During the observation time window, and whenever the system was at the desired trait configuration j/Z , the associated network configuration was stored with probability $\approx 10^{-3}$, thus lowering the chances of storing two consecutive network configurations.

On both **HoSW** and **HeSW** networks we analyze the peer influence patterns for $\lambda = 0.01$ while on EXP and BA populations we considered a harsher social dilemma with $\lambda = 1.25$. These values of λ can be shown to encapsulate the regimes of interest for the networks topologies under consideration [32, 28, 50].

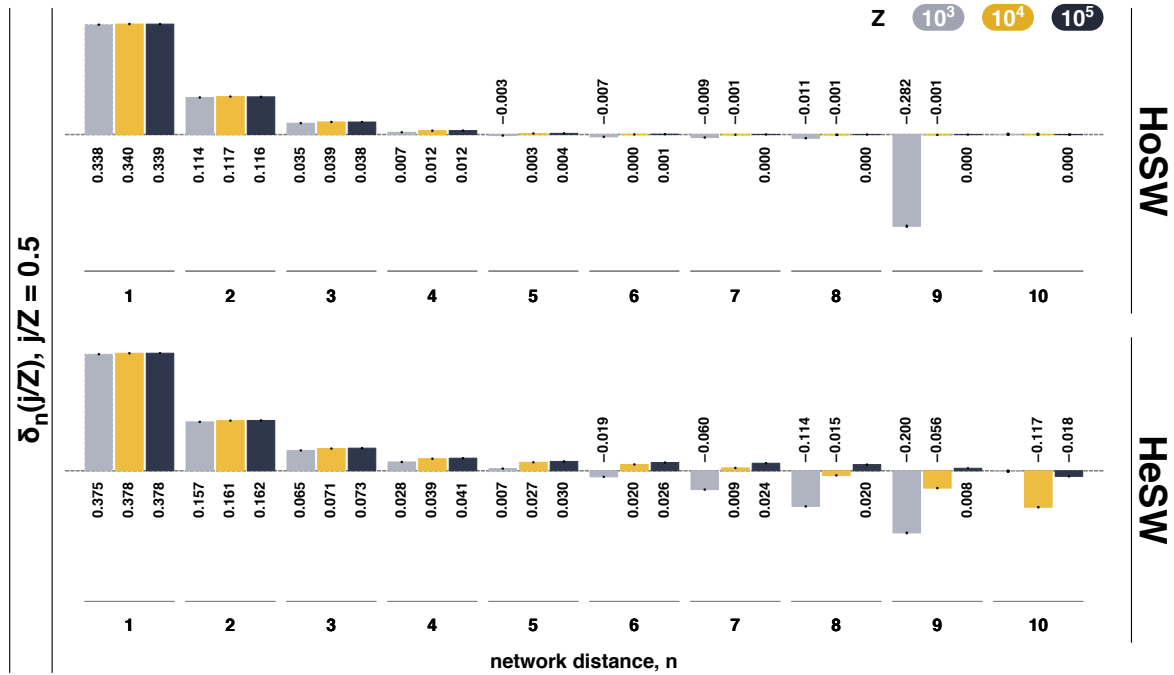


Figure 34: Peer Influence patterns on Homogeneous (upper panel) and Heterogeneous (bottom panel) Small World populations with different sizes. We assume populations composed by $Z = 10^3$ (gray), 10^4 (yellow) and 10^5 (black) individuals and average degree $\langle k \rangle = 4$ and show how the correlation values vary with the network distance

Once again we found that the critical network distance, n_c , tends to increase with increasing **APL** (white disks) – see Figure 33 – increasing as well with decreasing $\langle k \rangle$ or increasing **CC**.

We take into account the impact of each type of topology in the evolutionary dynamics of populations engaging in a **PD** by dividing our analysis in two different levels of λ : $\lambda = 0.01$ (Figure 34) and $\lambda = 0.25$ (Figure 35).

Figures 34 and 35 show the impact of population size (10^3 , 10^4 and 10^5) on the peer influence patterns generated from the EGT dynamics.

On **HoSW** populations we observe a consistent pattern that tends to zero with increasing network distance n . On heterogeneous populations, such as **HeSW**, **EXP** and **BA**, we obtain qualitatively the same pattern found in previous dynamics: a monotonic decrease with increasing network distance.

2.3 BIBLIOGRAPHY

- [1] Alun L Lloyd and Robert M May. How viruses spread among computers and people. *Science*, 292(5520):1316–1317, 2001.
- [2] Réka Albert and Albert-László Barabási. Statistical mechanics of complex networks. *Reviews of Modern Physics*, 74(1):47, 2002.
- [3] David Liben-Nowell and Jon Kleinberg. Tracing information flow on a global scale using internet chain-letter data. *Proceedings of the National Academy of Sciences*, 105(12):4633–4638, 2008.

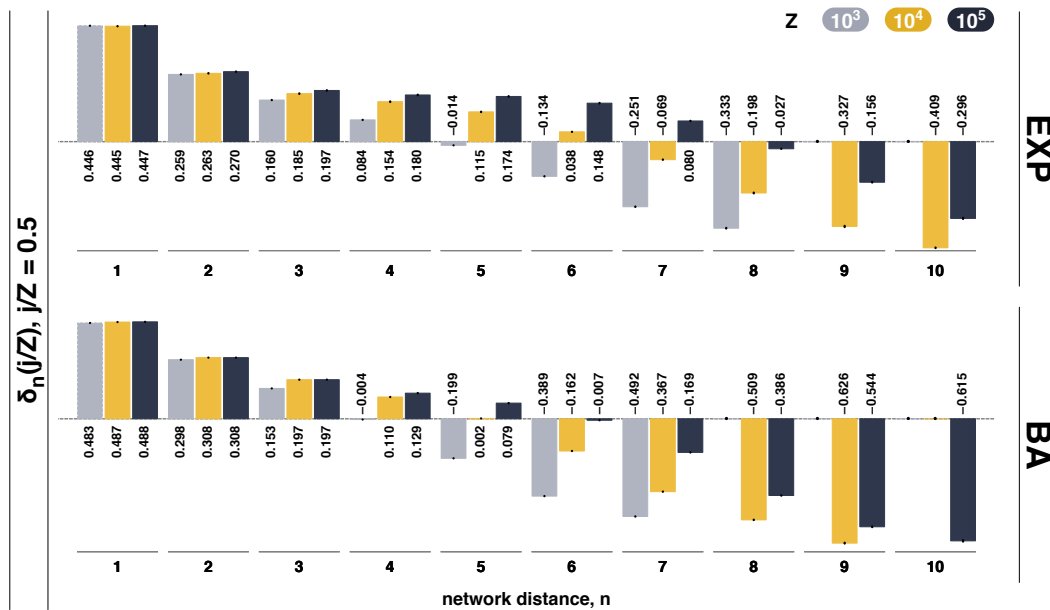


Figure 35: Peer Influence patterns on Exponential (upper panel) and scale free (bottom panel) populations of different sizes. We assume populations composed by $Z = 10^3$ (gray), 10^4 (yellow) and 10^5 (black) individuals and average degree $\langle k \rangle = 4$ and show how the correlation values vary with the network distance

[4] Meeyoung Cha, Hamed Haddadi, Fabricio Benevenuto, and P Krishna Gummadi. Measuring user influence in twitter: The million follower fallacy. *ICWSM*, 10:10–17, 2010.

[5] Ala Trusina, Martin Rosvall, and Kim Sneppen. Communication boundaries in networks. *Physical Review Letters*, 94(23):238701, 2005.

[6] Eytan Bakshy, Jake M Hofman, Winter A Mason, and Duncan J Watts. Everyone’s an influencer: quantifying influence on twitter. In *Proceedings of the fourth ACM international conference on Web search and data mining*, pages 65–74. ACM, 2011.

[7] Kevin Lewis, Jason Kaufman, Marco Gonzalez, Andreas Wimmer, and Nicholas Christakis. Tastes, ties, and time: A new social network dataset using facebook. com. *Social Networks*, 30(4):330–342, 2008.

[8] Jukka-Pekka Onnela and Felix Reed-Tsochas. Spontaneous emergence of social influence in online systems. *Proceedings of the National Academy of Sciences*, 107(43):18375–18380, 2010.

[9] Alain Barrat, Marc Barthélemy, and Alessandro Vespignani. *Dynamical processes on complex networks*, volume 1. Cambridge University Press Cambridge, 2008.

[10] Sergei N Dorogovtsev and José F F Mendes. *Evolution of networks: From biological nets to the Internet and WWW*. Oxford University Press, 2003.

[11] György Szabó and Gábor Fáth. Evolutionary games on graphs. *Physics Reports*, 446(4):97–216, 2007.

[12] Alex Arenas, Albert Díaz-Guilera, Jurgen Kurths, Yamir Moreno, and Changsong Zhou. Synchronization in complex networks. *Physics Reports*, 469(3):93–153, 2008.

2.3. Bibliography

- [13] Justin G Trogdon, James Nonnemaker, and Joanne Pais. Peer effects in adolescent overweight. *Journal of Health Economics*, 27(5):1388–1399, 2008.
- [14] Harikesh S Nair, Puneet Manchanda, and Tulikaa Bhatia. Asymmetric social interactions in physician prescription behavior: The role of opinion leaders. *Journal of Marketing Research*, 47(5):883–895, 2010.
- [15] Luís Bettencourt, Ariel Cintrón-Arias, David I Kaiser, and Carlos Castillo-Chavez. The power of a good idea: Quantitative modeling of the spread of ideas from epidemiological models. *Physica A: Statistical Mechanics and its Applications*, 364:513–536, 2006.
- [16] Edward L Glaeser, Bruce Sacerdote, and Jose A Scheinkman. Crime and social interactions. *The Quarterly Journal of Economics*, 111(2):507–548, 1996.
- [17] Antoni Calvó-Armengol and Yves Zenou. Social networks and crime decisions: The role of social structure in facilitating delinquent behavior*. *International Economic Review*, 45(3):939–958, 2004.
- [18] Antoni Calvó-Armengol. Job contact networks. *Journal of Economic Theory*, 115(1):191–206, 2004.
- [19] Lauren Cohen, Andrea Frazzini, and Christopher Malloy. The small world of investing: Board connections and mutual fund returns, 2007.
- [20] Bruce Sacerdote. Peer effects with random assignment: Results for dartmouth roommates. *The Quarterly Journal of Economics*, 116(2):681–704, 2001.
- [21] Pablo Brañas-Garza, Ramón Cobo-Reyes, María Paz Espinosa, Natalia Jiménez, Jaromír Kovářík, and Giovanni Ponti. Altruism and social integration. *Games and Economic Behavior*, 69(2):249–257, 2010.
- [22] James H Fowler and Nicholas A Christakis. Cooperative behavior cascades in human social networks. *Proceedings of the National Academy of Sciences*, 107(12):5334–5338, 2010.
- [23] Nicholas A Christakis and James H Fowler. The collective dynamics of smoking in a large social network. *New England Journal of Medicine*, 358(21):2249–2258, 2008.
- [24] Nicholas A Christakis and James H Fowler. The spread of obesity in a large social network over 32 years. *New England Journal of Medicine*, 357(4):370–379, 2007.
- [25] James H Fowler and Nicholas A Christakis. Dynamic spread of happiness in a large social network: longitudinal analysis over 20 years in the framingham heart study. *BMJ: British Medical Journal*, 337, 2008.
- [26] Coren L Apicella, Frank W Marlowe, James H Fowler, and Nicholas A Christakis. Social networks and cooperation in hunter-gatherers. *Nature*, 481(7382):497–501, 2012.
- [27] Karl Sigmund. *The calculus of selfishness*. Princeton University Press, 2010.
- [28] Francisco C Santos, Jorge M Pacheco, and Tom Lenaerts. Evolutionary dynamics of social dilemmas in structured heterogeneous populations. *Proceedings of the National Academy of Sciences*, 103(9):3490–3494, 2006.
- [29] György Szabó and Csaba Tóke. Evolutionary prisoner’s dilemma game on a square lattice. *Physical Review E*, 58(1):69, 1998.

Chapter 2. ORIGINS OF PEER INFLUENCE IN SOCIAL NETWORKS

- [30] Francisco C Santos and Jorge M Pacheco. Scale-free networks provide a unifying framework for the emergence of cooperation. *Physical Review Letters*, 95(9):098104, 2005.
- [31] Matjaž Perc and Attila Szolnoki. Coevolutionary games—a mini review. *BioSystems*, 99(2):109–125, 2010.
- [32] Flávio L Pinheiro, Jorge M Pacheco, and Francisco C Santos. From local to global dilemmas in social networks. *PLoS One*, 7(2):e32114, 2012.
- [33] Luis A Nunes Amaral, Antonio Scala, Marc Barthelemy, and H Eugene Stanley. Classes of small-world networks. *Proceedings of the National Academy of Sciences*, 97(21):11149–11152, 2000.
- [34] J-P Onnela, Jari Saramäki, Jorkki Hyvönen, György Szabó, David Lazer, Kimmo Kaski, János Kertész, and A-L Barabási. Structure and tie strengths in mobile communication networks. *Proceedings of the National Academy of Sciences*, 104(18):7332–7336, 2007.
- [35] Duncan J Watts and Steven H Strogatz. Collective dynamics of ‘small-world’ networks. *Nature*, 393(6684):440–442, 1998.
- [36] Elaine Hatfield, John T Cacioppo, and Richard L Rapson. Emotional contagion. *Current Directions in Psychological Science*, 2(3):96–99, 1993.
- [37] WO Kermack and AG McKendrick. Contributions to the mathematical theory of epidemics. iii. further studies of the problem of endemicity. *Proceedings of the Royal Society of London. Series A*, 141(843):94–122, 1933.
- [38] Tibor Antal, Sidney Redner, and Vishal Sood. Evolutionary dynamics on degree-heterogeneous graphs. *Physical Review Letters*, 96(18):188104, 2006.
- [39] Francisco C Santos, Flavio L Pinheiro, Tom Lenaerts, and Jorge M Pacheco. The role of diversity in the evolution of cooperation. *Journal of Theoretical Biology*, 299:88–96, 2012.
- [40] Francisco C Santos, JF Rodrigues, and Jorge M Pacheco. Epidemic spreading and cooperation dynamics on homogeneous small-world networks. *Physical Review E*, 72(5):056128, 2005.
- [41] Mark EJ Newman. The structure and function of complex networks. *SIAM Review*, 45(2):167–256, 2003.
- [42] Shweta Bansal, Shashank Khandelwal, and Lauren Meyers. Exploring biological network structure with clustered random networks. *BMC Bioinformatics*, 10(1):405, 2009.
- [43] Sven Van Segbroeck, Francisco C Santos, and Jorge M Pacheco. Adaptive contact networks change effective disease infectiousness and dynamics. *PLoS Computational Biology*, 6(8):e1000895, 2010.
- [44] Romualdo Pastor-Satorras and Alessandro Vespignani. Epidemic spreading in scale-free networks. *Physical Review Letters*, 86(14):3200, 2001.
- [45] Vishal Sood, Tibor Antal, and Sidney Redner. Voter models on heterogeneous networks. *Physical Review E*, 77(4):041121, 2008.
- [46] Thomas M Liggett. *Stochastic interacting systems: contact, voter and exclusion processes*, volume 324. Springer, 1999.
- [47] Arne Traulsen, Martin A Nowak, and Jorge M Pacheco. Stochastic dynamics of invasion and fixation. *Physical Review E*, 74(1):011909, 2006.

2.3. Bibliography

- [48] John Maynard Smith. *Evolution and the Theory of Games*. Springer, 1993.
- [49] Josef Hofbauer and Karl Sigmund. *Evolutionary games and population dynamics*. Cambridge University Press, 1998.
- [50] Flávio L Pinheiro, Francisco C Santos, and Jorge M Pacheco. How selection pressure changes the nature of social dilemmas in structured populations. *New Journal of Physics*, 14(7):073035, 2012.

FROM LOCAL TO GLOBAL DILEMMAS IN SOCIAL NETWORKS

PLOS ONE, 10.1371/journal.pone.0032114 (2012)

Flávio L. Pinheiro, Jorge M. Pacheco and Francisco C. Santos

In the previous chapter we developed a methodology to study and characterise the emerging peer influence patterns in complex networks. This was done for three different dynamical processes and tested over several network topologies. We have shown that these are a natural consequence of dynamical processes in complex networks, being largely independent of the way information spreads on a network, and that they show similar properties to the patterns already observed in empirical studies.

A more fundamental problem concerns the relation between local and collective dynamics in complex networks, similar to what happens in many other areas of Physics. Indeed, social networks affect in such a fundamental way the dynamics of the population they support that the global, population-wide behaviour that one observes often bears no relation to the individual processes it stems from. Up to now, linking the global networked dynamics to such individual mechanisms has remained elusive. Here we study the evolution of cooperation in networked populations and let individuals interact via a 2-person Prisoner's Dilemma – a characteristic defection dominant social dilemma of cooperation. We show how homogeneous networks transform a Prisoner's Dilemma into a population-wide evolutionary dynamics that promotes the coexistence between cooperators and defectors, while heterogeneous networks promote their coordination. To this end, we define a dynamic variable that allows us to track the self-organisation of cooperators when co-evolving with defectors in networked populations. Using the same variable, we show how the global dynamics – and effective dilemma – co-evolves with the motifs of cooperators in the population, the overall emergence of cooperation depending sensitively on this co-evolution.

3.1 MANUSCRIPT

3.1.1 *Introduction*

Dynamical processes involving populations of individuals constitute paradigmatic examples of complex systems. From epidemic outbreaks to opinion formation and behavioral dynamics [1, 2, 3, 4, 5, 6, 7, 8, 9], the impact of the underlying web of ties in the overall behavior of the population is well known. In this context, Evolutionary Games [10, 11] provide one of the most sophisticated examples of complex dynamics in which the role of the underlying network topology proves ubiquitous. For

instance, when cooperation is modeled as a Prisoner's dilemma game, cooperation may emerge (or not) depending on how the population is networked [12, 13, 14, 15, 16, 17, 18, 19, 20, 21, 22, 23, 24, 25, 26, 27, 28, 29, 30, 31, 32, 33, 34, 35, 36, 37, 38].

Up to now, it has been hard to characterize in detail the global dynamics by which local self-regarding actions lead to a collective cooperative scenario, relating it to the network topology. Indeed, most network studies have been focused on the analysis of the evolutionary outcome of cooperation [14] – either by means of the numerical analysis of steady states [12, 16, 18, 19, 24, 25, 30, 33, 35, 36, 39, 40, 41] or by means of the analytical determination of the conditions for fixation in the population or by means of the determination of positive inclusive fitness effects for particular homogeneous network interaction structures and low intensities of selection [17, 20, 22] – without characterizing the self-organization process by which one of the strategies outcompetes the other. Here we show how networked individuals, engaging in a Prisoner's dilemma (**PD**) of cooperation, give rise to a global, population wide, behavioral dynamics which deviates strongly from the original **PD**, depending sensitively on the underlying network of contacts: Homogeneous networks promote a coexistence dynamics between cooperators and defectors – akin to the Chicken or Snowdrift game [11, 39, 42, 43, 44] – whereas heterogeneous networks, from broad scale to scale-free [4, 27], favor the coordination between them, similar to the Stag-hunt game [45].

To this end we define a time-dependent variable – that we call the average gradient of selection (**AGoS**) – and use it to track the self-organization of cooperators when co-evolving with defectors under network reciprocity. Similar to existing analytical approaches [44, 46], the **AGoS** is able to provide a measure of the change in time of the frequency of cooperative traits under selection. The **AGoS** can be computed for arbitrary intensity of selection (see Section 3.1.5), arbitrary population structure and arbitrary game parameterization. We further prove that the global games are not fixed: they change in time, co-evolving with the motifs of cooperators in the population. The evolutionary outcome of such a self-organization process will depend sensitively on this co-evolution, which can be followed using a time-dependent **AGoS**.

3.1.2 Dynamical Model

Let us consider pairwise interactions between individuals who can behave either as a *Cooperator* (**C**) or *Defector* (**D**). Whenever cheated by a **D**, a **C** receives a payoff S (the sucker's payoff), while the **D** receives T (temptation to defect). Mutual cooperation provides R (reward) to each player, while mutual defection provides P (punishment). One obtains the Prisoner's dilemma (**PD**) – the most famous metaphor of cooperation – whenever $T > R > P > S$. We formalize the dilemma in terms of a single parameter b (benefit) by defining $T = B > 1$, $R = 1$, $S = 1 - B$ and $P = 0$. The results remain quantitatively unaltered if one adopts the more popular parameterization $T = b$, $R = b - c$, $S = -c$ and $P = 0$.

In the framework of evolutionary game theory, we adopt a stochastic update rule of social learning, where in each time step a random individual i imitates the strategy of a randomly selected neighbor j with a probability that increases with the fitness difference between them [14, 24, 48, 49, 50, 51] (see Section 3.1.5). In the limit of well-mixed populations of size N [10, 11], the frequency j/N of

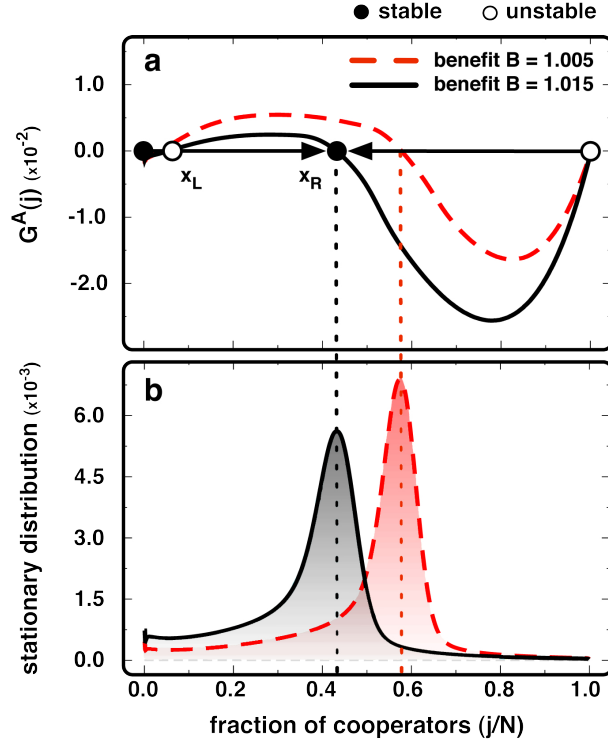


Figure 36: Time-independent AGoS. (a) We plot $G^A(j)$ for a population of players interacting via a **PD** in a homogeneous random network, for two values of the benefit b . Globally, $G^A(j)$ indicates that the population evolves towards a co-existence scenario. (b) Stationary distributions showing the pervasiveness of each fraction j/N in time. In line with the **AGoS** in a), the population spends most of the time in the vicinity of the stable-like root x_R of $G^A(j)$. When $j/N \approx 0$, *Cooperators* become disadvantageous, giving rise to an unstable-like root x_L of $G^A(j)$ which, however, plays a minor role as shown ($N = 10^3$, $\langle k \rangle = 4$ and $\beta = 1.0$). Homogeneous random networks were obtained by repeatedly swapping the ends of pairs of randomly chosen links of a regular lattice [47].

Cooperators will increase (decrease) in time depending on whether the gradient of selection [52, 53] $G(j) = T^+(j) - T^-(j)$ is positive (negative), where T^\pm [48] represent the probabilities to increase and decrease the number of *Cooperators* in the population by one. For the **PD**, $G(j) < 0$ for all j and, as a result, cooperation will most probably die out. The same scenario is obtained when $N \rightarrow \infty$, where we recover the scenarios described by the famous replicator dynamics [11, 48, 49, 50, 51]. The elegance of this result (despite the doomsday scenario for *Cooperators*) is best appreciated when we realize that the population ends up adopting the Nash-equilibrium of a **PD** game interaction between two individuals: everybody defects. Consequently, there is no difference in the outcome of the game, from an individual or from a (collective) population wide perspective, a feature that, as discussed below, will not remain true in structured populations.

3.1.3 Results

The previous analysis assumes finite yet structureless populations, a feature which is seldom observed in practice, with strong implications in many natural phenomena. A homogeneous network of size N represents the simplest case of a structured population, where all individuals engage in the same number of games k with their first neighbors, also imitating their behavior. Let us consider a homogeneous random network – also called a regular random graph – in which all links are randomly connected, while all nodes have each the same number of links [4, 54, 47]. In this case, individuals with the same strategy no longer share the same fitness: fitness becomes context-dependent. The same happens to $G(j)$, becoming hard to define it analytically. Consequently, we define the **AGoS** – denoting it by $G^A(j)$ – as the average *i*) over all possible transitions taking place in every node of the network throughout evolution, and *ii*) over a large number of networked evolutions (see Section 3.1.5). This **AGoS**, which must be computed numerically, becomes therefore network dependent but context independent, as it recovers its population averaged, or mean-field, character. Hence, the **AGoS** may constitute a powerful tool to understand dynamical processes at a population-wide scale stemming from individually defined, but often seemingly unrelated, rules.

The results for $G^A(j)$ on homogeneous networks of size $N = 10^3$, $k = 4$ and different values of a are shown in Fig. 36a. Unlike well-mixed populations where cooperation has no chance, homogeneous networks can sustain cooperation [12, 14, 15, 24, 47]. The shape of $G^A(j)$ no longer pictures a defection dominance dilemma typical of a **PD**, but a gradient of selection similar to what one observes under co-existence dilemmas in well-mixed populations [44]. In other words, even though every individual engages in a **PD**, from a global, population-wide perspective, homogeneous networks are able to create an emerging collective dynamics promoting the co-existence between *Cooperators* and *Defectors*. As we show below, the emergence of an unanticipated global (macroscopic) dynamics from a distinct individual (microscopic) dynamics pervades throughout all evolutionary dynamical processes in structured populations studied here. The co-existence point x_R (see Fig. 36a) is associated with the internal root ($x_R \in]0, 1[$) of $G^A(j)$ – inexistent in well-mixed populations – whose location decreases with increasing B . Together with x_R one obtains a coordination root ($x_L \approx 0$, see Fig. 36a) of $G^A(j)$ since, in the absence of cooperative partners, *Cooperators* will always be disadvantageous. However, the impact of x_L is minor, as shown in Fig. 36b (see discussion below). Remarkably, this characterization remains valid for other types of homogeneous networks, such as lattices and regular rings (as well as for other possible mechanisms of strategy update) whereas differences in the positions of the stable root (x_R) in of $G^A(j)$ and their dependence on b correlate perfectly with results obtained previously [14, 18, 24, 47, 55, 56, 57, 58], where steady-states of evolution were analyzed for such structures (see Section 3.2.1).

Fig. 36a shows that, as we change focus from an individual to a population wide perspective, one witnesses the emergence of an effective game transformation, as evidenced by $G^A(j)$, which brings along important consequences: For instance, the fixation time – the time required for cooperators to invade the entire population – becomes much larger in homogeneous networks when compared to well-mixed populations, as the population spends a large period of time in the vicinity of the x_R , mainly when selection is strong (see Section 3.1.5). This, in turn, is responsible for computer simulations to

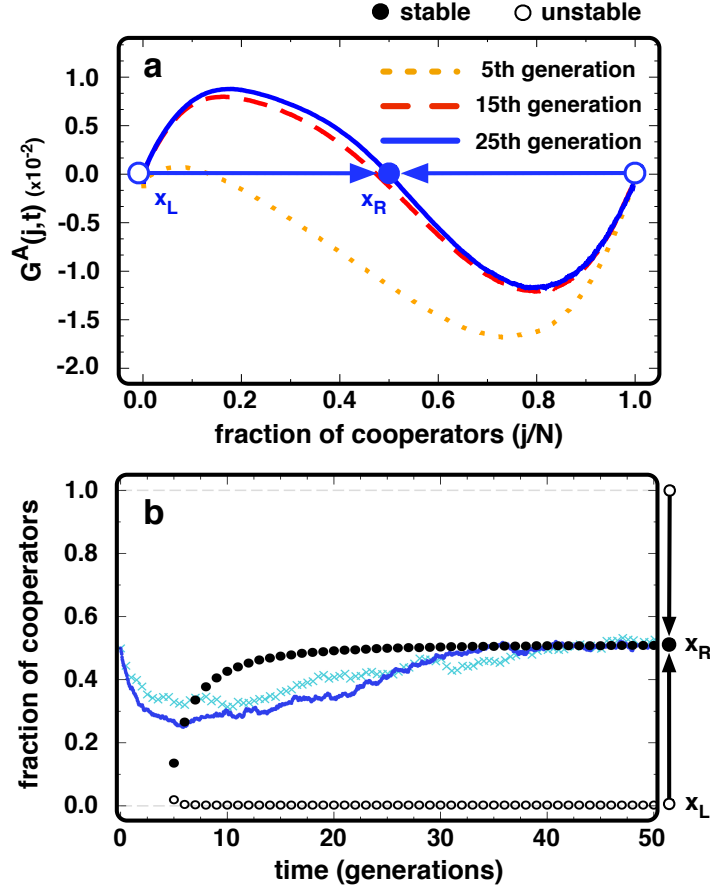


Figure 37: Time-dependent AGoS. (a) We plot $G^A(j,t)$ for three different instants of evolutionary time. Each line provides a snapshot for a given moment, portraying the emergence of a population-wide (time-dependent) co-existence-like dilemma stemming from an individual (time-independent) defection dominant dilemma (PD). (b) The circles show the position of the different interior roots of $G^A(j,t)$, whereas the solid (dark blue) line and (light blue) crosses show two independent evolutionary runs starting from 50% of *Cooperators* and *Defectors* randomly placed in the networked population. Open (full) circles stand for unstable, x_L (stable, x_R) roots of $G^A(j,t)$ ($b = 1.01$, $N = 10^3$, $\langle k \rangle = 4$ and $\beta = 10.0$).

spend arbitrary amounts of time in the same configuration, even when, in the absence of mutations (as is the case here), the only absorbing states are associated with monomorphic configurations of the population, that is, with configurations comprising cooperators-only or defectors-only. The stationary distribution (Fig. refpone2012:Fig1b), which represents the pervasiveness of each fraction of *Cooperators* in time, confirms the scenario portrayed by in Fig. 36a, stressing the similarities with the evolutionary dynamics in (finite) well-mixed populations under co-existence dilemmas [51, 59, 60], and putting in evidence the marked difference between individual preferences and the population-wide dynamics.

In Fig. 36, our analysis was limited to $G^A(j)$ that is, we averaged over the entire time span of all runs. However, the AGoS itself evolves in time – $G^A(j,t)$ – as detailed in section 3.2.1. Let us explore

this time dependence of the **AGoS**. If, at the beginning of each simulated evolution, *Cooperators* and *Defectors* are randomly spread in the network, the occurrence of clusters of the same strategy will not occur in general. Hence, for the **PD** we have that $G^A(j, t = 0) < 0$ in general. As populations evolve, *Cooperators* (*Defectors*) breed *Cooperators* (*Defectors*) in their neighborhood, promoting the assortment of strategies, with implications both on the fitness of each player and on the shape (and sign) of $G^A(j, t)$. In Fig. 37a we plot for three particular generations, whereas Fig. 37b portrays the time evolution of the internal roots of $G^A(j, t)$, on which we superimposed two evolutionary runs starting with 50% of *Cooperators* randomly placed in the population. As $G^A(j, t = 0) < 0$, the fraction of cooperators will start decreasing (Fig.37a). However, with time, strategy assortment leads to the emergence of a co-existence root, toward which the fraction cooperators converges. The ensuing coexistence between *Cooperators* and *Defectors*, entirely described by the shape of $G^A(j, t)$, steams from the self-organization of *Cooperators* and *Defectors* in the network, defining a global dynamics which is impossible to foresee solely from the nature of the local (**PD**) interactions.

It is now generally accepted, however, that homogeneous networks provide a simplified picture of real interaction networks [5, 27, 61, 62]. Most social structures share a marked heterogeneity, where a few nodes exhibit a large number of connections, whereas most nodes comprise just a few. The fingerprint of this heterogeneity is provided by the associated degree distributions, which exhibit a broad-scale shape, often resembling a power-law [4, 27, 61]. In the following we use $G^A(j, t)$ to understand how heterogeneity shifts the internal roots in Fig. 36 to the right, thereby transforming a co-existence scenario into a coordination one. To this end, we compute $G^A(j, t)$ employing scale-free (SF) networks of Barabási and Albert (BA) (see Section 3.2.1) [61].

Fig. 38a shows $G^A(j)$ for **BA** networks of $N = 10^3$ nodes and an average degree $k = 4$, whereas the circles in Fig. 38b portray the time evolution of the internal roots of $G^A(j, t)$. Heterogeneous networks lead to a global dynamics dominated by a coordination threshold, originating the appearance of two basins of attraction split by an unstable root $x_{Skymrms} : 2001aa_L$ of $G^A(j, t)$, analogous to the evolutionary dynamics under 2-person and N-person Stag-hunt dilemmas in unstructured populations [45, 52, 63, 64]. This unstable root represents the critical fraction of *Cooperators* above which they are able to assort, thereby invading highly connected nodes, rendering cooperation an advantageous strategy, as *Cooperators* acquire a higher probability of being imitated than *Defectors*. On SF networks the requirement to reach the hubs, which ensures the formation of cooperative star-like clusters [40, 53], makes invasion harder for isolated *Cooperators*. This moves the unstable root located close to $j/N \approx 0$ in homogeneous networks (see Fig. 36) to higher fractions of *Cooperators*. Yet, once this coordination is overcome, *Cooperators* benefit from the strong influence of hubs to rapidly spread in the population, eventually leading to fixation. As a result, the stable internal root which characterizes $G^A(j)$ in homogeneous networks collapses into the vicinity of $j = N$ on heterogeneous structures, promoting the evolution towards fully cooperative populations. Naturally, the location of the unstable root of $G^A(j)$ is an increasing function of b (see Fig. 38a)¹.

¹ It is noteworthy that our results remain qualitatively valid for other update rules, such as the discrete analogue of the replicator dynamics on graphs, used in many references, e.g., [16, 28, 39, 65]. In fact, the **AGoS** is capable of identifying particular features of such dynamics: For instance, the partially deterministic nature of such update rule may lead to evolutionary deadlocks in heterogeneous (scale-free) networks, creating stationary states close to full cooperation [16, 28]. In such situa-

The existence of a coordination barrier for *Cooperators* in heterogeneous networks, which must first occupy the hubs before outcompeting *Defectors*, leads to an intricate interplay between the time-dependent decline of x_L (see Fig. 36b) and the global fraction of *Cooperators*. In Fig. 38b we show, with full lines, two evolutions in **BA** networks (for the same value of $b = 1.25$): One, which fixates in full cooperation and another, which fixates in full defection. Whenever the fraction of cooperators j/N remains sizeable for long enough, x_L will eventually decrease to values satisfying $j/N > x_L$, such that the global coordination barrier is overcome and the population will fixate into full cooperation (light blue line). Otherwise, j/N may remain always below x_L with the population fixating into full defection (dark blue line). Clearly, heterogeneous networks lead to the emergence of a global coordination barrier and associated basins of attraction that evolve in time, in a way which is well described by the time-dependent **AGoS**.

3.1.4 Discussion

To establish the link between individual and collective behavior constitutes, undeniably, one of the main goals of the analysis of any complex multi-particle or multi-component system [66]. Here we establish such a link showing how it depends on the underlying network topology. Our study shows that behavioral dynamics of individuals facing a cooperation dilemma in social networks can be understood as though the network structure is absent but individuals face a different dilemma: The structural organization of a population of self-regarding individuals helps circumventing the Nash equilibrium of a cooperation dilemma by creating a new dynamical system that can be globally characterized by two internal fixed points, x_L (unstable) and x_R (stable). While a single defector will be always advantageous (creating an unstable fixed point at $x = 1.0$), a single cooperator will be always disadvantageous (prompting a stable equilibrium at $x = 0.0$). As cooperators assort into stable clusters, they may also become advantageous above a certain critical fraction of cooperators ($k/N > x_L$, associated with a critical cluster size) and below another critical fraction of cooperators x_R , above which defectors will be able to reap again the benefits of exploiting the many surrounding cooperators. Whereas in homogeneous networks the stable equilibria dictate the overall dynamics – as in co-existence dilemmas – heterogeneous networks create a global dynamics mainly dominated by the unstable equilibria, creating a coordination problem.

Strictly speaking, such a dynamical system resulting from individuals interacting (locally) via a two-person game, cannot be mapped onto a two-person evolutionary game in a well-mixed population, since the latter can only comply with a maximum of one internal fixed point [44]. On the contrary, such dynamics resembles that from, *e.g.*, N-person dilemmas [67, 68] in the presence of coordination thresholds [52, 64, 69]. It is as if the global dynamics of a 2-person dilemma in structured populations can be properly described as a time-dependent N-person dilemma, in which the coordination or co-existence features emerge from the population structure itself, with different network topologies emphasizing differently this co-existence/coordination dichotomy.

tion, the **AGoS** will reflect the occurrence of these stationary configurations by shifting to the left-hand side the stable (x_R) equilibrium, which may no longer coincide with $j = N$, remaining, however, in its vicinity.

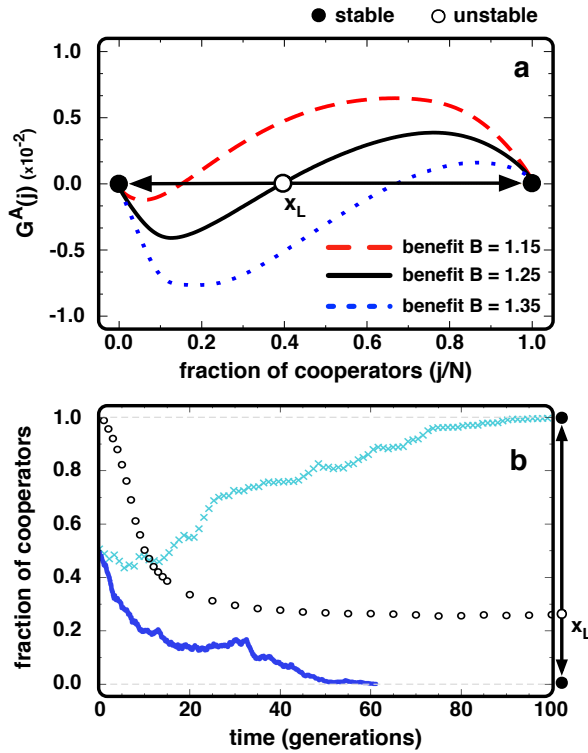


Figure 38: AGoS on BAnetworks. (a) Starting from a defection dominant **PD** played at an individual level, a coordination dynamics emerges at a global, population-wide scale, for the three values of b depicted. (b) Evolution of the unstable root x_L of $G^A(j, t)$ (open circles), exhibiting the time-dependence of the global dynamics; solid (dark blue) line and (light blue) crosses show two independent evolutionary runs starting from 50% of *Cooperators* and *Defectors* randomly placed. The ultimate fate of *Cooperators* in each run depends on whether the population composition crosses over the time-dependent value x_L of $G^A(j, t)$ thereby overcoming the dynamical coordination barrier during evolution. ($b = 1.25$, $N = 10^3$, $\langle k \rangle = 4$ and $\beta = 0.1$). **BAnetworks** were obtained combining growth and preferential attachment, following the model proposed by Barabási and Albert [61].

It is worth emphasizing that the approach developed here in the context of the two-person **PD** may be useful – and immediately applicable – in understanding the evolutionary dynamics of other game interactions, as well as in understanding other aspects of human sociality that extend beyond cooperation. From human behaviors and ideas, to diseases spreading or to individual preferences, most have been modeled as a person-to-person spreading process embedded in a social network [5, 8, 62]. In such frameworks, the identification and categorization of the global, population-wide dynamics which emerges from the apparently unrelated nature of the local interactions may enable one to anticipate the emergent outcomes of such complex biological and social systems.

3.1.5 Methods

Evolution is modelled via a stochastic birth-death process [48, 70, 71]. Each individual x adopts the strategy of a randomly selected neighbour y with probability given by the Fermi function $p = [1 +$

$\exp(-\beta(f_y - f_x))^{-1}$ [14, 48], where f_x (f_y) stands for the accumulate payoff of x (y) and controls the intensity of selection. In structured populations, the difference of the probabilities to increase and decrease the number of *Cooperators* ($G(j) = T^+(j) - T^-(j)$) becomes context dependent, but can be computed numerically. For each individual i we compute the probability of changing behavior at time t ,

$$T_i(t) = \frac{1}{k_i} \sum_{m=1}^{\bar{n}_i} [1 + \exp(-\beta(f_m - f_i))]^{-1}, \quad (59)$$

where k_i stands for the degree of node i and \bar{n}_i for the number of neighbors of i having a strategy different from that of i . The time-dependent AGoS at a given time t of simulation p , where we have j *Cooperators* in the population of size N , is defined as

$$G_p(j, t) = T_A^+(j, t) - T_A^-(j, t) \quad (60)$$

where

$$T_A^\pm(j, t) = \frac{1}{N} \sum_{i=1}^{AllDs/AllCs} T_i(t) \quad (61)$$

For a given network type, we run $\Omega = 2 \times 10^7$ simulations (using 10^3 randomly generated networks) starting from all possible initial fractions j/N of cooperators. Each configuration of the population is defined here by the fraction j/N of cooperators. Evolutions run for $\Lambda = 10^5$ time steps. Hence, the overall, time-independent, **AGoS** is given by the average

$$G_A^\pm(j) = \frac{1}{\Omega \Lambda} \sum_{t=1}^{\Lambda} \sum_{p=1}^{\Omega} G_p(j, t) \quad (62)$$

over all simulations and time-steps. The time-dependent gradients $G^A(j, t_0)$ for a particular generation t_0 (and corresponding roots shown in Fig. 36 and 36b) were computed averaging over the configurations occurring during N previous time-steps (1 generation):

$$G_A^\pm(j, t_0) = \frac{1}{\Omega \Lambda} \sum_{t=t_0-N}^{\Lambda} \sum_{p=1}^{\Omega} G_p(j, t). \quad (63)$$

The stationary distributions pictured in Fig. 36b were obtained computing the fraction of time the population spent in each overall configuration j/N . In some specific limits – in particular, for weak selection or well-mixed populations – our numerical approach will provide results analogous to those obtained with other methods (see for instance [20, 22, 44, 46, 48, 51, 60, 71, 72, 73, 74]).

Homogeneous random networks were obtained by repeatedly swapping the ends of pairs of randomly chosen links of a regular network [47]. **BA** networks were obtained combining growth and preferential attachment, following the model proposed by Barabási and Albert [4, 61]. All networks used have $N = 10^3$ nodes and an average degree $k = 4$.

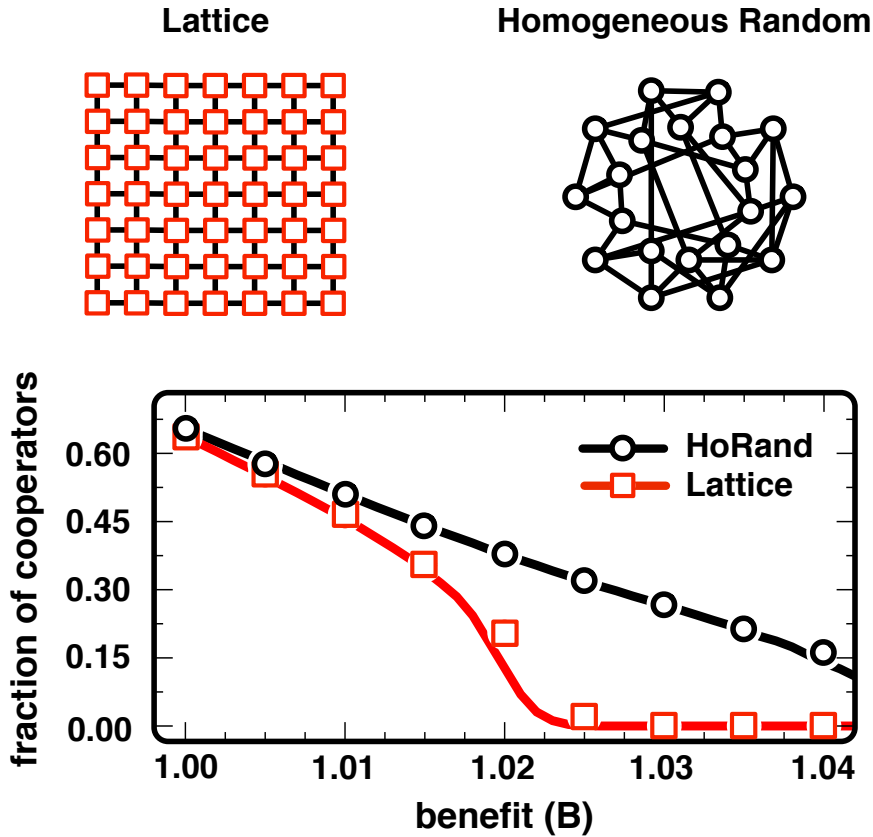


Figure 39: Evolutionary dynamics cooperation in homogeneous networks. We plot the interior roots x_R of (circles) for a **PD** ($T = b, R = 1, P = 0, S = 1 - b$) in homogeneous networks, from random networks (black circles) to ordered lattices (red circles), as a function of the benefit b . indicates that the population evolves towards a stationary fraction x_R of *Cooperators*. This is confirmed by the stationary states (lines) obtained via computer simulations starting from 50% of *Cooperators* and *Defectors* randomly placed in each network. ($N = 10^3, k = 4$ and $\beta = 0.1$).

3.2 SUPPORTING INFORMATION

3.2.1 Evolutionary steady states in homogeneous networks

As we argue in the main text, the shape of the time independent $G^A(j)$ obtained for homogeneous networks indicates that these topologies induce a co-existence game dynamics in a population of individuals engaging in a Prisoner's Dilemma (**PD**). Moreover, the stationary regime is associated with the interior root of $G^A(j)$. Thus, it is reasonable to expect that the stable roots of $G^A(j)$ will coincide with the steady states obtained from computer simulations carried out on the same networks.

In Fig. 39 we compare the interior roots of $G^A(j)$ (circles) with the stationary states (lines) obtained via computer evolutions [1, 2, 3, 4, 5] carried out for several values of the benefit b and for homogenous networks, ranging from ordered lattices (Lattice) to random networks (HoRand). Fig. 39 confirms that the information offered by remains valid and strikingly accurate for a broad range of game parameters for both types of networks. In accord with the results in the main text, the stationary

states were computed for networks with $N = 10^3$ individuals and an average connectivity of $z = 4$. As before, each individual revise his or her strategy adopting the one of a randomly selected neighbour with probability given by the Fermi function (see Section 3.1.5) [2, 6]. Each equilibrium fraction of cooperators in a simulation was obtained by averaging over 500 generations after a transient period of 10^4 generations starting from 50% of *Cooperators* randomly placed on the network. Both red and black lines in Fig. 39 correspond to a subsequent average over 10^4 simulations.

$G^A(j)$ and its interior roots (full circles in Fig. 39) were computed for the same game and network parameters by averaging $G^A(j, t)$ over 100 generations after a transient of 50 generations (see Section 3.1.5 for details of computation of $G^A(j, t)$).

3.3 BIBLIOGRAPHY

- [1] Mark S Granovetter. The strength of weak ties. *American Journal of Sociology*, pages 1360–1380, 1973.
- [2] Duncan J Watts. A twenty-first century science. *Nature*, 445(7127):489–489, 2007.
- [3] Alun L Lloyd and Robert M May. How viruses spread among computers and people. *Science*, 292(5520):1316–1317, 2001.
- [4] Sergei N Dorogovtsev. *Lectures on complex networks*, volume 24. Oxford University Press Oxford, 2010.
- [5] James H Fowler and Nicholas A Christakis. Cooperative behavior cascades in human social networks. *Proceedings of the National Academy of Sciences*, 107(12):5334–5338, 2010.
- [6] Damon Centola. The spread of behavior in an online social network experiment. *Science*, 329(5996):1194–1197, 2010.
- [7] Claudio Cioffi-Revilla. Computational social science. *Wiley Interdisciplinary Reviews: Computational Statistics*, 2(3):259–271, 2010.
- [8] Alain Barrat, Marc Barthelemy, and Alessandro Vespignani. *Dynamical processes on complex networks*, volume 1. Cambridge University Press Cambridge, 2008.
- [9] Jukka-Pekka Onnela and Felix Reed-Tsochas. Spontaneous emergence of social influence in online systems. *Proceedings of the National Academy of Sciences*, 107(43):18375–18380, 2010.
- [10] John Maynard Smith. *Evolution and the Theory of Games*. Springer, 1993.
- [11] Karl Sigmund. *The calculus of selfishness*. Princeton University Press, 2010.
- [12] Martin A Nowak and Robert M May. Evolutionary games and spatial chaos. *Nature*, 359(6398):826–829, 1992.
- [13] Mayuko Nakamaru, H Matsuda, and Y Iwasa. The evolution of cooperation in a lattice-structured population. *Journal of Theoretical Biology*, 184(1):65–81, 1997.
- [14] György Szabó and Csaba Tóke. Evolutionary prisoner’s dilemma game on a square lattice. *Physical Review E*, 58(1):69, 1998.
- [15] Ch Hauert. Effects of space in 2×2 games. *International Journal of Bifurcation and Chaos*, 12(07):1531–1548, 2002.
- [16] Francisco C Santos and Jorge M Pacheco. Scale-free networks provide a unifying framework for the emergence of cooperation. *Physical Review Letters*, 95(9):098104, 2005.

Chapter 3. FROM LOCAL TO GLOBAL DILEMMAS IN SOCIAL NETWORKS

- [17] Erez Lieberman, Christoph Hauert, and Martin A Nowak. Evolutionary dynamics on graphs. *Nature*, 433(7023):312–316, 2005.
- [18] Francisco C Santos, Jorge M Pacheco, and Tom Lenaerts. Evolutionary dynamics of social dilemmas in structured heterogeneous populations. *Proceedings of the National Academy of Sciences*, 103(9):3490–3494, 2006.
- [19] F C Santos, J F Rodrigues, and J M Pacheco. Graph topology plays a determinant role in the evolution of cooperation. *Proceedings of the Royal Society B: Biological Sciences*, 273(1582): 51–55, 2006.
- [20] Hisashi Ohtsuki, Christoph Hauert, Erez Lieberman, and Martin A Nowak. A simple rule for the evolution of cooperation on graphs and social networks. *Nature*, 441(7092):502–505, 2006.
- [21] Hisashi Ohtsuki and Martin A Nowak. The replicator equation on graphs. *Journal of Theoretical Biology*, 243(1):86–97, 2006.
- [22] Peter D Taylor, Troy Day, and Geoff Wild. Evolution of cooperation in a finite homogeneous graph. *Nature*, 447(7143):469–472, 2007.
- [23] Peter D Taylor, Troy Day, and Geoff Wild. From inclusive fitness to fixation probability in homogeneous structured populations. *Journal of Theoretical Biology*, 249(1):101–110, 2007.
- [24] György Szabó and Gábor Fáth. Evolutionary games on graphs. *Physics Reports*, 446(4):97–216, 2007.
- [25] J Gómez-Gardeñes, M Campillo, LM Floría, and Y Moreno. Dynamical organization of cooperation in complex topologies. *Physical Review Letters*, 98(10):108103, 2007.
- [26] Hisashi Ohtsuki, Martin A Nowak, and Jorge M Pacheco. Breaking the symmetry between interaction and replacement in evolutionary dynamics on graphs. *Physical Review Letters*, 98 (10):108106, 2007.
- [27] Luis A Nunes Amaral, Antonio Scala, Marc Barthelemy, and H Eugene Stanley. Classes of small-world networks. *Proceedings of the National Academy of Sciences*, 97(21):11149–11152, 2000.
- [28] Jesús Gómez-Gardeñes, Julia Poncela, Luis Mario Floría, and Yamir Moreno. Natural selection of cooperation and degree hierarchy in heterogeneous populations. *Journal of Theoretical Biology*, 253(2):296–301, 2008.
- [29] Julia Poncela, Jesús Gómez-Gardeñes, LM Floría, and Yamir Moreno. Robustness of cooperation in the evolutionary prisoner’s dilemma on complex networks. *New Journal of Physics*, 9(6): 184, 2007.
- [30] Naoki Masuda. Participation costs dismiss the advantage of heterogeneous networks in evolution of cooperation. *Proceedings of the Royal Society B: Biological Sciences*, 274(1620):1815–1821, 2007.
- [31] L Lehmann, L Keller, and David JT Sumpter. The evolution of helping and harming on graphs: the return of the inclusive fitness effect. *Journal of Evolutionary Biology*, 20(6):2284–2295, 2007.
- [32] Attila Szolnoki, Matjaž Perc, and Zsuzsa Danku. Towards effective payoffs in the prisoner’s dilemma game on scale-free networks. *Physica A: Statistical Mechanics and its Applications*,

- 387(8):2075–2082, 2008.
- [33] György Szabó and Christoph Hauert. Evolutionary prisoner’s dilemma games with voluntary participation. *Physical Review E*, 66(6):062903, 2002.
- [34] Matjaž Perc. Evolution of cooperation on scale-free networks subject to error and attack. *New Journal of Physics*, 11(3):033027, 2009.
- [35] LM Floría, C Gracia-Lázaro, J Gómez-Gardeñes, and Y Moreno. Social network reciprocity as a phase transition in evolutionary cooperation. *Physical Review E*, 79(2):026106, 2009.
- [36] Matjaž Perc and Attila Szolnoki. Coevolutionary games—a mini review. *BioSystems*, 99(2):109–125, 2010.
- [37] Matjaz Perc and Zhen Wang. Heterogeneous aspirations promote cooperation in the prisoner’s dilemma game. *PLoS One*, 5(12):e15117, 2010.
- [38] James AR Marshall. Ultimate causes and the evolution of altruism. *Behavioral Ecology and Sociobiology*, 65(3):503–512, 2011.
- [39] Christoph Hauert and Michael Doebeli. Spatial structure often inhibits the evolution of cooperation in the snowdrift game. *Nature*, 428(6983):643–646, 2004.
- [40] Francisco C Santos, Marta D Santos, and Jorge M Pacheco. Social diversity promotes the emergence of cooperation in public goods games. *Nature*, 454(7201):213–216, 2008.
- [41] György Szabó, Jeromos Vukov, and Attila Szolnoki. Phase diagrams for an evolutionary prisoner’s dilemma game on two-dimensional lattices. *Physical Review E*, 72(4):047107, 2005.
- [42] John Maynard Smith and Geoffrey A Parker. The logic of asymmetric contests. *Animal Behaviour*, 24(1):159–175, 1976.
- [43] Herbert Gintis. *Game theory evolving: A problem-centered introduction to modeling strategic behavior*. Princeton University Press, 2000.
- [44] Josef Hofbauer and Karl Sigmund. *Evolutionary games and population dynamics*. Cambridge University Press, 1998.
- [45] Brian Skyrms. *The stag hunt and the evolution of social structure*. Cambridge University Press, 2004.
- [46] George R Price et al. Selection and covariance. *Nature*, 227:520–21, 1970.
- [47] Francisco C Santos, JF Rodrigues, and Jorge M Pacheco. Epidemic spreading and cooperation dynamics on homogeneous small-world networks. *Physical Review E*, 72(5):056128, 2005.
- [48] Arne Traulsen, Martin A Nowak, and Jorge M Pacheco. Stochastic dynamics of invasion and fixation. *Physical Review E*, 74(1):011909, 2006.
- [49] Arne Traulsen, Jorge M Pacheco, and Martin A Nowak. Pairwise comparison and selection temperature in evolutionary game dynamics. *Journal of Theoretical Biology*, 246(3):522–529, 2007.
- [50] Arne Traulsen, Martin A Nowak, and Jorge M Pacheco. Stochastic payoff evaluation increases the temperature of selection. *Journal of Theoretical Biology*, 244(2):349–356, 2007.
- [51] Arne Traulsen, Jorge M Pacheco, and Lorens A Imhof. Stochasticity and evolutionary stability. *Physical Review E*, 74(2):021905, 2006.

Chapter 3. FROM LOCAL TO GLOBAL DILEMMAS IN SOCIAL NETWORKS

- [52] Jorge M Pacheco, Francisco C Santos, Max O Souza, and Brian Skyrms. Evolutionary dynamics of collective action in n-person stag hunt dilemmas. *Proceedings of the Royal Society B: Biological Sciences*, 276(1655):315–321, 2009.
- [53] Jorge M Pacheco, Flávio L Pinheiro, and Francisco C Santos. Population structure induces a symmetry breaking favoring the emergence of cooperation. *PLoS Computational Biology*, 5(12):e1000596, 2009.
- [54] Béla Bollobás. *Random graphs*. Springer, 1998.
- [55] Christoph Hauert and György Szabó. Game theory and physics. *American Journal of Physics*, 73(5):405–414, 2005.
- [56] Matjaž Perc. Coherence resonance in a spatial prisoner’s dilemma game. *New Journal of Physics*, 8(2):22, 2006.
- [57] Matjaž Perc and Attila Szolnoki. Social diversity and promotion of cooperation in the spatial prisoner’s dilemma game. *Physical Review E*, 77(1):011904, 2008.
- [58] György Szabó and Attila Szolnoki. Cooperation in spatial prisoner’s dilemma with two types of players for increasing number of neighbors. *Physical Review E*, 79(1):016106, 2009.
- [59] Tibor Antal and Istvan Scheuring. Fixation of strategies for an evolutionary game in finite populations. *Bulletin of Mathematical Biology*, 68(8):1923–1944, 2006.
- [60] Fabio ACC Chalub and Max O Souza. From discrete to continuous evolution models: a unifying approach to drift-diffusion and replicator dynamics. *Theoretical Population Biology*, 76(4):268–277, 2009.
- [61] Albert-László Barabási and Réka Albert. Emergence of scaling in random networks. *Science*, 286(5439):509–512, 1999.
- [62] Nicholas A Christakis and James H Fowler. The collective dynamics of smoking in a large social network. *New England Journal of Medicine*, 358(21):2249–2258, 2008.
- [63] Brian Skyrms. The stag hunt. In *Proceedings and Addresses of the American Philosophical Association*, pages 31–41. JSTOR, 2001.
- [64] Francisco C Santos and Jorge M Pacheco. Risk of collective failure provides an escape from the tragedy of the commons. *Proceedings of the National Academy of Sciences*, 108(26):10421–10425, 2011.
- [65] Francisco C Santos and Jorge M Pacheco. A new route to the evolution of cooperation. *Journal of Evolutionary Biology*, 19:726–733, 2006.
- [66] T.C. Schelling. *Micromotives and Macrobehavior*. New York: Norton, 1978.
- [67] P. Kollock. Social dilemmas: The anatomy of cooperation. *Annual Review of Sociology*, 24:183–214, 1998.
- [68] C.S. Gokhale and Arne Traulsen. Evolutionary games in the multiverse. *Proceedings of the National Academy of Sciences*, 107(12):5500, 2010.
- [69] Max O Souza, Jorge M Pacheco, and Francisco C Santos. Evolution of cooperation under n-person snowdrift games. *Journal of Theoretical Biology*, 260(4):581–588, 2009.
- [70] Samuel Karlin. *A first course in stochastic processes*. Academic press, 2014.

3.3. Bibliography

- [71] Martin A Nowak, Akira Sasaki, Christine Taylor, and Drew Fudenberg. Emergence of cooperation and evolutionary stability in finite populations. *Nature*, 428(6983):646–650, 2004.
- [72] Karen M Page and Martin A Nowak. Unifying evolutionary dynamics. *Journal of Theoretical Biology*, 219(1):93–98, 2002.
- [73] Thomas M Liggett. *Stochastic interacting systems: contact, voter and exclusion processes*, volume 324. Springer, 1999.
- [74] Fabio ACC Chalub and Max O Souza. Continuous models for genetic evolution in large populations. In *Dynamics, Games and Science I*, pages 239–242. Springer, 2011.

HOW SELECTION PRESSURE CHANGES THE NATURE OF SOCIAL DILEMMAS IN STRUCTURED POPULATIONS

New Journal of Physics, 14, 073035 (2012)

Flávio L. Pinheiro, Francisco C. Santos and Jorge M. Pacheco

In Chapter 3 we have introduced a new methodology to characterize the evolutionary dynamics of cooperation in structured populations. We have shown that the degree distribution of the underlying network of interactions between individuals plays an important role in defining the emerging collective behavior of the population. In particular, when individuals interact according to the *Prisoner's Dilemma* we concluded that degree homogeneous networks, in which individuals share a similar number of neighbors, lead to a population-wide coexistence dynamics. In contrast, degree heterogeneous networks prompts a coordination towards a monomorphic configuration dominated either by Cooperators or Defectors. Both these global, population-wide dynamics present a milder challenge for the evolution of cooperation when compared with the *Prisoner's Dilemma* locally faced by individuals.

Here, we investigate the role of selection pressure (associated with the stochasticity of the decision making of individuals) in the emergence of these collective scenarios. We find that homogeneous networks are very sensitive to selection pressure, whereas strongly heterogeneous networks are more resilient to natural selection, dictating an overall robust evolutionary dynamics of coordination. Between these extremes, a whole plethora of behaviors is predicted, showing how selection pressure can change the nature of dilemmas populations effectively face. We further show how the present results for homogeneous networks bridge the existing gap between analytic predictions obtained in the framework of the pair-approximation from very weak selection and simulation results obtained from strong selection.

4.1 MANUSCRIPT

4.1.1 Introduction

Complex networks are ubiquitous and known to profoundly affect the processes that take place on them [3, 4, 5]. From a theoretical perspective, some of the most complex processes studied to date, occurring on complex networks, are related with behavioral dynamics and decision-making, often described by means of social dilemmas of cooperation [6]. Among these, the *Prisoner's Dilemma* (**PD**) provides the most popular metaphor of such dilemmas, given that its only Nash equilibrium is

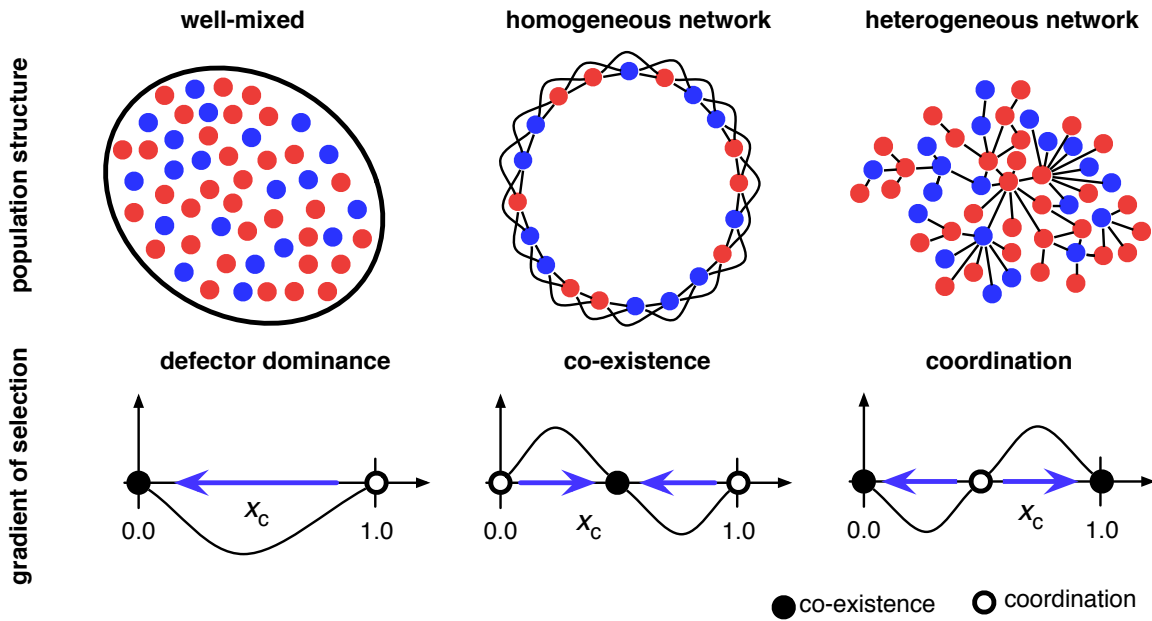


Figure 40: Effective games in structured populations. Depending on the underlying network structure, the evolutionary dynamics of a population may exhibit an *Average Gradient of Selection (AGOS)* which may coincide with the expectations from standard evolutionary game theory (panel A), or not (panels B and C), reflecting the fact that the network structure changes the effective game played at a population-wide level. Similar to the replicator equation [1], the AGoS [2] provides a characterization of the change in time of the fraction of cooperators under natural selection, being positive (negative) when the fraction of cooperators tends to increase (decrease).

mutual defection, despite mutual cooperation providing higher returns [7] – thus the dilemma. We may also assume a dynamical (evolutionary) approach to game theory [1, 8] where individuals revise their behavior based on the perceived success of other individuals, creating a gradient of selection [9] which dictates the evolution of cooperation in time. In this context, such gradient of selection will always favor free-riders irrespectively of the fraction of cooperators and of the relative importance of fitness in the evolutionary process, a result that dictates the demise of cooperation in the population [8].

This result, which translates the forecast stemming from a game-theoretical analysis based on the Nash-equilibrium into a population-wide, dynamical setting, assumes that populations are large and well mixed, that is, everyone interacts with everyone else with equal probability [1]. Yet, when members of a population interact along the links of an underlying complex network this scenario is altered, as the assumption of a well-mixed population no longer holds [6, 10, 11]. Only recently it has become possible to analyze the population-wide evolutionary dynamics of a game played on an arbitrarily complex network, very much in the same manner that games were analyzed in well mixed populations [2]. The so-called *Average Gradient of Selection (AGOS)*, see Section 4.1.2 for details) has unraveled the fundamental changes in evolutionary game dynamics introduced in populations structured along the links of complex networks. The results show that, at a population-wide level (what

we call macro-dynamics) the effective game at stake can be very different from that in which pairs of individuals engage (what we call micro-dynamics). In particular, homogeneous networks seem to favor the coexistence of strategies, whereas heterogeneous networks, in turn, favor their coordination [2], irrespective of the fact that the game individuals perceive and play, individually, is a **PD** – see Fig. 40.

The scenarios illustrated in Fig. 40, however, do not take into account the role of selection pressure in the overall evolutionary dynamics of a networked population [12, 13, 14, 15]. Selection pressure provides the relative significance of individual fitness in the evolutionary process, as opposed to an arbitrary or random adoption of strategies. This is important, as selection pressure can be very different depending on the processes at stake. Indeed, in many social interactions, errors in decision making, perhaps induced by stress or exogenous confounding factors, which often translate into a bounded rational behavior of the players [16], may lead to an overall weak selection environment. This contrasts with many situations in nature where selection may be strong [17] as well as in cases where cultural evolution is at stake [8]. Moreover, the fate of cooperation in social networks may depend on how the success of the others are locally perceived – which is related with the number of partners of each player and their social context [10, 15, 18, 19] – turning selection pressure into a central variable in the ongoing challenge of understanding the impact of each social structure on global outcomes [6, 10, 11, 2, 20, 21, 22, 23, 24, 25, 26, 27, 28, 29, 30, 31, 32, 33, 34, 35, 36, 37, 38].

Here we study the role played by selection pressure in the overall evolutionary dynamics of a population. We find that, for a given class of population structure, there is an optimum level of selection pressure for which cooperation is maximized. We stick here to paradigmatic examples of homogeneous and strongly heterogeneous classes of population structure, deferring to section 4.2 the study of other classes of population structure which enlarges the variety of topological features studied here, thereby providing an overall view of the role of selection pressure in a wider range of contexts.

4.1.2 Model

We take a population of individuals organized by means of a complex network of social interactions, where individuals are placed on the nodes and interactions are restricted to individuals connected by links. We focus on two classes of population structures: homogeneous, where every individual shares the same number of neighbors, and heterogeneous, where individuals have variable number of partners. For the former class, we adopt *Homogeneous Random* networks (**HR**) that are built by randomizing the links of initial homogeneous regular ring networks [39], whereas for the latter we choose the strong heterogeneous case of Scale-free network structures generated with the *Barabási-Albert* algorithm (**BA**) of growth and preferential attachment [40]. All networks have an average degree of 4 and population size is $N = 1000$. In section 4.2 we extend our analysis to other classes of population structures [5] [4] [41], in order to ensure a more complete picture of the effect under study: *Exponential* (**EN**) [42], *Random* (**RN**) [43] and the highly clustered Scale-free networks generated with the *Minimal Model* algorithm (**MM**) [44]; these, while having a degree of heterogeneity similar to **BA** networks, exhibit a high cluster coefficient, in stark contrast with **BA** networks. We confirmed that our results, obtained for $N = 1000$, remain valid for much larger population sizes.

Individuals can assume one of two possible strategies: to Cooperate or to Defect. Each strategy obtains a payoff that depends on the strategy composition of its neighborhood, given by $\Pi_i = n_C(S_i(R - T) + T) + n_D(S_i(S - P) + P)$, where n_C (n_D) is the number of cooperators (defectors) in the vicinity of node i while S_i is 1 if individual i is a *Cooperator* (**C**) or 0 if a *Defector* (**D**). Finally T (*Temptation*), R (*Reward*), P (*Punishment*) and S (*Sucker's Payoff*) are the game parameters that define all possible pair outcomes in a symmetric two-person-two-strategy interaction (from a game theory perspective). Here we consider $R = 1.0$, $P = 0.0$, $T = \lambda$ and $S = 1 - \lambda$, where $\lambda > 1$ stands both for the temptation to defect towards a **C** and for the fear of being cheated [18, 45], thus combining two social tensions in a single parameter. Given that $\lambda > 1.0$, we have that $T > R > P > S$, which means that the game at stake is a *Prisoner's Dilemma* (**PD**). Further social dilemmas can be considered for different rankings of the game parameters, in particular the *Stag Hunt* (a coordination dilemma, for which $R > T > P > S$) and the *Snowdrift Game* (a coexistence dilemma, for which $T > R > S > P$).

Evolutionary dynamics proceeds as long as individuals with higher fitness will tend to reproduce more or, in the context of cultural evolution and social learning, successful individuals will be imitated; in both cases, the fitter behavior will spread in the population. Here we adopt the pairwise comparison rule [46, 47, 48] which allows us to explore in terms of a single parameter (β) the full range of possible selection pressures, from neutral evolution to pure imitation dynamics. At each time step we allow one randomly chosen individual, i , from the population to imitate the strategy of a randomly chosen neighbor, j , with probability p given by $(1 + \exp(-\beta(f_j - f_i)))^{-1}$ where f_i denotes the fitness of individual i (here associated with the accumulated payoff obtained from playing with all neighbors). As stated above, $\beta \geq 0$ defines the selection pressure: for $\beta = 0$ we obtain neutral evolution, in which case the evolutionary dynamics proceeds by random drift; at the other extreme, for very large values of β , imitation becomes deterministic, in the sense that any chosen neighbor who is more fit will be always imitated.

The final fraction of cooperators were computed by averaging over 2.5×10^5 evolutionary runs, after a transient of 5×10^3 generations starting with a population composed by equal fractions of strategies randomly placed on the network. We also computed the quasi-stationary distributions, corresponding to the fraction of time that the population spent in each non-absorbing state during the first 5×10^3 generations over 2.5×10^5 distinct evolutions that started with a random initial condition.

The Gradient of Selection is defined as $G(i) = T^+(i) - T^-(i)$ [9], where $T^+(i)$ ($T^-(i)$) is the probability of increasing (decreasing) the number of cooperators by one in a population with i cooperators. For structured populations this quantity becomes context dependent, but can be computed numerically [14]. For each individual i we compute the probability of changing behavior at time t , $\pi_i(t)$, where k_i stands for the degree of node i and for the number of neighbors of i having a different strategy. At a give time t of simulation p the *Averaged Gradient of Selection* (**AGOS**), is defined as $\bar{G}^A(j, g)$, with $\bar{G}^A(j, g)$ for a state with j Cs in a population of size N . The time-dependent **AGOS**, $G^A(j, g)$, for a particular generation g is thus computed by averaging over N time-steps (1 generation), $\bar{G}^A(j, g) = \frac{1}{N} \sum_i G^A(j, g)$, where $c_j(g)$ accounts for the number of times the system was observed in state j at generation g . For a given network type,

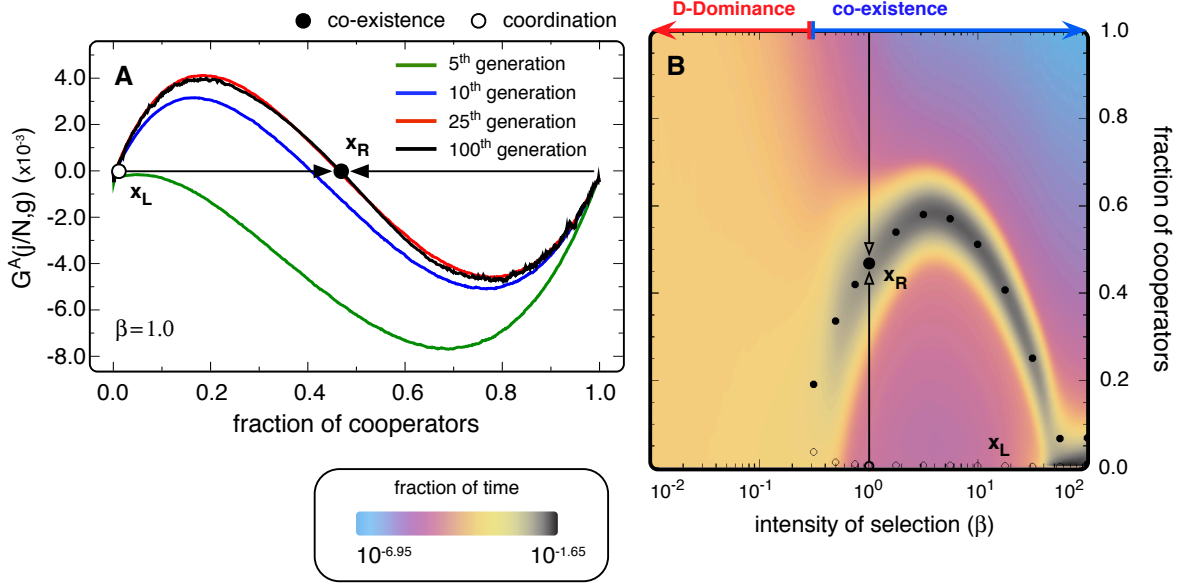


Figure 41: Average Gradient of Selection (AGOS) on HR structured populations. A: time-dependent AGOS for populations engaging in a PD with $\lambda = 1.01$ and $\lambda = 1.0$ at 4 different generations ($g = 5, 10, 25$ and 100) showing that the position of x_R does not change after the 25th generation. B: Location of the internal fixed points of the time-dependent AGOS, at the 100th generation, for a broad range of values of β ($\lambda = 1.01$). The color gradient is used to plot the quasi-stationary distribution (see Section 2), i.e., the prevalence in time of each fraction of cooperators.

we run $\Omega = 2.5 \times 10^7$ simulations (using 10^3 networks of each type) starting from random initial conditions.

4.1.3 Results and Discussion

As discussed in [14], the evolutionary game dynamics taking place on structured populations leads to the emergence of an effective game, at a macro (population-wide) level, characterized by exhibiting, typically, a pair of internal roots (of coordination and coexistence type) in the AGOS, more akin to the dynamics of N-Person games [9, 15, 49, 50, 51, 52]. However, as shown, while in homogeneous population structures the dynamics is dominated by the coexistence root, in heterogeneous populations the coordination root characterizes the overall dynamics (cf. Fig. 41).

In Fig. 41A we show a typical profile of the AGOS at different moments of the evolutionary dynamics of a PD played in a population structured according to a HR network, for $\beta = 1.0$ and $\lambda = 1.01$. We observe a gradual stabilization of the overall shape of the AGOS such that, by the 100th generation, the internal fixed point (and the shape) of the AGOS has already stabilized. Hence, in Fig. 41B, we show the location of the internal fixed points of the AGOS at the 100th generation, as a function of β , on top of the corresponding quasi-stationary distributions computed along the lines specified in Section 2.

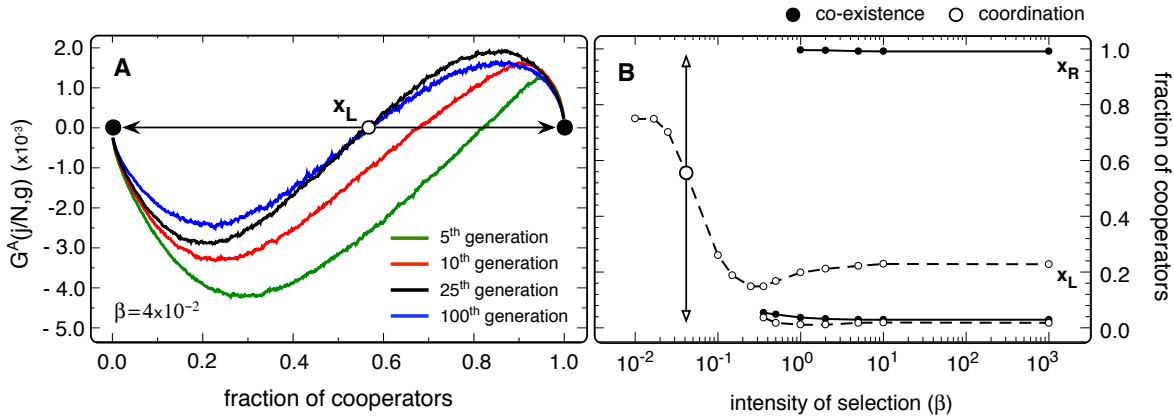


Figure 42: AGoS on BA structured populations. A: time-dependent AGoS for BA populations with $\lambda = 1.25$ and $\beta = 4 \times 10^{-2}$ at 4 different generations ($g = 5, 10, 25$ and 100) showing that the position of x_L does not change after the 25th generation. Panel B shows the position of the internal points of the AGoS at the 100th generation for different values of λ , dashed (full) lines follow the trajectory of coordination (co-existence) points

Fig. 41B shows that, whenever $\beta < 0.3$ the AGoS indicates no trace of internal roots, which indicates that we are in a **PD** (or defector dominance) regime, approaching random drift as $\beta \rightarrow 0$ (leading to a flat quasi-stationary distribution). As soon as $\beta > 0.3$ the effective dilemma changes abruptly, associated with the appearance of two internal points. The dynamics becomes mainly dominated by the co-existence point (x_R , whereas the coordination point x_L essentially collapses to $x = 0$), a feature also reflected in the contour profiles displayed for the quasi-stationary distribution. It is noteworthy the excellent agreement between the AGoS results and those obtained for the quasi-stationary distribution. For $\beta > 50$ we observe the appearance of yet another pair of fixed points between x_R and $x = 0.0$, in an overall dynamical scenario close to a defection dominance. Hence, homogeneous networks are able to promote cooperation within a small window of selection pressures in which cooperators may co-exist with defectors.

In Fig. 42 we show the same results as in Fig. 41 but now for a population structured along the links of a BA network. Again, by the 100th generation, roots of the AGoS have stabilized, and hence in Fig. 3B the location of the internal fixed points (computed at the 100th generation) is shown as a function of β . Whenever $\beta < 0.28$ the macro-dynamics is dominated by a single coordination point x_L that moves closer to $x = 0.0$ for increasing β . However for $\beta > 0.28$ a pair of internal points appear below $x = 0.1$ which occurs simultaneously with the slight increase in the location of the coordination point (x_L) above which the population reaches full cooperation. For increasing β the co-existence point (x_R) reaches almost $x = 1.0$. The discussion of the detailed mechanisms giving rise to these roots near the monomorphic states falls beyond the scope of the present work, and will be deferred to future work, being related with multitude of evolutionary deadlocks that may appear at the leaves of scale-free networks [26], which become more significant for high selection pressure.

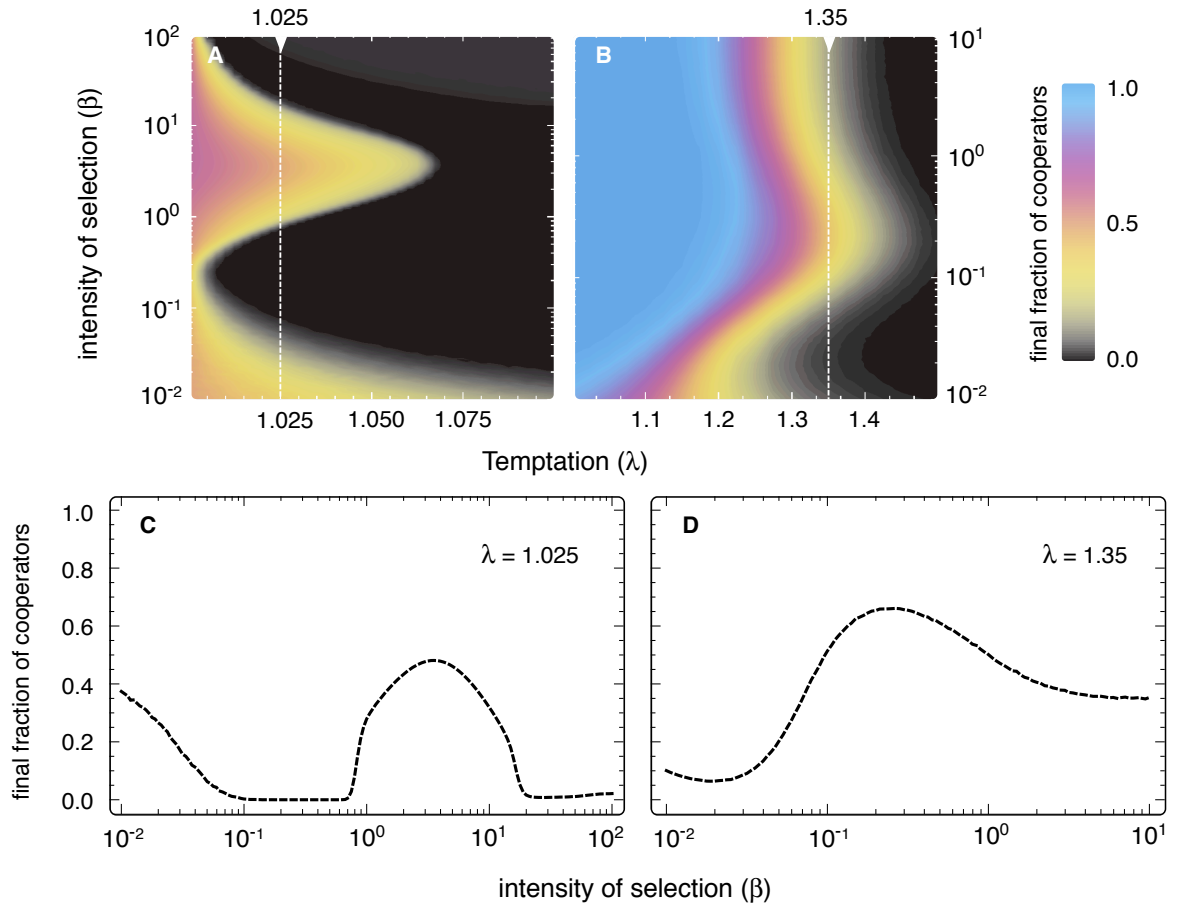


Figure 43: *Final Fraction of Cooperators* on networked populations. Panels A and B ? We plot the final fraction of cooperators as function of both the intensity of selection (β) and of the temptation (λ) for **BA** and **HR** structured populations, respectively. Panels C and D – Examples of the final fraction of cooperators for fixed temptation values ($\lambda = 1.025$ and 1.35) as a function of β (these results correspond to the dashed white lines in upper panels). In both cases there is an optimal value of β for which cooperation is maximized.

In both cases (**HR** and **BA**, see Figs. .41 and .42) the positions of the internal points of the **AGOS** put into evidence the existence of an optimal selection pressure for which cooperation levels are maximized.

Fig. 43 shows the result of standard computer simulations (e.g., see [6]) in which, starting from 50% Cs ($x_i = 0.5$) placed at random in the population, one computes the stationary *final fraction of cooperators* (**FFC**) as a function of β and λ . Fig. 43A shows results for **HR** networks, whereas Fig. 43B shows the corresponding results for **BA** networks. For a wide range of values of λ , there is a value of β that optimizes the final fraction of Cs in both network types. We have confirmed that this behavior is independent of both λ and the population structure.

For strong selection ($\beta \gg 1.0$) individuals approach a more deterministic regime in which the update process consists of copying the strategy of their neighbors whenever these are doing better, however slightly. In such a regime, the population outcome is strongly dependent on the population structure.

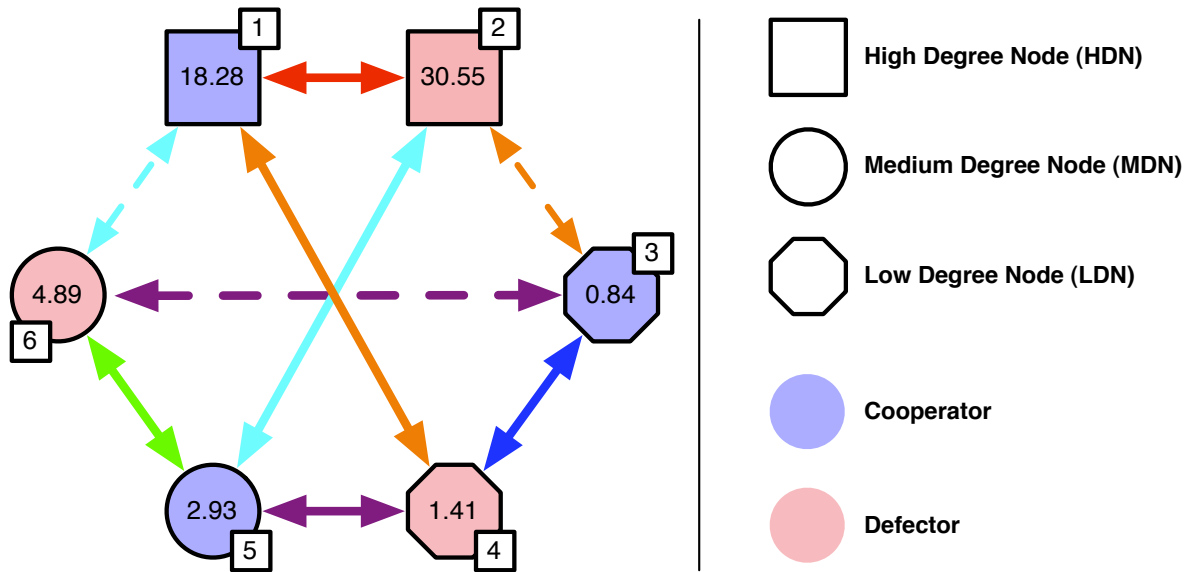


Figure 44: Meta-Network depicting the several classes of nodes present in scale-free population (squares, circles and hexagons) and the possible strategies (blue and pink colors). In each node the numeric value indicates the average payoff accumulated by nodes of such strategy and structural class in population configurations comprising an equal fraction of **Cs** and **Ds**, randomly distributed ($\lambda = 1.25$). To simplify the discussion in connection with Fig. 45 below, we label each node by a number (square box in the corner of each node).

Between these two extremes one obtains a transition region, characterized by the existence of a local maximum of the **FFC** in β for a given λ .

On **HR** populations, as long as **Cs** succeed in forming compact clusters, they may prevent the invasion from **Ds** [6, 11]. Given that the underlying game is a **PD**, for weak selection, clusters of **Cs** are easier to form, but errors in imitation also allow their destruction and/or invasion by **Ds**.

As we increase β we decrease the incidence of errors of imitation, hindering the feasibility of forming clusters of **Cs**, but also hindering the feasibility of them getting destroyed or invaded as a result of errors of imitation. Hence, it is not surprising that the population evolves to a stationary regime in which **Cs** and **Ds** may coexist in the population. From a population wide perspective, the macrodynamics will be characterized by an effective co-existence dilemma as was shown in Fig. 41.

On **BA** heterogeneous populations the situation is more complex, although we can identify the basic mechanism that leads to the results shown in Fig. 43. Indeed, we observe a decoupling in the effective intensity of selection between interactions that involve at least one hub (nodes of high degree) and those that involve none (involving mostly leaves, that is, nodes of smallest degree). Because hubs are able to accumulate a large fitness – at least one order of magnitude higher than that of other nodes (see below) – they are seen as preferential role models. Hence, potential behavioral imitation between hubs and leaves occur at an effectively higher β than interactions among leaves. This mechanism is discussed in further detail in Section 3.3.

From an individual perspective this mechanism hints at how each individual should interact with his peers so that cooperation levels at the population-wide level are maximized: imitate deterministically the strategy of the most influential (high fitness) individuals and less so all those that are at a similar level of influence than you. In sum, for a greater good, social and context diversity must be taken seriously [19, 53].

To put into evidence the mechanism responsible for the optimal intensity of selection in what regards cooperation levels in **BA** populations, we divide the nodes of a **BA** network into three degree classes, similar to [57]. We classify nodes as *High Degree Nodes (HDN)* if $k_i > k_{max}/3$, *Medium Degree Nodes (MDN)* if $z < k_i \leq k_{max}/3$ or *Low Degree Nodes (LDN)* whenever $k_i < z$.

Taking into account that a node from a degree class can either be a **C** or a **D** we consider six possible classes of nodes. We can thus collapse all interactions between nodes in the original network into interactions taking place on a meta-network of 6 (meta-) nodes, where we shall consider only links between nodes of different strategies. Fig 5 exemplifies such a meta-network. The values provided for each node correspond to the average payoff of nodes of the respective class computed for 10^3 configurations obtained by randomly distributing an equal fraction of **Cs** and **Ds** on **BA** networks. Fig 5 shows that, indeed, **HDN** can accumulate payoffs one order of magnitude higher than nodes of other classes.

We can take the average payoffs of each type of node and compute the average probabilities of imitation in each possible **C-D** link of the meta-network. Whenever any of these processes occurs under weak selection we expect to obtain a probability of imitation near 0.5, whereas deterministic imitation occurs whenever probabilities approach 1.0.

In Fig 45 we show the probability of imitation between nodes with different strategies as a function of β . The lines in each panel correspond to the links in the meta-network identified using the node-numbers in Fig. 44. Black dashed lines display the corresponding **FFC**.

For low β all three types of transitions occur near random imitation ($p = 0.5$) but as we increase β we observe a change of behavior, as some transitions reach a deterministic regime ($p = 1.0$) before others, that is, for lower values of β . On the other hand, for high β all transitions group again and become deterministic. This trend is observed in all panels. In Fig 45A we plot the probability of imitation for transitions between nodes of the same degree class but different strategy, whereas in Figs 45B and 45C we show how the probability of imitation changes with the intensity of selection for transitions that involve at least one **HDN**. Clearly, these interactions reach a deterministic regime for values of β below those in Fig 6A. This is so because the higher fitness difference between hubs and leaves leads to an effect similar to what one would obtain for smaller fitness differences but high intensity of selection β . Note further that the values of β at which we observe the transition in these interactions fit quite well the sharp increase of **FFC** with β . For the other type of interactions available, involving a **MDN** and a **LDN** (see Fig 45D), we observe that the transition to a deterministic regime occurs for higher values of β (compared to the other panels in Fig. 45), leading to a 'decoupling' between these transitions and those discussed before. In fact it appears that the transition to a deterministic regime in these interactions is positively correlated with the decrease of the **FFC**.

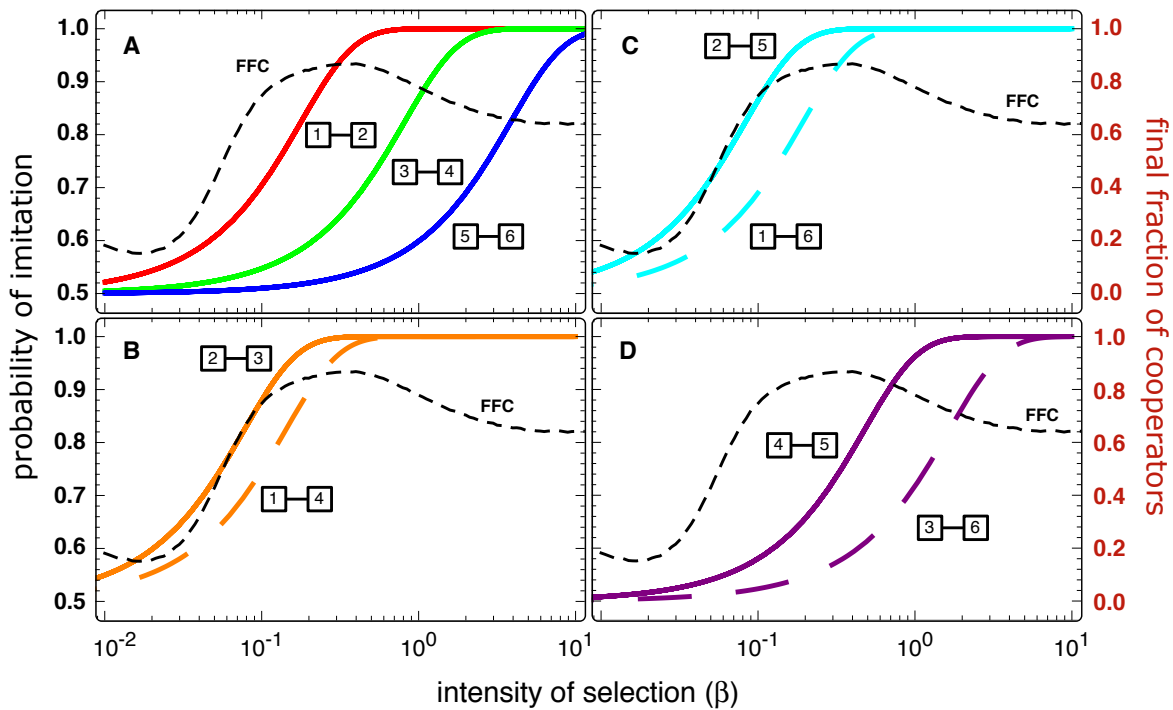


Figure 45: Probability of imitation in the meta-network. Colored curves represent the probability of imitation between different nodes in the meta-network (as depicted in Fig 44), the color and type of the line is associated with a different link of Fig 44 connecting the nodes shown in the Legend. The dashed black lines in all panels represents the final fraction of cooperators for $\lambda = 1.25$ and is associated with the scale in the right side of the frame.

In this manuscript we have shown that the macro-dynamics of a population – whose individuals engage in a *Prisoner’s Dilemma* of cooperation – strongly depends on two aspects: the network of interactions in which individuals are embedded on and of the intensity of selection associated with strategy revision. For scale-free populations the macro-dynamics is more akin to a coordination game, regardless of the intensity of selection, whereas for homogeneous networked populations it depends on the intensity of selection: for strong selection we observe a dynamics similar to a co-existence game while for weak selection regimes we recover a typical dynamics of a *Prisoner’s Dilemma*.

The fact that the game at the macro-level remains a *Prisoner’s Dilemma*, in which Cs have no chance, has been obtained previously for homogeneous random graphs, in the framework of the pair-approximation [28, 54, 55]. The pair-approximation, however, was leading to an apparent contradiction with early results from computer simulations by Szabó and collaborators (see [6] for details), which were evidencing a window of opportunity for the *Prisoner’s Dilemma* game played on homogeneous networks under strong selection. The present results resolve the apparent contradiction, showing how the macro-game changes with β .

The present work also provides evidence for the existence of an optimal intensity of selection at which levels of cooperation on structured populations are maximized. We discussed the fundamental

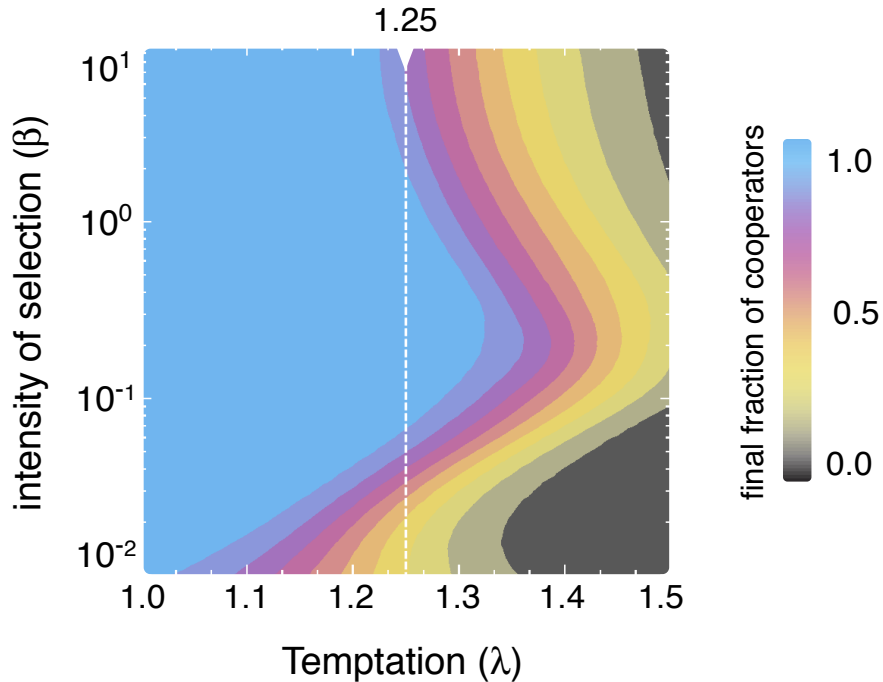


Figure 46: *Final Fraction of Cooperators* for a Scale Free (SF) population structured according to the *Minimal Model* of [44] as a function of the temptation (λ) and of the intensity of selection (β). Initially, the population was composed by equal frequencies of each strategy placed at random. We observe that for fixed λ there is an optimal value of β at which cooperation levels are maximized. These results show the same type of behavior identified in the other SF populations discussed in the main text

topological and dynamical mechanisms that led to these results on both homogeneous and scale free networks. In section 4.2 we further discuss these issues for other types of networks.

On scale free populations the mechanism that induces the existence of an optimal level for cooperation results from the high levels of social diversity [19](here, network heterogeneity) that give to a decoupling in the effective intensities of selection at which the imitation between individuals of different degree classes occur.

4.2 ADDITIONAL RESULTS

In Fig 46 we show the *final fraction of cooperators* (**FFC**) for a scale-free population whose structure was generated with the *Minimal Model* (**MM**) algorithm [44], which unlike **BA** exhibit high values of the *Cluster Coefficient* (**CC**) [5].

The behavior obtained is similar to that already identified and discussed in Figs 42 and 43 of the main text, allowing us to conclude that the underlying mechanism that generates this optimal behavior for a specific intensity of selection (β) does not depend on the **CC**. Instead these results seem to be a direct consequence of the **SF** nature of the network of interactions that give rise to the decoupling mechanism discussed in Section 3.3. Moreover, Fig. 46 corroborates the idea [56, 18]

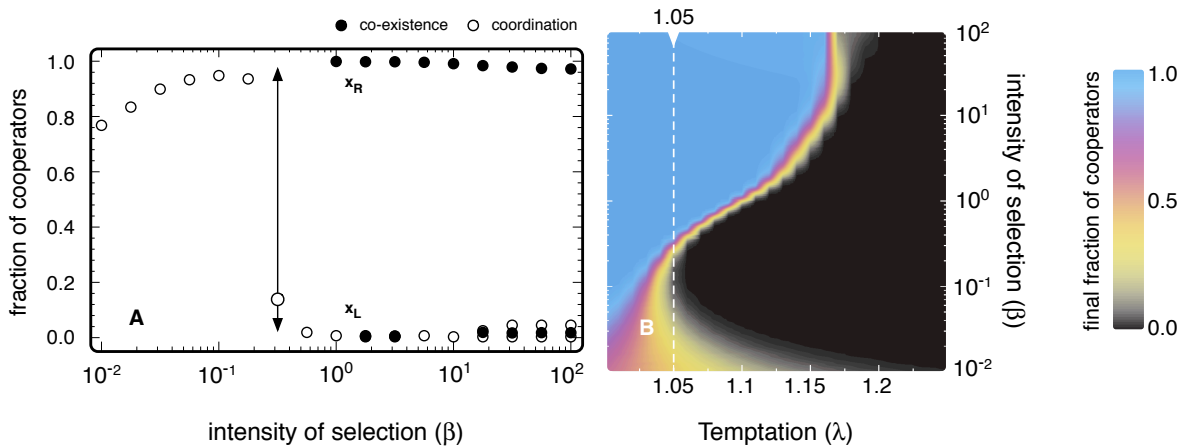


Figure 47: Evolutionary Dynamics on Random Networked Populations. A shows the internal points of the **AGoS** at the 100th generation as a function of the intensity of selection with $\lambda = 1.05$. B final fraction of cooperators, starting from 50% placed at random in the population, as a function of the Temptation (λ) and of the intensity of selection (β). Dashed line represents the results that correspond to the **AGoS** shown in A.

that high clustering combined with a heterogeneous network structure offers a clear enhancement of cooperation, when compared to the results obtained in the absence of such clustering.

Fig 47 shows the overall dynamics of a population that is organized by means of Erdős- Rényi random networks of interactions. We used random networks with 1000 nodes and average degree of 4 [5]. These random networks possess a low level of heterogeneity, exhibiting a single-scale degree distribution [41].

Fig. 47 A shows the internal points of the **AGoS** at the 100th generation as a function of the intensity of selection, where one observes that that the macro-dynamics is mainly dominated by a coordination point that, for strong selection regimes ($\beta > 1.0$) is located close to $x = 0.0$, in agreement with the final fraction of cooperators shown in Fig 47B.

Figure 48 shows the overall dynamics of populations organized on random networks exhibiting an exponential degree-distribution. Such exponential networks with 1000 nodes and average degree of 4 were generated using an algorithm similar to the *Barabási and Albert* [6], in which preferential attachment is replaced by random attachment [5, 57]. These networks exhibit levels of heterogeneity which fall in between those accruing to random and to scale free networks [41].

Figure 48A shows the internal fixed points of the **AGoS** at the 100th generation as a function of the intensity of selection. Again we see a population-wide dynamics dominated mainly by the coordination point that, for strong selection regimes ($\beta > 1.0$) is located close $x = 0.0$, making the game resemble a *Harmony Game*, a Cooperation dominance dilemma.

These results are in full agreement with what we observe in Figure 48B for the final fraction of cooperators as a function of the intensity of selection β and of the temptation parameter λ . The results in both Figures 47 and 48 show no evidence for the existence of a value of β at which cooperation is maximized; instead, we obtain a threshold value, above which cooperation is sustained. Furthermore, the analysis of these two cases puts into evidence the impact of degree heterogeneity on the

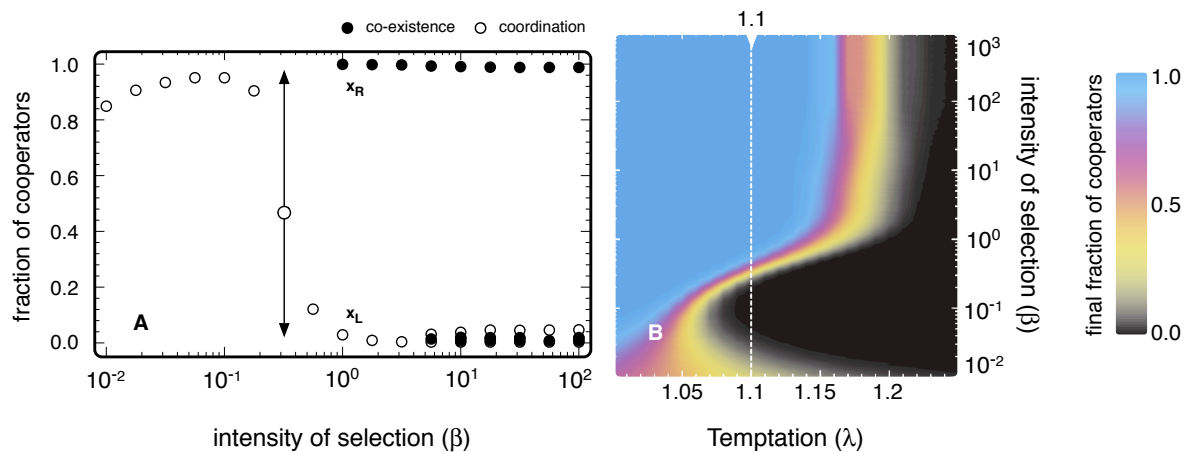


Figure 48: Evolutionary Dynamics on Exponential Networked Populations. A shows the internal points of the AGoS at the 100th generation as a function of the intensity of selection on Exponentially structured populations with $\lambda = 1.1$. B final fraction of cooperators, starting from 50% Cs placed at random in the population, as a function of the temptation (λ) and of the intensity of selection (β). Dashed line represents the results that correspond to the AGoS shown in A.

overall cooperation dynamics, as cooperation successfully dominates for a broad range of intensities of selection and temptations to defect in populations structured by Exponential networks.

4.3 BIBLIOGRAPHY

- [1] Josef Hofbauer and Karl Sigmund. *Evolutionary games and population dynamics*. Cambridge University Press, 1998.
- [2] Flávio L Pinheiro, Jorge M Pacheco, and Francisco C Santos. From local to global dilemmas in social networks. *PLoS One*, 7(2):e32114, 2012.
- [3] Nicholas A Christakis. *Connected: the amazing power of social networks and how they shape our lives*. HarperCollins UK, 2010.
- [4] Albert-László Barabási. *Linked: How everything is connected to everything else and what it means*. Plume Editors, 2002.
- [5] Sergei N Dorogovtsev and José F F Mendes. *Evolution of networks: From biological nets to the Internet and WWW*. Oxford University Press, 2003.
- [6] György Szabó and Gábor Fáth. Evolutionary games on graphs. *Physics Reports*, 446(4):97–216, 2007.
- [7] Martin A Nowak. *Evolutionary dynamics: exploring the equations of life*. Harvard University Press, 2006.
- [8] Karl Sigmund. *The calculus of selfishness*. Princeton University Press, 2010.
- [9] Jorge M Pacheco, Francisco C Santos, Max O Souza, and Brian Skyrms. Evolutionary dynamics of collective action in n-person stag hunt dilemmas. *Proceedings of the Royal Society B: Biological Sciences*, 276(1655):315–321, 2009.

- [10] Francisco C Santos and Jorge M Pacheco. Scale-free networks provide a unifying framework for the emergence of cooperation. *Physical Review Letters*, 95(9):098104, 2005.
- [11] Martin A Nowak and Robert M May. Evolutionary games and spatial chaos. *Nature*, 359(6398): 826–829, 1992.
- [12] György Szabó, Jeromos Vukov, and Attila Szolnoki. Phase diagrams for an evolutionary prisoner’s dilemma game on two-dimensional lattices. *Physical Review E*, 72(4):047107, 2005.
- [13] Attila Szolnoki, Jeromos Vukov, and György Szabó. Selection of noise level in strategy adoption for spatial social dilemmas. *Physical Review E*, 80(5):056112, 2009.
- [14] Jeromos Vukov, György Szabó, and Attila Szolnoki. Cooperation in the noisy case: Prisoner’s dilemma game on two types of regular random graphs. *Physical Review E*, 73(6):067103, 2006.
- [15] Sven Van Segbroeck, Francisco C Santos, Tom Lenaerts, and Jorge M Pacheco. Selection pressure transforms the nature of social dilemmas in adaptive networks. *New Journal of Physics*, 13 (1):013007, 2011.
- [16] H Simon. *Models of man, continuity in administrative science*, 1987.
- [17] Graham Bell. Fluctuating selection: the perpetual renewal of adaptation in variable environments. *Philosophical Transactions of the Royal Society B: Biological Sciences*, 365(1537):87–97, 2010.
- [18] Francisco C Santos, Jorge M Pacheco, and Tom Lenaerts. Evolutionary dynamics of social dilemmas in structured heterogeneous populations. *Proceedings of the National Academy of Sciences*, 103(9):3490–3494, 2006.
- [19] Francisco C Santos, Flavio L Pinheiro, Tom Lenaerts, and Jorge M Pacheco. The role of diversity in the evolution of cooperation. *Journal of Theoretical Biology*, 299:88–96, 2012.
- [20] Jorge M Pacheco, Flávio L Pinheiro, and Francisco C Santos. Population structure induces a symmetry breaking favoring the emergence of cooperation. *PLoS Computational Biology*, 5 (12):e1000596, 2009.
- [21] Mayuko Nakamaru, H Matsuda, and Y Iwasa. The evolution of cooperation in a lattice-structured population. *Journal of Theoretical Biology*, 184(1):65–81, 1997.
- [22] LM Floría, C Gracia-Lázaro, J Gómez-Gardeñes, and Y Moreno. Social network reciprocity as a phase transition in evolutionary cooperation. *Physical Review E*, 79(2):026106, 2009.
- [23] Jesús Gómez-Gardeñes, Julia Poncela, Luis Mario Floría, and Yamir Moreno. Natural selection of cooperation and degree hierarchy in heterogeneous populations. *Journal of Theoretical Biology*, 253(2):296–301, 2008.
- [24] J Gómez-Gardeñes, M Campillo, LM Floría, and Y Moreno. Dynamical organization of cooperation in complex topologies. *Physical Review Letters*, 98(10):108103, 2007.
- [25] Julia Poncela, Jesús Gómez-Gardeñes, LM Floría, and Yamir Moreno. Robustness of cooperation in the evolutionary prisoner’s dilemma on complex networks. *New Journal of Physics*, 9(6): 184, 2007.
- [26] Christoph Hauert and Michael Doebeli. Spatial structure often inhibits the evolution of cooperation in the snowdrift game. *Nature*, 428(6983):643–646, 2004.

- [27] Christoph Hauert. Spatial effects in social dilemmas. *Journal of Theoretical Biology*, 240(4): 627–636, 2006.
- [28] Hisashi Ohtsuki and Martin A Nowak. The replicator equation on graphs. *Journal of Theoretical Biology*, 243(1):86–97, 2006.
- [29] Stephen Devlin and Thomas Treloar. Cooperation in an evolutionary prisoner’s dilemma on networks with degree-degree correlations. *Physical Review E*, 80(2):026105, 2009.
- [30] Naoki Masuda. Participation costs dismiss the advantage of heterogeneous networks in evolution of cooperation. *Proceedings of the Royal Society B: Biological Sciences*, 274(1620):1815–1821, 2007.
- [31] Jochen BW Wolf, Arne Traulsen, and Richard James. Exploring the link between genetic relatedness r and social contact structure k in animal social networks. *The American Naturalist*, 177(1):135–142, 2011.
- [32] Matjaž Perc and Attila Szolnoki. Social diversity and promotion of cooperation in the spatial prisoner’s dilemma game. *Physical Review E*, 77(1):011904, 2008.
- [33] Attila Szolnoki, Matjaz Perc, and Zsuzsa Danku. Making new connections towards cooperation in the prisoner’s dilemma game. *EPL (Europhysics Letters)*, 84(5):50007, 2008.
- [34] Attila Szolnoki, Matjaž Perc, and György Szabó. Diversity of reproduction rate supports cooperation in the prisoner’s dilemma game on complex networks. *The European Physical Journal B*, 61(4):505–509, 2008.
- [35] Christoph Hauert and György Szabó. Game theory and physics. *American Journal of Physics*, 73(5):405–414, 2005.
- [36] Matjaž Perc. Evolution of cooperation on scale-free networks subject to error and attack. *New Journal of Physics*, 11(3):033027, 2009.
- [37] Matjaž Perc and Attila Szolnoki. Coevolutionary games—a mini review. *BioSystems*, 99(2): 109–125, 2010.
- [38] Peter D Taylor, Troy Day, and Geoff Wild. Evolution of cooperation in a finite homogeneous graph. *Nature*, 447(7143):469–472, 2007.
- [39] Francisco C Santos, JF Rodrigues, and Jorge M Pacheco. Epidemic spreading and cooperation dynamics on homogeneous small-world networks. *Physical Review E*, 72(5):056128, 2005.
- [40] Albert-László Barabási and Réka Albert. Emergence of scaling in random networks. *Science*, 286(5439):509–512, 1999.
- [41] Luis A Nunes Amaral, Antonio Scala, Marc Barthelemy, and H Eugene Stanley. Classes of small-world networks. *Proceedings of the National Academy of Sciences*, 97(21):11149–11152, 2000.
- [42] Albert-László Barabási, Réka Albert, and Hawoong Jeong. Mean-field theory for scale-free random networks. *Physica A: Statistical Mechanics and its Applications*, 272(1):173–187, 1999.
- [43] Duncan J Watts and Steven H Strogatz. Collective dynamics of ‘small-world’ networks. *Nature*, 393(6684):440–442, 1998.
- [44] S N Dorogovtsev, J F F Mendes, and A N Samukhin. Size-dependent degree distribution of a scale-free growing network. *Physical Review E*, 63(6):062101, 2001.

- [45] Michael W Macy and Andreas Flache. Learning dynamics in social dilemmas. *Proceedings of the National Academy of Sciences*, 99(Suppl 3):7229–7236, 2002.
- [46] Arne Traulsen, Martin A Nowak, and Jorge M Pacheco. Stochastic dynamics of invasion and fixation. *Physical Review E*, 74(1):011909, 2006.
- [47] Arne Traulsen, Jorge M Pacheco, and Martin A Nowak. Pairwise comparison and selection temperature in evolutionary game dynamics. *Journal of Theoretical Biology*, 246(3):522–529, 2007.
- [48] György Szabó and Csaba Tóke. Evolutionary prisoner’s dilemma game on a square lattice. *Physical Review E*, 58(1):69, 1998.
- [49] Max O Souza, Jorge M Pacheco, and Francisco C Santos. Evolution of cooperation under n-person snowdrift games. *Journal of Theoretical Biology*, 260(4):581–588, 2009.
- [50] Francisco C Santos and Jorge M Pacheco. Risk of collective failure provides an escape from the tragedy of the commons. *Proceedings of the National Academy of Sciences*, 108(26):10421–10425, 2011.
- [51] João A Moreira, Flavio L Pinheiro, Ana Nunes, and Jorge M Pacheco. Evolutionary dynamics of collective action when individual fitness derives from group decisions taken in the past. *Journal of Theoretical Biology*, 298:8–15, 2012.
- [52] Sven Van Segbroeck, Jorge M Pacheco, Tom Lenaerts, and Francisco C Santos. Emergence of fairness in repeated group interactions. *Physical Review Letters*, 108(15):158104, 2012.
- [53] Francisco C Santos, Marta D Santos, and Jorge M Pacheco. Social diversity promotes the emergence of cooperation in public goods games. *Nature*, 454(7201):213–216, 2008.
- [54] Hisashi Ohtsuki, Jorge M Pacheco, and Martin A Nowak. Evolutionary graph theory: breaking the symmetry between interaction and replacement. *Journal of Theoretical Biology*, 246(4):681–694, 2007.
- [55] Hisashi Ohtsuki, Martin A Nowak, and Jorge M Pacheco. Breaking the symmetry between interaction and replacement in evolutionary dynamics on graphs. *Physical Review Letters*, 98(10):108106, 2007.
- [56] F C Santos, J F Rodrigues, and J M Pacheco. Graph topology plays a determinant role in the evolution of cooperation. *Proceedings of the Royal Society B: Biological Sciences*, 273(1582):51–55, 2006.
- [57] Réka Albert and Albert-László Barabási. Statistical mechanics of complex networks. *Reviews of Modern Physics*, 74(1):47, 2002.

EVOLUTION OF COOPERATION UNDER VARIABLE MUTATION RATES

To be Submitted

Flávio L. Pinheiro, Francisco C. Santos and Jorge M. Pacheco

In this work we analyze how constant and variable mutation rates influence the evolutionary dynamics of cooperation in structured populations. In biology, mutations account for mistakes in the replication process, whereas in behavioral dynamics they can account for innovations and exploration of new strategies, ideas or traits. In a sense, mutations equip an evolving system with the necessary stochasticity to explore the strategy space independent of the current state of a population .

While many works have explored the impact of mutations in the context of population dynamics, few have studied how mutations impact the evolutionary dynamics in structured populations. Here we show that when individuals engage in a Prisoner's Dilemma game in heterogeneous networks, the introduction of mutation rates induce striking regime shifts, from the defection dominance that characterizes the standard Prisoner's Dilemma into a regime of coexistence among Cooperators and Defectors, as well as into a regime of coordination, often revealing more than one basin of attraction. Moreover, we show that under strong selection regimes, cooperation is undermined by variations in the mutation rate, whereas under weak selection one witnesses a subtle balance between selection and mutation, which is favorable to defectors. Interestingly, there exists a range of selection pressures in which structured populations are most resilient to variations in mutation rates.

5.1 MANUSCRIPT

Selection and Mutation are two of the fundamental mechanisms that drive the evolutionary dynamics of social and biological systems [1]. Both these mechanisms have an intuitive interpretation from a biological point of view: Mutations account for mistakes during the replication of individual's traits, giving rise to new types; Selection exists as long as different types of individuals reproduce at different rates by consequence of environmental or/and peer pressure. In many respects, cultural/social evolution, and many socio-economic systems proceed in a way which closely mimics that of its biological counterpart [2, 3]. We replicate behaviours of others by means of social learning and peer-influence [4, 5, 6] with mutations accounting for errors or innovations [7]. Moreover, we all recognize that certain behaviours are favoured with respect to others, thus being preferentially selected, depending on the context they are embedded in.

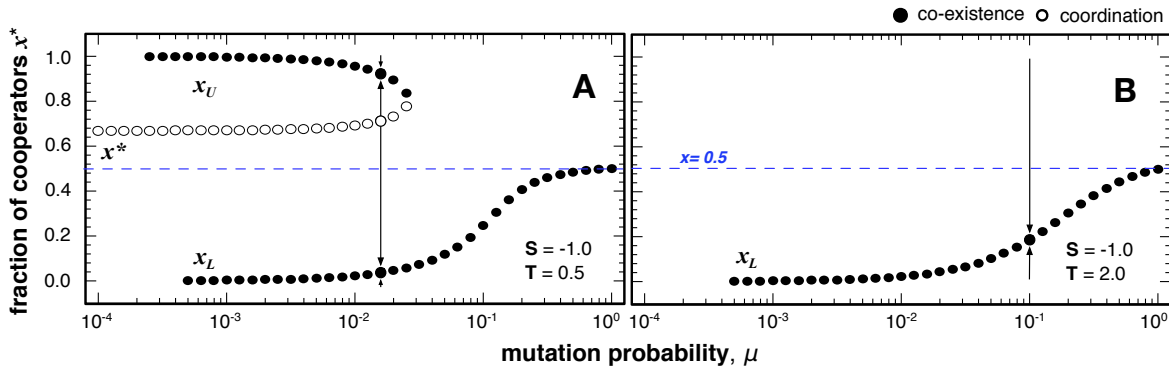


Figure 49: Internal points of the gradient of selection $G_\mu(k)$ on finite and well-mixed populations for a wide range of mutation probabilities. Each panel concerns different game parameters as indicated. We used $\beta = 1.0$ and, given the well-mixed nature of the dynamics, used the average payoff as a measure of individual fitness. Arrows point towards the direction of selection.

Theoretical models, in turn [8, 9, 10, 11, 12, 13, 14, 15], often rely on a constant selection pressure and mutation rates to investigate the evolution of traits within a population. This line of research collides with the evidence that populations undergo changes in mutation rates, as stated above. It is thus important to understand the impact of a variable mutation rate in the evolutionary outcome of populations. This is the purpose of this work, in which we investigate the role of a variable mutation in what concerns the evolution of cooperation in both well-mixed and structured populations. To this end, we adopt an Evolutionary Game Theory [1] framework and consider the Prisoner's dilemma [16], which is commonly regarded as the prototypical social dilemma of cooperation.

Following past works [8, 10, 14, 17] we model population structure by means of a complex network, where individuals correspond to nodes and interactions are defined by the links connecting pairs of nodes. We shall focus in a network structure that mimics the topology of scale-free networks [18], which are commonly regarded as good representatives of the heterogeneous nature of real-world social networks. Recent works have shown that, in the absence of mutations, the evolutionary dynamics in structured populations is decoupled from the dilemma faced locally by individuals [9, 19]. Indeed, in strongly heterogeneous populations it was found that the global dynamics is dominated by a coordination of strategies, which closely resembles a Stag Hunt game on a well-mixed population.

In the following section we shall start by detailing the model adopted and discuss how variable mutations impact the evolutionary dynamics of the *Prisoner's Dilemma* and *Stag Hunt* games in well-mixed populations, thus providing the necessary intuition to understand the unfolding dynamic on networked populations (see Section 5.1.3).

5.1.1 Model

Let us consider a finite population of individuals that adopt one of two possible behaviours/strategies: to Cooperate (C) or to Defect (D). Each individual collects a payoff from each interaction he/she participates with his/her neighbours. The total payoff gathered by an individual is computed by $\Pi_i =$

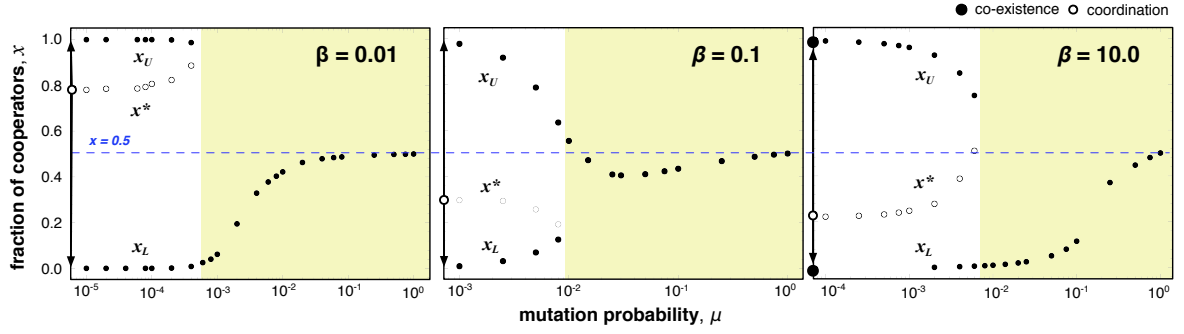


Figure 50: Internal fixed points of the $\Gamma_\mu(k, g)$ at $g = 100$ on structured populations as a function of the mutation probability μ . Each panel regards the results under a different selection pressure, A) $\beta = 0.01$, B) $\beta = 0.1$ and C) $\beta = 10.0$. The yellow background denotes the dynamical region after the coalescence of the internal roots points of the $\Gamma_\mu(k, g)$, location which is denoted by a red cross. Other parameters are $T = 1.25$, $S = -0.25$, $Z = 10^3$, and average degree of 4.

$n_i^C(S_i(R - T) + T) + n_i^D(S_i(S - P) + P)$ where n_i^C (n_i^D) is the number of cooperators (defectors) in the vicinity of i while S_i is 1 if individual i is a C being 0 when he is a D. The parameters **T** (Temptation), **R** (Reward), **P** (Punishment) and **S** (Sucker's Payoff) define the social dilemma faced locally by each individual in a two-person-two-strategy interaction. It is customary to consider a simplified domain of parameters bounded by $R = 1.0$, $P = 0.0$, $-1 \leq S \leq 0.0$ and $0.0 \leq T \leq 2.0$ [17], thus depending on the ordering of the parameters one can define the Stag Hunt ($R > T > P > S$) [20] or the Prisoner's Dilemma ($T > R > P > S$) [16].

Here we shall consider that the change of strategy abundance in the population is modelled by means of a stochastic Birth-Death process, in which Selection is implemented by the pairwise-comparison rule [11] and mutation occurs at different rates. The co-evolution of both processes can be summarized as follows: at each time step a randomly selected individual, A, adopts a different strategy (selected at random) with probability μ or, with probability $1 - \mu$, imitates the strategy of a random neighbour, B, with probability $p = [1 + \exp(-\beta(f_B - f_A))]^{-1}$, where f_i denotes the fitness of individual i and β the intensity of selection.

$$\begin{aligned}
 T_\mu^+(k) &= (1 - \mu) \frac{Z - k}{Z} \frac{k}{Z - 1} \frac{1}{1 + \exp(-\beta(f_C - f_D))} + \mu \frac{Z - k}{Z} \\
 T_\mu^-(k) &= (1 - \mu) \frac{k}{Z} \frac{Z - k}{Z - 1} \frac{1}{1 + \exp(\beta(f_C - f_D))} + \mu \frac{k}{Z}
 \end{aligned} \tag{64}$$

When populations are well-mixed the dynamics is fully characterized by the gradient of selection (with mutations) $G_\mu(k) = T_\mu^+(k) - T_\mu^-(k)$, where $T_\mu^+(k)$ (Equation 66) refers to the probability of increasing the number of Cs by one and $T_\mu^-(k)$ (Equation 66) the probability of decreasing the number of Cs by one, for a given configuration with k Cs [11]. Hence from $T_\mu^+(k)$ and $T_\mu^-(k)$, $G_\mu(k)$ simplifies to

$$G_\mu(k) = (1 - \mu) \frac{Z - k}{Z} \frac{k}{Z - 1} \tanh\left(\frac{\beta \Delta f}{2}\right) + \mu \left(1 - \frac{2k}{Z}\right) \tag{65}$$

where $\Delta f = f_C - f_D$. This quantity when negative (positive) implies that the tendency of cooperators to decrease (increase). It is intuitive to conclude that there is a critical mutation probability μ_C above which the second term of Equation 65 dominates, and selection will not operate at a population-wide level. Thus, in the extreme scenario of $\mu = 1.0$ the population evolves towards a stationary state in which half of the individuals are Cooperators and the remaining half are Defectors, resembling a coexistence dynamics characterized by a stable probability attractor (a finite population analogue of a stable fixed point) located at $x \equiv \frac{k}{Z} = 0.5$. This strong mutation limit is indicated by a blue dashed line in Figure 49, 51 and 52.

On the other hand, when $\mu = 0.0$ each social dilemma/game prompts a characteristic dynamical picture: for $T < R$ and $S < P$ the G_μ is dominated by an interior unstable fixed point at $x^* \equiv (k/Z)^* \approx (P - S)(R + P - S - T)^{-1}$, which works as a probability repeller resulting in coordination-like dynamics of a Stag Hunt game; in the Prisoner's Dilemma ($T > R$ and $S < P$) $G_\mu(k)$ is negative for all values of k and defectors are always advantageous, irrespectively of their prevalence.

The addition of mutations prompts the emergence of additional internal fixed points. In the case of the Stag Hunt we see the emergence of two stable fixed points near $x = 0.0$ and $x = 1.0$ (x_L and x_U respectively), while in the Prisoner's Dilemma we see the emergence of a single stable fixed (x_L) point near $x = 0.0$. In both cases the internal fixed points x_L and x_U move towards $x = 0.5$ with increasing μ . Hence when $S > T - 1$ ($< T - 1$) the repeller (x^*) lies bellow (above) 0.5 and will coalesce with x_L (x_U) at a critical μ_C , as exemplified in Figure 49A for $T = 0.5$ and $S = -1.0$. When $S = T - 1$ the internal repeller is located at $x^* = 0.5$ leading to a bifurcation at μ_C . In the case of the Prisoner's Dilemma the single probability attractor x_L that emerges move towards $x = 0.5$ with increasing μ , as shown in Figure 49B. It is noteworthy that the particular choice of game parameters and intensity of selection (β) influence the value of μ_c (see Equation 65, and Section 5.1.3).

The above-mentioned dynamical portraits can generate distinct outcomes when a well-mixed population faces variations in the overall mutation rates. Let us now consider a case in which, during the course of evolution, a population that started from a monomorphic configuration (*i.e.* entirely composed by Cs or Ds) experiences a transition from a low to a high level of mutation rate (for instance, a change of the habitat due to a radioactive exposure) followed by a return to its initial state (the time scales of these two processes may be very different, a feature we are not including here). Let us further assume that the mutation rate rises above the critical value μ_C , that is, into a scenario dynamically dominated by the mutation process.

When well-mixed populations inexorably evolve into full defection as the mutation rate decreases. Thus, under a Prisoner's Dilemma, the evolutionary dynamics remains, on average, unchanged by variations in the mutation level. A different outcome is observed in the other social dilemmas, in particular under the Stag Hunt game (see Figure 49A), the existence of an unstable internal fixed point (*i.e.* a coordination dynamics) implies that the outcome will be dictated by the largest basin of attraction — full cooperation for $S > T - 1$ or full defection if $S < T - 1$ — regardless of the initial composition of strategies prior to variations in mutation levels. Hence, variation in mutation rates may imply regime shift for a population that was initially composed solely by Cs. Finally, it is worth

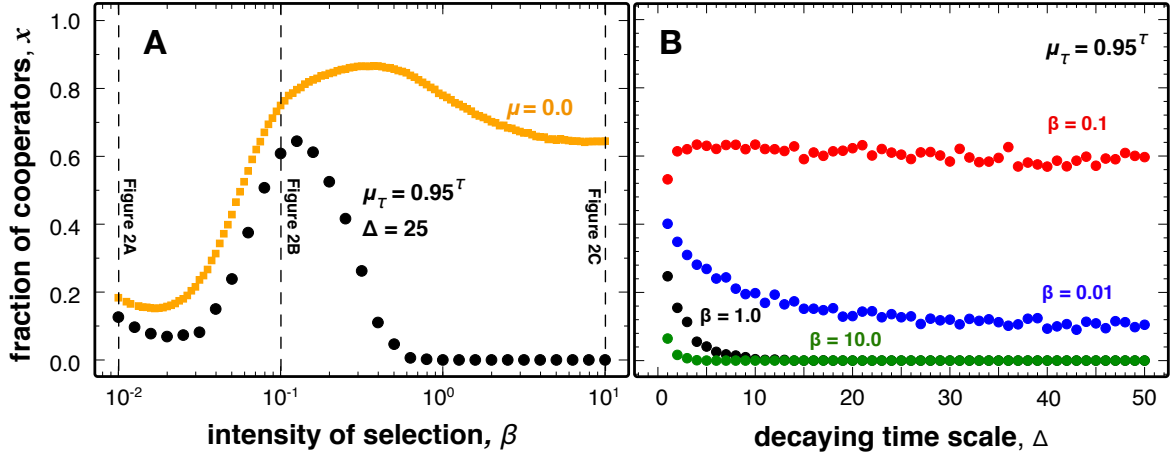


Figure 51: Level of cooperation under variable mutations for a wide range of selection pressures (panel A) and decaying time scales (panel B) on structured populations. Panel A shows the average final fraction of cooperation under variable mutation (black disks) when compared with the level of cooperation attained in a scenario without mutations (orange squares). Dashed lines indicate the values used in Figure 51. Panel B shows the average final fraction of cooperation for different decaying time scales of the mutation rate for different selection pressures. Other parameters are $S = -0.25$, $T = 1.25$, $Z = 10^3$ and average degree of 4.

mentioning that variations of the selection pressure do not change qualitatively these scenarios they do however change the values of μ at which the fixed points bifurcate.

5.1.2 Materials and Methods

The gradient of selection $G_\mu(k)$, as defined in the previous section, is not valid for structured populations. An analytical estimation is also hard to compute in closed form, since transition probabilities depend on the particular assortment of strategies in the network, thus $G_\mu(k)$ is context and time dependent. To overcome such limitations we numerically compute an average over all possible transitions through simulations, obtaining an average gradient of selection (AGoS, denoted by $\Gamma_\mu(k, g)$). This approach has the advantage of being independent of the network structure, mutation probabilities and intensity of selection. The AGoS is defined as $\Gamma_\mu(k, g) = \xi_\mu^+(k, g) - \xi_\mu^-(k, g)$, where $\xi_\mu^+(k, g)$ and $\xi_\mu^-(k, g)$ account for the population averaged probability to increase and decrease the number of Cs by one (i.e. the numerical equivalents of $T^+(k)$ and $T^-(k)$ respectively) at the g^{th} generation, for mutation probability μ and for a given configuration with Cs.

The $\Gamma_\mu(k, g)$, was numerically estimated during the first 150 generations (1 generation corresponds to Z time steps), which accounts for a total of $t_{max} = Z \times g = 1.5 \times 10^5$ iterations. In order to obtain a good estimate of these quantities a total of $\Omega = 2.5 \times 10^7$ independent simulations were conducted, each starting from a random configuration with Cs. A total of 10^3 Scale-Free networks were generated and used in the simulations.

Finally, for each simulation $\xi_{\mu}^{+}(k, g)$ and $\xi_{\mu}^{-}(k, g)$ account respectively for the average probabilities to increase and decrease the number of Cs by one at generation (g) in configuration (k), which can be written as

$$\begin{aligned}\xi_{\mu}^{-}(k, g) &= \frac{1 - \mu}{\Lambda_g(k)} \sum_{\omega=1}^{\Omega} \sum_{t=1}^{t_{max}} [\delta(k, k_t) \Theta(\frac{t}{Z}, g) \frac{1}{Z} \sum_{i=1}^Z \frac{1}{z_i} \sum_{j \in \zeta_i} \frac{S_i - S_j S_i}{1 + \exp[-\beta(f_j - f_i)]]] \\ &\quad + \mu \frac{k}{Z} \\ \xi_{\mu}^{+}(k, g) &= \frac{1 - \mu}{\Lambda_g(k)} \sum_{\omega=1}^{\Omega} \sum_{t=1}^{t_{max}} [\delta(k, k_t) \Theta(\frac{t}{Z}, g) \frac{1}{Z} \sum_{i=1}^Z \frac{1}{z_i} \sum_{j \in \zeta_i} \frac{S_j - S_i S_j}{1 + \exp[-\beta(f_j - f_i)]]] \\ &\quad + \mu \frac{Z - k}{Z}\end{aligned}\tag{66}$$

where S_i is 1 (0) if the strategy of individual i is **C** (**D**), $\Lambda_g(k)$ is the number of times the system was observed at configuration k of generation g , $\delta(a, b)$ is equal to 1 if $a = b$ being 0 otherwise, $\Theta(a, b)$ is one when $b - 1 \leq a < b$ and 0 otherwise. The first summation is over all time-series, the second is over all iterations of a given time-series, the third is over each individual in the population and the fourth along the entire neighborhood of an individual. The internal points of $\Gamma_{\mu}(k, g)$ in Figure 50 concern the results at the 100th generation at which the evolution of $\Gamma_{\mu}(k, g)$ arrived has achieved an equilibrium.

5.1.3 Results and Discussion

The previous considerations set the right framework and stage for the ensuing analysis, in which we abandon the assumption that populations are well-mixed. In fact, this is usually a strong assumption that is seldom realized. In some simple cases, one may have populations spatially and quasi-regularly distributed [10]. More often, populations exhibit sizable levels of irregularities, which translate into a population structure well represented by heterogeneous graphs, often exhibiting fat-tails whenever populations are sufficiently large [18]. Hence, in the remainder of the manuscript we probe the impact of variable mutation levels on structured populations [9], where structure will translate into scale-free complex networks of interactions, generated using the Barabási-Albert algorithm of growth and preferential attachment [18]. Consequently, the structures we will consider exhibit sizable heterogeneity in what concerns the distribution of the number of interactions, a feature which is found to be ubiquitous in real world networks [21, 22].

Figure 50 shows the location of internal roots of $\Gamma_{\mu}(k, g)$ (the equivalent of $G_{\mu}(k)$ in structured populations, see Section 5.1.1) for a broad μ range of (fixed) mutation rates ($10^{-4} \leq \mu \leq 1.0$) and for the case with $T = 1.25$ and $S = -0.25$ (Prisoner's Dilemma domain). Each panel of Figure 50 shows the results obtained for different selection pressures: $\beta = 0.01$ (panel A), $\beta = 0.1$ (panel B) and $\beta = 10.0$ (panel C).

For $\mu = 0.0$ with $\beta = 0.001$ and $\beta = 0.01$ the population-wide dynamics is dominated by a single internal probability repeller at x^* . For strong selection additional roots appear in the vicinity of $x = 1.0$ and $x = 0.0$ which, while playing no relevant role in the present analysis, result from

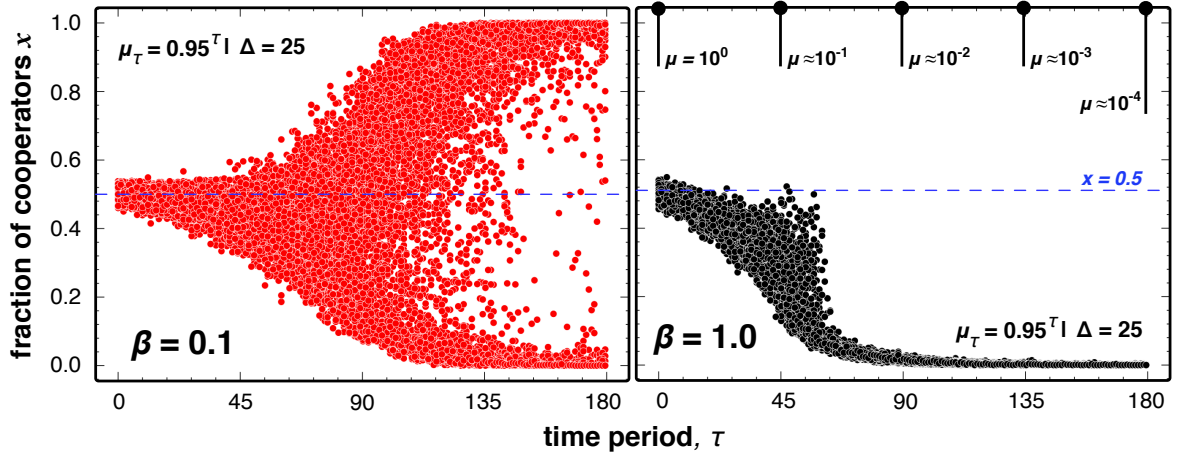


Figure 52: Time evolutions under variable mutation rates on structured populations. Each evolution starts with $\mu_0 = 1.0$, which decreases every period (j) of $i = 25$ generations while $\mu > 10^{-4}$. Each point concerns the fraction of cooperators at the end of each period on 103 independent evolutions. Other parameters are $\beta = 0.1$ (panel A) and 1.0 (panel B), $S = -0.25$, $T = 1.25$, $Z = 10^3$ with average degree of 4.

specific assortments of strategies which lead, in the absence of mutations, to long fixation times [19]. The coordination nature of the population-wide dynamics implies that an increasing μ leads to the emergence of two internal probability attractors near $x = 1.0$ (x_U) and $x = 0.0$ (x_L), that move towards $x = 0.5$ with increasing μ .

From Figure 50 one may easily infer that, as in many other complex adaptive systems [2, 23, 24, 25, 26], evolution in structured populations portrays critical thresholds (or tipping points) at which the population-wide dynamics abruptly shifts from one regime to another. In this case, two distinct dynamical pictures result with increasing μ , depending on the selection pressure. For $\beta = 0.01$ (Figure 50A) x^* coalesces with x_L (similar to the results on well-mixed populations whenever $x^* < 0.5$), whereas for $\beta = 0.01$ and 10.0 (Figure 50B) x^* coalesces with x_U . Hence, and unlike the scenario associated with well-mixed populations, the evolutionary outcome under variable mutation rates on structured populations will also depend on the overall selection pressure: An increase in the mutation rate will drive populations towards a coexistence of strategies, regardless of both *i*) initial configuration of the population and *ii*) selection pressure. However, a decrease in the mutation rate implies the demise of cooperation for a wide range of selection pressures ($\beta < 0.1$ and $\beta > 0.5$, see panel A of Figure 51). However in between these two domains ($0.1 < \beta < 0.5$) coordination is again favored, thus recovering the initial dynamics. These results highlight the idea of the existence of an optimal selection pressure in what concerns the evolution of cooperation.

In the following we check the evolutionary dynamics discussed in Figure 50 by simulating the evolution of cooperation on structured populations undergoing a transition between strong and weak mutation regimes. Hence, let us consider a structured population evolving from an initially random composition of strategies with constant T , S and β and initial $\mu_0 = 1.0$. At the end of each period (τ) of Δ generations the population undergoes a decrease in the mutation levels according to the expression $\mu_{\tau+1} = 0.95\mu_\tau$; this process is repeated 180 times, that is, while $\mu > 10^{-4}$. Figure 51A

Chapter 5. EVOLUTION OF COOPERATION UNDER VARIABLE MUTATION RATES

shows the final fraction of cooperators under variable mutations (black dots) and in the absence of mutations (orange squares) for a wide range of selection pressures. Figure 51B shows the dependence of cooperation on the adopted decaying timescale, for different selection pressures.

A population undergoing a period of variable mutation rates (as described above) will always attain lower levels of cooperation, which for $\beta > 0.5$ results in the complete demise of cooperation. For lower selection pressures the stochastic effects compensate the harsher dynamical picture (also evidenced in Figure 50A). Moreover, as shown in Figure 51B, the decrease of cooperation becomes emphasized whenever the mutation rates decay slowly (that is, for higher Δ).

Finally, as suggested by the dynamical picture of Figure 50B and 3A there is window of hope for cooperators within a range of selection pressures (around $\beta = 0.1$) which optimizes the resilience of populations to such events of variable mutation rates. In what concerns the time scale of decay (Figure 50B), for $\beta = 0.01$ the evolutionary outcome remains unchanged for periods larger than $\Delta > 8$.

Figure 52 shows how the cooperation levels change with the decrease of the mutation rates for $\beta = 0.1$ and $\beta = 1.0$. In both panels, each dot represents the level of cooperation at the end of each period of 25 generations before the decrease of the mutation rates. Each example reflects the predicted dynamical picture discussed in Figure 50.

In sum this work shows how mutation rates and its variation impact the evolutionary outcome of cooperation on well-mixed and structured populations. When populations are taken as well-mixed, four prototype scenarios were identified in the domains of the Stag Hunt and Prisoner's Dilemma, which are qualitatively invariant for changes in the selection pressures (see Figure 49). For the more realistic case of structured populations we have shown the important role of selection pressure in providing the population with resilience to defectors fixation, identifying a range of selection pressures that optimize populations resilience to changes in the mutation rates (see Figure 50 and 51).

5.2 BIBLIOGRAPHY

- [1] Martin A Nowak. *Evolutionary dynamics*. Harvard University Press, 2006.
- [2] Robert M May, Simon A Levin, and George Sugihara. Complex systems: Ecology for bankers. *Nature*, 451(7181):893–895, 2008.
- [3] Simon Levin, Tasos Xepapadeas, Anne-Sophie Crépin, Jon Norberg, Aart De Zeeuw, Carl Folke, Terry Hughes, Kenneth Arrow, Scott Barrett, Gretchen Daily, et al. Social-ecological systems as complex adaptive systems: modeling and policy implications. *Environment and Development Economics*, 18(02):111–132, 2013.
- [4] Flavio L Pinheiro, Marta D Santos, Francisco C Santos, and Jorge M Pacheco. Origin of peer influence in social networks. *Physical Review Letters*, 112(9):098702, 2014.
- [5] Nicholas A Christakis and James H Fowler. The collective dynamics of smoking in a large social network. *New England journal of medicine*, 358(21):2249–2258, 2008.
- [6] James H Fowler and Nicholas A Christakis. Cooperative behavior cascades in human social networks. *Proceedings of the National Academy of Sciences of the United States of America*, 107(12):5334–5338, 2010.

- [7] Arne Traulsen, Christoph Hauert, Hannelore De Silva, Martin A Nowak, and Karl Sigmund. Exploration dynamics in evolutionary games. *Proceedings of the National Academy of Sciences of the United States of America*, 106(3):709–712, 2009.
- [8] Francisco C Santos, Flavio L Pinheiro, Tom Lenaerts, and Jorge M Pacheco. The role of diversity in the evolution of cooperation. *Journal of Theoretical Biology*, 299:88–96, 2012.
- [9] Flavio L Pinheiro, Jorge M Pacheco, and Francisco C Santos. From local to global dilemmas in social networks. *PLoS One*, 7(2):e32114, 2012.
- [10] György Szabó and Gabor Fath. Evolutionary games on graphs. *Physics Reports*, 446(4):97–216, 2007.
- [11] Arne Traulsen, Jorge M Pacheco, and Martin A Nowak. Pairwise comparison and selection temperature in evolutionary game dynamics. *Journal of Theoretical Biology*, 246(3):522–529, 2007.
- [12] Chaitanya S Gokhale, Yoh Iwasa, Martin A Nowak, and Arne Traulsen. The pace of evolution across fitness valleys. *Journal of Theoretical Biology*, 259(3):613–620, 2009.
- [13] Sven Van Segbroeck, Francisco C Santos, Tom Lenaerts, and Jorge M Pacheco. Selection pressure transforms the nature of social dilemmas in adaptive networks. *New Journal of Physics*, 13(1):013007, 2011.
- [14] Matjaž Perc and Attila Szolnoki. Coevolutionary games—a mini review. *BioSystems*, 99(2):109–125, 2010.
- [15] Benjamin Allen, Arne Traulsen, Corina E Tarnita, and Martin A Nowak. How mutation affects evolutionary games on graphs. *Journal of Theoretical Biology*, 299:97–105, 2012.
- [16] Karl Sigmund. *The calculus of selfishness*. Princeton University Press, 2010.
- [17] Francisco C Santos, Jorge M Pacheco, and Tom Lenaerts. Evolutionary dynamics of social dilemmas in structured heterogeneous populations. *Proceedings of the National Academy of Sciences of the United States of America*, 103(9):3490–3494, 2006.
- [18] Albert-László Barabási and Réka Albert. Emergence of scaling in random networks. *Science*, 286(5439):509–512, 1999.
- [19] Flavio L Pinheiro, Francisco C Santos, and Jorge M Pacheco. How selection pressure changes the nature of social dilemmas in structured populations. *New Journal of Physics*, 14(7):073035, 2012.
- [20] Brian Skyrms. *The stag hunt and the evolution of social structure*. Cambridge University Press, 2004.
- [21] Guido Caldarelli. Scale-free networks: complex webs in nature and technology. *OUP Catalogue*, 2007.
- [22] Luis AN Amaral and Julio M Ottino. Complex networks. *The European Physical Journal B-Condensed Matter and Complex Systems*, 38(2):147–162, 2004.
- [23] Marten Scheffer. *Critical transitions in nature and society*. Princeton University Press, 2009.
- [24] Marten Scheffer, Steve Carpenter, Jonathan A Foley, Carl Folke, and Brian Walker. Catastrophic shifts in ecosystems. *Nature*, 413(6856):591–596, 2001.

Chapter 5. EVOLUTION OF COOPERATION UNDER VARIABLE MUTATION RATES

- [25] Marten Scheffer, Stephen R Carpenter, Timothy M Lenton, Jordi Bascompte, William Brock, Vasilis Dakos, Johan Van De Koppel, Ingrid A Van De Leemput, Simon A Levin, Egbert H Van Nes, et al. Anticipating critical transitions. *Science*, 338(6105):344–348, 2012.
- [26] Steven J Lade, Alessandro Tavoni, Simon A Levin, and Maja Schlüter. Regime shifts in a social-ecological system. *Theoretical Ecology*, 6(3):359–372, 2013.

LINKING INDIVIDUAL AND COLLECTIVE BEHAVIOR IN ADAPTIVE SOCIAL NETWORKS

Submitted

Flávio L. Pinheiro, Francisco C. Santos and Jorge M. Pacheco

In the previous chapters we have dealt with the characterization of dynamical processes on complex networks. So far we have assumed that networks are static, that is, individuals interactions remain fixed along the entire timespan of the evolutionary dynamics. This assumption, however, is but a simplification that does not take into account the natural adaptive nature of social structures. Indeed, individuals not only adapt their dynamical states (*i.e.* behaviors, traits, etc) they also choose with whom they interact. It is thus important to consider the co-evolution of structure along with the evolution of traits.

Previous works have shown that adaptive social structures promote the evolution of Cooperation. However, up to now the characterization of the macroscopic, population wide dynamics hat stems from such co-evolutionary processes has remained illusive, mainly due to the same challenges already faced in the characterization of dynamical processes in static networks. Here we establish such link by connecting individual decision making to the self-organizing collective behavior in a manner that allows to study and compare the results with the previous analysis and thus factor the contribution that co-evolution of structure introduces to the overall dynamical portrait.. We demonstrate that adaptive social structures change the 2-person social dilemma locally faced by individuals into an evolutionary dynamics that resembles that of a N -person coordination game, whose characteristics depend sensitively on the relative time-scales between behavioral and network co-evolution. Indeed, we show that faster the relative rate of adaptation of the network, the smaller the critical fraction of Cooperators required for cooperation to prevail, thus establishing a direct link between network adaptation and the evolution of cooperation. The framework developed here is not only general but readily applicable to other dynamical processes occurring on adaptive networks, notably the spreading of contagious diseases or the diffusion of innovations.

6.1 MANUSCRIPT

Complex networks provide a rich and powerful representation of the underlying web of social ties that interconnects individuals in a given community, society or population [1, 2, 3, 4]. As time unfolds,

individuals adapt their behaviors and preferences in the context of the position they occupy in the social network they are part of [5, 6], adaptations that often induce changes in the structure of the social network. Hence, the socially heterogeneous structures ubiquitous among empirical analysis are but the natural result from the interplay between the co-evolution of the different mechanisms.

The emerging features of an evolving structure are contingent on the underlying mechanism driving interactions between peers. For instance, if what is at stake is the spreading of a disease, healthy individuals ought to break (secure) the links with infected (healthy) individuals, provided they know they are (not) infected [7, 8], while social dilemmas of cooperation [9, 10] often pitch individuals with competing preferences, which unfolds into a more complex decision process. To understand the time dependence of both social structure and individuals' choices it is necessary a co-evolutionary process [11] where individual behavior is allowed to evolve *at par* with the structure of the underlying interaction network. The latter implies that links are possibly rewired depending on whether individuals are satisfied or not with a given interaction. A simple implementation of such a model [11, 12, 13, 14, 15, 16, 17, 18] is expected to account for many of the stylized facts that characterise social-structure [19]: individual preferences; resolution of conflicts of interest and an adaptive heterogeneous network that co-evolves with the process at stake.

Figure 53 provides an overview of what is known to date by means of computer simulations, regarding the co-evolution of cooperation and network topology [11], when the social dilemma at stake is a Prisoner's Dilemma (**PD**) of cooperation (details provided below). The relative time-scales of network adaptation and behavioral evolution are controlled by the parameter τ : When $\tau = 0$ no network adaptation occurs; when $\tau = 1$ no behavioral adaptation occurs. Inspection of Fig. 1 clearly shows that adaptation favors cooperation, and not defection, at a population wide level. Consequently, and despite the fact that, individually, every individual engages in a **PD** game, globally, the game being played must be a different one.

But which one? Of which type? With which features? These questions remain open and are of fundamental importance given that, often, all we can gather empirically (e.g. from microbes populations or human societies [20, 21, 22]) are time-series of aggregate information at a population wide scale, without direct information on individual behavior. An intuitive example of our empirical constraints regards epidemic outbreaks: What one often collects is aggregate statistical information of the community as a whole, instead of individual information that may allow practitioners to infer directly from the data the characteristics of the, say, virus infectiousness [7]. Thus, and similar to many other areas of Physics, it becomes ubiquitous to establish a (reversible) link between individual and collective behavior in the analysis of co-evolutionary processes.

In the simulations in Fig. 1 one starts from a homogeneous network [23], where all individuals have the same number of links, and let individual behavior and network structure co-evolve at variable rates. Individuals engage in a **PD** in which mutual cooperation provides a reward $R = 1$, mutual defection a punishment $P = 0$, whereas when a **C** meets a **D**, the **C** gets a sucker's payoff $S = -\lambda$ while the **D** gets a temptation $T = 1 + \lambda$ ($\lambda \geq 0$ is the dilemma strength, such that increasing λ implies a stronger attraction into a Full-**D** configuration). Time proceeds in discrete steps, with the co-evolutionary process allowing, in each step, for link-rewiring with probability τ and behavioral

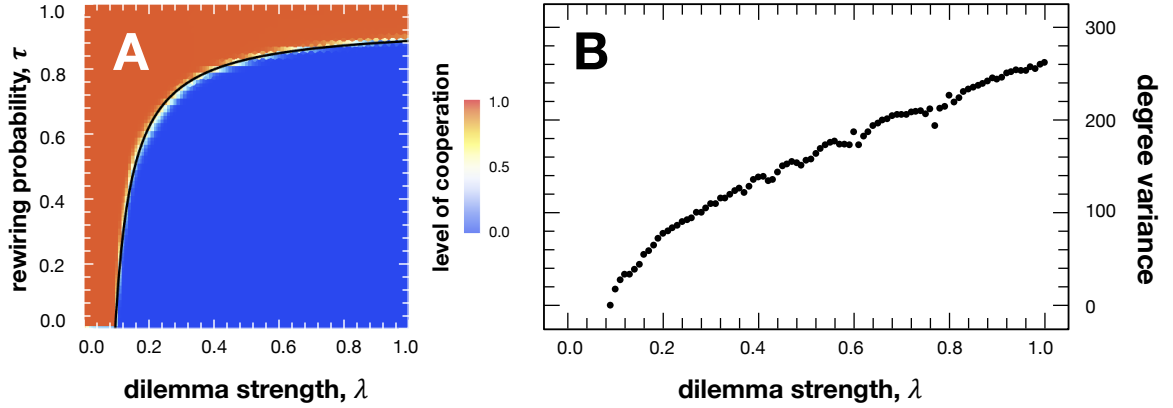


Figure 53: Level of Cooperation and network heterogeneity under co-evolutionary dynamics.

A) We computed numerically the level of cooperation in the domain bounded by $0.0 \leq \lambda \leq 1.0$ and $0.0 \leq \tau \leq 1.0$. It corresponds to the average final fraction of cooperators after 5×10^3 generations (1 generation equals Z discrete strategy time steps, where Z is the population size) and averaged over 10^5 independent simulations starting from a configuration with equal abundance of strategies. Orange (blue) regions denote parameter values for which Cooperators (Defectors) dominate. These two regions are separated by a narrow transition line, interpolated from the simulations to allow an easier visual inspection. **B)** Variance of the degree distribution of the equilibrium network as a function of λ , obtained along the curve $\tau(\lambda)$. Clearly, the stronger the social dilemma, the more heterogeneous the network becomes, in this way allowing for cooperators to increase their chances of overturning defectors in the population. Furthermore, network heterogeneity is most pronounced along the line $\tau(\lambda)$ marking the transition between full cooperation and full defection [11]. Other parameters are $\beta = 10.0$, $Z = 10^3$ and average network connectivity of $\langle k \rangle = 8$.

update with probability $(1 - \tau)$. Behavioral update is modelled via the so-called pairwise comparison rule [24, 25], a birth-death process in which an individual i with strategy s_i (here **C** or **D**) imitates a neighbor m with (a different) strategy s_m with probability given by the Fermi distribution from statistical physics (where the inverse temperature β provides here a measure of the strength of natural selection): $p_{i,m} = [1 + \exp(-\beta(f_m - f_i))]^{-1}$, with f_j accounting for the fitness of individual j , associated with the payoff accumulated over all interactions with her/his neighbors [24, 25]. Network adaptation assumes that **Cs** (**Ds**) seek for **Cs** to cooperate with (to exploit), while avoiding connections with **Ds**. Thus, an individual is satisfied with all his **C**-neighbors, being dissatisfied with the remaining. Hence, given a link between individuals A and B, if A is satisfied, she will try to keep the link; if dissatisfied, she will try to rewire the link to one of her second neighbors, accounting for the myopic nature of individuals regarding the entire social network. Following [11], when linked individuals A and B have a conflict regarding rewiring, resolution is fitness driven, the will of A prevailing with probability $\sigma = [1 + \exp(-\beta(f_A - f_B))]^{-1}$. Different variants of this model have been considered [12, 13, 14, 15, 16, 17, 18], leading to qualitatively similar results. Naturally, the methods and results discussed below are applicable to other choices of link rewiring.

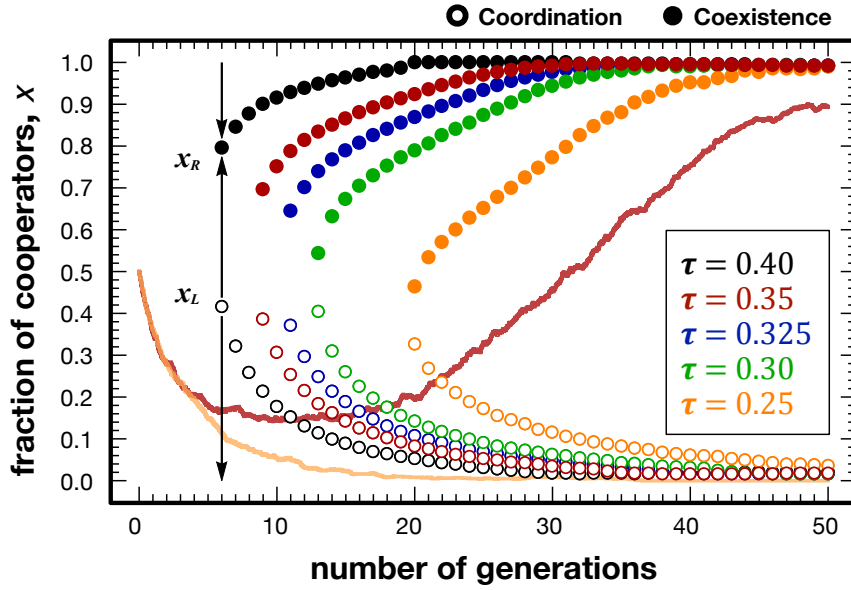


Figure 54: Global Evolutionary Dynamics in Adaptive Networks. Evolution of the internal fixed points of for the different rewiring probabilities τ indicated. Solid lines display two prototype time-series that start at $k/Z = 0.5$, one co-evolving towards 100% **Ds** ($\tau = 0.25$) and the other co-evolving towards 100% **Cs** ($\tau = 0.35$) this latter succeeding after crossing the coordination threshold provided by $\Gamma^A(k, t_g)$. Other parameters are $\lambda = 0.2$, $\beta = 10.0$, $N = 10^3$ and network average connectivity $\langle k \rangle = 4$.

As is well known [10, 26, 27, 28], in the mean-field approximation (a structureless, well-mixed population), **Cs** are not evolutionary viable. But when individuals interact with their peers along the links of a social network, **Cs** do not necessarily get extinct [29], even when no network adaptation takes place ($\tau = 0$), as shown at the bottom of Figure 53A. Most importantly, however, network adaptation paves the way for cooperation to prevail, even for game parameters that would render cooperation unfeasible in non-adaptive networks, as one can easily check by following trajectories of constant λ in Figure 53A. The faster the rate τ of network adaptation, the more **Cs** get an evolutionary edge over **Ds**. Moreover, for $\tau > 0$, our results suggest that the adaptive nature of the network nicely accounts for the heterogeneity observed in realistic social networks [1, 2, 3], in which a minority of nodes has a much larger degree than the majority. This is shown in Figure 53B, where we plot the degree variance of the networks emerging from co-evolutionary simulations, as a function of λ (and τ) as we move along the critical line $\tau(\lambda)$ depicted in Figure 53A. Figure 53B clearly shows how heterogeneous network structures prevail in the transition between Full **C** and **D**, highlighting also the tight interplay between the behavioral and network evolution.

To shed light on the link between individual and collective behavior, let us consider a network with Z nodes and L (undirected) links, and let every pair of linked individuals play a **PD** game of strength λ . Let us consider a large ensemble (Ω) of co-evolutionary time-series, each of which starting from an arbitrary fraction k/Z of **Cs** placed at random on the initial network, that we shall take to be a homogeneous random network of degree $\langle k \rangle$ [23, 30]. At any time t and co-evolutionary simulation

w , we compute the quantity $T_{i,w}(k, t) = \frac{1}{k_i} \sum_{m=1}^{k_i} p_{i,m} [1 - \delta(s_i, s_m)]$, where $\delta(a, b) = 1$ if $a = b$, being 0 otherwise, and $p_{i,m}$ stands for the probability that an individual i imitates a neighbor m (see above). Making use of $T_{i,w}(k, t)$ we can now compute the (ensemble) average probability that, in each behavioral update time step t , the number of **Cs** in the population increases (+) or decreases (−) by one individual:

$$T^\pm(k, t) = \frac{1}{Z\Omega(k)} \sum_{w=1}^{\Omega(k)} \sum_{i=1}^{D_s, C_s} T_{i,w}(k, t) \quad (67)$$

In Eq. 1, $\Omega(k)$ ($0 \leq \Omega(k) < \Omega$) is the number of times that a population configuration containing k **Cs** was observed at time t in the ensemble Ω of all simulations performed. Equation 1 allows us now to numerically compute the (time-dependent) drift term

$$\Gamma^A(k, t) = T^+(k, t) - T^-(k, t) \quad (68)$$

that constitutes a network (mean-field) analog of the gradient of selection used in the analysis of the stochastic evolutionary dynamics in finite well-mixed populations [28, 25]. Thus, $\Gamma^A(k, t)$ provides a population-wide information of the co-evolutionary dynamics, which now carries, nonetheless, (mean-field) information on the adaptive network structure. In the following, we shall re-write $\Gamma^A(k, t)$ in generation units (by performing a partial time average over 1 generation, given by Z discrete behavioral update steps) as $\Gamma^A(k, t_g) = \frac{1}{Z} \sum_{t=Z(t_g-1)}^{Zt_g} \Gamma^A(k, t)$.

Figure 2 shows what happens at a population-wide scale as a function of time t_g in the co-evolution of cooperation and adaption. At $t_g = 0$, the whole population engages in a **PD** game; this means that $\Gamma^A(k, 0) < 0$ for any value of k . At this stage, what is best for an individual is also true for the population as a whole. As time unfolds, however, there is typically a critical number of generations (g_C) above which we observe the emergence of two (finite population analogues of) internal fixed points, that we denote by x_L and x_R ; systematically, x_L has the structure of a probability repeller (analogue of an unstable fixed point, represented by open circles) whereas x_R has the structure of a probability attractor (analogue of a stable fixed point, solid circles).

As Figure 54 shows, x_L and x_R separate from each other with time until they reach a stable location associated with a stationary phase of $\Gamma^A(k, t_g)$. Importantly, the emergence of x_L and x_R depends sensitively on the value of τ : The larger the value of τ , the sooner x_L and x_R emerge as a result of the co-evolutionary process. This is clearly shown in Figure 54, where the order of appearance of the pair (x_L, x_R) follows the values of τ from top to bottom in the Figure legend. Needless to say, the sooner the emergence of the pair (x_L, x_R) , the more likely the process of self-organization of **Cs** and **Ds** will favor **Cs** to fall into the basin of attraction of x_R , which will dictate the overall prevalence of cooperation. This, of course, reflects the predominant scenario, which is valid in a stochastic sense.

Solid lines in Figure 54 display the evolution of **Cs** for two representative co-evolutionary time-series, where the initial fraction of **Cs** is 50%. Their color code uniquely identifies the rewiring probability τ ($\tau = 0.25$ for the orange line – lower curve, and $\tau = 0.35$ for the brown line – upper curve). At start, and in both simulations, the number of **Cs** tends to decrease, as one would expect under a population-wide **PD**-like evolutionary dynamics. However, as we have discussed, this is a

transient regime: As strategy correlations build up *at par* with a co-evolving network, we observe the emergence of a new population-wide dynamics at g_C , where the pair (x_L, x_R) emerges into the dynamics. In this new co-evolutionary landscape, **Cs** are now able to succeed provided $x > x_L$. Failing to achieve that will lead to the demise of Cooperation. Both outcomes are illustrated in Figure 54. Indeed, while for $\tau = 0.35$ the transient state is short enough (≈ 6 generations) thus allowing the survival of a sufficiently large fraction of cooperators x to remain above the time dependent location of x_L , for $\tau = 0.25$ the transient is so large (≈ 20 generations) that by the time the pair (x_L, x_R) appears, x is already below x_L (recall we started from 50% **Cs** in the population), compromising the viability of cooperators in the population, as shown by the corresponding solid line.

This analysis shows that, in adaptive networked populations, there will be a critical value of τ above which cooperation prevails (in a stochastic sense). This prevalence is associated with the capacity of the population to overcome the coordination barrier that emerges, at a population-wide scale, out of the co-evolutionary processes of strategy and structure adaptation. Naturally, the larger the rewiring probability, the easier it becomes to solve the coordination dilemma.

It is also worth commenting on the significance and impact of the emergence of the pair of internal equilibria (x_L, x_R) . As Figure 54 suggests, this pair converges to the approximate limits $x_L \approx 0$ and $x_R \approx 1$ as $t_g \rightarrow \infty$. This is, however, highly unlikely, mostly for large values of the selection pressure β , for which strategy update becomes increasingly deterministic. Strictly speaking, a single **D** in a population of $Z - 1$ **Cs** will always be advantageous, independent of the underlying network structure, whereas a single **C** in a population of $Z - 1$ **Ds** will always be disadvantageous, and thus the pair (x_L, x_R) cannot converge exactly to $(0, 1)$. However, network adaptation, which naturally induces a network heterogeneity that is maximal at the critical point when **Cs** overturn **Ds** in the population (see Figure 53) optimizes the error in the approximate limit above and, to the extent that x_R emerges at values higher than the actual fraction x of **Cs** present in the population at that time, x_R will foster the increase of **Cs** in the population, which in turn will promote an increase in the value of x_R . In this sense, the role of x_L is more important than that of x_R in what concerns the viability of cooperation. This said, however, it is also important to note that, work carried out in the framework of N-person coordination games shows that one of the most prominent features of the associated evolutionary dynamics resides, precisely, in the emergence of a pair (x_L, x_R) with exactly the same structure and nature [28], in a wide region of the game parameter spectrum, a feature that does not occur in 2-person games, such as the **PD** we started from here. Thus, and qualitatively, one may state that, globally, 2-person games on adaptive networks are transformed into effective N-person coordination games. This is more so if we establish the analogy that, on networked populations, the average connectivity of the network provides the natural proxy for the average group size appearing in N-person coordination games.

Overall, both processes under consideration – strategy evolution and structural evolution – contribute to a positive assortment of **Cs**. Indeed, the strategy update process leads to what can be qualitatively described as a “**Cs (Ds) breed Cs (Ds)**” type dynamics. As already discussed before [31], however, the complexity inherent to the underlying **PD** social dilemma leads to an asymmetry in the outcome of the update process, in which, unlike **Cs**, **Ds** become victims of their own success: When co-evolving

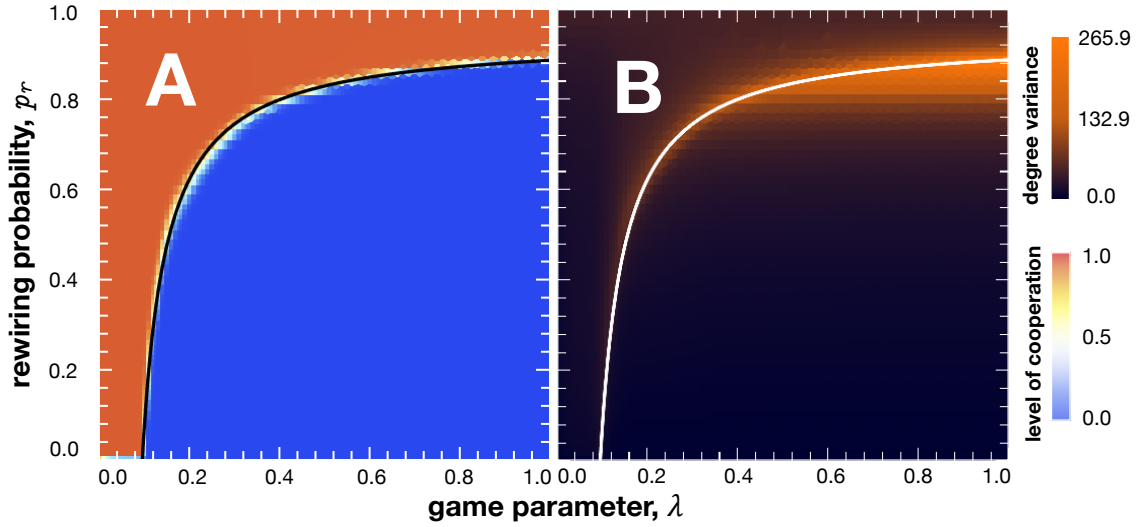


Figure 55: Level of Cooperation (panel **A**) and degree Heterogeneity (panel **B**) as a function of the rewiring probability ($0.0 \leq \tau \leq 1.0$) and the dilemma strength parameter ($0.0 \leq \lambda \leq 1.0$). Black/white line divides the parameter space in two regions: one of Cooperation dominance and another of Defectors dominance. Other parameters are, $\beta = 10.0$, $Z = 10^3$ and $\langle k \rangle = 8$.

at par with network adaptation, this evolutionary asymmetry is further extended to links that connect 2 Cs and links that have at least one D: the former are resilient to adaptation, contrary to the latter, which will be resilient only if Ds are much more fit than Cs. As our results demonstrate, such asymmetry also contributes to an assortment of Cs at the same time that it fosters the segregation of Ds. The joint contribution of both processes facilitates the emergence of cooperation, which becomes feasible in the entire parameter range of the PD as long as network adaptation proceeds fast enough. This prevalence results from the emergence of a pair (x_L, x_R) at a global scale that appears the sooner the faster the rate of adaptation of the underlying network of contacts. Moreover, as time proceeds, one observes a systematic separation between the two internal fixed points (x_L, x_R) which, as $t_g \rightarrow \infty$, approach 0 and 1 asymptotically.

A crucial issue of complex systems research and, more recently, of computational social science, is to understand how societies behave as a collective, knowing beforehand how individuals interact with each-other. Conversely, if all we know is how societies behave collectively (as happens all too often in micro-biology) is there anything we can say about how individuals interact with each-other? This manuscript shows how to develop a reversible link between individual and collective behavior. We show how network adaptation changes the cooperation dilemma, as it is locally perceived, into a coordination problem at a global level. Interestingly, such coordination problem ultimately dictates the collective dynamics and therefore each individual's choices, even if, locally, individual perception remains unchanged and individuals cannot observe or even anticipate such global dynamics. The simplicity of the present implementation renders this framework readily applicable to other time-dependent processes that occur on adaptive networks, notably the spreading of contagious diseases and the diffusion of innovations [6].

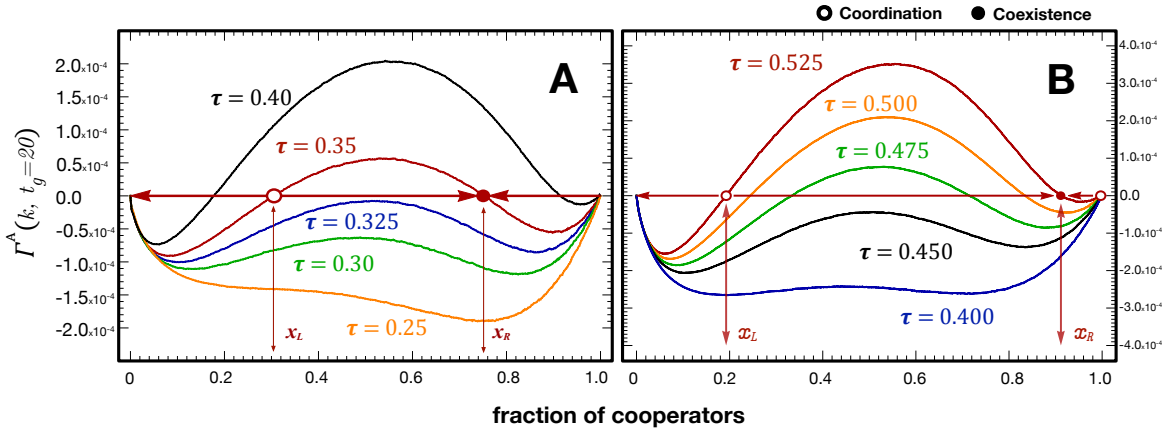


Figure 56: Time-Dependent Gradient of Selection in Adaptive Networks. Profile of the average gradient of selection, $\Gamma^A(k, t_g)$, after $t_g = 20$ generations, plotted for different values of the rewiring probabilities τ . Panel **A** corresponds to $\langle k \rangle = 4$ and panel **B** to $\langle k \rangle = 8$. Other parameters are $\lambda = 0.2$, $\beta = 10.0$ and $Z = 10^3$.

6.2 SUPPLEMENTAL MATERIAL

6.2.1 Computer Simulations

In order to validate the results obtained with the Averaged Gradient of Selection and to have a better grasp of the parameter space under analysis we have also run extensive Monte Carlo simulations. These allow us to evaluate the evolutionary outcome of populations that translates into the expected level of cooperation.

In each independent simulation a population of individuals starts from a Homogeneous Random Network [23] with a total of $Z \langle k \rangle / 2$ links. The number of links remains constant throughout the evolutionary process, thus the average degree $\langle k \rangle$ also remains constant. However, as individuals adapt their social network, the distribution of degrees $D(k)$ changes its shape, from the single-peak over $\langle k \rangle$ into a broader distribution. This naturally implies that the variance of the degrees changes with the evolutionary process.

At the beginning of each simulation an initial fraction (x_i) of individuals are randomly selected to be Cooperators, while the remaining $(1 - x_i)$ are Defectors. Simulations run for a total of 10^6 generations¹ or until the population reaches a monomorphic configuration. The level of cooperation is thus the number of cooperators in the population at the end of a simulation. We average this quantity over 10^5 independent simulations. At each time step we follow the update dynamics described in the manuscript, namely the pairwise comparison rule [25, 32] for strategy update and its counterpart [11] for structure adaptation. Figure 55 depicts the level of cooperation (panel A) along with the average degree heterogeneity (panel B) of the population structure that results from the evolutionary process. In Figure 53B of the main manuscript shows the degree heterogeneity along the white line of

¹ A generation corresponds to Z strategy updates

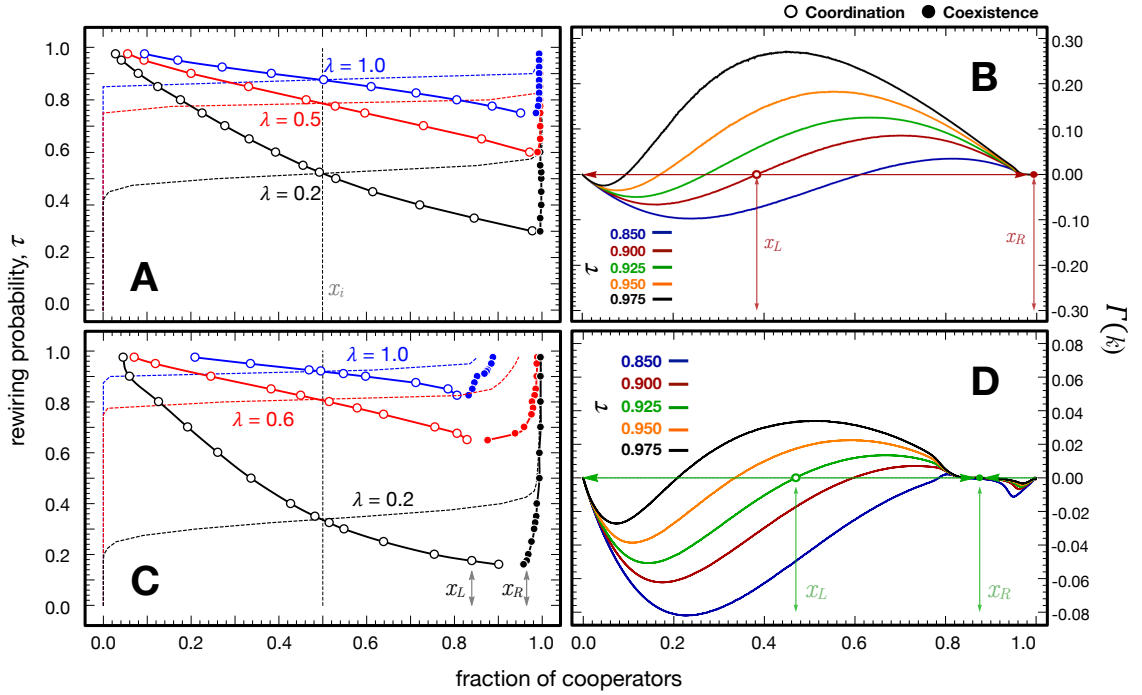


Figure 57: Shape of the Time-Independent Gradient of Selection as a function of the rewiring probability (τ). **A** and **C** show the Bifurcation diagram that depicts the trajectories of the internal fixed points of $\Gamma^A(k)$ for changes in the rewiring probabilities, τ . Dashed lines indicate the level of cooperation for simulations with an initial fraction of cooperators of $x_i = 0.5$ for each of the scenarios. **B** and **D** show the shape of for different rewiring probabilities, τ . **A** and **B** show results for $\langle k \rangle = 8$ while **C** and **D** consider $\langle k \rangle = 6$. Other parameters are $\beta_s = 10.0$, $\beta_r = 10^{-3}$ and $Z = 10^3$.

Figure 53B, which corresponds to the parameters and that divides the parameter space in two regions: one characterized by Full Cooperation and another by Full Defection evolutionary outcomes.

6.2.2 Time-Dependent Gradient of Selection

Figure 56 shows the shape of $\Gamma^A(k, t_g)$ after $t_g = 20$ generations for different values of the rewiring probabilities τ . It supports the idea that faster network adaption prompts a faster response of the population to the social dilemma at hand and, thus, generates a population-wide dynamics that is more favorable for the emergence of cooperation.

As mentioned in the main manuscript, the shape of $\Gamma^A(k, t_g)$ closely resembles that of a N-Person coordination game [33], characterized by a coordination threshold (x_L) and a basin of attraction dominated by a coexistence point (x_R), which does not correspond to the Full Cooperation configuration.

Figure 54 of the main manuscript shows the positions of the internal roots of $\Gamma^A(k, t_g)$, which fully describe the evolutionary dynamics of the population at each generation.

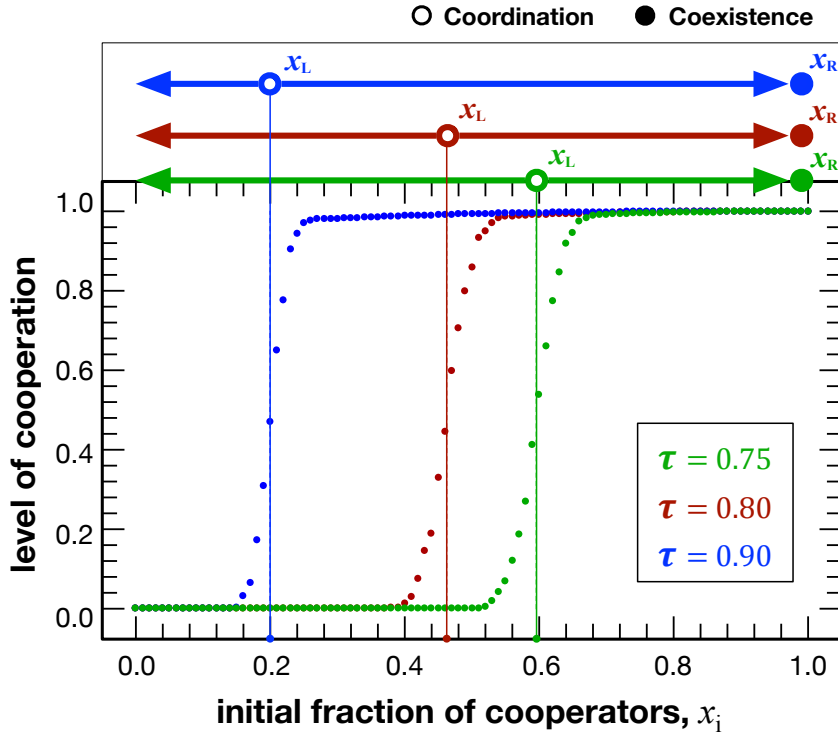


Figure 58: Relationship between Time-Independent Gradient of Selection internal fixed points (upper box) and the level of cooperation (dots) dependence on the initial fraction of cooperators. Other parameters are $\lambda = 0.5$, $\beta_s = 10.0$, $Z = 10^3$ and $\langle k \rangle = 8$.

6.2.3 Time-Independent Gradient of Selection

The Time-Dependent description conveyed by $\Gamma^A(k, t_g)$ allows us to better understand how the emerging strategy assortments (*i.e.* correlations between strategies), that naturally arise from the ensuing co-evolutionary dynamics, lead to a reshape of the population-wide social dilemma along its evolutionary pathway.

However, in order to compare with other quantities that measure the evolutionary outcome of populations and that are widely popular in the literature, it is useful to define a Time-Independent description of the gradient of selection.

Let us denote by $\Gamma^A(k)$ the Time-Independent Gradient of Selection, which is defined as $\Gamma^A(k) = T^+(k) - T^-(k)$, where

$$T^\pm(k) = \frac{1}{Z\Theta(k)} \sum_{w=1}^{\Theta(k)} \sum_{i=1}^{D_s, C_s} \frac{1}{k_i} \sum_{m=1}^{k_i} p_{i,m} (1 - \delta(s_i, s_m)) \quad (69)$$

where $\Theta(k)$ is the number of times the population was observed in a configuration containing k Cooperators during the time of integration (from $t_g = 0$ to $t_g = 150$), which effectively corresponds to the quasi-stationary distribution. Moreover, as defined in the main manuscript $p_{i,m}$ is the probability that an individual i imitates a neighbour m , which is given by the Fermi Distribution (see Main text),

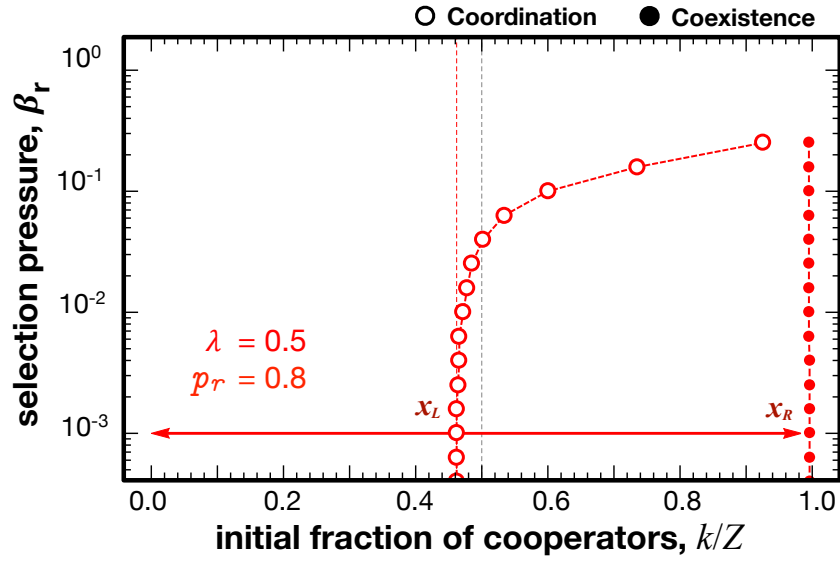


Figure 59: Internal fixed points of the Time-Independent Gradient of Selection in Adaptive Networks as a function of the rewiring selection pressure (β_r). Other parameters are $\tau = 0.8$, $\lambda = 0.5$, $\beta_s = 10.0$, $Z = 10^3$ and $\langle k \rangle = 4$.

and $\delta(a, b)$ is the Kronecker delta being 0 if $a \neq b$ and 1 otherwise. Hence we have a quantity that measures the direction of selection at each configuration of k over the entire time of evolution. As we show below, many of the patterns and conclusions attained from the analysis of $\Gamma^A(k, t_g)$ are recovered through $\Gamma^A(k)$ as well.

Figure 57 shows how the internal fixed points of $\Gamma^A(k)$ change with different rewiring probabilities (τ) under fixed β_r and β_s and three values of λ . In all cases there is a critical rewiring probability that leads to a bifurcation and corresponding emergence of two internal fixed points. The location of $\Gamma^A(k)$ the internal fixed points of are a good indicator of the evolutionary fate of populations and particularly of the coordination threshold that characterizes the evolutionary dynamics of the population. In particular, as shown in Figure 58, it predicts very well the necessary initial fraction of cooperators required for the evolutionary dominance of Cooperation

6.2.4 Selection Pressure

In the implemented model two parameters regulate the stochasticity of each decision making process. Namely β_r regulates how deterministic is the rewiring process of an individual when choosing whether to maintain or sever a link, and β_s plays a similar role for the behavioural dynamics in strategy update.

In both cases, the probability of an event is conveniently computed from the Fermi Distribution. This distribution traces back to Statistical Physics, and in that context β plays the role of the inverse of the temperature, thus here when $\beta \rightarrow \infty$ implies that individuals take a deterministic action (always take the most advantageous action) while with $\beta \rightarrow 0$ individuals decide at random.

Overall in the main manuscript we explore a situation where $\beta_r \ll 1$ and $\beta_s = 10$.

Figure 59 shows the trajectory of the internal fixed points of the $\Gamma^A(k)$ along changes of the network adaptation selection pressure (β_r). It shows that under variation of β_r the system interpolates between two regimes: under strong selection pressures ($\beta > 10^{-1}$) evolution is dominated by Defectors as indicated by the fully negative $\Gamma^A(k)$; for weaker selection pressures $\beta_r < 10^{-1}$ we see the emergence of internal fixed points of $\Gamma^A(k)$ lead to a more favourable evolutionary dynamics for cooperation.

6.3 BIBLIOGRAPHY

- [1] Luis A Nunes Amaral, Antonio Scala, Marc Barthélemy, and H Eugene Stanley. Classes of small-world networks. *Proceedings of the National Academy of Sciences*, 97(21):11149–11152, 2000.
- [2] Albert-László Barabási. *Linked: How everything is connected to everything else and what it means*. Plume Editors, 2002.
- [3] Sergei N Dorogovtsev and José FF Mendes. *Evolution of networks: From biological nets to the Internet and WWW*. Oxford University Press, 2003.
- [4] Mark EJ Newman. The structure and function of complex networks. *SIAM review*, 45(2):167–256, 2003.
- [5] James H Fowler and Nicholas A Christakis. Dynamic spread of happiness in a large social network: longitudinal analysis over 20 years in the framingham heart study. *BMJ: British Medical Journal*, 337, 2008.
- [6] Flávio L. Pinheiro, Marta D. Santos, Francisco C. Santos, and Jorge M. Pacheco. The origin of peer influence in social networks. *Physical Review Letters*, 2014.
- [7] Sven Van Segbroeck, Francisco C Santos, and Jorge M Pacheco. Adaptive contact networks change effective disease infectiousness and dynamics. *PLoS Computational Biology*, 6(8): e1000895, 2010.
- [8] Thilo Gross, Carlos J Dommar D’Lima, and Bernd Blasius. Epidemic dynamics on an adaptive network. *Physical Review Letters*, 96(20):208701, 2006.
- [9] Peter Kollock. Social dilemmas: The anatomy of cooperation. *Annual Review of Sociology*, pages 183–214, 1998.
- [10] Karl Sigmund. *The calculus of selfishness*. Princeton University Press, 2010.
- [11] Francisco C Santos, Jorge M Pacheco, and Tom Lenaerts. Cooperation prevails when individuals adjust their social ties. *PLoS Computational Biology*, 2(10):e140, 2006.
- [12] Jorge M Pacheco, Arne Traulsen, and Martin A Nowak. Coevolution of strategy and structure in complex networks with dynamical linking. *Physical Review Letters*, 97(25):258103, 2006.
- [13] Jorge M Pacheco, Arne Traulsen, Hisashi Ohtsuki, and Martin A Nowak. Repeated games and direct reciprocity under active linking. *Journal of Theoretical Biology*, 250(4):723–731, 2008.
- [14] Sven Van Segbroeck, Francisco C Santos, Ann Nowé, Jorge M Pacheco, and Tom Lenaerts. The evolution of prompt reaction to adverse ties. *BMC Evolutionary Biology*, 8(1):287, 2008.
- [15] Sven Van Segbroeck, Francisco C Santos, Tom Lenaerts, and Jorge M Pacheco. Reacting differently to adverse ties promotes cooperation in social networks. *Physical Review Letters*, 102(5):

- 058105, 2009.
- [16] Feng Fu, Christoph Hauert, Martin A Nowak, and Long Wang. Reputation-based partner choice promotes cooperation in social networks. *Physical Review E*, 78(2):026117, 2008.
 - [17] Julia Poncela, Jesús Gómez-Gardeñes, Arne Traulsen, and Yamir Moreno. Evolutionary game dynamics in a growing structured population. *New Journal of Physics*, 11(8):083031, 2009.
 - [18] Feng Fu, Te Wu, and Long Wang. Partner switching stabilizes cooperation in coevolutionary prisoner’s dilemma. *Physical Review E*, 79(3):036101, 2009.
 - [19] Katrin Fehel, Daniel J van der Post, and Dirk Semmann. Co-evolution of behaviour and social network structure promotes human cooperation. *Ecology Letters*, 14(6):546–551, 2011.
 - [20] Kirill S Korolev, Joao B Xavier, and Jeff Gore. Turning ecology and evolution against cancer. *Nature Reviews Cancer*, 14(5):371–380, 2014.
 - [21] David Lazer, Alex Sandy Pentland, Lada Adamic, Sinan Aral, Albert Laszlo Barabasi, Devon Brewer, Nicholas Christakis, Noshir Contractor, James Fowler, Myron Gutmann, et al. Life in the network: the coming age of computational social science. *Science (New York, NY)*, 323(5915):721, 2009.
 - [22] J-P Onnela, Jari Saramäki, Jorkki Hyvönen, György Szabó, David Lazer, Kimmo Kaski, János Kertész, and A-L Barabási. Structure and tie strengths in mobile communication networks. *Proceedings of the National Academy of Sciences*, 104(18):7332–7336, 2007.
 - [23] Francisco C Santos, JF Rodrigues, and Jorge M Pacheco. Epidemic spreading and cooperation dynamics on homogeneous small-world networks. *Physical Review E*, 72(5):056128, 2005.
 - [24] György Szabó and Csaba Tóke. Evolutionary prisoner’s dilemma game on a square lattice. *Physical Review E*, 58(1):69, 1998.
 - [25] Arne Traulsen, Martin A Nowak, and Jorge M Pacheco. Stochastic dynamics of invasion and fixation. *Physical Review E*, 74(1):011909, 2006.
 - [26] Josef Hofbauer and Karl Sigmund. *Evolutionary games and population dynamics*. Cambridge University Press, 1998.
 - [27] Brian Skyrms. *The stag hunt and the evolution of social structure*. Cambridge University Press, 2004.
 - [28] Jorge M Pacheco, Francisco C Santos, Max O Souza, and Brian Skyrms. Evolutionary dynamics of collective action in n-person stag hunt dilemmas. *Proceedings of the Royal Society B: Biological Sciences*, 276(1655):315–321, 2009.
 - [29] György Szabó and Gábor Fáth. Evolutionary games on graphs. *Physics Reports*, 446(4):97–216, 2007.
 - [30] Hisashi Ohtsuki, Martin A Nowak, and Jorge M Pacheco. Breaking the symmetry between interaction and replacement in evolutionary dynamics on graphs. *Physical Review Letters*, 98(10):108106, 2007.
 - [31] Francisco C Santos and Jorge M Pacheco. A new route to the evolution of cooperation. *Journal of Evolutionary Biology*, 19(3):726–733, 2006.
 - [32] Arne Traulsen, Jorge M Pacheco, and Martin A Nowak. Pairwise comparison and selection temperature in evolutionary game dynamics. *Journal of Theoretical Biology*, 246(3):522–529,

Chapter 6. LINKING INDIVIDUAL AND COLLECTIVE BEHAVIOR IN ADAPTIVE SOCIAL NETWORKS

2007.

- [33] Jorge M Pacheco, Francisco C Santos, Max O Souza, and Brian Skyrms. Evolutionary dynamics of collective action in n-person stag hunt dilemmas. *Proceedings of the Royal Society B: Biological Sciences*, 276(1655):315–321, 2009.

EVOLUTION OF ALL-OR-NONE STRATEGIES IN REPEATED PUBLIC GOODS DILEMMAS

PLOS Computational Biology, 10.1371/journal.pone.0032114 (2014)

Flávio L. Pinheiro, Vitor V. Vasconcelos, Francisco C. Santos and Jorge M. Pacheco

The previous chapters discuss how complex networks impact the dynamical processes they support. We have considered dynamical processes that only involve pairwise interactions between individuals and explored in particular the problem of Cooperation, which in turn is not limited to the study of pairwise interactions. Indeed many problems of Cooperation involve repeated interactions among the same groups of individuals. When collective action is at stake, groups often engage in *Public Goods Games*, where individuals contribute (or not) to a common pool, subsequently sharing the resources. Such scenarios of repeated group interactions materialize situations in which direct reciprocation to groups may be at work. Here we study direct group reciprocity considering the complete set of reactive strategies, where individuals behave conditionally on what they observed in the previous round. We study both analytically and by computer simulations the evolutionary dynamics encompassing this extensive strategy space, witnessing the emergence of a surprisingly simple strategy that we call *All-Or-None* (AoN). AoN consists in cooperating only after a round of unanimous group behavior (Cooperation or Defection), and proves robust in the presence of errors, thus fostering Cooperation in a wide range of group sizes. The principles encapsulated in this strategy share a level of complexity reminiscent of that found already in 2-person games under direct and indirect reciprocity, reducing, in fact, to the well-known *Win-Stay-Lose-Shift* strategy in the limit of the repeated 2-person Prisoner's Dilemma.

7.1 MANUSCRIPT

7.1.1 Introduction

The emergence and sustainability of Cooperation constitutes one of the most important problems in social and biological sciences [1]. It revolves around the clash between individual and collective interest, which becomes particularly clear when one considers the evolution of collective action involving *Public Goods Games* (**PGG**), such as the stereotypical N-person *Prisoner's Dilemma* (**NPD**) [2, 3]. In the absence of additional mechanisms, such as the presence of thresholds [4, 5], risk [6], an embedding network of interactions [7, 8, 9, 10, 11, 12], institutions [13, 14, 15], punishment or

voluntary participation [16, 17, 18, 19], evolutionary game theory predicts a population fated to fall into a tragedy of the commons [20].

Collective action problems, however, often involve repeated interactions between members of the same group [21, 22, 23], as exemplified by the repeated attempts from country leaders to cooperate in reducing emissions of greenhouse gases [6, 24, 25, 26, 27, 28, 29] or in finding a solution to the Euro monetary crisis [30, 31, 32]. In such scenarios, where collective action is more difficult to achieve in larger groups [6], one is naturally led to question whether a generalization of the direct reciprocity [33] mechanism to problems of collective action may provide an escape hatch to the aforementioned tragedy of the commons. Moreover, N -player interactions pose many additional difficulties, in particular in what concerns the emergence of reciprocation: If one interacts repeatedly in a group of N -players it is hard to identify towards whom should one reciprocate [3]. In fact, only recently direct reciprocity has been generalized to **PGGs** [22, 23], studying the co-evolution of unconditional defectors with generalized reciprocators, that is, individuals who, in a group of size N , only cooperate if there were at least M ($0 \leq M \leq N$) individuals who cooperated in the previous round. Results show [22, 23] that generalized reciprocators are very successful in promoting Cooperation. Moreover, for a given group size N , there is a critical threshold level of fairness, M^* , at which reciprocation optimizes the emergence of Cooperation [22].

Generalized reciprocators [22] provide an intuitive generalization of the **TFT** strategy to repeated N -player games. However, and despite the underlying intuition, they constitute but a small subset of all possible individual (reactive) strategies one can envisage in a group of size N . Here we explore the complete set of reactive strategies that individuals may adopt when engaging in repeated *Public Goods Games* with $N - 1$ other individuals, assuming that the decision to cooperate or not is based on the behavioral decisions of the group in the previous round (see below). We find that, in the context of *Public Goods Games*, a reactive strategy not belonging to the set of generalized reciprocators emerges as ubiquitous, ensuring the emergence and sustainability of Cooperation.

7.1.2 Model

Let us consider a finite and well-mixed population of Z individuals, who assemble in groups of size N randomly formed, and play a repeated version of the **NPD** [34]. In each round individuals either *cooperate* (**C**) by contributing an amount c to a public good or *defect* (**D**) by not doing so. The aggregated contributions of the group are multiplied by an enhancement factor F and equally divided among the N individuals of the group. Hence, in each round, **Ds** achieve a payoff of $\pi_D(k) = kFc/N$, while **Cs** attain $\pi_C(k) = \pi_D(k) - c$ where k is the number of contributions in that round. We consider a repeated **PGG** with an undetermined number of rounds, such that at the end of each round, another round will take place with probability w [3], leading to an average number of rounds – m – given by $m = (1 - w)^{-1}$. At the beginning of each round (with the exception of the first), each individual decides to contribute (*i.e.* to play **C**) or not (*i.e.* to play **D**), depending on the total number of contributions that took place in the previous round.

Each strategy S_i defines how an individual behaves in each round (*i.e.* if she/he decides to cooperate or defect) and is encoded in a string with $N + 2$ bits ($b^{-1}b^0b^1\dots b^{N-1}b^N$). The first bit (b^{-1})

N	\bar{b}^{-1}	\bar{b}^0	\bar{b}^1	\bar{b}^2	\bar{b}^3	\bar{b}^4	\bar{b}^5	\bar{b}^6	\bar{b}^7	\bar{b}^8	\bar{b}^9	\bar{b}^{10}
2	0.46	0.89	0.00	0.95								
3	0.36	0.99	0.02	0.00	1.00							
4	0.37	0.99	0.06	0.13	0.01	1.00						
5	0.33	0.99	0.09	0.27	0.14	0.04	0.99					
6	0.34	0.98	0.12	0.29	0.24	0.14	0.09	0.99				
7	0.33	0.97	0.15	0.28	0.31	0.28	0.13	0.16	0.99			
8	0.35	0.95	0.21	0.28	0.35	0.29	0.28	0.14	0.27	0.99		
9	0.36	0.93	0.26	0.29	0.35	0.34	0.32	0.27	0.15	0.40	0.99	
10	0.38	0.91	0.31	0.30	0.36	0.37	0.32	0.33	0.27	0.17	0.53	0.99

Figure 60: Stationary bit distribution as a function of N . Each bit (square) corresponds to the weighted sum of the fraction of time (*i.e.* the analytically computed stationary distribution) the population spends in strategy configurations in which $b^q = 1$. Blue (red) cells identify those bits that are employed at least 3/4 of the time with value $b^q = 1.0$ ($b^q = 0.0$). The analysis provided extends for groups sizes (N) between 2 and 10 (rows). Other model parameters: $Z = 100$, $\beta = 1.0$, $F/N = 0.85$, $w = 0.96$, $\epsilon = 0.05$, $\mu \ll 1/Z$.

dictates the behavior in the initial round, while the remaining $N + 1$ bits ($b^0 b^1 \dots b^{N-1} b^N$) correspond in sequence to the player's behavior depending on the number of Cs in the previous round. In this definition a bit 1 corresponds to a cooperative act and a bit 0 to a defective one. Hence, one obtains a maximum of 2^{N+2} strategies, corresponding to all possible combinations of 0s and 1s in a string of size $N + 2$.

We consider groups of N individuals, randomly sampled from a finite population of size Z , playing a repeated **NPD**. Individuals revise their strategies through the Fermi update rule [35, 36, 37, 38], a stochastic birth-death process with mutations. At each time step a randomly selected individual A (with strategy S_A and fitness f_{S_A}) may adopt a different strategy i) by mutation with probability μ or ii) by imitating a random member B of the population (with strategy S_B and fitness f_{S_B}) with probability

$$(1 - \mu)(1 + e^{-\beta(f_{S_A} - f_{S_B})}) \quad (70)$$

where β is the intensity of selection that regulates the randomness of the decision process. The fitness of each strategy f_{S_i} is the average payoff attained over all rounds and possible groups by individuals adopting strategy S_i . It is well known that execution errors profoundly affect the evolutionary dynamics of repeated 2-person games [39, 40, 41, 42, 43, 44, 45]. Consequently, we shall also consider that,

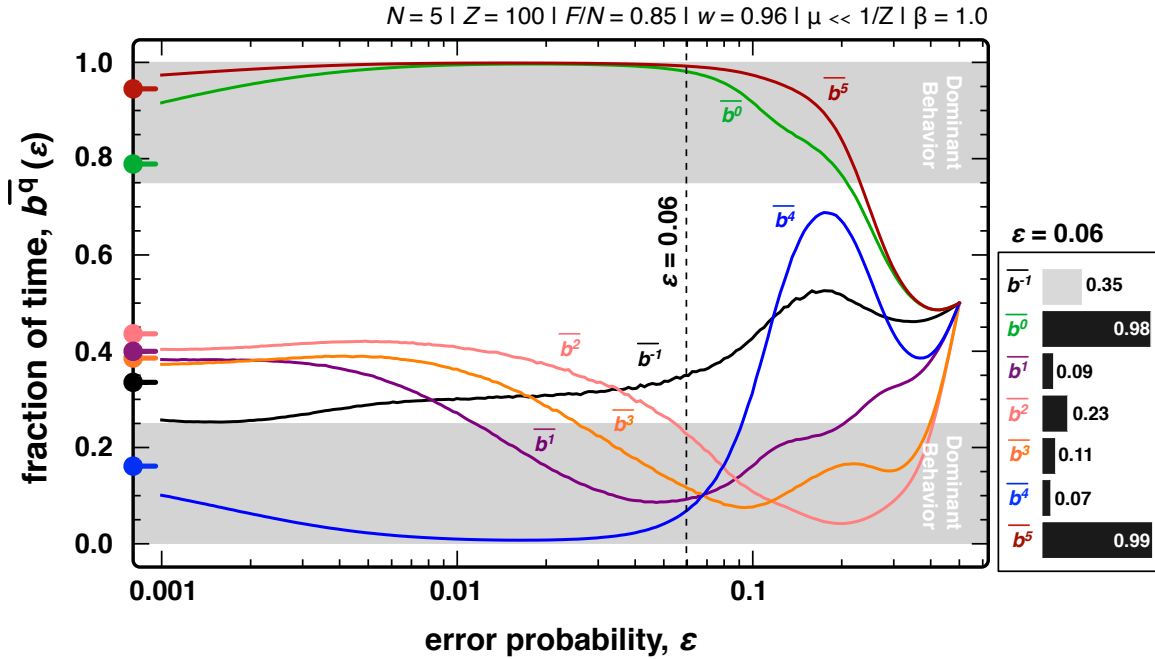


Figure 61: Stationary bit distribution as a function of the error rate. We plot (log-linear scale) the fraction of time the population spends in a strategy with $b^q = 1$ for a broad range of error probabilities ϵ . Circles on the left indicate the values obtained for $\epsilon = 0.0$, gray areas show the range of values for which bits were defined to have a dominant behavior. Note that for $\epsilon = 0.5$ all strategies behave randomly. The bar plot on the right shows the results for $\epsilon = 0.06$ (vertical dashed line). Other model parameters: $Z = 100, \beta = 1.0, N = 5, F/N = 0.85, w = 0.96$ and $\mu \ll 1/Z$.

in each round, and after deciding to contribute or not according to b^q , an individual may act with the opposite behavior ($1 - b^q$) with a probability ϵ , thus making an execution error.

7.1.3 Results and Discussion

Let us start by investigating the evolutionary dynamics of the population in the small mutation limit approximation [46]. This allows us to compute analytically the relative pervasiveness of each strategy in time. It is noteworthy, however, that the results obtained through this approximation remain valid for a wide range of mutation probabilities, as we show explicitly in Section 7.2.1 via comparison with results from computer simulations. In a nutshell, and whenever mutations are rare, a new mutant that appears in the population will either get extinct or invade the entire population before the occurrence of the next mutation. Hence, in each time-step there will be, at most, 2 strategies present in the population, which allows one to describe the evolutionary dynamics of the population in terms of an embedded (and reduced) Markov Chain with a size equal to the number of strategies available. Each state represents a monomorphic population adopting a given strategy, whereas transitions are defined by the fixation probabilities of a single mutant [47]. The resulting stationary distribution τ_i will then indicate the fraction of time the population spends in each of the 2^{N+2} states (or strategies S_i). We

shall also make use of τ_i to compute the fraction of time the population spends in a configuration/s-
strategy with $b_i^q = 1$, a quantity we call stationary bit strategy, defined as

$$\bar{b}^q = \sum_{i=1}^{s^{N+2}} \tau_i b_i^q \quad (71)$$

where b_i^q corresponds to the bit q of strategy i . The stationary bit strategy allows us to easily quantify the relative dominance of each behavior and extract the most pervasive strategic profiles.

Figure 60 shows the stationary bit distribution, \bar{b}^q , for different group sizes. Colored cells highlight those bits (b^q) that retain the same value more than 75% of the time, with $b_q \geq 0.75$ (blue) and $b_q \leq 0.25$ (red). For simplicity, we associate this feature with what we call dominant bit.

Analysis of the stationary bit distributions for different group sizes under small error probabilities puts into evidence the overall evolutionary success of strategies that conform with a particular profile: $b_0 = b_N = 1$ and $b_q = 0$ for $0 < q < N$. A similar trend is obtained if instead we analyze the stationary distribution τ_i for all possible strategies S_i : This strategy – or minor variations on this profile (see below) – shows the highest prevalence for a wide range of parameters even in the absence of errors of execution (see Section 7.2.1). The philosophy encapsulated in this strategy is a simple yet efficient one: cooperating only after a round of unanimous group behavior (Cooperation or Defection). Hence we refer to this strategy as All-Or-None (**AoN**), highlighting the two situations in which these individuals are prone to cooperate. As group size increases, so does the number of expected errors per round, which leads to an overall reduction of the number of dominant bits found in the intermediate sector (*i.e.* b^q for $0 < q < N$) without affecting the “edge bits”, which again reveals the prevalence of **AoN** behaviour in the population.

A monomorphic population of **AoN** players can easily sustain unanimous group Cooperation, even in the presence of errors. Indeed, after an occasional individual Defection, a round of full Defection ensues, resuming back to unanimous Cooperation in the following round. Therefore, **AoN** allows a prompt recovery from errors of execution, which constitutes a key feature that allows Cooperation to thrive.

To investigate the robustness of **AoN** we show, in Figure 61, the effect of execution errors on the stationary bit distribution (\bar{b}^q) for a fixed group size (here $N = 5$): Clearly, both b_0 and b_N remain associated with Cooperation for a wide range of error probabilities ($\mu \leq 0.2$). The internal bits, in turn, remain qualitatively close to the **AoN** profile (*i.e.* $b^q = 0$ for $0 < q < N$), undergoing changes as the error rate increases, allowing an efficient resume into full Cooperation, after (at least) one behavioral error. In particular, for $0.01 < \epsilon < 0.1$, evolution selects for Defection in bits b^1 to b^{N-1} , with particular incidence to adjacent bits of b^0 and b^N , allowing a fast error recovery. This feature gets enhanced with increasing ϵ . For larger values of ϵ ($\epsilon > 0.1$), unanimity becomes less likely and we witness an adaptation of the predominant strategy that acts to reduce the interval of bits in which Defection prevails. In other words, it is as if execution errors redefine the notion of unanimity itself or, alternatively, individuals become more tolerant as execution errors become more likely. It is also noteworthy that the non-monotonous response to errors shown in Figure 61 has been previously observed in other evolutionary models of Cooperation [48] where intermediate degrees of

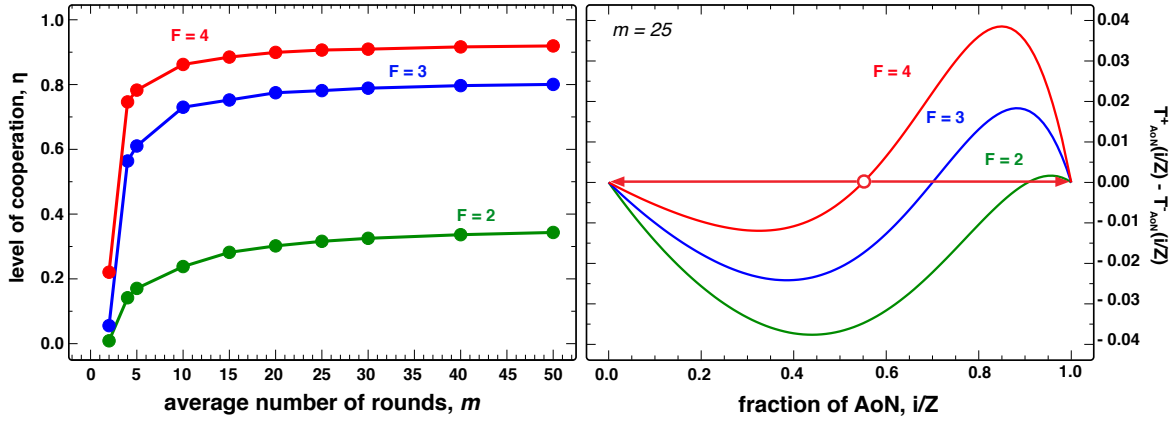


Figure 62: **Left:** Level of Cooperation as a function of average number of rounds, m for three different values of the enhancement value F (4, 3 and 2) with $N = 5$ and in the absence of behavioral errors. **Right:** Gradients of Selection [5] for the evolutionary game between ALLD and AoN ($b^{-1} = 0$, $N = 5$, $w = 0.96$ or $m = 25$; other model parameters: $Z = 100$ and $\beta = 1.0$).

stochasticity emerge as maximizers of Cooperation. We confirmed that the results remain qualitatively equivalent for different group sizes.

In the following we investigate the relevant issue of asserting whether the introduction of this strategy can efficiently promote the average fraction of cooperative actions. The level of Cooperation, η , may be defined as the average number of contributions per round divided by the maximum number of contributions possible. Denoting by C_i the average number of contributions per round associated with strategy S_i , η reads

$$\eta = \frac{1}{N} \sum_{i=1}^{2^{N+2}} \tau_i C_i \quad (72)$$

where τ_i is the fraction of time the population spends in the configuration S_i and N is the group size. As shown in Figure 62, the overall levels of Cooperation remain high as long as the average number of rounds is sizeable (left panel, for different values of the PGG enhancement factor F).

The success of AoN can also be inferred by assessing its evolutionary chances when interacting with unconditional defectors (AllD). To do so, we compute the gradient of selection [5] – $G(k)$ – which provide information on the most likely direction of change of the population configuration with time. This is given by the difference between the probabilities of increasing and decreasing the number of AoN players in a population of k AoNs and $Z - k$ AllDs. The result is depicted in the right panel of Figure 62, a profile characteristic of a coordination game, in which case the AoN strategy dominates whenever the population accumulates a critical fraction of AoN players. Moreover, the size of coordination barrier decreases with increasing values of the enhancement factor F . In Section 7.2.1 we further show that the location of the coordination point is rather insensitive to other game parameters, in particular when the number of rounds is large. Notably, the evolutionary chances of the AoN strategy remain qualitatively independent from alterations on the first bit (b^{-1}). Similarly, we have checked the robustness of the AoN strategy when interacting with random strategists (RS), *i.e.*,

individuals that cooperate or defect with equal probability. It can be shown that both **AoN** and **AllD** are advantageous with respect to **RS** strategists (regardless of their prevalence in the population), while these should drive **AllC** to extinction. Finally, contrary to the generalized versions of **TFT** strategies, in the presence of errors, the **AoN** strategy is robust to invasion of unconditional cooperators (**AllC**) by random drift, as the former can efficiently exploit the latter.

To sum up, we have shown that the strategy **AoN** emerges as the most viable strategy that leads to the emergence of Cooperation under repeated **PGGs**. This strategy, despite its remarkable simplicity, cannot be encoded within the subspace of generalized reciprocators studied before in this context [22]. When we consider individuals capable of making behavioral errors, **AoN** is dominant as suggested by analyzing both the stationary bit strategy (Figures 60 and 61) and the stationary distribution in the monomorphic configuration space (see Section 7.2.1). More importantly, our results suggest that **AoN** dominates independently of the group size and over a wide range of error rates.

Previous works have identified similar strategy principles in different contexts. For instance, the *Win-Stay-Lose-Shift* [39, 40, 41, 49] strategy discovered in the context of the repeated 2-person *Prisoner's Dilemma* constitutes the $N = 2$ limit of **AoN**. In the context of repeated N -Person games on the multiverse [34], the strategy entitled *generic Pavlov* [50] encapsulates a behavioral principle which is similar to that underlying **AoN**. In fact, one may argue that the principles underlying **AoN** may very well be ubiquitous: The simplicity of this strategy can be seen as equivalent – in the context of problems of collective action [5, 6, 14] involving *Public Goods Games* – to the simplicity of tit-for-tat or *Win-Stay-Lose-Shift* strategies discovered in the context of 2-person direct reciprocity, or the stern-judging social norm of indirect reciprocity [51]. In these cases, we observe a fine balance between strict replies towards defective actions and prompt forgiving moves, allowing the emergence of unambiguous decision rules (or norms) that may efficiently recover from past mistakes. Thus, despite the inherent complexity of N -person interactions and the individual capacity to develop complex strategies, it is remarkable how evolution still selects simple key principles that lead to widespread cooperative behaviors.

7.2 SUPPORTING INFORMATION

7.2.1 *The Small Mutation Limit*

Whenever a population evolves under sufficiently small mutation rates, such that the fixation time of any mutant in a population is much smaller than the waiting time between any two mutations, the population is said to be evolving under the small mutation limit [46] and therefore at any moment in time it hosts a maximum of two different strategies (S_i and S_j).

Under such conditions the stochastic evolutionary dynamics may be conveniently described by means of a reduced Markov Chain, whose transitions T_{ij} between configurations are defined by the renormalized fixation probabilities ρ_{ij} , that is

$$T_{ij} = \frac{\rho_{ij}}{2^{N+2}} (i \neq j) \quad (73)$$

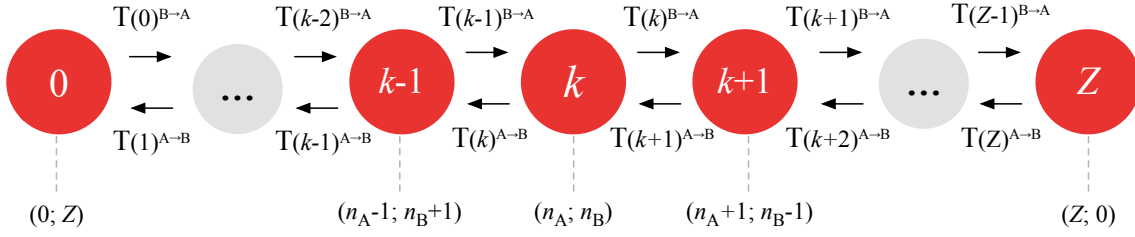


Figure 63: Markov Chain that depicts the $Z + 1$ configurations and respective one-step transitions, which describes the evolution of a system composed by Z individuals that can adopt one of two strategies.

The fixation probability (ρ_{ij}) represents the probability with which a mutant with strategy S_j is able to invade a resident population, reaching fixation, using strategy S_i . For birth-death processes, as is the case, this quantity can be computed whenever all transition probabilities between configurations are known (see Fig. 63).

Let us consider that each configuration corresponds to a different combination ($k, Z - k$) of two strategies in a population with Z individuals, where k is the number of individuals with the first strategy and $Z - k$ the remaining individuals, adopting the other strategy. Probability of transitions that increase the number individuals with the first strategy by one (from configuration k to $k + 1$) are written as $T^+(k)$ while those that decrease that number by one are written as $T^-(k)$. This can be used to compute the fixation probability of a mutant i in a population of $Z - 1$ m 's. Following [52, 53, 47, 35] this can be written as

$$\rho_{ij} = \left(1 + \sum_{l=1}^{Z-1} \prod_{k=l}^l \frac{T^+(k)}{T^-(k)} \right)^{-1} \quad (74)$$

For the particular case of the fermi update rule [35] the fixation probability is given by

$$\rho_{ij} = \left(1 + \sum_{l=1}^{Z-1} \prod_{k=l}^l e^{\beta(f_{S_i}(k) - f_{S_j}(k))} \right)^{-1} \quad (75)$$

where β is the intensity of selection and $f_{S_i}(k)$ the fitness of strategy S_i . These fitnesses are computed by averaging the payoffs $\Pi_{S_i}(l)$ and $\Pi_{S_j}(l)$ over all groups of size N composed by l other individuals playing S_i :

$$\begin{aligned} f_{S_i}(k) &= \binom{Z-1}{N-1}^{-1} \sum_{l=0}^{N-1} \binom{k-1}{l} \binom{Z-k}{N-1-l} \Pi_{S_i}(l+1) \\ f_{S_j}(k) &= \binom{Z-1}{N-1}^{-1} \sum_{l=0}^{N-1} \binom{k}{l} \binom{Z-1-k}{N-1-l} \Pi_{S_j}(l) \end{aligned} \quad (76)$$

Both $\Pi_{S_i}(l)$ and $\Pi_{S_j}(l)$ are computed numerically given the large number of strategies under study for all $0 \leq l < N$.

N	\bar{b}^{-1}	\bar{b}^0	\bar{b}^1	\bar{b}^2	\bar{b}^3	\bar{b}^4	\bar{b}^5	\bar{b}^6	\bar{b}^7	\bar{b}^8	\bar{b}^9	\bar{b}^{10}
2	0.60	0.52	0.01	0.91								
3	0.45	0.65	0.34	0.05	0.89							
4	0.49	0.65	0.38	0.33	0.16	0.91						
5	0.33	0.79	0.40	0.44	0.39	0.16	0.95					
6	0.34	0.78	0.44	0.45	0.38	0.38	0.25	0.95				
7	0.24	0.84	0.45	0.46	0.45	0.43	0.38	0.29	0.96			
8	0.27	0.83	0.46	0.47	0.47	0.41	0.44	0.40	0.32	0.96		
9	0.20	0.87	0.47	0.48	0.47	0.46	0.45	0.44	0.41	0.34	0.97	
10	0.20	0.87	0.48	0.48	0.48	0.48	0.45	0.46	0.44	0.42	0.37	0.97

Figure 64: Stationary-bit-Strategy in the absence of behavioral errors. Rows refer to different group sizes (N) and columns to different strategy bits (b^q). Each cell indicates the fraction of time the population spends in a strategy with bit $b^q = 1$. Blue (red) cells highlight group for which the population spends more (less) than $3/4$ of the time employing strategies with $b^q = 1$. Parameters are $Z = 100$, $\beta = 1.0$, $N = 5$, $F/N = 0.85$, $w = 0.96$, $\epsilon = 0.00$ and $\mu \ll 1/Z$.

The set of transition probabilities T_{ji} build up a Transition Matrix (a stochastic matrix) whose eigenvector associated with the largest eigenvalue (*i.e.* 1) returns the stationary distribution (τ_i) of the population [54]. τ_i conveniently describes the average fraction of time the population spends in each of the 2^{N+2} possible monomorphic population configurations corresponding to situations in which every member employs the same strategy.

7.2.2 Evolution without errors

The exponential growth of strategies that takes place with increasing group size precludes the use of numerically computed fixation probabilities or stationary distributions to carry out a detailed comparison of strategy profiles involving different group sizes. Instead, it is convenient to compute, numerically, the stationary bit strategy (see main text and previous section for details) which amounts to compute the pervasiveness, in time, of bit $b^q = 1$ in the population. Indeed, this quantity allows us to best assess the evolutionary dynamics of populations, as shown in Fig. 64 in the case where no execution errors are allowed. Fig. 64 stands as the counterpart of Fig. 60 of main text where execution errors occur with probability $\epsilon = 0.05$.

The results in Fig. 64 confirm the trend already present in Fig. 60 of main text pointing out to the emergence of the **AoN** as the prevailing strategic profile. In the absence of errors, Fig. 64 shows that

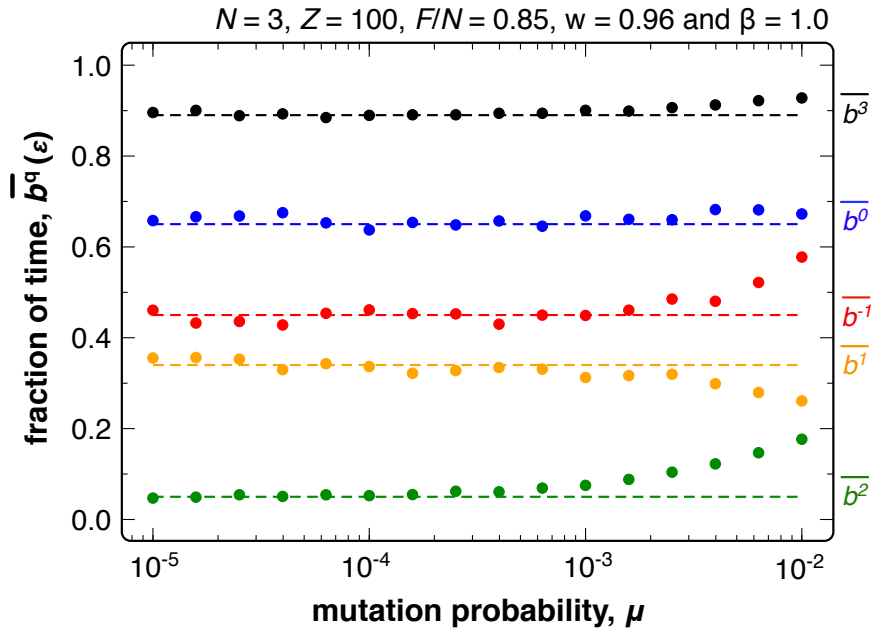


Figure 65: Comparison between numerical simulations and analytical results under the small mutation limit in the absence of errors ($\epsilon = 0.0$). Dots represent the results from numerical simulations with different levels of mutation probability whereas dashed lines display the results obtained in the small mutation limit. Different colors are associated with the different bits indicated.

the remaining (intermediate) bits are weakly dominated by defective behavior. The values obtained for $N = 5$ correspond to the positions of the dots in the left panel of Fig. 61 of main text.

7.2.3 Validity of the Small-Mutation Limit

In what follows, we check the validity of the small mutation limit comparing the results obtained for $N = 3$ with numerical simulations. Fig. 65 shows the stationary bit strategy obtained for a population of $Z = 100$ individuals evolving for a wide range of mutation probabilities (μ from 10^{-4} to 10^{-2}). Dots represent the results of computer simulations while dashed lines reproduce the results under the small mutation limit. Each simulation starts from a random configuration of strategies and evolves for 10^6 generations after an appropriate transient of 10^3 generations. In order to compute the stationary bit strategy we computed the average frequency of strategies along the 10^6 generations over a total of 150 different evolutions. As depicted in Fig. 65 the agreement between numerical and analytical results is good and holds in general for $\mu < (10 \times Z)^{-1}$.

7.2.4 All-or-None versus ALLD

Here we determine the location of the internal roots of the gradient of selection [7] for evolutionary games between AllD and AoN as a function of the number of rounds. The first bit ($b - 1$) of strategy AoN – dictating the behavior in the initial round – is assumed to be 0 (Defection), yet the results remain

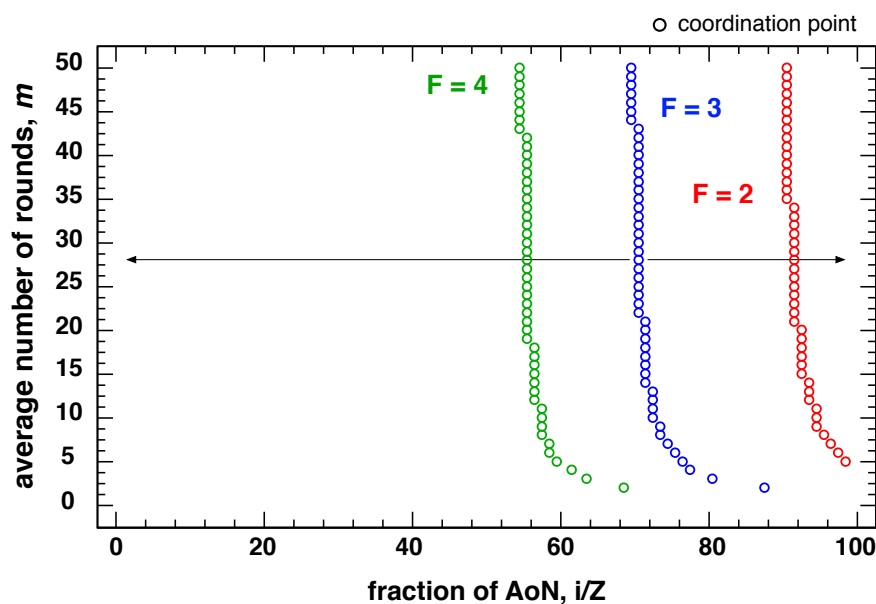


Figure 66: Internal points of the Gradient of Selection [] for the evolutionary game between AllD and AoN when $N = 5$ as a function of the number of rounds m and for different enhancement levels F (2, 3 and 5), other model parameters: $Z = 100$, $\beta = 1.0$.

qualitatively equivalent whenever one assumes $b^{-1} = 1$. We obtain a single coordination point (see Fig. 66) below which greedy AoN is driven towards extinction, while above it AoN outcompetes AllD. Above $m \sim 20$, the location of the coordination point converges, for every value of F , to a constant value. Moreover, increasing F also increases the basin of attraction of the AoN.

7.3 BIBLIOGRAPHY

- [1] Karl Sigmund. *Games of life: Explorations in ecology. Evolution, and Behaviour. London, GB [etc.]: Penguin, 1993.*
- [2] Peter Kollock. Social dilemmas: The anatomy of cooperation. *Annual Review of Sociology*, pages 183–214, 1998.
- [3] Karl Sigmund. *The calculus of selfishness*. Princeton University Press, 2010.
- [4] Max O Souza, Jorge M Pacheco, and Francisco C Santos. Evolution of cooperation under n-person snowdrift games. *Journal of Theoretical Biology*, 260(4):581–588, 2009.
- [5] Jorge M Pacheco, Francisco C Santos, Max O Souza, and Brian Skyrms. Evolutionary dynamics of collective action. In *The Mathematics of Darwin's Legacy*, pages 119–138. Springer, 2011.
- [6] Francisco C Santos and Jorge M Pacheco. Risk of collective failure provides an escape from the tragedy of the commons. *Proceedings of the National Academy of Sciences*, 108(26):10421–10425, 2011.
- [7] Francisco C Santos, Marta D Santos, and Jorge M Pacheco. Social diversity promotes the emergence of cooperation in public goods games. *Nature*, 454(7201):213–216, 2008.

Chapter 7. EVOLUTION OF ALL-OR-NONE STRATEGIES IN REPEATED PUBLIC GOODS DILEMMAS

- [8] Marta D Santos, Flavio L Pinheiro, Francisco C Santos, and Jorge M Pacheco. Dynamics of n-person snowdrift games in structured populations. *Journal of Theoretical Biology*, 315:81–86, 2012.
- [9] Matjaž Perc and Attila Szolnoki. Coevolutionary games—a mini review. *BioSystems*, 99(2): 109–125, 2010.
- [10] Matjaž Perc, Jesús Gómez-Gardeñes, Attila Szolnoki, Luis M Floría, and Yamir Moreno. Evolutionary dynamics of group interactions on structured populations: a review. *Journal of The Royal Society Interface*, 10(80):20120997, 2013.
- [11] Zhen Wang, Attila Szolnoki, and Matjaž Perc. Interdependent network reciprocity in evolutionary games. *Scientific Reports*, 3, 2013.
- [12] Attila Szolnoki, Jeromos Vukov, and Matjaž Perc. From pairwise to group interactions in games of cyclic dominance. *Physical Review E*, 89(6):062125, 2014.
- [13] Tatsuya Sasaki, Åke Brännström, Ulf Dieckmann, and Karl Sigmund. The take-it-or-leave-it option allows small penalties to overcome social dilemmas. *Proceedings of the National Academy of Sciences*, 109(4):1165–1169, 2012.
- [14] Vítor V Vasconcelos, Francisco C Santos, and Jorge M Pacheco. A bottom-up institutional approach to cooperative governance of risky commons. *Nature Climate Change*, 3(9):797–801, 2013.
- [15] Karl Sigmund, Hannelore De Silva, Arne Traulsen, and Christoph Hauert. Social learning promotes institutions for governing the commons. *Nature*, 466(7308):861–863, 2010.
- [16] Christoph Hauert, Silvia De Monte, Josef Hofbauer, and Karl Sigmund. Volunteering as red queen mechanism for cooperation in public goods games. *Science*, 296(5570):1129–1132, 2002.
- [17] Hannelore Brandt, Christoph Hauert, and Karl Sigmund. Punishing and abstaining for public goods. *Proceedings of the National Academy of Sciences*, 103(2):495–497, 2006.
- [18] Ernst Fehr and Simon Gächter. Altruistic punishment in humans. *Nature*, 415(6868):137–140, 2002.
- [19] György Szabó and Gabor Fath. Evolutionary games on graphs. *Physics Reports*, 446(4):97–216, 2007.
- [20] Garrett Hardin. The tragedy of the commons. *Science*, 162(3859):1243–1248, 1968.
- [21] Robert Boyd and Peter J Richerson. The evolution of reciprocity in sizable groups. *Journal of Theoretical Biology*, 132(3):337–356, 1988.
- [22] Sven Van Segbroeck, Jorge M Pacheco, Tom Lenaerts, and Francisco C Santos. Emergence of fairness in repeated group interactions. *Physical Review Letters*, 108(15):158104, 2012.
- [23] Shun Kurokawa and Yasuo Ihara. Emergence of cooperation in public goods games. *Proceedings of the Royal Society of London B: Biological Sciences*, 276(1660):1379–1384, 2009.
- [24] Manfred Milinski, Ralf D Sommerfeld, Hans-Jürgen Krambeck, Floyd A Reed, and Jochem Marotzke. The collective-risk social dilemma and the prevention of simulated dangerous climate change. *Proceedings of the National Academy of Sciences*, 105(7):2291–2294, 2008.
- [25] Valentina Bosetti, Carlo Carraro, Romain Duval, and Massimo Tavoni. What should we expect from innovation? a model-based assessment of the environmental and mitigation cost implica-

- tions of climate-related r&d. *Energy Economics*, 33(6):1313–1320, 2011.
- [26] Scott Barrett. Why cooperate?: the incentive to supply global public goods. *OUP Catalogue*, 2010.
- [27] Scott Barrett and Astrid Dannenberg. Climate negotiations under scientific uncertainty. *Proceedings of the National Academy of Sciences*, 109(43):17372–17376, 2012.
- [28] WMO and UNEP. Ipcc, 2013. URL <http://www.ipcc.ch/>.
- [29] Vítor V Vasconcelos, Francisco C Santos, Jorge M Pacheco, and Simon A Levin. Climate policies under wealth inequality. *Proceedings of the National Academy of Sciences*, 111(6):2212–2216, 2014.
- [30] Klau T. Two challenges for europe’s politicians, 2011. URL http://www.ecfr.eu/content/entry/commentary_two_challenges_for_europes_politician:
- [31] Stiglitz J. Eurozone’s problems are political, not economic. URL <http://blogs.ft.com/the-a-list/2011/07/20/eurozones-problems-are-political-not-economic/-axzz2Rrr973yy>.
- [32] Soros G. A european solution to the eurozone’s problem, 2013. URL <http://www.social-europe.eu/2013/04/a-european-solution-to-the-eurozones-problem/>.
- [33] Robert L Trivers. The evolution of reciprocal altruism. *Quarterly review of biology*, pages 35–57, 1971.
- [34] Chaitanya S Gokhale and Arne Traulsen. Evolutionary games in the multiverse. *Proceedings of the National Academy of Sciences*, 107(12):5500–5504, 2010.
- [35] Arne Traulsen, Martin A Nowak, and Jorge M Pacheco. Stochastic dynamics of invasion and fixation. *Physical Review E*, 74(1):011909, 2006.
- [36] Lawrence E Blume. The statistical mechanics of strategic interaction. *Games and Economic Behavior*, 5(3):387–424, 1993.
- [37] György Szabó and Csaba Tóke. Evolutionary prisoner’s dilemma game on a square lattice. *Physical Review E*, 58(1):69, 1998.
- [38] William H Sandholm. *Population games and evolutionary dynamics*. MIT press, 2010.
- [39] Martin A Nowak, Karl Sigmund, et al. A strategy of win-stay, lose-shift that outperforms tit-for-tat in the prisoner’s dilemma game. *Nature*, 364(6432):56–58, 1993.
- [40] Martin Posch et al. Win stay—lose shift: An elementary learning rule for normal form games. Technical report, Santa Fe Institute, 1997.
- [41] Lorens A Imhof, Drew Fudenberg, and Martin A Nowak. Tit-for-tat or win-stay, lose-shift? *Journal of Theoretical Biology*, 247(3):574–580, 2007.
- [42] Drew Fudenberg and Eric Maskin. Evolution and cooperation in noisy repeated games. *The American Economic Review*, pages 274–279, 1990.
- [43] John Gale, Kenneth G Binmore, and Larry Samuelson. Learning to be imperfect: The ultimatum game. *Games and Economic Behavior*, 8(1):56–90, 1995.
- [44] Robert Boyd. Mistakes allow evolutionary stability in the repeated prisoner’s dilemma game. *Journal of Theoretical Biology*, 136(1):47–56, 1989.

Chapter 7. EVOLUTION OF ALL-OR-NONE STRATEGIES IN REPEATED PUBLIC GOODS DILEMMAS

- [45] Martin A Nowak, Karl Sigmund, and Esam El-Sedy. Automata, repeated games and noise. *Journal of Mathematical Biology*, 33(7):703–722, 1995.
- [46] Drew Fudenberg and Loren A Imhof. Imitation processes with small mutations. *Journal of Economic Theory*, 131(1):251–262, 2006.
- [47] Martin A Nowak, Akira Sasaki, Christine Taylor, and Drew Fudenberg. Emergence of cooperation and evolutionary stability in finite populations. *Nature*, 428(6983):646–650, 2004.
- [48] Flavio L Pinheiro, Francisco C Santos, and Jorge M Pacheco. How selection pressure changes the nature of social dilemmas in structured populations. *New Journal of Physics*, 14(7):073035, 2012.
- [49] David Kraines and Vivian Kraines. Evolution of learning among pavlov strategies in a competitive environment with noise. *Journal of Conflict Resolution*, 39(3):439–466, 1995.
- [50] CH Hauert and Heinz Georg Schuster. Effects of increasing the number of players and memory size in the iterated prisoner’s dilemma: a numerical approach. *Proceedings of the Royal Society of London B: Biological Sciences*, 264(1381):513–519, 1997.
- [51] Jorge M Pacheco, Francisco C Santos, and FACC Chalub. Stern-judging: A simple, successful norm which promotes cooperation under indirect reciprocity. *PLoS Computational Biology*, 2(12):e178, 2006.
- [52] Warren J Ewens. *Mathematical Population Genetics 1: Theoretical Introduction*, volume 27. Springer Science & Business Media, 2012.
- [53] Samuel Karlin. *A first course in stochastic processes*. Academic press, 2014.
- [54] Nicolaas Godfried Van Kampen. *Stochastic processes in physics and chemistry*, volume 1. Elsevier, 1992.

CONCLUSION

"There is no perfection, only life."

Milan Kundera

The structure of social interactions in a population is often modeled by means of a complex network representing individuals and their social ties [1]. These structures are known to fundamentally impact the dynamical processes they support [2]. The characterization of how structure impacts a dynamical process is by no means an easy task. Indeed, the large configuration space spanned tends to limit the systematic applicability of numerical methods, while analytical treatments have failed to provide a good description of the system dynamics. The goal of this thesis was to develop methods and tools inspired in statistical and computational physics in order to obtain a deeper insight on how population structure, modeled in terms of a complex network, impacts dynamical processes.

Chapter 2 explored the nature of correlations among members of a social network that do emerge as a result of different interaction processes [3]. These correlations, associated with the likelihood with which a trait is shared by two individuals that are at a given social distance¹, provide a convenient way to peer through the influence that individuals exert on each other in social networks. Empirical evidence suggests that individuals tend to be positively correlated with others up to a social distance of three contacts, a phenomena coined as the three degrees of influence [4]. Our work shows that these 'peer-influence' patterns are universal and emerge as a natural consequence of having dynamical processes (*e.g.* opinion formation, behavior evolution and disease spreading) on structured populations. We have also shown that, counter-intuitively, the range of influence of individuals increases with increasing network sparsity, that is, with decreasing density of the network connectivity, and increasing clustering. Future work should explore how *peer-influence* patterns are affected by *i*) topological features not considered in our study (*e.g.* hierarchal organization) and by *ii*) dynamical processes that rely on group interactions (*e.g.* Public Goods Games) contrary to the pairwise scheme that we have studied.

A central question associated with the study of dynamical processes in complex networks, and to a certain extent with the entire field of complex systems, concerns the dichotomy between the dynamical rules that govern pairwise interactions (local scale) and the collective dynamics exhibited

¹ In a social network the social distance between two individuals is measured as the minimum number of links that separates them.

Chapter 8. CONCLUSION

by the population (global scale). Here we approached this question formulating it as a problem of Cooperation [5], resorting to Evolutionary Game Theory [6].

Chapter 3 introduces a numerically computed *mean-field* quantity that captures the evolutionary dynamics of structured populations [7]. This quantity, coined as the *Average Gradient of Selection*, returns a dynamical description that is qualitatively similar to that conveyed by the replicator equation but that takes into account the topological features of the network of interactions between individuals. Moreover, since it is computed through the analysis of all pairs of connected individuals in a population, it effectively connects both local and global scale dynamics. With the *Average Gradient of Selection* we have shown a fundamental connection between the connectivity structure of the underlying network of interactions and the resulting collective dynamics. In particular, when individuals interact according to the two-person *Prisoner's Dilemma*, degree homogeneous networks² promote a population-wide coexistence dynamics, while degree heterogeneous networks³ lead to a coordination of strategies. These scenarios, that result from the different connectivity structures of the interaction network, are dynamically similar to other social dilemmas of Cooperation, namely to the N -person variants of the Snowdrift Game (coexistence) and the Stag Hunt (coordination) games, which in turn contrast with the defector dominance dynamics characteristic of the *Prisoner's Dilemma* that individuals face locally. Hence, population structure effectively leads to the emergence of a collective social dilemma, whose dynamical properties contrast with the social dilemma that individuals face locally and that constitutes a milder challenge for Cooperation. It is precisely because of this transformation, induced by networks, that Cooperation has a chance of being evolutionary (self)-sustainable in a population. In this sense, not only Cooperation (modeled in terms of a *Prisoner's Dilemma*) requires at least two individuals to emerge, it becomes inherently a collective phenomenon.

Chapters 4, 5 and 6 made use of the *Average Gradient of Selection* to characterize the evolutionary dynamics of the *Prisoner's Dilemma* in structured populations under different dynamical conditions. In particular, Chapter 4 explored how selection pressure (the uncertainty associated with the decision making) impacts the population-wide dynamics of structured populations [8]. We show that the coexistence dynamics, characteristic of homogeneous networks, only emerges under strong selection regimes. In heterogeneous networks the coordination dynamics is independent of the selection pressure. However, the specific features depend on the particular choice of selection pressure. Furthermore, we show that in both topological scenarios there is an optimal selection pressure that optimizes the level of Cooperation, while the underlying mechanism from which it stems is distinct in both cases.

Chapter 5 explores how the introduction of mutations (the spontaneously adoption of new behaviors by individuals) impacts the evolutionary dynamics of Cooperation in structured populations. We show that when individuals engage in a *Prisoner's Dilemma* game in heterogeneous networks, the introduction of mutation rates induce drastic regime shifts, from the defection dominance that characterizes the standard *Prisoner's Dilemma* into a regime of coexistence among Cooperators and Defectors, as well as into a regime of coordination, often revealing more than one basin of attraction. Moreover, we show that the evolutionary outcome in heterogeneous networks that results from variations in the

² A network whose degree distribution has zero variance.

³ A network whose degree distribution has non-zero variance.

mutation rates is quite sensible to the particular selection regime under which population evolves. In particular we show that under strong selection regimes, Cooperation is undermined by variations in the mutation rate, whereas under weak selection one witnesses a subtle balance between selection and mutation, which is favorable to defectors. Interestingly, there exists a range of selection pressures in which structured populations are most resilient to variations in mutation rates.

Chapter 6 extends the methodology employed for the computation of the *Average Gradient of Selection* to the co-evolutionary scenario where structure evolves along with strategy. We show that the fate of Cooperation is directly related with the relative time-scales of both dynamical processes and that for increasing rates of structure adaptation it becomes easier for cooperators to coordinate towards a full Cooperation scenario. Furthermore, the collective dynamical profile that emerges is similar to that found in games that involve interactions between groups of individuals.

In sum, the *Average Gradient of Selection* constitutes a powerful tool to study evolutionary dynamics of Cooperation in structured populations. It provides a context dependent description that is both sensitive to the underlying structure of interactions and to different dynamical scenarios, being able, for instance, to account for co-evolutionary dynamics, the presence of mutations and variations in the dynamical parameters (*e.g.* selection pressure and payoff parameters). These aspects, which have a dramatic impact in the dynamics of structured populations and that are an important part of the real world systems that we aim at modeling, are not accountable, at present, by current alternatives. For example, *pair-approximation* techniques [9] are unable to distinguish between networks with similar degree distributions but distinct topological features, fail also to account for degree heterogeneity and are unable to take into account the impact of mutations. On the other hand, the major drawback of the *Average Gradient of Selection* is that it is computed numerically, thus, being constrained to the computational resources available. Despite of this, we and others [10] believe that at the present the *Average Gradient of Selection* provides the most promising and efficient means to characterize the evolutionary dynamics in structured populations, being able to establish a reversible link between individual and collective behavior in those populations. The usefulness of the *Average Gradient of Selection* should not be limited to dynamical processes involving decision making modeled in terms of games. Indeed, in a broad perspective the methodology here developed should be considered as a contribution to the characterization of Complex Systems involving populations in which who interacts with whom is well-defined by a complex network. Future work should extend its applicability to other dynamical processes, such as disease spreading and opinion formation, and also to non-trivial interaction structures that involve multiplex or interdependent structures [11, 12]. The ongoing improvement of the computational efficiency in the computation of *Average Gradient of Selection* should remain a goal of future work.

The problem of Cooperation is not limited to the study of situations/games involving only two individuals, neither it is restricted to the characterization of the role of population structure in the evolution of Cooperation. Indeed, many situations are better modeled by assuming group interactions [13]. In that context, Chapter 7 explores the evolutionary dynamics of a population whose individuals engage in a repeated Public Goods Games [14]. We resort to the small mutation limit to explore the strategy space of strategies in which individuals' actions are conditional to the group achievements in the pre-

Chapter 8. CONCLUSION

vious round. We have found that a strategy of *All-or-None*, in which individuals only cooperate after a round of unanimous group behavior, outperforms all other strategies. *All-or-None* is also resilient to behavioral errors, performing well when individuals are prone to commit decision errors, in the sense of not acting according to what is defined by their strategies. The *All-or-None* strategy profile provides a quick route for coordination towards to the best group outcome (full Cooperation) in error prone environments, is risk-dominant against free-riders, leads to (overall) high levels of cooperative behavior and builds from the same (simple) intuition found in strategies studied in the scope of the two-person repeated *Prisoner's Dilemma*, namely the famous *Pavlov* and *Win-Stay-Lose-Shift* strategic profiles [15, 16, 17]. Future work should look to understand the robustness of *All-or-None* in the space of more generic strategies that do not imply explicitly a conditional action towards the group's previous achievements.

Not included in this thesis are other works to which I have contributed and that explore the evolutionary dynamics of Cooperation. In [18] we explore the impact of fitness delay in the *N*-Person games with payoff thresholds. In this context, fitness delay implies that the payoff attained through game theoretical interactions only contributes to the fitness in the future. In [19] we provide a summary of previous works, detailing how social diversity, when modeled through different perspectives, seems to be a key ingredient for the evolution of Cooperation. In [20] we have used the *Average Gradient of Selection* to characterize the evolutionary dynamics of *N*-Person Snowdrift Games in structured populations. Finally, in [21] we have shown that the joint effect of population structure and *peer-punishment* (another mechanism regarded to provide a positive impact for the evolution of Cooperation) does not necessarily generate a better scenario for Cooperation.

8.1 BIBLIOGRAPHY

- [1] Albert-László Barabási. *Linked: How everything is connected to everything else and what it means*. Plume Editors, 2002.
- [2] Alain Barrat, Marc Barthélemy, and Alessandro Vespignani. *Dynamical processes on complex networks*, volume 1. Cambridge University Press Cambridge, 2008.
- [3] Flavio L Pinheiro, Marta D Santos, Francisco C Santos, and Jorge M Pacheco. Origin of peer influence in social networks. *Physical Review Letters*, 112(9):098702, 2014.
- [4] Nicholas A Christakis and James H Fowler. *Connected: The surprising power of our social networks and how they shape our lives*. Little, Brown, 2009.
- [5] Karl Sigmund. *The calculus of selfishness*. Princeton University Press, 2010.
- [6] Martin A Nowak. *Evolutionary dynamics: exploring the equations of life*. Harvard University Press, 2006.
- [7] Flávio L Pinheiro, Jorge M Pacheco, and Francisco C Santos. From local to global dilemmas in social networks. *PLoS One*, 7(2):e32114, 2012.
- [8] Flávio L Pinheiro, Francisco C Santos, and Jorge M Pacheco. How selection pressure changes the nature of social dilemmas in structured populations. *New Journal of Physics*, 14(7):073035, 2012.

- [9] György Szabó and Gábor Fáth. Evolutionary games on graphs. *Physics Reports*, 446(4):97–216, 2007.
- [10] Cong Li, Boyu Zhang, Ross Cressman, and Yi Tao. Evolution of cooperation in a heterogeneous graph: Fixation probabilities under weak selection. *PLoS One*, 8(6):e66560, 2013.
- [11] Zhen Wang, Attila Szolnoki, and Matjaž Perc. Interdependent network reciprocity in evolutionary games. *Scientific Reports*, 3, 2013.
- [12] Stefano Boccaletti, G Bianconi, R Criado, Charo I Del Genio, J Gómez-Gardeñes, M Romance, I Sendina-Nadal, Z Wang, and M Zanin. The structure and dynamics of multilayer networks. *Physics Reports*, 544(1):1–122, 2014.
- [13] P. Kollock. Social dilemmas: The anatomy of cooperation. *Annual Review of Sociology*, 24: 183–214, 1998.
- [14] Flávio L Pinheiro, Vítor V Vasconcelos, Francisco C Santos, and Jorge M Pacheco. Evolution of all-or-none strategies in repeated public goods dilemmas. *PLoS Computational Biology*, 10(11):e1003945, 2014.
- [15] Martin Posch et al. Win stay—lose shift: An elementary learning rule for normal form games. Technical report, Santa Fe Institute, 1997.
- [16] David Kraines and Vivian Kraines. Evolution of learning among pavlov strategies in a competitive environment with noise. *Journal of Conflict Resolution*, 39(3):439–466, 1995.
- [17] Martin A Nowak, Karl Sigmund, et al. A strategy of win-stay, lose-shift that outperforms tit-for-tat in the prisoner’s dilemma game. *Nature*, 364(6432):56–58, 1993.
- [18] João A Moreira, Flavio L Pinheiro, Ana Nunes, and Jorge M Pacheco. Evolutionary dynamics of collective action when individual fitness derives from group decisions taken in the past. *Journal of Theoretical Biology*, 298:8–15, 2012.
- [19] Francisco C Santos, Flavio L Pinheiro, Tom Lenaerts, and Jorge M Pacheco. The role of diversity in the evolution of cooperation. *Journal of Theoretical Biology*, 299:88–96, 2012.
- [20] Marta D Santos, Flavio L Pinheiro, Francisco C Santos, and Jorge M Pacheco. Dynamics of n-person snowdrift games in structured populations. *Journal of Theoretical Biology*, 315:81–86, 2012.
- [21] Jeromos Vukov, Flavio L Pinheiro, Francisco C Santos, and Jorge M Pacheco. Reward from punishment does not emerge at all costs. *PLoS Computational Biology*, 9(1), 2013.

